Physiol Rev 98: 1493–1590, 2018
Published May 30, 2018; doi:10.1152/physrev.00047.2017

CLC CHLORIDE CHANNELS AND TRANSPORTERS: STRUCTURE, FUNCTION, PHYSIOLOGY, AND DISEASE

Thomas J. Jentsch and Michael Pusch

Leibniz-Forschungsinstitut für Molekulare Pharmakologie (FMP) and Max-Delbrück-Centrum für Molekulare Medizin (MDC), Berlin, Germany; and Istituto di Biofisica, Consiglio Nazionale delle Ricerche, Genova, Italy

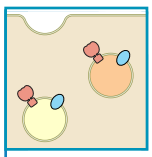

Jentsch TJ, Pusch M. CLC Chloride Channels and Transporters: Structure, Function, Physiology, and Disease. *Physiol Rev* 98: 1493–1590, 2018. Published May 30, 2018; doi:10.1152/physrev.00047.2017.—CLC anion transporters are found in all phyla and form a gene family of eight members in mammals. Two CLC proteins, each of which completely contains an ion translocation parthway, assemble to homo- or heteromeric dimers that sometimes require accessory β-subunits for function. CLC proteins come in two flavors: anion channels and anion/proton exchangers. Structures of these two CLC protein classes are surprisingly similar. Extensive structure-function analysis identified residues involved in ion permeation, anion-proton coupling and gating and led to attractive biophysical models. In mammals, ClC-1, -2, -Ka/-Kb are plasma membrane Cl^- channels, whereas ClC-3 through ClC-7 are $2Cl^-/H^+$-exchangers in endolysosomal membranes. Biological roles of CLCs were mostly studied in mammals, but also in plants and model organisms like yeast and *Caenorhabditis elegans*. CLC Cl^- channels have roles in the control of electrical excitability, extra- and intracellular ion homeostasis, and transepithelial transport, whereas anion/proton exchangers influence vesicular ion composition and impinge on endocytosis and lysosomal function. The surprisingly diverse roles of CLCs are highlighted by human and mouse disorders elicited by mutations in their genes. These pathologies include neurodegeneration, leukodystrophy, mental retardation, deafness, blindness, myotonia, hyperaldosteronism, renal salt loss, proteinuria, kidney stones, male infertility, and osteopetrosis. In this review, emphasis is laid on biophysical structure-function analysis and on the cell biological and organismal roles of mammalian CLCs and their role in disease.

I. INTRODUCTION

Chloride is the most abundant anion and serves many different biological roles. As a counterion for Na^+ and K^+, chloride ensures electroneutrality both under steady state and during transport across cellular membranes, as exemplified by transepithelial transport and acidification of intracellular vesicles. Owed to its high concentration, it serves, together with positively charged counterions, as important osmolyte to drive water across cellular membranes in cell volume regulation and transepithelial secretion or absorption of water. Chloride may also have "chemical" roles by binding to proteins and thereby modifying their function. Examples are given by the lysosomal enzyme cathepsin C, the activity of which is modulated by the binding of chloride to the protein (138) and WNK protein kinases (616, 646, 830), but many other proteins are known to be chloride sensitive (207). Chloride transport across cellular membranes generates electrical currents if its transport is not strictly coupled to that of other ions, such as in "electroneutral" K^+-Cl^- or Na^+-K^+-$2Cl^-$ cotransporters or Cl^-/HCO_3^- exchangers. Cl^- channels can therefore change the voltage across the plasma membrane and thereby influence the electrical excitability of neurons, muscle, and endocrine cells (310, 423, 477, 572, 702). Cl^- channels might also influence the voltage of intracellular organelles, but most likely the main Cl^- transporters of endosomes and lysosomes are $2Cl^-/H^+$ exchangers of the CLC gene family, which encompasses both these exchangers and Cl^- channels. These exchangers also generate currents (are "electrogenic"), but, as discussed below, coupling of Cl^- to H^+

transport has additional important implications for their biological roles.

The direction of Cl^- transport through channels is entirely determined by the transmembrane gradient of the electrochemical potential, which is given by the difference in Cl^- concentration and the transmembrane voltage according to the Nernst equation. Whereas in mammals the serum concentration of Cl^- is universally high (~120 mM) and intracellular chloride concentration ($[Cl^-]_i$) much lower, different cell types display a wide range of $[Cl^-]_i$ (from ~5–10 mM in most mature neurons up to ~40 mM in epithelial cells). This large difference in $[Cl^-]_i$ is mainly due to differential expression of secondarily active Cl^- transporters that either increase (e.g., Na^+-K^+-$2Cl^-$ cotransporters or Cl^-/HCO_3^- exchangers) or decrease (like K^+-Cl^- cotransporters) $[Cl^-]_i$ (201, 889). Hence, opening of Cl^- channels may either hyperpolarize or depolarize the plasma membrane. In stark contrast, opening of Na^+ and Ca^{2+} channels will almost always depolarize the cell owing to the large inwardly directed ion gradient and the inside-negative voltage.

For a long time, the study of chloride channels had been neglected. The interest focused on voltage- or ligand-gated cation channels that underlie action potential conduction and synaptic transmission (343). In fact, Cl^- channels were often considered a nuisance and their currents were often eliminated when studying cation channels. Notable exceptions are the large chloride conductance of skeletal muscle, that amounts to ~80% of the resting conductance (83, 364, 477, 617), and inhibitory GABA and glycine receptor anion channels (300, 572, 752). In the 1980s, the application of the patch-clamp technique revealed the presence of cation and anion channels in practically all cells (95, 343, 776).

The first voltage-gated chloride channel to be molecularly identified was ClC-0, the founding member of the CLC gene family (393). Thomas Jentsch and colleagues cloned it from the electric organ of the marine ray *Torpedo* which is a rich source for ion channels that are needed to generate the large currents that these animals use to stun their prey. Besides the nicotinic acetylcholine receptor cation channel, which also was first cloned from this organ (596), the *Torpedo* electroplax contained a peculiar chloride channel that had been discovered by Chris Miller upon reconstituting electric organ membrane proteins into lipid bilayers (905), in this way establishing the first high-resolution single-channel recordings from lipid bilayers (548). Detailed biophysical analysis by Miller and colleagues strongly suggested that the channel contained two largely independent pores (324, 548, 549), a prescient conclusion amply confirmed after its molecular identification (211, 491, 492, 543, 897). Thomas Jentsch at first tried to identify the channel protein by its ability to covalently bind DIDS (388), which Chris Miller had shown to irreversibly inhibit the channel at micromolar concentrations (549). Following the failure of his approach (388), Jentsch and colleagues finally identified the channel using a painstaking combination of hybrid depletion and functional expression in *Xenopus* oocytes (393). After having identified the mammalian skeletal muscle chloride channel, which they named ClC-1 (for Cl^- Channel 1), they proposed to name the prototype *Torpedo* channel ClC-0 (807). Personal accounts of Jentsch's and Miller's initial discoveries can be found in two recent reviews (385, 547).

With the use of homology-based methods, first in wet-laboratory experiments using hybridization of cDNA libraries with radioactive probes (807, 808, 832) and later in silico once large-scale DNA sequencing took off, CLC proteins were subsequently identified in all phyla, with nine human CLC genes (384, 385) **(FIGURE 1)**.[1] Apart from the skeletal muscle ClC-1 channel, whose function was known before its molecular identification (807), the function of the remaining CLCs was unknown. The study of their biochemical and biophysical properties and of their physiological role and their involvement in human genetic diseases led to the clarification and discovery of many biological and pathological processes (384, 802). A particularly important discovery was that several CLCs reside in the endo/lysosomal system (307, 429) and that these intracellular CLCs are actually not chloride channels but secondarily active, strictly coupled $2Cl^-/1H^+$ antiporters (5, 651, 742). The precise physiological role of these intracellular transporters is still not fully understood.

It should be mentioned that there are several structurally unrelated Cl^- channel classes besides CLCs. These include the cystic fibrosis transmembrane conductance regulator (CFTR) (480, 703), pentameric ligand-gated anion channels like GABA and glycine receptors (300, 752), Ca^{2+}-activated Cl^- channels of the bestrophin (327, 818) and TMEM16 (or Anoctamin) (104, 605, 756, 928) gene families, LRRC8 proteins that form volume-regulated anion channels (VRACs) (681, 865), and maxi-anion channels (723) that may be formed by the organic anion transporter SLCO2A1 that is known as prostaglandin transporter (724). This list is not complete, and several biophysically characterized anion channels remain to be identified at the molecular level. However, several protein classes previously postulated to represent Cl^- channels are now known not to function as ion channels, such as CLCAs (chloride channel,

[1]We use the most widely accepted CLC nomenclature in this review. As a generic name, CLC with three capital letters is used, with individual proteins using lowercase l (for Cl) and a dash to connect to the number or letter specifying the individual isoform, e.g., ClC-1 [as originally proposed by Steinmeyer et al. (807)]. Species specifiers are added at the beginning, for example, EcClC-1 for *Escherichia coli* (210, 335), AtClC-a for *Arabidopsis thaliana* (335), or hClC-1 and mClC-1 for the human and mouse ClC-1 channels. The corresponding human and mouse genes are, e.g., *CLCN1* and *Clcn1*, respectively, according to the genome nomenclature.

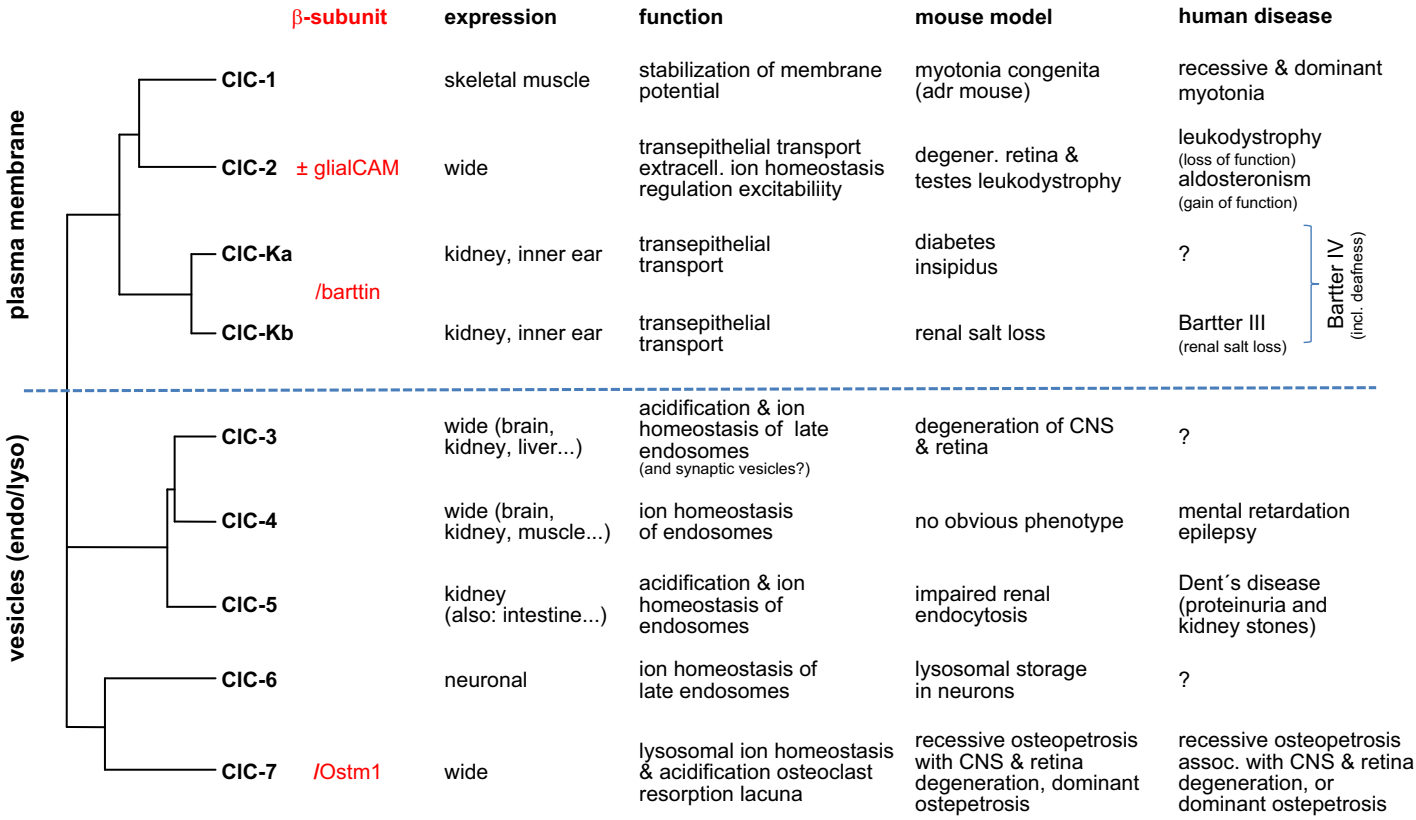

FIGURE 1. The family of mammalian CLCs and associated proteins. In mammals, three homology branches can be identified (shown in dendrogram at *left*). Whereas members of the first branch function as plasma membrane voltage-gated anion channels like the *Torpedo* channel ClC-0 (most closely related to ClC-1), proteins of the two other branches are rather $2Cl^-/H^+$ exchangers that reside predominantly on endosomes and lysosomes. ClC-1 and the two ClC-K isoforms show highly specific tissue expression patterns, whereas ClC-2 and the vesicular Cl^-/H^+ exchangers (with the exception of ClC-6) are widely and probably even ubiquitously expressed across tissues. Both ClC-K isoforms and ClC-7 need specific auxiliary proteins ("β-subunits") for functional expression and protein stability (222, 445). ClC-2 can function without a β-subunit, but associates with the cell adhesion molecule GlialCAM in glia, which changes its localization, stability, and biophysical properties (346, 395). These differential requirements for ancillary proteins are symbolized by "/" and "±", respectively. The main phenotypes of *Clcn* mouse models or human diseases caused by *CLCN* mutations are indicated. The loss of the common β-subunit barttin (65, 222), or the loss of both ClC-K isoforms (748), leads to a combination of severe renal salt loss and congenital deafness, which in humans is known as Bartter syndrome type IV.

Ca^{2+}-activated) (75, 288) and CLICs (chloride intracellular channel) (30). The names given to these proteins are misnomers and a source of confusion.

In this review we first provide a description of the general structural architecture of CLC proteins, general mechanisms of ion transport in CLC channels and transporters, and mechanisms of gating in the prototype ClC-0 channel, a well-studied channel that serves as a reference for other CLCs.

We then review the current knowledge on the properties of the nine mammalian CLCs and their associated β-subunits **(FIGURE 1)**. A particular focus will be put on their physiological functions as highlighted by mouse models and human inherited disease. The associated pathologies impressively demonstrate the important, and often unexpected, role of chloride transport in many different tissues and cellular organelles.

Finally, we summarize briefly the literature on CLC proteins in various model organisms and in plants.

II. BIOPHYSICAL PROPERTIES OF CLC PROTEINS

CLC proteins exhibit several unique peculiar properties. These include the homodimeric architecture with independent ion transport in each subunit, the existence of passive channels as well as secondary active transporters, and the exquisite voltage-dependent regulation of CLC function by the transported substrates: anions and protons (126, 384, 385, 802, 964).

A. The Double-Barreled *Torpedo* ClC-0 Channel

The first electrophysiological recordings of the *Torpedo* electroplax Cl^- channel in planar lipid bilayers by Miller and colleagues revealed a peculiar "double-barreled" single-channel behavior **(FIGURE 2*A*)**. Single channels opened in bursts, separated by long closures. During each burst two equally spaced open conductance levels were visible that appeared to originate from the independent gating of two physically separated Cl^- channels (324, 548, 828). Collectively, this behavior could be explained by a "double-barreled shotgun" model: Two identical protopores are present in the complex, each bearing a proper "fast gate" giving rise to the binomial gating behavior within a burst. A common "slow gate" is able to shut off both pores simultaneously (548, 550). The protopore gate was found to be voltage-dependent with an apparent gating valence around 1 elementary charge (324, 548). Direct evidence for the model was obtained by applying low concentrations of DIDS which led to the sequential, irreversible inhibition of single protopores (549) **(FIGURE 2*A*)**. A further peculiarity of the *Torpedo* channel gating, namely, a violation of microscopic reversibility, was revealed by single-channel recordings in bilayers: Channels entered a burst predominantly into a state with both protopores being open, while bursts terminated predominantly from a state in which only one of the protopores was open (697). Such a time asymmetry is only possible in a system that is not in thermodynamic equilibrium and requires the dissipation of free energy to fuel the gating process. Initially, Richard and Miller (697) concluded that the electrochemical Cl^- gradient was the underlying source of free energy. More recently, Lísal and Maduke (478) discovered that not the Cl^- gradient but instead the electrochemical H^+ gradient quantitatively correlates with the degree of irreversibility of the gating process. This finding demonstrates unambiguously that protons are permeating through the ClC-0 channel in a manner that is coupled to the gating processes (970). In more general terms, such a behavior strongly favors the hypothesis that CLC anion channels evolutionarily arose from stoichiometrically coupled anion/proton exchangers, losing most, but not all, of their coupling efficiency (479, 546). It is nevertheless still a mystery how the common gate of the

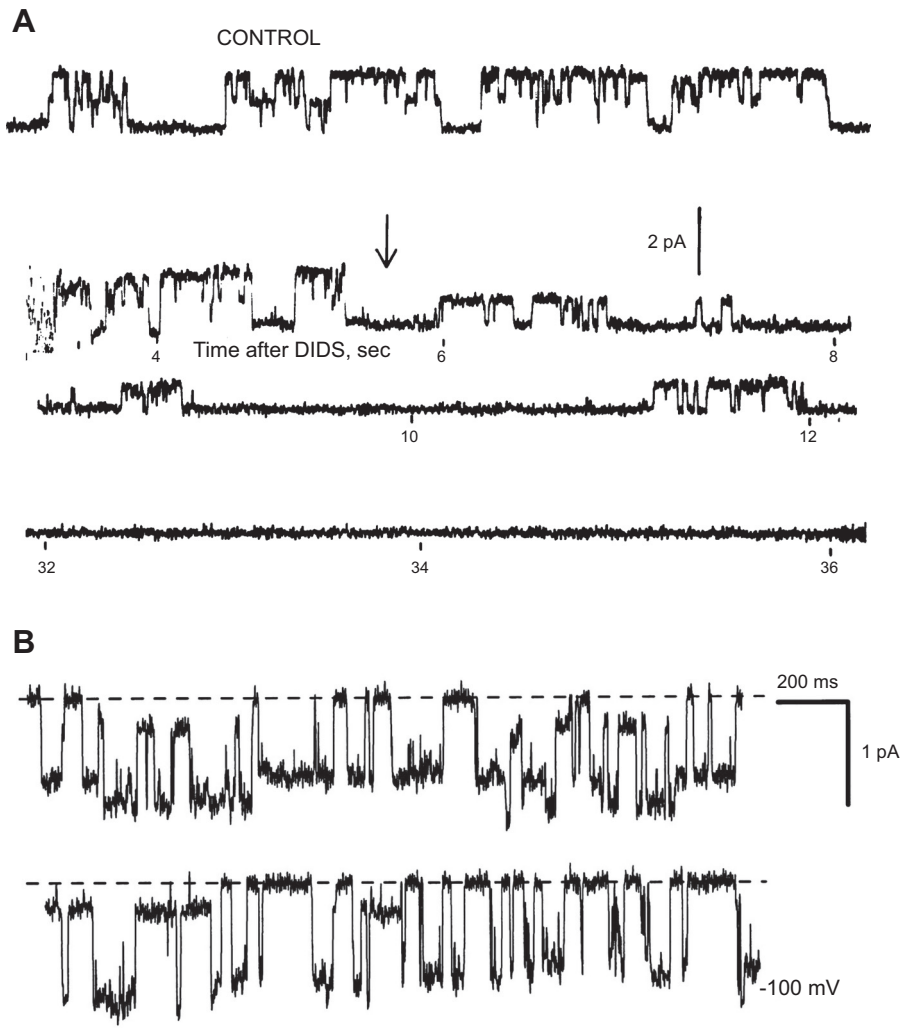

FIGURE 2. Double-barreled CLC Cl^- channels with independent pores. *A*: a recording of a single *Torpedo* Cl^- channel incorporated into a lipid bilayer before the application of DIDS (top trace) and after addition of 10 mM DIDS (lower traces). Note the grouping of openings in bursts during which two equally spaced conductance levels are visible, being caused by the opening of two independent pores. After DIDS addition, first one and later both pores stop opening, suggesting that both pores are physically distinct. [From Miller and White (549).] *B*: a recording of a single concatemeric channel composed of one subunit of ClC-0 and the other subunit of ClC-2. The observed conductance levels are fully consistent with the linear superposition of a larger ClC-0 and a smaller ClC-2 pore, demonstrating that pore properties are entirely determined by the structure of the corresponding protein subunit. [From Weinreich and Jentsch (897).]

Torpedo channel that acts on both pores simultaneously is related to the better understood fast protopore gate or to the anion/proton exchange mechanism of CLC antiporters. The question is even more intriguing considering that the anion/proton exchange mechanism is independent of the dimeric structure (446, 705, 941).

The cloning of the ClC-0 *Torpedo* channel (393), followed by the rapid identification of mammalian CLC genes (see Ref. 387), allowed the investigation of the architecture of CLC proteins using molecular methods. Importantly, the single cDNA encoding the 805-amino acid ClC-0 protein was able to fully reproduce the biophysical behavior of the *Torpedo* channel (50), demonstrating that the channel is homomeric. Early functional experiments using the ClC-2 channel showed that the NH_2 terminus and the large COOH-terminal domain (after amino acid E526) are entirely cytoplasmic (303). A multimeric structure of ClC-1 could be inferred from dominant negative functional effects of dominant myotonia causing mutations (806). Biochemical analysis, and concatamers and/or coexpression of wild-type (WT) and mutant ClC-0 or ClC-1 channels with different functional properties unambiguously showed that CLC channels are homodimers (492, 543, 544). Importantly, single-channel analysis demonstrated that each subunit forms a proper protopore (492, 543) (see **FIGURE 2*B***), whose gating was completely independent from the neighboring pore (491). Such an architecture is quite different from that of classic ion channels like voltage-gated cation channels, in which a central ion conducting pore is formed at the interface of identical or homologous subunits (343), imposing thus a straight pore perpendicular to the membrane plane.

The transmembrane topology of CLC proteins had been explored using a variety of techniques, correctly identifying the orientation of several membrane helices and intra/extracellular localization of loops (228, 303, 415, 437, 489, 544, 750). However, in retrospect, given the complex architecture revealed by CLC crystal structures, a full determination of the membrane topology was extremely challenging. It is also interesting to note that functional CLC channels can be formed from the separate expression of various pieces of the protein (223, 505, 512, 560, 749), suggesting that CLC proteins are composed of modular domains that can fold independently and then associate.

B. Structure of CLC Proteins

Eukaryotic, and in particular mammalian, membrane proteins are generally more difficult to purify in large quantities needed for crystallization compared with prokaryotic proteins. As for K^+ channels (200), bacterial homologues have been extremely useful to obtain direct structural information on CLC proteins. In pioneering studies, Maduke et al. (511) purified a CLC-homologue from *Escherichia coli* and biochemically confirmed a dimeric structure. A two-dimensional projection structure of EcClC-1 was in agreement with a homodimeric double-pore structure, but the resolution of 6.5 Å was too low to allow further structural insight (553). A breakthrough was the determination of the crystal structures of EcClC-1 and of the highly homologous StClC from *Salmonella typhimurium* (210, 211). In full agreement with the double-pore architecture deduced from the functional studies, the crystal structures revealed a homodimeric structure with anion binding sites in the center of each subunit **(FIGURE 3, *A* AND *B*)**. Each subunit has a triangular shape (viewed from the outside or from the inside), and the subunits are interacting with a large, mostly hydrophobic and roughly planar interface of ~2,300 $Å^2$, suggesting a very strong binding of the two monomers. Indeed, using single molecule photobleaching of fluorescently labeled EcClC-1 subunits reconstituted into liposomes at very low density, Chadda et al. (114) could estimate the free energy of dimerization finding that the CLC dimer is one of the strongest protein complexes measured so far.

The subunits are composed of 18 alpha helices (denominated A-R), 17 of which are partially embedded in the membrane **(FIGURE 3*C*)**. Most helices are tilted, and in addition, several helices are not traversing the membrane completely, resulting in the presence of small loops within the membrane, which have important roles in anion coordination. A surprising feature emerging from the crystal structure was that each monomer presents an internal pseudo-symmetry: helices A-I assume a structure similar to that of helices J-R but with an inverted membrane orientation (210) **(FIGURE 3*C*)**. Similar inverted repeat topology architectures have been found in many classes of membrane transporters (262), and in most cases the substrate binding sites are located at the interaction face of the two repeats. Two anion binding sites could be identified in the WT structure, called S_{cen} and S_{int} **(FIGURE 4*A*)**. The ion bound at S_{cen} is completely buried in the protein, whereas the ion in S_{int} appears to be in direct contact with the intracellular solution. Access of the anion bound at S_{cen} to the extracellular solution is impeded by the presumably negatively charged side chain of E148 **(FIGURE 4*A*)** (E148 and the homologous residue in other CLCs is also called "gating glutamate"). In fact, in the crystal structure of the charge neutralizing mutant E148Q, a third anion was found to be bound at the position of the E148 side chain of the WT structure, defining a third anion binding site, S_{ext} **(FIGURE 4*B*)** (211). The glutamine side chain of Q148 was instead found to be oriented towards the extracellular solution. Interestingly, in E148Q crystals grown in fluoride, the Q148 side chain was instead found to occupy S_{ext}, as the gating glutamate in the WT structure, probably being stabilized by a fluoride ion bound in S_{cen} (469).

The CmClC crystal structure gave further insight into ion binding properties of CLC proteins. The transmembrane

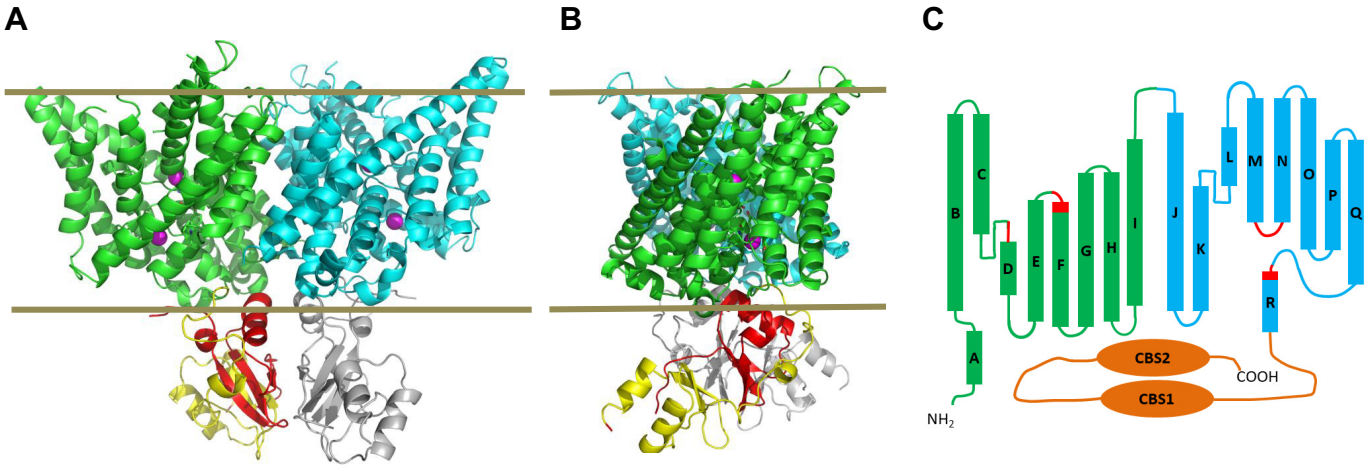

FIGURE 3. Structure and membrane topology of CmClC. *A* and *B*: the crystal structure of CmClC (pdb entry 3ORG) in a lateral view in cartoon representation with the approximate position of the membrane indicated by brown lines. The view in *B* is rotated by ~90° with respect to that of *A*. The membrane embedded parts of the two subunits are shown in light blue and green, respectively. The intracellular CBS domains are colored in yellow (CBS1) and red (CBS2) in one of the subunits and in gray for the other subunit. Bound chloride ions are shown as pink spheres. *C*: the complex toplogy of the CLC structure with the α-helices (A-R) shown as cylinders. The two halves of the transmembrane part of each subunit are differently colored. Partial positive charges in Cl^- binding regions are schematically shown in red. [Adapted from Dutzler et al. (210).]

part of the CmClC is very similar to that of EcClC-1 [main-chain root mean square deviation (RMSD) of 1.7 Å] (242). However, the amino acid side chain of the gating glutamate of CmClC occupies the S_{cen} binding site, whereas S_{ext} is occupied by an anion. The S_{int} site is occupied by an anion in CmClC as found in EcClC-1 **(FIGURE 4*C*)**.

The crystallized prokaryotic CLCs lack the extended cytosolic COOH-terminal domain present in eukaryotic CLC proteins. Based on sequence analysis, Bateman (49) and Ponting (665) found that the COOH termini of mammalian CLC proteins harbor two so-called CBS domains (from cystathionine-β-synthase). CBS domains are found in many different proteins and are usually not involved in the main protein function but are rather believed to exert a modulatory role. In general, as in CLCs, CBS domains are organized in pairs that dimerize to form a stable globular domain (365). Isolated COOH-terminal fragments containing

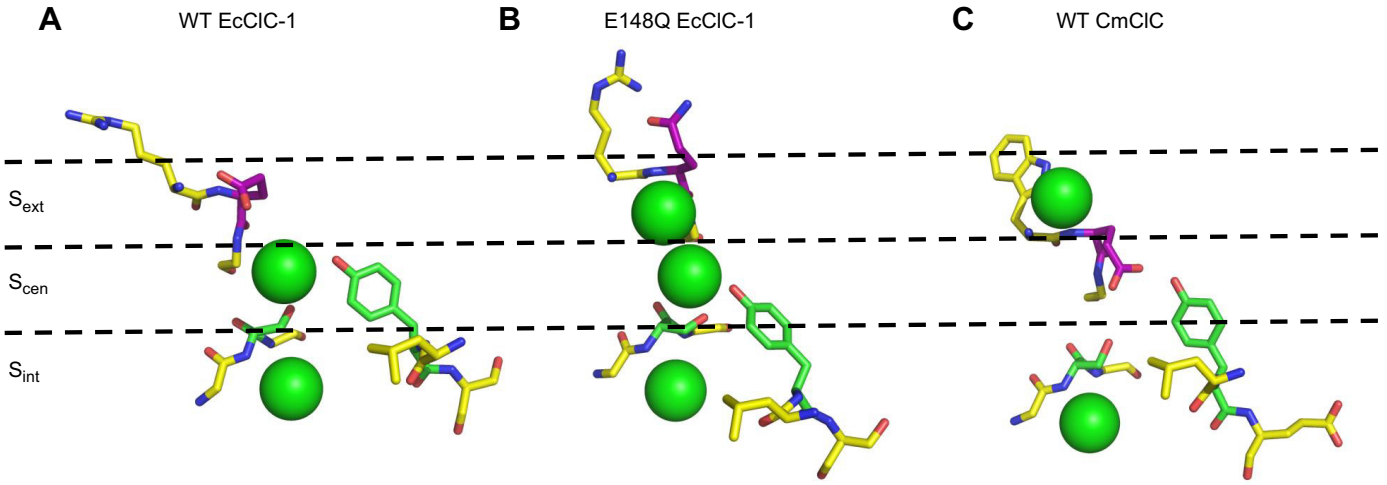

FIGURE 4. The Cl^- transport pathway and Cl^- binding sites. Key amino acids involved in gating and anion selectivity and pore-bound Cl^- ions are shown for three different crystal structures that are assumed to represent different conformations during the transport cycle of CLC exchangers. *A*: WT EcClC-1 (pdb entry 1OTS). *B*: mutant E148Q of EcClC-1 (pdb entry 1OTU). *C*: WT CmClC (pdb entry 3ORG). Positions of anion binding sites are indicated by dashed lines. The gating glutamate (and Q148 in *B*) is shown in red stick. The pore serine (S107 in EcClC-1) and the pore tyrosine (Y445 in EcClC-1) are shown in green stick. The external site is occupied by the side chain of the gating glutamate in *A*, and by a Cl^- ion in *B* and *C*. The side chain of the gating glutamate points to the outside in *B* and occupies S_{cen} in *C*.

the CBS domains have been crystallized from ClC-0, ClC-Ka, and ClC-5 (526, 541, 542). As in other proteins, CBS1 and CBS2 form a sandwich structure via their beta strands, with an adenine nucleotide bound between the two domains in the fragment of ClC-5, but not in those of ClC-Ka or ClC-0. However, the relative orientation of the CBS-domain pairs with regard to the membrane embedded part remained unclear. This question was answered by the crystallization of a eukaryotic CBS domain-containing CLC from the thermophilic red alga *Cyanidioschyzon merolae*, called CmClC (242) and recently in the cryo-EM structure of the bovine ClC-K homologue (628). As illustrated in **FIGURE 3**, in CmClC, the CBS domains form a similar sandwich structure as in the isolated fragments. Interestingly, CBS1 is relatively far away from the membrane domain, whereas CBS2 is in close contact with the membrane part. Overall, the cytosolic, COOH-terminal part of the proteins interacts with the membrane part involving an interacting area of ~2,300 Å^2 (242). The organization of the CBS domains is very similar in the ClC-K structure, but their orientation relative to the transmembrane part is rotated by ~20 degrees compared with the CmClC structure (628).

Several studies have addressed the role of the CBS domains in CLC proteins by deletion and transplantation assays and expression of "split" constructs (223, 259, 280, 332, 356, 505, 512, 560, 749, 813). Depending on the channel/transporter and on the precise location of deletions, divergent results regarding the effect on channel function have been reported. There is ample evidence that the COOH terminus, including the CBS domains, is involved in the common gate mechanisms of ClC-0 and ClC-1 (93, 223, 259, 512). However, the specific roles of CBS1 or CBS2 or the various linker regions are difficult to nail down because any alteration of the COOH terminus by mutagenesis, and in particular employing deletions or chimeric constructs, is expected to cause non-local structural changes. This problem is profound if the crystal structure of CmClC is applicable to other CLCs as well. In this structure, the COOH terminus, including the CBS domains, interacts with the membrane-embedded part of the proteins through an extensive interface of 3,600 Å^2 with a large shape similarity "similar to an antibody-antigen interface" (242). In light of this, it is actually very surprising that in several cases in-frame deletions of single or even both CBS domains were functionally tolerated with sometimes only relatively mild consequences (223, 280, 332, 813). Also the large physical separation (by ~20 Å) of the COOH termini of the ClC-0 dimer upon slow gate opening reported by Bykova et al. (93) is surprising if the COOH terminus is so tightly bound to the membrane embedded part. CBS domains have also been proposed to be important for for correct trafficking of ClC-5 to endosomes and of the yeast CLC to the Golgi, respectively (107, 760). However, unspecific effects caused by structural alterations cannot be easily excluded. The COOH terminus of ClC-1 contains a unique proline-rich region downstream of CBS2, in which point mutations cause myotonia by altering the common gate and which might form a poly-proline helix (507). It will be interesting to obtain direct structural insight on how this putative helix interacts with the rest of the protein.

The interaction of the COOH-terminal domains with the transmembrane part has been studied rather extensively by Strange (816) in the CeClC-3 homologue from *C. elegans*, as discussed in more detail below. Activity of this channel is regulated by the phosphorylation of serine residues in the linker connecting CBS1 and CBS2, and it has been proposed that the phosphorylation status is communicated via CBS2 to the transmembrane helices H and I, which are presumably close to CBS2 (816).

An exciting finding was that CBS domain pairs from a variety of proteins including AMP-activated protein kinase, IMP dehydrogenase-2, ClC-2, ClC-5, and CBS itself bind AMP, ATP, and other adenine nucleotides, suggesting that CBS domains serve as sensors of the cellular energy status (763, 898). No nucleotides were found in X-ray structures of COOH-terminal fragments from ClC-0 and ClC-Ka and the full-length structures of CmClC and ClC-K (242, 526, 541, 628), but ATP or ADP molecules were tightly bound between the two CBS domains in crystal structures of the isolated COOH-terminal fragment from ClC-5 (542). For ClC-1, mutant cycle analysis, in combination with a homology model based on the ClC-5 CBS domain structure, confirmed that the mode of nucleotide binding in ClC-1 is very similar to that in ClC-5 (842). Functional studies confirmed a regulatory role of nucleotide binding for ClC-1 and ClC-5 (55, 57, 58, 841, 968). The physiological role of nucleotide regulation, however, remains unclear, since all adenine nucleotides are almost equally effective, and their summated cellular concentration is generally in the millimolar range.

In summary, CBS domains are clearly important for CLC function, highlighted also by the numerous mutations found in the COOH termini of ClC-1, ClC-Kb, ClC-5, and ClC-7 causing diseases. In ClC-1, several myotonia causing mutations in the COOH terminus lead to a shift of the common gate to more positive potentials (51, 89, 507, 535). Interestingly, in the lysosomal ClC-7 transporter, some COOH-terminal mutations actually cause a gain-of-function effect in that the opening kinetics are significantly faster than in WT (453), probably acting via the common gate of the dimer. However, intracellular ATP had no effect on ClC-7-mediated currents (453). In general, the physiological relevance of nucleotide binding to the CBS domains of CLC proteins is far from being understood. *Knock in* mice (or other organisms) carrying mutations that abrogate nucleotide binding might help to uncover potential physiological roles of nucleotide regulation.

At the time of the publication of the EcClC-1 crystal structures (210, 211), only rudimentary knowledge of the functional properties of the protein was available (375, 511). It was however implicitly assumed that EcClC-1 is a Cl^- channel because it showed anion transport activity in a reconstituted system with a $Cl^- > I^-$ preference (511), typical of CLC channels (389, 673). In addition, EcClC-1 was found to be dramatically activated by acidic pH (375). It was found only later, in the breakthrough study of Accardi and Miller (5), that EcClC-1 is actually a secondary active, strictly coupled and highly electrogenic $2Cl^-/1H^+$ antiporter, as described in detail below. Furthermore, because of the low overall sequence identity of EcClC-1 with mammalian CLCs (<20%), it was unclear if the structure was representative for other CLCs. However, several lines of evidence supported the relevance of the EcClC-1 structure for mammalian CLCs. First of all, in the EcClC-1 and also in CmClC crystal structures, the ion binding sites are formed by four separate protein regions that are highly conserved in CLC proteins (210, 242) and that are located at the NH_2 terminus of various helices, including the GSGIP sequence of helix D, the G(K/R)EGP sequence of helix F, the GXFXP sequence of helix N, and a highly conserved tyrosine in helix R. Most of these regions had been identified in earlier work as being important for gating and permeation of ClC-0 and ClC-1 channels (227, 228, 231, 234, 470, 489, 492, 677, 806, 912). The above-mentioned helices are pointing their NH_2 terminus towards S_{cen}, potentially contributing to the stabilization of anion binding via the electrical helix dipole (210). However, several theoretical studies doubted a significant contribution of the helix dipole to the free energy of anion binding (142, 236). Interestingly, the bound anions are not directly coordinated by positively charged lysine or arginine residues but by side-chain hydroxyls (S107, Y445 in EcClC-1) and by main-chain amides (I356, F357 in EcClC-1). However, significant long-distance electrostatic interactions have been inferred to arise from the highly conserved K131 (helix E) that is pointing its positively charged side chain towards S_{cen}, but is shielded from it by amino acids from the loop connecting helices C and D and by the glycine residue following the gating glutamate (236). In support of a conserved role of this residue, Chen and colleagues (952) found that mutating the corresponding residue in ClC-0 had dramatic effects on ion conduction and gating. Several other studies, using the EcClC-1 structure as a guide for mutational analysis, fully confirmed the overall conservation of the CLC structure from bacteria to vertebrates (121, 219, 224, 471, 648, 691). A further, more extracellularly located Cl^- binding site had been postulated by theoretical studies (236). However, this binding site could not be confirmed experimentally by site-directed mutagenesis (952).

A puzzling feature of the available CLC crystal structures was that despite the presence of bound anions, no clear continuous aqueous permeation pathway for ions could be seen, different from to crystal structures of classical voltage-gated or ligand-gated ion channels (959a). In retrospect, such an "occluded state" with bound substrate shielded from either aqueous face is not surprising for the structure of a stoichiometrically coupled antiporter. To avoid slipping, coupled transporters must make sure that the substrates are not simultaneously accessible to both aqueous compartments (277). The centrally bound anion in EcClC-1 is completely buried in the protein. In particular, the passage towards the outside is impeded by the side chain of the gating glutamate (E148) that is occupying S_{ext}. Access of the anion bound at S_{cen} to the inside is impeded by the side chains of S107 and Y445 **(FIGURE 4)**, even though in several computational studies it has been suggested that local protein fluctuations could allow an efficient passage through this intracellular constriction (142, 929). However, this view was not shared by other authors (149, 552), and it is still disputed if Y445 constitutes a physical "gate" of the EcClC-1 transporter (1).

The recent cryo-EM structure of the bovine ClC-K homologue provided the first view of the structure of a CLC channel pore at ~3.8 Å resolution, even though no bound anions were identified (628). The overall architecture of the pore is very similar to the Cl^- ion translocation pathway of CLC exchangers. The side chain of V166, the corresponding residue of the gating glutamate, does not appear to obstruct the pathway towards the extracellular solution, pointing somewhat parallel to the channel wall, and the conserved tyrosine Y520 (corresponding to Y445 of EcClC-1) is similarly positioned, probably interacting with pore transiting Cl^- (628). The major difference in the pore structure, compared with CLC exchangers, regards the conformation of the loop connecting helices C and D which results in a rotation of the side-chain orientation of the conserved S121 (corresponding to S107 of EcClC-1). The different conformation of the loop C-D reshapes the internal vestibule such that the side chain of S121 points away from the pore. This configuration frees the ion passage between the pore and the intracellular solution, with an estimated pore radius at the intracellular constriction of around 1.7 Å, significantly wider than in CLC exchangers (628). In addition, in ClC-K, the cytosolic vestibule is positively charged which could lead to a local increase in the concentration of Cl^- (628). It remains to be seen if this configuration is typical of all CLC channels, and it will be interesting to find out why mutations of the tyrosine residue in ClC-0 have little effect on ion conductance properties (7, 471), while mutations of the serine quite strongly affect ion conductance and selectivity (471, 492).

C. Conductance and Anion Selectivity of CLC Channels

The reconstituted *Torpedo* channel as well as the heterologously expressed ClC-0 have a linear single-channel cur-

rent-voltage relationship with a single pore conductance around 8–9 pS at "physiological" Cl^- concentrations (50, 492, 543, 548). It saturates at ~16 pS at high Cl^- concentrations with a half-maximal concentration of ~60–80 mM in a manner that is consistent with single pore occupancy (121, 904). However, anomalous mole fraction effects in anion mixtures indicate multiple ion occupancy in ClC-0 (677) as well as in ClC-1 (722) and ClC-2 (730). Noise analysis indicated that the single-channel conductance of ClC-1 is only 1–2 pS (at negative voltages) (678, 912). Single-channel recordings confirmed this result and demonstrated the double-barreled architecture of this channel as well (739). ClC-2 has a slightly larger protopore conductance of ~3 pS (595, 815, 897) (see **FIGURE 2*B***). ClC-K channels exhibit the largest protopore conductance values among all studied CLC channels ranging from ~15 to 22 pS for various isoforms (249, 293, 296, 441, 754). The Fahlke group reported that association with barttin altered the single-channel conductance of rat ClC-K1 (249, 754), an effect that was not seen in mouse ClC-K1 (441).

Several residues at the intracellular pore entry or in the intracellular part of the narrow pore region have been identified that lead to reductions of the ClC-0 single-channel conductance when mutated, including I515 and K519 of helix R (121, 127, 492, 543), S123 of helix D, the equivalent of which is coordinating the central chloride (Cl^-_{cen}) in the EcClC-1 structure (210, 492), E127 of helix D (121). These residues appear to exert an electrostatic control on the local intracellular Cl^- concentration (121, 127). Surprisingly, mutating the highly conserved Y512, equivalent to the Cl^- coordinating Y445 of EcClC-1, has only relatively small effects on single-channel conductance and ion selectivity (7, 121, 127, 224).

ClC-1 shows a unique feature among CLC channels in that its "instantaneous current voltage relationship," whose shape mirrors that of the single-channel current-voltage relationship, is extremely inwardly rectifying (678, 807): outward currents do hardly increase further for voltages above ~40 mV. The molecular basis for this rectification is still unknown. The mutation G230E, affecting the highly conserved glycine two residues upstream of the gating glutamate, appears to eliminate the rectification (227, 234), suggesting that structures in the external pore are involved. In agreement with this idea, a permeation model with a high-affinity Cl^- binding site very close to the outside was able to reproduce the rectifying phenotype (721).

CLC channels are practically impermeable to cations (905) (Pusch, unpublished result), even though a relative sodium permeability as large as 0.1 has been reported for ClC-1 (234). Such a large Na^+ permeability is, however, very unlikely because it would be disastrous for the excitability of skeletal muscle. Among halides, CLC channels generally exhibit a $Cl^- \geq Br^- > I^-$ selectivity sequence with iodide actually leading to channel block (222, 489, 677, 722, 806, 832, 869, 904). Large organic anions like cyclamate and glutamate are almost completely impermeable, SCN^- and ClO_4^- block ClC-0 (490, 904), whereas NO_3^- is relatively permeable (677). The conductance of ClC-0 exhibits an anomalous mole fraction effect in Cl^-/NO_3^- mixtures, indicating that two anions can be simultaneously present in the pore (677). Similar results have been obtained for ClC-2, which shows anomalous mole-fraction effects in SCN^-/Cl^- mixtures (730).

Permeability has been extensively studied for ClC-1 resulting in the following permeability sequence based on reversal potential measurements: $SCN^- \sim ClO_4^- > Cl^- > Br^- > NO_3^- \sim ClO_3^- > I^- >> BrO_3^- > HCO_3^- >>$ methanesulfonate ~ cyclamate ~ glutamate (722). The minimum pore diameter was estimated to be ~4.5 Å, and anomalous mole fraction effects were found for mixtures of Cl^-/SCN^- and Cl^-/ClO_4^-, suggesting a multi-ion pore (722). Surprisingly, small organic acids showed a significant permeability [Cl^- (1) > benzoate (0.15) > hexanoate (0.12) > butyrate (0.09) > propionate (0.047) ~ formate (0.046)] (721), showing that ClC-1 is more permeable to larger hydrophic anions than to smaller less hydrophobic one. A paradoxical block of inward currents by these organic acids applied from the outside could be accounted for by a rate constant model that explained both the strong rectification of ClC-1 and the block of inward currents induced by these acids by a high-affinity superficial anion binding site (721). The pore diameter of the bovine ClC-K homologue at the narrowest point was found to be ~3.4 Å based on a cryo-EM structure (628), substantially smaller than the size estimated from the permeability ratios. Possibly, organic anions interact with the pore in a dynamic manner, which is not easy to capture in a static structure.

Interestingly, also intracellularly applied benzoate blocked ClC-1 in a voltage-dependent manner, in a complex interplay with ClC-1 gating, which will be described in a separate paragraph (721).

D. Interaction of Gating and Permeation of the Prototype *Torpedo* ClC-0 Channel

At the single-channel level, the double-barreled ClC-0 exhibits two qualitatively distinct mechanisms of gating (see **FIGURE 2**). Within a burst, the two protopores fluctuate between open and closed states with relatively fast kinetics (ms time range). This gating mechanism is called "fast" or "protopore" gate. In contrast, burst lengths and interburst durations are much longer, and the mechanism underlying this gating is called slow gate or common gate. Miller and colleagues (324, 548, 549) found that within bursts the protopore dwell time distributions are single exponential and thus the fast gate of a single protopore can be phenomenologically extremely well described by a two-state system

$$C \underset{\beta}{\overset{\alpha}{\rightleftarrows}} O$$

with opening rate constant α, closing rate constant β, and open probability $p_{open} = \alpha/(\alpha + \beta)$. At positive voltages, p_{open} reaches practically unity, and the voltage dependence of the open probability can be roughly approximated by a Boltzmann distribution with an apparent gating valence of ~1 elementary charge and a voltage of half-maximal activation depending strongly on pH (324). In contrast, the slow gate shows an inverted voltage dependence, opening at negative voltages (550, 905)). Pusch et al. (677) discovered that the open probability of the fast gate of ClC-0 strongly depends on the extracellular Cl^- concentration. Decreasing extracellular Cl^- concentration ($[Cl^-]_o$) reduced p_{open} by "shifting" the voltage dependence to more positive voltages. Pusch et al. (677) postulated that voltage-dependent binding of extracellular Cl^- opens the fast gate, resulting in a channel that is opened by the transported substrate. This simple model provides an explanation for the fact that the apparent gating charge of the fast gate is ~1 elementary charge. Furthermore, the voltage dependence of the open probability in mixtures of NO_3^- and Cl^- showed an anomalous mole fraction effect, in parallel to an anomalous mole fraction effect of conduction (677). Anomalous mole fraction effects are considered as good evidence for the presence and the interaction of more than one ion in the pore of an ion channel (343). Thus these findings strongly support the conclusion of a tight coupling of permeation with gating. Chen and Miller (128) investigated the Cl^- dependence of fast gating at the single-channel level, dissecting effects on the opening and on the closing rate constants, α and β. Interestingly, they found that $[Cl^-]_o$ only affects α, with almost no effect on β. In addition, α showed a biphasic dependence on voltage, increasing exponentially at positive voltage with a slope corresponding to 0.6 elementary charges. Surprisingly, at negative voltages, both α and β increase with more negative voltage, roughly in parallel, resulting in a non-zero open probability (P_{min}) at negative voltages (128). P_{min} depends mostly on $[Cl^-]_i$ via the closing rate constant, in an apparent "foot-in-the-door" mechanism (124, 127, 128, 489). P_{min} is also significantly influenced by mutation at the intracellular pore entrance. For example, mutants of lysine 519 (now known to be located at the end of helix R) dramatically increase P_{min} (489, 677), probably by influencing the ability of $[Cl^-]_i$ to stabilize the open state. Chen and Miller (128) also found that the effect of $[Cl^-]_o$ on the opening rate α saturated with an apparent K_D of roughly 50 mM. From their studies, Chen and Miller (128) concluded that, in contrast to the original hypothesis that voltage-dependent binding to the pore confers the voltage-dependence of gating (677), Cl^- binds in a voltage-independent manner to a superficial site. Opening is, however, coupled to Cl^- permeation in subsequent voltage-dependent translocation step (128, 669). A further detailed analysis of the $[Cl^-]_o$ dependence of fast gating was performed by Engh and Maduke (218), who found that their data but also the data of Chen and Miller (128) are actually more compatible with the idea that voltage-dependent binding of extracellular Cl^- leads to fast gate opening (218) as in the original proposal (677).

The dependence of the fast gate on intracellular Cl^- and on amino acid residues at the intracellular pore entrance has been studied in great detail by Chen et al. (127). As a general rule, similar to $[Cl^-]_i$ itself, also mutations at the intracellular end of the pore mostly affect gating by altering the closing rate constant with litte effect on the opening rate constant, via an electrostatic control of Cl^- passage between the cytoplasmic solution and the deeper pore.

The crystal structures of EcClC-1 provided important insight into possible molecular mechanisms underlying the Cl^- dependence of fast gating (210, 211). Mutating E148 in EcClC-1 to glutamine "freed" the external anion binding site to be occupied by a third Cl^- **(FIGURE 4)**. The analogous mutations in ClC-0 (E166Q, E166A) led to constitutively open, voltage-independent channels (211, 838). This simple result pointed to E166 of ClC-0 as the essential structural part of the fast gate (hence the name "gating glutamate"). Furthermore, Dutzler et al. (209, 211) found, in agreement with Chen and Chen (120), that extracellular acidification led to large increase of the open probability of WT ClC-0. This was interpreted as being caused by a protonation of the gating glutamate from the outside, resulting in a structure mimicking the E166Q mutant, with the side chain of the gating glutamate moving out of the permeation pathway. Thus a simple negatively charged side chain obstructing the pore in the closed state, and being dislodged either by competition with permeating Cl^- or by protonation mediated neutralization to open the channel is a very attractive simple model for the protopore gating process.

However, the dependence of the fast gating process on voltage and intra- and extracellular pH (pH_o) and Cl^- concentration is complex, and several details are still not fully understood. Furthermore, some experimental results are difficult to reconcile with this simple picture. For example, using the small molecule blocker *p*-chloro-phenoxy acetic acid (CPA) as a tool, Accardi et al. (7) and Traverso et al. (838) concluded that fast gating is accompanied by conformational changes in addition to the simple side-chain movement of the gating glutamate. However, it cannot be excluded that the effects of the CPA blocker on gating were indirectly caused by effective alterations of local pH or Cl^- concentration. In this respect, it is interesting to note that the affinity of CPA and other small molecules, which act exclusively when applied from the intracellular side, strongly depends on the chemical nature of the side present at the place of the gating glutamate (838, 954). Mutating E166 in amino acids with small side chains (Ala, Gly) results in high-affinity block, whereas larger side chains result

in low-affinity block (954) even though practically all of these mutants have a completely open fast gate. Removing the side chain of the gating glutamate in mutant E166G allowed even the punch-through of small molecules like CPA through the pore of the channel (951). Thus these small molecules clearly interact with the side chain in position 166, which is relatively difficult to reconcile with the idea that the side chain is oriented towards the outside in the open mutants.

Among all studied mutants of the gating glutamate, E166D, in which the side chain is shortened by just one CH_2 group, has the most complicated effect (839). Using tandem-dimeric constructs with E166A, Traverso et al. (839) could demonstrate that this mutant has an extremely low open probability. Low pH_o induced an inward Cl^- current with a small single-channel conductance (deduced from noise analysis), and intracellular pH (pH_i) dependence indicated that the aspartate residue might be directly protonated from the inside (839).

The dependence of the protopore gate on pH_i had been investigated in early studies by Hanke and Miller (324) who found that acidification activated the fast gate. They could describe their data by an allosteric effect involving the protonation of an amino acid side chain that changes its p*K* from 6 to 9 upon protopore opening (324). In an extensive mutagenic screen, Zifarelli et al. (963) could not identify such an allosteric pH sensor. An attractive idea was that the proton glutamate could be directly protonated from the intracellular side leading to pH_i-dependent opening. The mechanism underlying such a direct protonation could be related to the Cl^-/H^+ antiport activity of EcClC-1 and has been dubbed the "broken antiporter hypothesis of gating" (546). However, this scenario would predict that the opening rate constant α, but less so the closing rate constant β depends on pH_i. In contrast to this prediction, Zifarelli et al. (963) found that only β is dependent on pH_i, whereas α is practically independent of pH_i. To explain this discrepancy, Zifarelli et al. (963) hypothesized that the protonation of the gating glutamate does not occur directly from a "free" proton, but stems from the dissociation of a water molecule into OH^- and H^+. Fast water dissociation reactions have been described also in other enzymes like carbonic anhydrase with rates up to 10^6 s^{-1} (474). The dissociation could in fact be favored by the stabilization of the OH^- in one of the anion binding sites. This model could explain an essentially pH-independent protonation rate and was in quantitative agreement with various other observations (963). It would be important to obtain more direct evidence for this mechanism, and it is unclear if it has any relevance for proton transfer in CLC Cl^-/H^+ antiporters.

In short summary, the fast gate of ClC-0 appears to involve mostly the displacement of the gating glutamate side chain from its blocking position. This somehow requires a synergistic action of Cl^- and protons, the movement of which from the aqueous solutions depends on voltage. Open questions are, for example, whether the gating glutamate has to be protonated before it can be displaced from its binding site, how much its own movement contributes to the voltage dependence of opening, and if it can reach the central anion binding site, as in the crystal structure of CmClC **(FIGURE 4)**. One remarkable aspect of fast gating is that despite all these various influences on fast gating, the time course of fast gate relaxations can be extremely well described by a single exponential function. This supports the hypothesis that the same major rate-limiting steps underlie fast gate opening and fast gate closing, respectively, under all conditions, which might be the movement of the side chain of the gating glutamate.

E. The Slow Gate of ClC-0

The common or slow gate of ClC-0 governs the appearance of the double-barreled bursts **(FIGURE 2)**. It acts on a much slower time scale than the fast gate and is activated by hyperpolarization, i.e., has an inverted voltage dependence compared with the fast gate (548, 550). Due to the very slow kinetics, in particular at positive voltages (676), the slow gate has been little studied in quantitative terms. Its voltage dependence can be relatively well studied using macroscopic current recordings and exploiting the vast difference in time scales of the two gates (259, 489, 492, 676). The gate does not close completely at positive voltages, resulting in a minimal open probability, $P_{min} > 0$. The voltage-dependent component that is activated by hyperpolarization can be phenomenologically described by a Boltzmann distribution with an apparent gating valence of ~2 elementary charges (259, 489, 676). At very negative voltages (less than about -140 mV), however, the open probability tends to decrease again, a phenomenon called hyperpolarization-induced current decrease (HICD) (259).

By definition, the slow gate acts simultaneously on both pores of the double-barreled channel. In agreement with complex structural rearrangements associated with slow gating, the kinetics of slow gate closure show a very large temperature dependence with a Q_{10} ~40 (676). Furthermore, properties of slow gating are altered by mutations in many protein regions, including the inner selectivity filter [e.g., S123 (492) and Y512 (54)], helix R and the region between helix R and CBS1 (489), the COOH terminus in general (223, 259, 507, 512), the intersubunit interface (933), the gating glutamate and the conserved lysine preceding the gating glutamate (470, 839), helix G (472), and others. These widespread mutational effects are in accord with large-scale conformational changes during slow gating. Chen (125) discovered that extracellularly applied Zn^{2+} reversibly inhibits ClC-0 at micromolar concentrations by stabilizing the closed state of the common gate. In search of the Zn^{2+} binding site, Lin and Chen (472) mu-

tated all cysteine residues of ClC-0 and found that mutating C212 to serine or alanine completely abolished the slow gate, locking it in a permanently open state. Additionally, the C212S mutant was almost completely insensitive to Zn^{2+} (125). However, because of the abolition of the slow gate, it could not be concluded that C212 is directly involved in Zn^{2+} binding. In fact, the corresponding residue of EcClC-1, A188, located at the COOH-terminal end of helix G, is not directly accessible from the extracellular solution. Thus the extracellular Zn^{2+} binding site of ClC-0 is still unknown. The fast gate of C212S is practically indistinguishable from that of WT ClC-0 (472), and the mutant serves as a simpler model system to study the fast gate in isolation (472).

Similar to ClC-0, all mammalian CLC channels (ClC-1, ClC-2, ClC-Ka, ClC-Kb) are inhibited by extracellular Zn^{2+} and/or Cd^{2+} (139, 294, 438, 719). For ClC-1 it has been shown that Zn^{2+}/Cd^{2+} binding stabilizes the closed state of the common gate and possibly induces a deeply inactivated state that is normally not present (125, 206). A characteristic feature of ClC-2 is its rather high sensitivity to extracellularly applied Cd^{2+} and Zn^{2+} (139), which has helped to identify endogenous Cl^- currents as being carried by ClC-2. The mechanism of Cd^{2+} and Zn^{2+} inhibition is probably similar to that of ClC-0 and ClC-1, i.e., binding of these divalent cations stabilizes the closed state of the common gate (971). Zn^{2+} binding sites in proteins involve histidine, cysteine, or acidic residues. Kürz et al. (439) mutated several histidine and cysteine residues in ClC-1 and found that the triple mutant C242A/C254A/C546A had a drastically reduced Zn^{2+} sensitivity. However, these residues are not close to each other in 3D and C242 and C254 are not exposed to the outside. Another interesting cysteine residue that is conserved among ClC-0, ClC-1, and ClC-2 has been indirectly implicated in Zn^{2+}/Cd^{2+} binding: mutating C212 in ClC-0, C277S in ClC-1, or C256 in ClC-2 drastically reduces Zn^{2+}/Cd^{2+} sensibility (206, 472, 971). However, these mutations lead also to a dramatic stabilization of the open state of the common gate (2, 472, 971). Thus the reduced Zn^{2+}/Cd^{2+} block seen with these mutations is probably caused indirectly. This is also supported by the finding that other mutations, e.g., in the COOH terminus, that activate the common gate, are less sensitive to Zn^{2+} (223). Furthermore, the conserved cysteine residue (C212 in ClC-0), even though located at the extracellular end of helix G, does not appear to be directly accessible to the external solution (210), and it is not conserved in ClC-K channels, which are equally sensitive to Zn^{2+} (294). Recently, also intracellular Cd^{2+} binding in ClC-0 was found to modulate the common gate via a binding site close to the subunit interface (933).

The presence of large conformational changes associated with slow gating has been experimentally tested using FRET of COOH-terminally fused fluorescent proteins (93). Maneuvers predicted to perturb slow gate opening were associated with FRET changes corresponding to a separation of the COOH-terminally fused GFP tags on the order of 20 Å (93). This finding is in agreement with the fact that mutations in many part of the COOH terminus affect slow gating (223, 259, 507, 512). However, it is unclear if these inferred conformational changes of the COOH termini are causally involved in the slow gate, i.e., if the "gate" is constituted by a COOH-terminal structure, or if these conformational changes are secondary to gate-opening conformational changes of the transmembrane part of the protein. Furthermore, large conformational changes of the COOH termini are surprising in light of the CmClC crystal structure, in which the COOH terminus forms an extended interface with the transmembrane part (242).

The slow gate is also markedly dependent on the extracellular and intracellular Cl^- concentrations, with low concentrations favoring the closure of the slow gate (128, 674). This hints to a strong coupling of slow gating to the pore occupancy by anions. Complex interactions of the slow gate with ion pore occupancy has been described for mutant T484S, located at the extracellular end of helix P: the mutant is characterized by an inwardly rectifying phenotype in normal extracellular Cl^- solutions, but extracellular ClO_4^-, which blocks WT ClC-0, partially recovers the fast gate deactivating currents, probably by stabilizing the slow gate in an open confirmation (490). Furthermore, charge neutralizing mutations of the gating glutamate (e.g., E166A) lock the slow gate in an open state (839). Also the charge preserving mutation E166D eliminates slow gating transitions (839). Interestingly, heteromeric WT/E166A or WT/E166D ClC-0 channels partially recover slow gating transitions (839). On the contrary, charge neutralization of the conserved lysine K165, a residue that points its side chain in the extracellular pore just above the gating glutamate (210), locks the slow gate completely shut (470). Modifying K165C channels with positively charged cysteine reactive probes recovers channel activity, and heteromeric WT/K165C showed only one pore in single-channel recordings (470). In light of these findings, the reported hyperpolarization activation exhibited by the charge conserving mutation K165R (490) is most likely caused by a dramatic destabilization of the slow gate open state. In agreement with this, combining the slow gate activating mutation C212S with K165R (double mutant K165R/C212S) leads to a channel with almost WT like behavior (Pusch, unpublished observation).

A further pore residue that has been implicated in slow gating only recently is Y512, one of the two residues in the inner selectivity filter of EcClC-1 (210). Mutating Y512 to Ala, Phe, or His locked the slow gate open similar to mutations of C212 or E166 (54). These results were interpreted in the framework of a possible direct hydrogen bond interaction between Y512 and the gating glutamate with its side

chain in the S_{cen} position as in the CmClC structure (54). However, it has not been noted that the analogous mutation in ClC-Ka, Y520A, caused a similar dramatic increase of the open probability (296). Since ClC-K channels lack the gating glutamate, carrying instead a valine residue (415, 869) at the equivalent position, the interaction proposed by Bennetts et al. (54) is not possible in this case. Thus a different mechanism underlying the activation of the common gate by the tyrosine mutations needs to be considered also for ClC-0 and ClC-1.

In summary, there is an obvious link of pore ion occupancy with slow gating. In addition, as shown by Lisal and Maduke (478), the irreversible gating transitions manifested by time-asymmetric bursting kinetics is coupled to the transmembrane pH gradient. These findings suggest that CLC channels are degraded anion/proton exchangers, in which certain mechanisms important for exchange are "used" as modifiers of gating. Nevertheless, we are still lacking a clue on the essential conformational changes associated with the slow gating process. A conformational change associated with a relative rearrangement of the two monomers of a CLC channel was suggested by the presence of two structural classes present in the single particle images used to obtain the cryo-EM structure of the bovine ClC-K channel (628). The two classes differed by a movement of the two transmembrane domains with a ~6 degrees tilt relative to each other, involving a quite substantial difference in the subunit interface (628). It will be interesting to explore if this conformational difference is related to the common gate of CLC proteins.

F. The Transport Mechanisms of CLC Cl^-/H^+ Exchangers

It was a breakthrough discovery of Accardi and Miller (5) that the bacterial homologue EcClC-1 is not a passive Cl^- channel, but a secondary active, strictly coupled 2:1 Cl^-/H^+ antiporter. This finding has dramatically changed our view of CLC proteins in general. In particular, it was subsequently found that all intracellular mammalian CLCs, i.e., ClC-3 through ClC-7, and several plant CLCs are actually anion proton antiporters (164, 316, 453, 576, 651, 742), whose physiological functions we are only beginning to fully understand. The biophysical mechanisms of the Cl^-/H^+ exchange are best understood for the *E. coli* homolog, which serves as an important model for the eukaryotic CLCs as well.

Accardi et al. (3) succeeded in producing extremely pure EcClC-1 at high yield, allowing the reconstitution of large amounts of the protein into planar lipid bilayers without significant contamination. Careful analysis of electrophysiological experiments in various Cl^- and pH gradients clearly excluded a passive anion permeability and demonstrated that EcClC-1 is a strictly coupled 2:1 Cl^-/H^+ antiporter (5). Flux measurements demonstrated that EcClC-1 is able to transport Cl^- or protons against their respective electrochemical gradient exploiting the gradient of the other substrate, a hallmark of secondary active transport (5). The tight 2:1 coupling was confirmed directly using H^+ flux measurements at different imposed voltages (583), and the same 2:1 stoichiometry was found for the human ClC-5 (966), human ClC-7 (453), plant CLCs (164), other prokaryotic CLCs (379, 645), and the red algal CmClC (242), demonstrating that the basic mechanism of coupling and transport is conserved in these evolutionary divergent antiporters. Quite surprisingly, a clade of distantly related CLC proteins from several bacteria called CLC^F proteins are fluoride/proton antiporters with a 1:1 stoichiometry (78, 811). However, the sequence of these CLC^F proteins is quite distinct from that of mammalian CLCs and of EcClC-1 in the core anion binding regions.

In retrospect, the fact that EcClC-1 is a transporter and not a channel is not surprising considering the crystal structure of the protein (210, 211). Contrasting with K^+ channel structures, no open aqueous diffusion pathway for Cl^- can be seen in EcClC-1. The centrally bound Cl^- is completely buried in the protein. Its access to the outside is impeded by the side chain of the gating glutamate E148, whereas it is shielded from the inside by the side chains of S107 and Y445. In fact, these three amino acids appear to play the most important roles in determining anion selectivity and gating of both CLC channels and CLC transporters.

Since coupled transport requires concerted conformational rearrangements in response to substrate binding and unbinding, the turnover rate of transporters is generally much smaller than that of ion channels (545, 546). Using the "Cl^- dump assay," reconstituting EcClC-1 at low density in proteoliposomes, a turnover of ~2,000 s^{-1} at 0 mV (with valinomycin in symmetrical K^+) in a 300 mM: 1 mM Cl^- concentration gradient at pH 4.5 was determined (378, 870). This is a small number compared even to the low conductance ClC-1 Cl^- channel, whose single-channel conductance of ~1.5 pS (739) corresponds to a movement of 10^6 ions/s at −100 mV, but is large in the transporter world (546). No direct turnover measurements have been reported for animal or plant CLC exchangers but indirect noise analysis indicated an extremely fast turnover of ~10^5 s^{-1} at 100 mV for ClC-5 (941, 966, 967) and ClC-4 (334). However, the latter estimate has been obtained with iodide in the intracellular solution, limiting its relevance for coupled Cl^-/H^+ exchange, because the coupling efficiency is critically dependent on the anion species (583, 941). In any case, it is highly desirable to achieve direct estimates of the turnover rate of these mammalian CLC transporters. High turnover is, however, not a defining characteristic of CLC transporters. For example, homologues from cyanobacteria or from *Citrobacter koseri* exhibit a turnover of only ~20 s^{-1} (379, 645).

Without doubt, the most fundamental role in coupled CLC anion/proton exchange is played by the gating glutamate, E148 in EcClC-1, which blocks the communication of the central Cl^- ion with the extracellular bulk solution (210, 211). Neutralizing the gating glutamate by mutation to alanine, glutamine or serine completely abolishes H^+ transport, resulting in a passive Cl^- transport activity (5). The same uncoupling is seen in eukaryotic CLC transporters (60, 453, 576, 651, 742). As discussed above, in several CLC channels, the equivalent neutralization of the gating glutamate results in an almost constitutive activation (211, 224, 588, 838). Interestingly, neutralization of the gating glutamate does not increase the throughput of Cl^-, but rather slightly decreases it in EcClC-1 (378), and it reduces currents also in ClC-5 (941). In fact, a structure distinct from the available crystal structures corresponding to an outward facing open state has been inferred from NMR studies, in which the narrow constriction between S_{ext} and the extracellular solution is widened transiently, suggesting that a small conformational change above S_{ext} is involved in the transport cycle (412). In CLC channels, the pore conductance is not significantly altered by mutations of the gating glutamate (211, 838, 954). Quite surprisingly, the recent cryo-EM structure of the bovine ClC-K homologue revealed that the ion pore is very similar to that of the transporter homologues in the vicinity of the position of the gating glutamate (which is a valine in the bovine ClC-K) (628).

Also mutations of the inner tyrosine residue, Y445, that is part of the constriction towards the inside do not dramatically alter Cl^- transport rates in EcClC-1 (378). At difference to the gating glutamate, mutations of Y445 drastically reduce but do not abolish H^+ transport (4). The simultaneous mutation of E148 and Y445 to alanine dramatically increases Cl^- throughput to ~20,000 s^{-1} (378). This result strongly favors the idea that two "gates" are involved in CLC transport: The extracellular gate is constituted by E148, whereas the intracellular gate is formed in part by Y445. Only removal of both gates allows fast diffusion of Cl^- through the permeation pathway. However, even these "opened" mutants do not present a large hydrated pore, but only a very narrow passage, even of smaller dimensions than a Cl^-, predicting that protein structure fluctuations must help in allowing Cl^- movement. In fact, so far, the crystal structures reported for practically all mutants of EcClC-1 are almost superimposable on the WT structure, except at the site of mutations (4, 9, 47, 211, 467–469, 482, 582, 583, 705).

Interestingly however, in the crystal structure of the uncoupled mutant Y445A, no Cl^- were found bound to the S_{cen} site, and the partially uncoupled mutation Y445L showed intermediate Cl^- occupancy (4). This suggested a correlation of Cl^-/H^+ flux coupling and the ion occupancy of S_{cen}. Such a correlation of anion binding with flux coupling was strengthened by the finding that H^+ transport coupling is practically absent if Cl^- is substituted by the polyatomic anions SCN^- and $SeCN^-$ and that the occupancy of S_{cen} in crystals grown in the presence of these anions correlated with the degree of uncoupling (583). NO_3^- had a similar but smaller effect on uncoupling. Similar uncoupling of H^+ transport in SCN^- and NO_3^- was seen in ClC-5 (941) and ClC-4 (22). The phenomenon of uncoupling in the Y445 mutants and in SCN^- probably reflects a "slippage" of the transport. The mechanism underlying this uncoupling, however, remains largely unknown. One possibility is that anion occupancy of S_{cen} electrostatically favors the H^+ passage from the proton glutamate to the gating glutamate, probably via transient water wires (321, 396, 434, 957).

Further detailed information of Cl^- binding to the EcClC-1 protein was provided by crystallography and isothermal titration calorimetry (ITC) (482, 650). Crystallographic analysis indicated that all three anion binding sites (S_{int}, S_{cen}, S_{ext}) can be occupied simultaneously with millimolar affinity (482). A major advancement was achieved by Picollo et al. (650), who measured thermodynamically well-defined equilibrium Cl^- binding affinities using ITC on detergent solubilized purified WT and mutant EcClC-1 proteins. The WT protein was found to bind Cl^- with an affinity of ~1 mM, probably reflecting the affinity of the central site, with the external site occupied by the negatively charged side chain of the gating glutamate (650). To correlate this equilibrium binding binding affinity with chloride binding during the transport cycle, Picollo et al. (650) determined the half-maximal "trans" chloride concentration that was necessary to reduce the transport rate in a large Cl^- gradient and found a value of the same order of magnitude of 1 mM. This result supported the relevance of the equilibrium binding affinities for the transport mechanism (650). Eliminating the putative inner gate in the mutant Y445A, in which Cl^- binding to S_{cen} was absent in crystal structures (4), almost completely abolished Cl^- binding also in ITC experiments (650). Very surprisingly, the E148A mutant, which lacks the gating glutamate, exhibited high-affinity Cl^- binding to two sites with an affinity of 12 μM, despite their spatial proximity (650). While a definite explanation for the high affinity is still lacking, tight binding of Cl^- in the E148A mutant may underlie its rather slow Cl^- transport rate (378).

Two residues form the constriction of the Cl^- pathway between S_{cen} and the intracellular solution: Y445 and S107. However, these two residues play clearly different roles. While mutations of the tyrosine affect Cl^- binding and transport coupling in EcClC-1 and slow gating in CLC channels (4, 54, 296), surprisingly the ion selectivity and turnover/single-channel conductance of tyrosine mutations is not much different from that of the respective WT proteins (7, 224, 870). In contrast, S107 and the respective residues in other CLCs are important for ion selectivity and

conductance. This was first shown for ClC-0 in which the quite conservative mutation S123T changes ion selectivity among halides and reduces the single-channel conductance to 1.5 pS (492). Interestingly, several plant homologues, which perform 2:1 NO_3^-/H^+ exchange and only poorly transport Cl^-, carry a proline residue at the corresponding position (164). The human ClC-5 exchanger could be converted to a NO_3^-/H^+ exchanger by simply substituting the serine by a proline residue, demonstrating the role of the serine/proline for ion selectivity in CLC exchangers (60, 966). Importantly, the NO_3^-/H^+ exchange was tightly coupled with 2:1 stoichiometry, and Cl^- was very poorly transported (966). The analogous mutation in EcClC-1 led to a loss of Cl^- binding and a significant increase in NO_3^- binding affinity assessed with ITC (650). Analogously, the reverse mutation in the plant AtClC-a homologue, P160S, leads to a loss of its NO_3^-/Cl^- selectivity (60, 893), and the mutant is not able to complement the defect in NO_3^- accumulation of AtClC-a knockout plants (893). Even in the ClC-0 channel, the S123P mutation increases NO_3^- permeability in the context of the gating glutamate neutralization mutant E166A (650). Surprisingly, the side chain of the corresponding serine was found to point away from the pore in the recent cryo-EM structure of the bovine ClC-K channel (628).

The potential involvement of the external binding site S_{ext} in ion selectivity in CLC exchangers or channels has been studied less extensively. Functional effects of mutations of the gating glutamate in CLC exchangers suggested that S_{ext} has no prominent role in anion selectivity (3, 269, 651, 941). In ClC-5, charge neutralizing mutations of the lysine residue that precedes the gating glutamate (K210) reversed the NO_3^- over Cl^- preference, but did not modify the H^+/anion coupling stoichiometry (179). Effects were however smaller at saturating anion concentrations, suggesting that K210 is critical for the association rate of extracellular anions to S_{ext} (179). Mutation of the equivalent lysine in ClC-1 has been reported to alter ion selectivity (234). However, these measurements are questionable because the mutant K210A is strongly inwardly rectifying and reversal potentials, which were measured in current clamp, are unreliable in such a condition.

While the Cl^- permeation pathway is clearly visible in the CLC crystal structures, protons are invisible in X-ray crystallography, and their transport pathway has been inferred indirectly from mutagenesis and theoretical studies. Related to this technical difficulty is the lack of a definite picture of the coupling mechanism, which will be discussed below. It is practically universally accepted that the gating glutamate is directly involved in proton transport from/to the extracellular solution in a protonation/deprotonation cycle, since its neutralization abolishes H^+ transport (5, 6, 211, 651, 742). In this picture, the coupling between Cl^- and H^+ transport involves the alternative occupation of S_{ext} and S_{cen} by Cl^- or by the negatively charged side chain of the gating glutamate. Even stronger evidence for this notion of competition of Cl^- and the glutamate side chain was obtained by Feng et al. (243) who could reconstitute H^+ transport in the E148A mutant by adding high concentrations of free glutamate or gluconate. This H^+ transport was blocked by submillimolar Cl^- (243) in agreement with the high Cl^- affinity of this mutant (650).

A more difficult question regards the pathway of H^+ between the gating glutamate and the intracellular solution. In a pioneering study, Accardi and co-workers (6, 9) identified E203 as the most likely intracellular proton acceptor of EcClC-1. For convenience, this residue is also called the "proton glutamate" (941). It is located in a highly conserved sequence stretch at the subunit interface at the end of helix H, close to the intracellular solution. It is preceded by another glutamate residue that is one of the most conserved residues in all CLC proteins. However, mutating E202 preserved coupled transport (9). Neutralizing the proton glutamate in the E203Q mutant resulted in a complete loss of proton transport, preserving however Cl^- transport at a rate about threefold slower than WT (9, 467), and showing Cl^- binding affinities similar to WT in ITC experiments (467). Also, the crystal structure of the E203Q mutant was almost identical to that of WT EcClC-1, except at the site of mutation (9). These results suggested divergent pathways for Cl^- and H^+ to or from the intracellular solution: Cl^- ions enter via S_{int}, whereas protons enter through a lateral pathway via the proton glutamate (9). The preservation of Cl^- transport in a mutation that presumably blocks the binding of one of the substrates is counterintuitive for a classical "ping-pong" antiporter mechanism, and is one of many signs that the coupling mechanism in CLC transporters is rather unique. More in line with a classical coupling mechanism, equivalent mutations of the proton glutamate in ClC-5 (E268Q, E268A) completely inhibit steady-state transport of Cl^- and protons (941). Interestingly, the E268A mutant in ClC-5 gives rise to transient, "pre-steady-state" currents upon voltage steps (788), which will be discussed in more detail below. For ClC-5 it was also found that mutating the proton glutamate to some other titratable residues including Asp and His allowed coupled Cl^-/H^+ exchange (941), a finding extended later to EcClC-1 (467).

All known CLC channels carry a nontitratable residue at the position of the proton glutamate (9), even though introducing a glutamate residue in the CLC channels is not sufficient to confer H^+ transport activity but rather alters gating characteristics (941). It was thus believed that a defining characteristic of CLC exchangers was the presence of a titratable residue at the position of the proton glutamate. However, this is not strictly necessary: coupled Cl^-/H^+ antiport was found in a homologue from *Citrobacter koseri* (645), which carries an isoleucine, and in the crystallized

CmClC (242), which carries a threonine at the equivalent position.

The access of the proton glutamate from the intracellular solution has been investigated in detail by Lim et al. (468), underlining that the proton glutamate is not freely accessible to the intracellular solution and suggesting that the glutamate E202 serves as a "water organizer" (468). The protein region between the proton glutamate and the gating glutamate is rather hydrophobic, raising the important question of how protons can move between these two residues. The crystal structure of CmClC shows the side chain of the gating glutamate in the S_{cen} position (242), which is closer to the proton glutamate than the S_{ext} position. Thus it is possible that protons are delivered from the inside to the deprotonated gating glutamate side chain in the S_{cen} site in CLC exchangers in general. Recently, flux measurements favor the possibility that the gating glutamate can reach the central binding site also in EcClC-1 (860). Transport activity decreased when Cl^- was elevated on both sides of the membrane, suggesting that the gating glutamate becomes trapped between two Cl^- and the trapped state was eliminated by mutations supposed to disrupt hydrogen bonds that stabilize the gating glutamate in the central binding site (860). Several theoretical studies highlighted the possibility of transient water wires between the two glutamates (434, 872, 957). Recently, a combination of theoretical and experimental studies provided strong evidence for water wires, involving residues A404 and I109 in the passage of protons (321). However, even though intriguing and theoretically possible, the involvement of water wires in the H^+ passage is extremely difficult to nail down with certainty.

G. The Mechanism of Transport Coupling

The homodimeric architecture with an extensive subunit interface of all CLC proteins studied so far might suggest an important role of this peculiar arrangement for transport. However, the functional properties of dimeric constructs of WT and uncoupled mutants of ClC-5 demonstrated that each monomer unit of the dimeric protein is able to carry out Cl^-/H^+ exchange independently from the neighboring subunit (941). For EcClC-1, "straight-jacketed" constructs in which the two subunits were covalently linked with cysteine bridges behaved almost like WT showing that no large rigid body movement of the two subunits is involved in coupled transport (582). Furthermore, by introducing tryptophan residues at the dimer interface at two positions, Robertson et al. (705) succeeded in obtaining monomeric EcClC-1 proteins that were fully functional, showing unambiguously that the fundamental unit of transport is the CLC monomer.

Many features of CLC Cl^-/H^+ exchange are conceptually different from a classical alternate access antiporter system. In such antiporters, like e.g., Cl^-/HCO_3^- exchangers (24), the exchanged substrates never bind simultaneously. The binding site is alternatively exposed to the inside or to the outside, and coupling is ensured by the condition that only the "loaded" transporter can undergo the conformational change between outwardly to inwardly exposed binding sites. "Slippage" or uniport activity occurs to the extent that the unloaded transporter is able to undergo this transition.

In contrast, in CLC anion/H^+ antiporters, both substrates bind simultaneously and synergistically. This has been demonstrated elegantly by Picollo et al. (652), who showed, using ITC, that Cl^- binding triggers protonation of the transporter with a 0.5 H^+ to Cl^- binding stoichiometry. Proton binding most likely reflects the protonation of the gating glutamate. However, since the measurements of Picollo et al. were performed under equilibrium conditions, they do not reveal the temporal order of the binding events, i.e., if Cl^- binding is followed by protonation or vice versa. Interestingly, mutating the tyrosine Y445 to leucine reduced the binding stoichiometry to ~0.12 H^+ per Cl^- bound (652) similar to its effect on transport stoichiometry (4). In contrast, neutralizing the proton glutamate (E203Q) had almost no effect on the synergistic Cl^-/H^+ binding (652), suggesting that protonation of E203 is not directly involved in transport coupling. Synergistic binding of Cl^- and protons has also been supported by theoretical calculations (130, 449).

Triggered by the CmClC crystal structure, in which the gating glutamate side chain occupies S_{cen}, Feng et al. (242) proposed a coupling mechanism without involvement of a steric intracellular gate, and rather suggested a "kinetic" gate **(FIGURE 5*A*)**. The model involves conformations of the transporter that are "open" for Cl^- to both sides of the membrane, and in which the protonated or deprotonated gating glutamate points to the extracellular side (see states 5 and 6 in **FIGURE 5*A***). These states allow passive diffusion of Cl^-. In a strictly coupled transporter such states are theoretically "forbidden" because they introduce slippage, i.e., a loss of tight coupling. In the model of Feng et al. (242), these conductive states are visited only transiently such that they introduce only a marginal degree of slippage. However, the model predicts that these uncoupled states are stabilized at acidic pH, predicting uncoupled Cl^- transport at acidic pH. This has, however, not been observed experimentally even at pH 3 (5). In addition, the model does not involve conformational changes associated with transport that have been inferred in other studies (47, 53, 216). In an alternative picture, a true intracellular gate, involving Tyr_{in}, strictly controls access of intracellular Cl^- (1), and opening of the gate involves conformational changes of helix O (1, 47) **(FIGURE 5*B*)**.

Additional insight into the sequence of events in transport was obtained by the analysis of transient currents measured in the proton glutamate mutant of ClC-5, E268A (788).

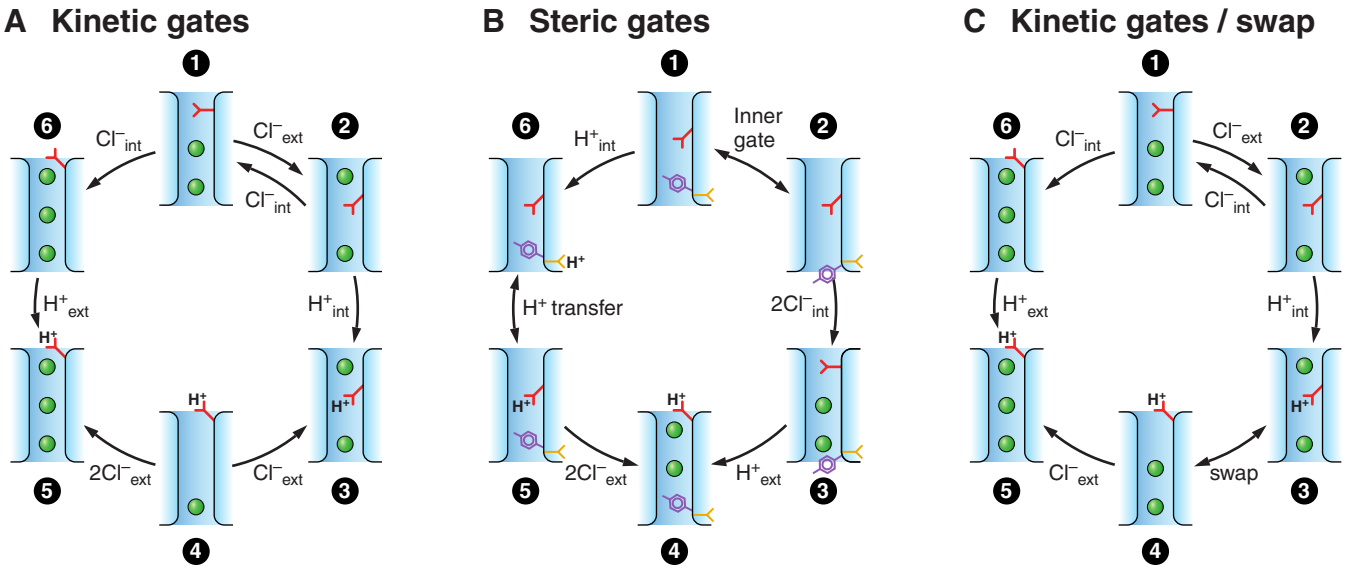

FIGURE 5. Different models of the transport cycle of CLC exchangers. In all three models, the anion binding sites correspond to those illustrated in **FIGURE 4** with Cl^- indicated as green spheres. The side chain of the gating glutamate, acting in all models as the external gate, is highlighted in red. The conserved tyrosine (Y445 in EcClC-1), suggested to play a role as internal gate (1, 47), is shown in violet in *B*, and the proton glutamate is shown in orange in *B*. The model in *A* was suggested by Feng and MacKinnon and incorporates only the external gating glutamate as a structural gating element (242). Here, the negatively charged side chain of the gating glutamate, E_{Gate}, occupies S_{ext} in state 1, which corresponds to the crystal structure of WT EcClC-1. In the clockwise direction, the first transport event is a downward movement of the side chain of E_{Gate} from S_{ext} to S_{cen}, pushing the Cl^- bound in S_{cen} to S_{int} and the ion bound in S_{int} into the cytoplasm, followed by rapid binding of an extracellular Cl^- ion into S_{ext} (state 2). A proton arriving from the cytoplasm protonates E_{Gate}, neutralizing its electrical charge (state 3). The Cl^- that previously occupied S_{ext} has to leave again its binding site towards the outside to allowing the E_{Gate} side chain to reorient towards the outside (state 4). Thus, in these first events, extracellular Cl^- binding/unbinding does not correspond to net transport, but extracellular Cl^- exerts a modulating function, controlling access of E_{Gate} to the outside. From state 4, binding of two extracellular Cl^- results in state 5. Deprotonation of E_{Gate} and release of the proton to the outside results in a state that corresponds to the E148Q mutant of EcClC-1 (state 6), from which the transporter returns to state 1 by the downward movement of E_{Gate} accompanied by the release of a Cl^- into the inside. All transitions are reversible, and the transport cycle can be operated in the reverse order. In this model, states 4–6 are conductive for Cl^-, i.e., allow Cl^- transport that is uncoupled from H^+ movement. *B* shows an alternative model proposed by Accardi (1) and Basilio et al. (47), in which strict coupling is ensured by an additional intracellular gate formed (in part) by the conserved tyrosine residue (Y445 in EcClC-1), as suggested by various pieces of experimental evidence (see main text). *C* shows a modified version of the kinetic model shown in *A*, which eliminates the modulatory Cl^- binding/unbinding step by introducing a hypothetical transition during which the protonated side chain of E_{Gate} and the Cl^- bound in S_{ext} swap their position and the side chain of the gating glutamate E_{Gate} moves further out (state 4 in *C*). In models *A* and *C*, approximate 2:1 Cl^-:H^+ transport coupling is achieved by "kinetic" gating that ensures that the conductive states are short-lived (242). However, preliminary model simulations using the parameters employed by Feng and MacKinnon (242; personal communication) show that at acidic pH values (<3) with the model shown in *A* the transporter becomes almost completely uncoupled, because the conductive states 4 and 5 are highly populated. This is in contrast to the experimental observation that EcClC-1 remains fully coupled for pH values as low as 3 (1, 3, 5). This behavior is partially remediated in the model shown in *C*, using similar parameters. The qualitative reason for this difference is that in model *C* the nonconductive state 3 is more highly populated at acidic pH and because of the different Cl^- occupancy of the various states (unpublished result). [*B* adapted from Accardi (1) and Basilio et al. (47).]

From a detailed analysis of such transient currents, it was concluded that the first events in the transport cycle are the movement of the gating glutamate from S_{ext} to S_{cen}, accompanied by a movement of a Cl^- from S_{cen} to the inside, which is then followed by the binding of an extracellular Cl^- to S_{ext} (961). A transport model that incorporates these initial events and a hypothetical swap of a Cl^- ion and the protonated gating glutamate is shown in **FIGURE 5*C***. A major difference to the model proposed by Feng et al. (242) **(FIGURE 5*A*)** is that after the initial downward movement of the gating glutamate and external Cl^- binding (transition from state 1 to state 2 in **FIGURE 5*C***), and protonation of the gating glutamate by an internal proton (transition from state 2 to state 3 in **FIGURE 5*C***), the previously bound Cl^- is not released back to the outside (as in the model of Feng et al., **FIGURE 5*A***) but moves further inside, swapping its position with the protonated gating glutamate (transition from state 3 to state 4 in **FIGURE 5*C***). Similar to the model of Feng et al. (242) **(FIGURE 5*A*)**, a "kinetic" gate has to be present to make the freely Cl^- conductive states 5 and 6

short-lived to avoid too much slipping. Preliminary simulations indicate that the model shown in **FIGURE 5*C*** largely prevents uncoupling of the transporter at acidic pH, which instead occurs in the model of Feng et al. **(FIGURE 5*A*)**, using comparable model parameters (Pusch, unpublished results). Such an uncoupling at acidic pH has in fact not been observed experimentally for pH values as low as 3 (1, 3, 5). However, the proposed "swapping" of the protonated glutamate side chain with a pore-bound Cl^- is purely hypothetical and requires experimental verification.

H. The Current-Voltage Relationship of CLC Transporters

The bacterial EcClC-1, reconstituted in planar lipid bilayers, shows a relatively linear current-voltage relationship, suggesting that none of the voltage-dependent translocation steps becomes significantly rate-limiting in the studied voltage ranges (3, 5). The mammalian CLC exchangers, ClC-3 to -7, are all expressed predominantly in endosomes and lysosomes, which are not simply accessible to directly electrophysiological recordings. Among these, ClC-4 and ClC-5 exhibit, however, significant plasma membrane localization in heterologous expression systems, allowing their analysis using the two-electrode voltage-clamp technique in *Xenopus* oocytes or the patch-clamp technique in transfected cells (269, 808, 855). Both transporters show an extremely pronounced outward rectification with no detectable inward currents, even using tail current protocols (269, 808, 855). The ion selectivity of the conductance at positive voltages is similar to that of CLC channels: $NO_3^- > Cl^- > Br^- > I^-$ (269, 334, 808, 855). ClC-5 is inhibited by pH_o (269), in a manner that is compatible with a voltage-dependent binding from the extracellular solution (649). ClC-3 behaves similarly to ClC-4 and ClC-5, even though its expression level is much smaller (456, 457, 651). Several other publications reporting different current phenotypes, including e.g., a phenotype similar to that of swelling activated anion currents, must be considered wrong as discussed by Stauber et al. (802) and below. More recently, several splice variants of ClC-3 have been studied, with some of them showing more pronounced plasma membrane expression than others (317). Neutralizing the gating glutamate, which abolishes H^+ transport in CLC transporters (964), completely eliminates the outwardly rectifying phenotype and any current relaxations in ClC-3, ClC-4, and ClC-5 (269, 457). These mutants yield currents with an almost linear current-voltage relationship and an anion selectivity that is similar to that of the WT (941). This suggests that anion permeation through the uncoupled transporters per se is not rectifying. An alternative explanation for the observed rectification is that one of the proton translocation steps is voltage dependent (941). However, even in the presence of SCN^-, which leads to almost complete uncoupling and loss of H^+ transport, currents are strongly rectifying (941), and also the H^+ block is similar in these conditions (649), arguing against a fundamental role of H^+ translocation as the basis of the rectification. A possible "gating phenomenon" underlying the strong rectification will be discussed below.

ClC-6 could be partially targeted to the plasma membrane by NH_2-terminal fusion of GFP (576). The electrophysiological activity was compatible with a Cl^-/H^+ exchange, and currents were strongly outwardly rectifying and small, such that reversal potentials could not be determined reliably (576). Neutralizing the gating glutamate eliminated the rectification, but currents remained very small. Simultaneous mutation of the internal tyrosine to serine augmented currents (576), similar to the enhanced turnover in EcClC-1 of the E148A/Y445S mutant (378). From a biophysical perspective, ClC-6 remains one of the least studied mammalian CLC proteins.

For a long time, ClC-7/Ostm1 transporters could not be studied electrophysiologically because of their very tight targeting to lysosomes (391). Using flux assays on native lysosomes, Graves et al. (298) found that the dominant Cl^- transport was characterized by $2Cl^-/1H^+$ antiport activity. A more direct investigation of the biophysical properties of ClC-7/Ostm1 became possible after the discovery that the proteins could be partially redistributed to the plasma membrane by the mutation of NH_2-terminal leucine targeting motifs (801), allowing for the first time their electrophysiological characterization (453). ClC-7/Ostm1 currents are strongly outwardly rectifying and reflect coupled 2:1 Cl^-/H^+ antiport, but unlike ClC-5, they exhibit very slow activation kinetics and inwardly directed tail currents (453). Similar to ClC-3, -4, and -5, neutralizing the gating glutamate results in voltage-independent, practically linear, uncoupled Cl^- transport (453).

Thus all mammalian CLC transporters exhibit strong outward rectification, in contrast to the linear current-voltage characteristics of EcClC-1. In the case of ClC-7, the rectification appears to almost exclusively reflect a gating phenomenon, since the instantaneous current-voltage relationship obtained by tail current protocols is almost linear (453). For ClC-3 to ClC-6, the mechanisms underlying the rectification are not yet fully understood.

I. Pharmacology of the Bacterial EcClC-1 Transporter

While not of immediate medical relevance, small molecule ligands of the bacterial EcClC-1 transporter have a great potential as mechanistic tools. In addition, the co-crystallization of potential ligands may provide important structural insights in ligand/protein interaction applicable to human CLCs. Initially, Matulef and Maduke (534) reported that DIDS inhibits EcClC-1 specifically from the intracellular side, allowing a "functional orientation" of the reconstituted protein. However, later the same group discovered

that DIDS is chemically highly unstable in aqueous solution and that the active fractions inhibiting EcClC-1 are polythiourea derivatives of DIDS (533). Building on these insights, Howery and co-workers designed an inhibitor of EcClC-1 combining 4,40-diaminostilbene-2,20-disulfonate (533) with the two aliphatic side chains present in octanoic acid, which blocks ClC-0 and ClC-1 (721, 954). The resulting compound, called OADS, inhibits EcClC-1-mediated transport with micromolar affinity and probably binds to the protein in a superficial position (353). Unfortunately, so far no high-resolution structure of any CLC with a bound inhibitor has been obtained.

III. CELL BIOLOGY, PHYSIOLOGY, AND PATHOLOGY OF MAMMALIAN CLC PROTEINS

When ClC-0, the founding member of the CLC family, was cloned in 1990 (393), most of the diverse and often crucial roles of Cl^- channels were not appreciated and largely unknown. Only two human pathologies were attributed to an inheritable impairment of Cl^- channels: myotonia congenita, a disorder of skeletal muscle excitability, and cystic fibrosis, a multisystem disorder associated with defects in transepithelial transport. The identification and characterization of nine mammalian CLCs **(FIGURE 1)** not only showed that myotonia congenita is indeed due to mutations in a muscle Cl^- channel (423, 805), but revealed many hitherto unexpected roles of Cl^- transport. These roles were most often gleaned from human genetic diseases or mouse models in which CLC genes were disrupted or specifically altered by point mutations. Mutations in seven of the nine human *CLCN* genes are now known to cause human disease (187, 246, 359, 423, 429, 481, 747, 748, 780). Likewise, mutations in the three genes encoding ancillary CLC "β-subunits" [barttin (65, 222), Ostm1 (116, 445), and GlialCAM (395, 483)] cause human pathologies which substantially overlap, or are sometimes identical to, those caused by a loss of the associated CLC "α-subunit." Genetic mouse models sometimes led the way to the corresponding human disease (68, 429) and always helped to unravel the underlying pathological mechanisms as well as the function of Cl^- transport for the cell and the organism.

In the following, we review the current knowledge of each mammalian CLC, beginning with the plasma membrane Cl^- channels ClC-1, ClC-2, ClC-Ka, and -Kb and proceeding to the overwhelmingly intracellular chloride/proton exchangers ClC-3 to ClC-7. As general features of CLC structure-function relationships have been discussed in detail in the preceding sections, we mention these aspects only shortly and when they are relevant and specific for the particular CLC isoform. We discuss their regulation, pharmacology, as well as their roles for cells, tissues, and the organism. Particular emphasis is placed on diseases and mouse phenotypes that are associated with their mutational disruption or alteration.

IV. CLC PLASMA MEMBRANE CHLORIDE CHANNELS

Among mammalian CLCs, only ClC-1, ClC-2, and the two highly homologous ClC-K channel isoforms, both of which require the β-subunit barttin, are Cl^- channels. They reside in the plasma membrane and display different tissue distributions. ClC-1 is highly specific for skeletal muscle, whereas the ClC-K isoforms are differentially expressed in epithelial cells of the nephron, the inner ear, and salivary glands. In contrast, ClC-2 is widely and almost ubiquitously expressed in epithelial and nonepithelial cells. By providing the major resting conductance of skeletal muscle, ClC-1 is crucial for ensuring appropriate excitability of that tissue, and ClC-K/barttin channels have well-defined roles in transepithelial transport. Functions of ClC-2 are more diverse and less defined. They may range from extra- and intracellular ion homeostasis over regulation of cellular excitability to transepithelial transport. Human genetic diseases and genetic mouse models demonstrate the physiological importance of all these plasma membrane channels.

V. ClC-1: THE SKELETAL MUSCLE Cl^- CHANNEL MUTATED IN MYOTONIA

ClC-1 was the first mammalian voltage-gated Cl^- channel that was identified at the molecular level (807). Skeletal muscle was an obvious choice for a tissue to look for a homologue of ClC-0 because the electric organ is derived from muscle during development (263, 264). Indeed, ClC-1 is the closest mammalian homologue of the *Torpedo* channel. With a mass of ~120 kDa (998 amino acids), ClC-1 is the largest mammalian CLC protein. This is owed to a relatively long cytosolic NH_2 terminus (larger only in ClC-7), a relatively large segment between the cytosolic CBS1 and CBS2 domains (also found in ClC-2 and ClC-6), and a particularly large cytosolic tail after CBS2 (the largest of mammalian CLCs). These relatively large cytosolic regions may be important for the trafficking and regulation of ClC-1 (358, 507, 710). In skeletal muscle, ClC-1 is strongly regulated both on the transcriptional and posttranscriptional levels. Its regulation, biophysical properties, structure-function relationship, pharmacology, and role in muscle physiology have been extensively investigated for more than 20 years (for excellent reviews, see Refs. 34, 367, 640, 827).

ClC-1 is almost exclusively found in skeletal muscle (807) where it mediates the bulk of plasma membrane Cl^- conductance (g_{Cl}) as evident from the close match of the properties of heterologously expressed ClC-1 with those of native g_{Cl} (reviewed in Ref. 34) and, above all, from the loss of skeletal muscle chloride conductance upon *Clcn1* disruption (537, 805). Skeletal muscle is unusual in that g_{Cl} provides ~80% of the resting conductance (83). This high level of g_{Cl} is crucial for the control of muscle excitability. In-

deed, *CLCN1* mutations abolishing or otherwise reducing ClC-1 plasma membrane currents lead to myotonia, a disorder associated with muscle hyperexcitability, in humans (423) and other mammals (51, 72, 568, 694, 805, 906) (for reviews on ClC-1 and myotonia, see Refs. 485, 670, 827, and for more general reviews on myotonia, see Refs. 97, 402, 817). The reduction of g_{Cl} due to aberrant splicing of the *CLCN1* mRNA contributes to myotonic symptoms in two neurodegenerative diseases, myotonic dystrophy (119, 518) and Huntington disease (890). Hence, ClC-1 plays a crucial role in muscle physiology and pathology.

A. Transcriptional Regulation of ClC-1 Expression

ClC-1 is almost exclusively expressed in skeletal muscle as demonstrated by Northern blots that compared skeletal muscle with with cardiac muscle (654) and several additional tissues (807). Whereas more sensitive RT-PCR/Northern analysis could detect ClC-1 transcripts also in liver, ClC-1 levels were reported to be only ~0.01% of those found in mature skeletal muscle (43). The recently reported expression of ClC-1 in brain and other organs (123) has to be viewed with considerable skepticism (see below).

In rodents, skeletal muscle Cl^- conductance (145) and the expression of ClC-1 (807, 909) strongly increase in parallel within a few weeks after birth and decrease again with aging (654). Northern blots were unable to detect the small amount of ClC-1 transcripts in myotubes which represent the embryonic stage of muscle (909), but sensitive RT-PCR showed that ClC-1 levels increased during the differentiation of myogenic cells to myotubes in cell culture (909). ClC-1 transcription may be controlled by MyoD and myogenin transcription factors (419). In addition, developmental regulation of *Clcn1* splicing may contribute to the postnatal increase in g_{Cl} and ClC-1 levels in rodents (495). Shortly after birth, a considerable fraction (~30%) of *Clcn1* mRNA contains an additional exon (exon7a+) that introduces a frameshift and reduces mRNA levels by nonsense-mediated mRNA decay. Over the next few weeks, skipping of this extra exon increases, resulting in a rise in *Clcn1* mRNA levels and functional channels (495).

ClC-1 is more highly expressed in fast-twitch than in slow-twitch muscles and is modulated by electrical activity as revealed by myotonic mouse models in which ClC-1 levels were increased, and denervation experiments which decreased ClC-1 transcript levels (419). These changes in ClC-1 expression correlate well with the previously described decrease of muscle Cl^- conductance upon denervation (145). Immobilization of muscles in a hindlimb unloading model appeared to moderately increase ClC-1 mRNA levels specifically in low-twitch soleus muscle of rats (655), an effect that may, however, be less important than the activation of ClC-1 that results from decreased protein kinase C (PKC) activity under these conditions (656). Hence, transcriptional regulation of ClC-1 not only plays a role during development, but also during the adaptation of muscle fibers to changed physiological conditions.

B. Basic Properties and Posttranslational Regulation of the ClC-1 Channel

ClC-1 is the closest mammalian ortholog of the electric organ chloride channel ClC-0. The general properties of heterologously expressed ClC-1 channels are in agreement with those of the skeletal muscle Cl^- conductance (83, 617, 807). However, before the cloning of ClC-1, the skeletal muscle Cl^- conductance had been studied mostly using current-clamp recordings of skeletal muscle fibers, which does not allow a precise determination of biophysical parameters (83). Recently, whole cell patch-clamp recordings and two-electrode voltage-clamp recordings have shown that the properties of the endogenous conductance are practically identical to that of heterologously expressed ClC-1 channels (196, 496, 497). Like this prototype channel, it shows a typical "double-barreled" electrophysiological fingerprint with two equally spaced, independent conduction levels (739). However, since its single-channel conductance is ~1.5 pS, as first determined by noise analysis (678) and later confirmed by single-channel recordings (739, 814, 894, 897), much lower than that of ClC-0 (~10 pS) (50, 548), it is technically more challenging to measure single-channel currents of ClC-1. Moreover, compared with ClC-0, it is more difficult to distinguish between common gating (that affects both pores of the dimeric channel) and protopore gating (that affects only one pore). Whereas the common gate activates ClC-0 very slowly (within seconds) upon hyperpolarization, the protopore gate is fast (in the 10 ms range) and opens upon depolarization. In contrast, both the common and protopore gates open upon depolarization and do not show drastic differences in gating kinetics at physiological voltages with slow and fast time constants that differ by less than roughly a factor of 5 and are smaller than 100 ms (8, 720, 721, 739). Hence, more sophisticated analysis is needed to distinguish both gates in ClC-1 (8, 739), which can be affected differentially by myotonic mutations. The voltage dependence of both gates contributes to the outward rectification of macroscopic currents. ClC-1 is ~40% open at resting voltages of skeletal muscle (894) and can be opened further by depolarization. It displays a $Cl^- > Br^- > NO_3^- > I^-$ selectivity sequence (722) that is typical for CLC channels.

Biophysical properties and structure-function aspects of ClC-1 have been studied extensively (2, 8, 35, 54–56, 113, 205, 206, 224, 356, 503–505, 719–722, 739, 749, 920). ClC-1 is voltage dependent, deactivating at negative voltages, with a steady-state open probability curve that can be approximated by a Boltzmann distribution with an

apparent gating valence of ~1 elementary charge (233, 678, 679, 720). This gating behavior is reminiscent of the fast gate of ClC-0, and, at physiological pH, the channel shows no sign of a slow, hyperpolarization activated gate (see **FIGURE 6**). Only at acidic extracellular pH (5.5), and keeping a positive holding potential, the channel exhibits activation by hyperpolarization, with some features similar to the slow gating of ClC-0 (720). Furthermore, single point mutations in various protein regions induce a gating phenotype that is fully or partially characterized by activation by hyperpolarization, some of which are causally involved in myotonia (230, 233, 319, 674, 718, 918, 947). In all cases studied, the hyperpolarization activation was sensitive to the intracellular Cl^- concentration (674, 718, 918), as is the gating of ClC-2 (588, 674). This suggests that the basic gating phenotypes seen in CLC channels share common mechanisms, possibly being ultimately attributable to a facilitation of opening by pore occupancy and competition with the gating glutamate.

In contrast to the fast gate of ClC-0, the deactivating current relaxations of ClC-1 cannot be described by a single-exponential function, but bear at least two exponential

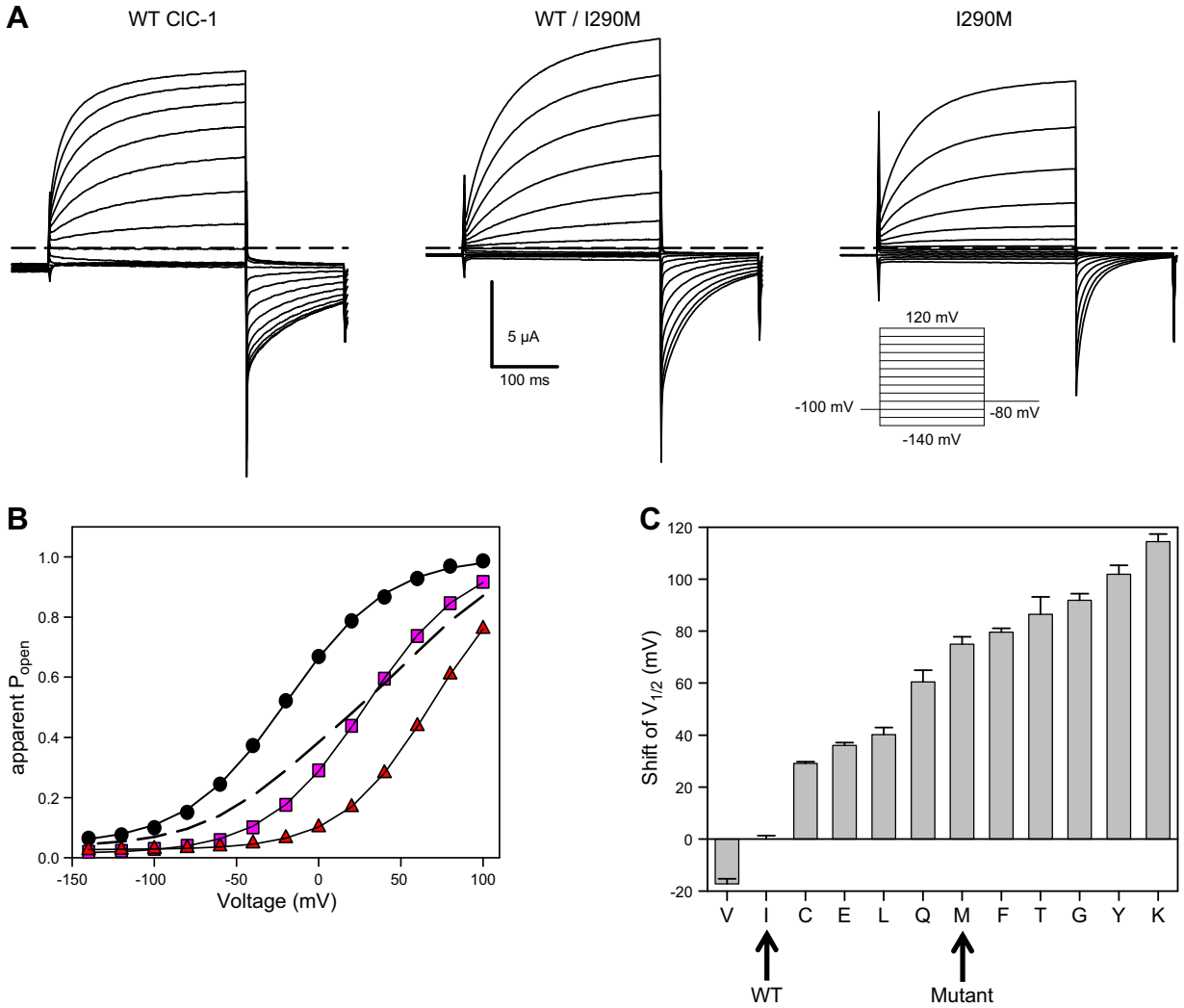

FIGURE 6. Shift of ClC-1 voltage dependence by dominant myotonia mutant I290M. *A*: typical voltage-clamp traces from individual oocytes injected with RNA coding for WT ClC-1 (*left*), mutant I290M (*right*), or coinjected with these RNAs (*middle*) elicited with the voltage-clamp protocol shown in the *inset* (holding potential −100 mV). The coinjection mimics the genotype of a heterozygous patient. *B*: apparent open probability obtained from the normalized initial tail currents measured at the −80 mV tail pulse (WT: black; I290M: red; WT/I290M: pink) together with the fit of a Boltzmann distribution (black lines) from which the voltage of half-maximal activation ($V_{1/2}$) was obtained. The dashed line was obtained by the average of the Boltzmann fits of WT and mutant I290M, which is less steep than the Boltzmann fit obtained for the coinjected oocyte, indicating that heteromeric WT/I290M channels gate with a dominantly shifted voltage dependence. In particular, the Cl^- conductance in the physiological (negative) voltage range is significantly reduced in the coinjected oocyte. *C*: shift of $V_{1/2}$ induced by mutations of I290 by the indicated amino acids. [Adapted from Pusch et al. (679).]

components (720). While Fahlke and colleagues concluded that intrinsic sensors of the protein are underlying its voltage dependence (232, 233), there is ample evidence that the basic mechanisms of voltage-dependent gating of ClC-1 are similar to those of ClC-0, and that gating is strongly coupled to anion/proton movements within the pore (8, 479, 719–721). In particular, reduction of the extracellular Cl^- concentration leads to a shift of the voltage dependence of the open probability to more positive voltages (720), similar to its effect on ClC-0 fast gating. Compared with ClC-0, gating of ClC-1 is relatively insensitive to the intracellular Cl^- concentration (720). Interestingly, the myotonia causing mutation A331T, located in the extracellular loop connecting helices I and J, induces a $[Cl^-]_i$ sensitivity of gating (886). Similar to the fast gate of ClC-0, gating of ClC-1 is dependent on pH_i, with faster deactivation at more alkaline pH (479, 720).

A major difference to ClC-0 is that certain impermeant anions, like methanesulfonate or cyclamate, can partially substitute for Cl^- in promoting gate opening (722). This somewhat paradoxical behavior could be related to a complex interrelationship between fast and slow gate, analogous to the effect of ClO_4^- in certain ClC-0 mutations (490). In fact, a major complication of the earlier studies on ClC-1 was that contributions of the single protopore gate and the common gate could not be distinguished. Single-channel analysis showed that both gates are present but that they show considerable kinetic overlap, with the single protopore gate being only about three- to fivefold faster than the common gate at negative voltages (739). Accardi and Pusch (8) discovered that the time constant of the protopore gate exhibits an exponential voltage dependence at positive voltages, becoming very fast and reaching values in the order of 10–20 μs at 200 mV. This finding by itself is interesting regarding the mechanism of fast gate opening, i.e., the rate-limiting step underlying fast gating has to be able to operate on a time-scale faster than this. By comparison, the fast gate time constant of ClC-0 showed a similar exponential voltage dependence, being, however, almost 10-fold slower (8). The exponential voltage dependence of the opening rate constant for voltages up to 200 mV additionally implies that the rate-limiting opening step of the fast gate is associated with the movement of an electric charge with an apparent valence of ~0.79 for ClC-1 and ~0.55 for ClC-0 (8).

Importantly, the slow gate time constant of ClC-1 is much less voltage dependent such that the two gating processes become kinetically distinct by a factor of more than 100 at large positive voltages, allowing an efficient separation of the two gating processes using adequate pulse protocols (8). In this way, assuming independence of the protopore and common gates, the voltage dependence of the two processes can be determined separately. It has to be underscored, however, that this procedure is approximate because of the relatively strong interdependence of the two gates.

Using this procedure, Accardi and Pusch (8) found that both gates are activated at positive voltages and that the common gate shows a significant minimal open probability even at negative voltage. The procedure allowed to dissect also the $[Cl^-]_o$ and pH_i dependence of the two gates, finding that both gates are in fact dependent on these parameters (8). The detailed analysis of Lisal and Maduke of the pH_i dependence of fast and slow gating of ClC-1 (479) revealed that ClC-1 behaves very similar in that respect compared with ClC-0. Bennetts et al. (56) reported that the common gate of ClC-1 has a much larger temperature dependence than the fast gate, however less so than the common gate of ClC-0 (676).

An important piece of evidence that the slow gate, defined through the prepulse protocols of Accardi and Pusch, corresponds to the common gate of ClC-0, was that the C277S mutation, which corresponds to C212S of ClC-0, almost completely abolished the slow gate, as does C212S in ClC-0 (2, 472). The same mutation almost abolished Zn^{2+} block of ClC-1 (206), similar to its effect in ClC-0 (472). From their studies of Zn^{2+} block of ClC-1, Duffield et al. (206) concluded that Zn^{2+} stabilizes a closed state of the channel, recovery from which is much slower and more temperature dependent than the regular gating kinetics. Such a deeply inactivated state is an interesting hypothesis, which might apply to other CLC proteins as well. The Zn^{2+} binding site, however, remains unknown for ClC-1 and for ClC-0.

More recently, Bennetts et al. (54) discovered that mutating the tyrosine of the selectivity filter (Y578 in ClC-1, Y512 in ClC-0) dramatically activated the common gate in both channels. Like in ClC-0, neutralizing the gating glutamate in ClC-1 completely eliminates slow and fast gating components (224, 234).

Thus there is highly convincing evidence that the common gate of ClC-1 shares many features with the slow gate of ClC-0, despite an inverted voltage dependence. Using FRET analysis of COOH-terminally fused fluorescent proteins, Ma et al. (504) reported a movement of the COOH-terminal regions upon maneuvers that are expected to manipulate the common gate open probability. The extent of the movement was, however, smaller than that reported for ClC-0 in analogous experiments (93).

Of likely physiological importance, the intracellular pH dependence of ClC-1 is highly dependent on intracellular nucleotide concentration. Whereas currents of heterologously expressed ClC-1 were rather increased by acidic pH_i when studied in whole cell patch-clamp or in inside-out patches without intracellular ATP (8, 720, 739), ClC-1 is inhibited by intracellular acidification when studied in the presence of

physiological ATP concentrations (55, 841). As discussed later, the inhibition of native ClC-1 channels by acidic intracellular pH may play an important role in the adaptation of muscle to intense exercise (639).

Two other means of modulating ClC-1 activity, namely, intracellular binding of ATP and modulation by PKC, are important for muscle physiology. ClC-1 conductance at resting voltages can be inhibited by intracellular ATP and other nucleotides which shift its current-voltage relationship to more positive potential, probably by acting on the common gate (55, 57, 841, 842). The inhibitory effect of ATP is stronger at acidic pH_i (841) and is controlled by oxidation and reduction (953), a finding that may explain why another study (968) failed to reproduce an influence of ATP on ClC-1. Site-directed mutagenesis provided convincing evidence that ATP acts by binding to the cytosolic CBS domains of ClC-1 (57, 842). Also intracellular β-nicotinamide dinucleotides (NAD) inhibit ClC-1 and endow an exquisite pH_i sensitivity on the channel (58). Like ATP, NAD probably exerts its effect by binding to the CBS domains and changing the common gating of ClC-1. Both modulation by pH_i and $[ATP]_i$ are posed to link ClC-1 activity to muscle metabolism, but are predicted to have qualitatively opposing effects on g_{Cl}: a drop of pH_i and $[ATP]_i$ upon muscle exercise should decrease and increase, respectively, muscle chloride conductance.

Currents of heterologously expressed ClC-1 could be inhibited by activating PKC with phorbol esters (711). However, the effect of phorbol esters is slow and PKC has pleiotropic effects that may include a reduction of surface expression. Thus a change in biophysical channel properties more convincingly demonstrates a direct effect of PKC than a change in current amplitudes (711). More recent studies reported that phorbol esters shifted the voltage dependence of ClC-1 by nearly 20 mV to more positive potentials (358, 701), predominantly by changing the common gate and without affecting maximal current amplitudes (701). Channels carrying double mutations of PKC consensus sites suggested that phosphorylation of COOH-terminal serines/threonines (891–893 in human ClC-1) may mediate the shift in voltage dependence (358). It remains an open question whether such a change in ClC-1 properties or other factors like the reported PKC-dependent change of its localization in myofibers (625) accounts majorly for the well-established inhibition of muscle g_{Cl} by PKC (84, 840). A role of PKC in regulating muscle g_{Cl} has recently been confirmed genetically by studying mice devoid of PKC-θ (96).

C. Role of ClC-1 in Muscle Physiology

Skeletal muscle is unusual in that ~80% of the resting conductance is mediated by Cl^- rather than K^+ as in most other tissues (12, 14, 83, 364, 477, 617). ClC-1 mediates the bulk of this conductance as is evident from myotonic animal models that carry inactivating *CLCN1* mutations. Although skeletal muscle expresses the Na^+-K^+-$2Cl^-$-cotransporter NKCC1 (851, 913) which uses the inwardly directed Na^+ gradient to accumulate Cl^- in cells, the high Cl^- conductance of skeletal muscle ensures that $[Cl^-]_i$ is nearly at its electrochemical equilibrium. ClC-1 therefore stabilizes the resting membrane potential of skeletal muscle (which is eventually determined by the interplay of the Na^+-K^+-ATPase and K^+ channels) and significantly contributes to the repolarization of action potentials in a role that resembles that of K^+ channels in most other cells. Muscle action potentials may further lead to incremental voltage-dependent activation of ClC-1 during repetitive firing (679, 843). As discussed below, however, regulation of ClC-1 by kinases, pH, and ATP may be physiologically more important than its voltage-dependent activation.

If skeletal muscle plasma membrane conductance would be carried predominantly by K^+, as is the case with loss-of-function mutations of *Clcn1* in myotonia, there would be a significant increase of extracellular K^+ concentration during the repolarization of action potentials, in particular in the narrow t tubules that penetrate and criss-cross the muscle to ensure efficient excitation-contraction coupling by voltage-gated L-type Ca^{2+} channels. Since extracellular $[K^+]$ is in the 5 mM range, a rather small repolarizing outward flow of K^+ into these tubules would lead to a relatively large increase in t-tubular $[K^+]$ (265). This may lead to a depolarization of t-tubular membranes with the danger of eliciting unwanted action potentials and muscle contraction (as actually observed as "myotonic runs" in myotonia). Since $[Cl^-]_o$ is much higher (~120 mM), the same amount of charge transfer during repolarization would lead to ~25-fold lower relative extracellular concentration change of Cl^- compared with K^+. The influx of Cl^- into the muscle fiber will not significantly change $[Cl^-]_i$ either because of the large intracellular volume of muscle fibers. Hence, for the repolarization of muscle action potentials, Cl^- is better suited than K^+.

These considerations rest largely on the assumption that ClC-1 is expressed in t tubules, which was indeed suggested by a substantial decrease of K^+ but not of Cl^- conductance, upon tubular disruption with glycerol (617), and by experiments on mechanically skinned muscle fibers (146, 177, 208, 639). However, immunohistochemistry did not detect ClC-1 on t tubules, but rather on the sarcolemma (313, 625). Two recent studies, both of which were commented (226, 969), come to opposite conclusions concerning the presence of ClC-1 on t tubules (196, 497). Hence, although a careful discussion tends to rather support a t-tubular expression of ClC-1 (640), this issue remains unresolved.

A recent series of elegant studies revealed that regulation of ClC-1 activity plays an important role in the control of

excitability of working muscle (176, 637, 638, 701). Repetitive action potential firing in muscle leads at first to an increase in the electrical resistance of the muscle membrane. The increased resistance, which increases the electrical excitability by reducing shunt currents, could be attributed to an inhibition of ClC-1 by PKC (176, 638) and also, to some degree, to an inhibition of ClC-1 by intracellular acidification (636). In fast-twitch, but not in slow-twitch muscle fibers, prolonged action potential firing later leads to a marked increase in membrane K^+ and Cl^- conductance that is mediated by an activation of K_{ATP} and ClC-1 channels, respectively (637). Since both channels are inhibited by intracellular ATP, their activation is probably caused by a decrease in $[ATP]_i$ during exercise. The resulting increased shunt conductance decreases action potential amplitudes and muscle excitability and is a correlate of muscle fatigue.

D. ClC-1 in Myotonia

Myotonia is a symptom of several neurological diseases and is associated with an impaired relaxation of skeletal muscles after voluntary contraction (97, 402, 712, 817). Electromyograms typically reveal "myotonic runs," trains of action potentials which are elicited by single stimuli that would trigger only one action potential in normal muscle. This suggests that myotonia is caused by a muscle-intrinsic electrical hyperexcitability. Myotonia can be caused by mutations in ion channels like ClC-1, the $Na_v1.4$ Na^+ channel, the $Ca_v1.1$ Ca^{2+} channel, or several inwardly-rectifying Kir K^+ channels (for review, see Ref. 97) and also by a more indirect decrease of channel activity [like aberrant splicing of ClC-1 in myotonic dystrophy (119, 518)]. The term *myotonia congenita* is reserved for myotonia caused by mutations in the *CLCN1* gene.

The first clinical description of myotonia was given by Julius Thomsen in 1876 (835). He himself suffered from the disease which segregated in his family in an autosomal dominant manner. The dominant form of myotonia congenita is therefore known as "Thomsen disease." We now know that Dr. Thomsen carried the P480L mutation in the *CLCN1* gene (806).

The first animal model for myotonia was the "fainting goat" which spontaneously arose as a probably dominantly inherited trait in North America. Early work indicated that the hyperexcitability of their muscles was not due to altered innervation (86). Bryant and colleagues discovered that their muscles displayed reduced Cl^- permeability (13, 476) and found similar changes in myotonic patients (477). A well-established animal model for recessive myotonia are *adr* mice (891) which also display severely reduced muscle Cl^- conductance (537). Almost immediately after the molecular identification of ClC-1 as the major skeletal muscle Cl^- channel (807), the *Clcn1* gene of *adr* mice was shown to be inactivated by the insertion of a transposon (805). Following this seminal finding, *CLCN1* mutations were identified in human myotonia (423), in the myotonic goat (51), and in several other mammals with myotonia, including dog (248, 694), sheep (568), horse (906), and water buffalo (72). To date, more than 200 *CLCN1* mutations (485, 667, 670) have been identified in patients with myotonia congenita, and many of these have been studied functionally after heterologous expression.

In humans, myotonia congenita can be inherited as an autosomal dominant or recessive trait (known as Thomsen disease and Becker disease, respectively). However, following the identification of the underlying gene, it became clear that low-penetrance dominant *CLCN1* mutations can be associated with dominant myotonia in some families, and recessive myotonia in others (435). Since only one *CLCN1* allele is mutated in dominant myotonia, Thomsen disease is in general clinically less severe, with particularly mild forms sometimes being called myotonia levior (452). In both recessive and dominant forms of the disease, muscle stiffness is particular severe after rest and gets better with exercise (the "warm-up" effect) (97, 712). A sudden, severe muscle stiffness after rest also explains the startle response of myotonic goats (86), *adr* mice (891), and myotonic buffalos (72), in which these animals fall down when trying to run away after being scared. This startle response has led to the misnomer "fainting goats" for myotonic goats. There is no muscle dystrophy in myotonia congenita and patients rather have an athletic appearance. Their muscles are hypertrophic owed to the increased muscle exercise caused by myotonia. Muscle hypertrophy is also seen in animal models of myotonia as impressively demonstrated for buffalos (72).

Reduction of skeletal muscle Cl^- conductance contributes in at least two ways to the pathogenesis of myotonia congenita. As discussed above, a decrease of muscle resting conductance (down to ~20% with a complete loss of ClC-1) causes electrical hyperexcitability because depolarizing currents are now less opposed by electrical shunting. Hence, action potentials can be elicited by smaller depolarizing currents. Second, and probably more important, a much larger proportion of the repolarizing currents terminating action potentials is now carried by K^+ which accumulates in the small extracellular space of the t-tubular system. The resulting depolarization may exceed the threshold for the activation of Na^+ channels and thereby elicits aberrant action potentials that result in the typical "myotonic runs" of patients.

Myotonia-causing mutations in *CLCN1* are scattered over the entire coding region and may also affect noncoding regions if they affect transcription or RNA processing. There is also a sizeable ~5% fraction of patients with recessive myotonia who display exon deletions or duplications in *CLCN1* (687). Protein-truncating and missense mutations

are scattered all over the transmembrane part of the protein, but can also be found in the cytosolic NH_2- and COOH-terminal parts of the protein. Nonsense or frameshift mutations are almost always associated with recessive myotonia with the exception of a few mutations that truncate only a short part of the long cytosolic tail of ClC-1 (540, 698). Premature stop codons can decrease mRNA levels by nonsense-mediated mRNA decay, and in most cases, the truncated protein will not form functional channels. Moreover, most truncated proteins (with the above-noted exceptions) will be unable to form a dimer with WT ClC-1 proteins and are therefore expected to lack dominant-negative effects in heterozygous patients. Conversely, almost all dominant *CLCN1* mutations result in single amino acid exchanges that still allow the mutated protein to interact with its WT partner and thereby change its function in a mutant/WT dimer. Random point mutations are less likely to produce such mutants than causing a complete loss of channel function, explaining why more recessive than dominant mutations have been found in myotonia (485, 670). It is presently impossible to predict whether a particular novel *CLCN1* missense mutation is associated with recessive or dominant myotonia.

Graded pharmacological inhibition suggested that muscle Cl^- conductance has to be decreased by roughly 75% to cause myotonia (274, 440). This result is consistent with the observation that complete loss-of-function *CLCN1* mutations on only one allele, which might be expected to reduce muscle Cl^- conductance by 50%, does not result in myotonia. However, despite having halved functional gene dosage, heterozygous *Clcn1*^{adr}/WT mice displayed normal muscle g_{Cl} owing to some type of posttranscriptional regulation (122). In dominant myotonia, g_{Cl} is reduced close to the critical 25% of WT level, thereby explaining that Thomsen disease is generally less severe than Becker-type myotonia in which there may be a total loss of ClC-1 function. If the efficiency of dimer formation is not changed in the dominant channel mutant, heterozygous patients will express 25% fully functional WT/WT ClC-1 channels. Even if mutant/mutant and WT/mutant channels would be nonfunctional, g_{Cl} would remain at 25% of WT levels.

Many, and probably most, dominant *CLCN1* mutations shift the voltage dependence of ClC-1 to positive voltages where the channel no longer contributes significantly to resting g_{Cl} and to the repolarization of action potentials (679) **(FIGURE 6)**. This shift is not only seen with mutant/mutant homodimers, but to a lesser degree [that depends on the particular mutation (435)] also in WT/mutant heterodimers (679) **(FIGURE 6)**. This dominant effect on gating is mediated by the common gate that affects both protopores and thereby allows for a cross-talk between the subunits (739). These mutations include I290M (679), which is located at the dimer interface (210). The residues of the two subunits corresponding to I290 in EcClC-1 (I201 in helix H) are directly contacting each other in the crystal structure of EcClC-1, underscoring the importance of the dimer interface for the common gate. Interestingly, the mutation I201W, together with the I422W mutation, was sufficient to yield monomeric EcClC-1 proteins (705). Another dominant mutation is P480L that was found to cause myotonia in Thomsen's own family (806). Homomeric mutant channels are nonfunctional, and the mutant exerts a strong dominant negative effect on the WT (806), by dramatically shifting the voltage dependence to more positive voltages (679). P480 is not located at the dimer interface but in the loop preceding helix N, close to the selectivity filter, suggesting that the strong effect of the mutant on the gating might be caused by alterations in ion binding properties. Mutant I556N, that has a mixed dominant/recessive inheritance, was found to shift the overall voltage dependence of gating but to have virtually no dominant negative effect in coexpression with WT (435). Dissection of fast and slow gating components revealed that indeed the I290M mutation has a large effect on the slow gate, whereas the I556N mutation has a stronger effect on the fast gate (8, 739). Over the past two decades, many more dominant mutations were found to shift the voltage dependence of ClC-1 (89, 305, 319, 369, 435, 485, 535, 670, 784, 912, 918, 946).

However, not all mutations shifting the ClC-1 voltage dependence exert dominant effects and are rather associated with recessive myotonia (like V236L or G190S) (189, 667, 770). Mutations that only confer a moderate shift in voltage dependence on mutant/WT heterodimers have sometimes been found in recessive and dominant pedigrees (435). In addition to an effect on the common gate, missense mutations may also affect the processing or trafficking of WT/mutant heteromers. Several missense mutations in the ClC-1 NH_2 terminus affected the surface expression of ClC-1, with Q43R also strongly affecting the surface expression of WT/mutant concatemeric channels (710). However, this mutation was associated with recessive myotonia, suggesting that the observed dominant effect on surface expression may just occur with covalently linked concatemers.

The mechanisms by which recessive *CLCN1* mutations can cause myotonia are manyfold as the required final outcome is just a significant reduction of ClC-1 currents under physiological conditions. Recessive *CLCN1* mutations may affect ClC-1 by abolishing protein expression altogether, by enhanced degradation of probably misfolded proteins (450, 626, 861), impaired surface expression (710), or changes in biophysical properties like single channel conductance (894, 912) and gating (189, 233, 667, 894, 912, 918, 947).

Myotonia is also a symptom of myotonic dystrophy, a multi-system disorder which is caused by $(CTG)_n$ expansion in the 3′-untranslated region of the DM1 protein kinase (DMPK) gene or $(CCTG)_n$ repeats in an intron of the zinc

finger protein-9 gene (*ZFN9*). Both DMPK and ZFN9 mutant transcripts accumulate in nuclei of skeletal muscle and sequester CUG-repeat binding proteins such as muscleblind-like which have a role in regulated splicing (119, 405, 551). This entails aberrant splicing with an inclusion of the frameshift-inducing exon7+, which is also observed in early postnatal muscle (495) and reduces ClC-1 mRNA and g_{Cl} to levels that cause myotonia (119, 496, 518). Several preclinical studies aim at restoring normal *Clcn1* splicing in mouse models for myotonic dystrophy using oligonucleotides (424, 903) or small molecules identified in reporter screens (602).

E. A Role for ClC-1/ClC-2 Heteromers in Skeletal Muscle?

Skeletal muscle not only expresses ClC-1, but also the widely expressed ClC-2 Cl^- channel (832) with which it shares roughly 55% identity. ClC-1 and ClC-2 can form heteromeric channels with altered properties when coexpressed (484). Whereas ClC-1 is opened by depolarization and ClC-2 opens slowly with hyperpolarization, ClC-1/ClC-2 heteromers showed almost time-independent, ohmic currents (484). Prominent and roughly similar changes in gating were also observed with ClC-1—ClC-2 concatemers in which both subunits were covalently linked (814). However, the covalent linkage affected the phenotype which was evident from different gating properties when subunits were arranged in the opposite order and which may relate to the role of the ClC-2 NH_2 terminus in slow gating (303). Very surprisingly, single-channel conductances of ClC-1—ClC-2 concatemers were reported to differ from those of ClC-1 or ClC-2 homodimeric channels (814). This contrasts with the unchanged single-channel amplitudes of ClC-1, ClC-2, and ClC-0 protopores with ClC-1—ClC-0 and ClC-2—ClC-0 concatemers (897). Unchanged single-channel properties would be expected from the observation that the permeation pathway is entirely contained in each CLC protein subunit (210).

Regardless of these discrepancies, the question arises whether ClC-1/ClC-2 heteromers, which do not yield significantly more currents than a superposition of currents from the respective homooligomers, play a significant physiological role. In view of the probably much higher skeletal muscle expression of ClC-1 compared with ClC-2, which is supported by the near-total loss of g_{Cl} and the appearance of myotonia upon genetic loss of ClC-1, but not of ClC-2, the answer is most likely negative.

F. Roles of ClC-1 Beyond Skeletal Muscle?

Northern blot analysis using a full-length ClC-1 cDNA as probe detected robust ClC-1 mRNA expression in skeletal muscle (807). ClC-1 transcripts were almost undetectable in tissues like brain, liver, kidney and lung, with heart possibly showing a very faint hybridization signal (807). Likewise, Northern analysis by Conte Camerino and colleagues detected ClC-1 in skeletal muscle, but not in heart (654). Surprisingly, Noebels and co-workers (123) recently suggested that ClC-1 shows widespread tissue expression that prominently includes brain and heart. However, the antibodies used to detect ClC-1 in Western blots of brain and muscle were not *knockout* controlled and the RT-PCR employed to detect *Clcn1* transcripts used a large number of amplification cycles (35 to 40). Indeed, the similar abundance of amplification products in brain, heart, and muscle suggests that PCR amplification had reached saturation (123). In particular, there was no difference in signal intensities when PCR was performed on RNA derived from 10-day-old or adult mouse skeletal muscle (123), which conflicts with the well-known increase of ClC-1 expression (807, 909) during that time.

Noebels and co-workers (123) also suggested a role of brain-expressed ClC-1 in human epilepsy. They reported a threefold increase of nonsynonymous single nucleotide polymorphisms in the *CLCN1* gene of patients with idiopathic epilepsy versus controls and identified a heterozygous nonsense mutation in *CLCN1* (R976X; which deletes the last 12 amino acids of the ClC-1 protein) in one of the patients. The functional effect of this truncation, which deletes a significantly shorter part of the COOH terminus than the well-characterized myotonia-associated R894X mutation (287, 333, 507, 540, 626), was not assessed functionally, and the patient carrying this mutation did not display myotonia (123). A recent report (466) found one patient with epilepsy and limbic encephalitis in a family affected by dominant (Thomsen) myotonia due to the well-characterized I290M mutation (670, 679), but epilepsy in that patient was likely due to the presence of anti-GAD antibodies. Hence, there is currently no convincing evidence for a role of ClC-1 in epilepsy. Moreover, such a role appears unlikely because patients with *CLCN1*-associated myotonia generally do not display epilepsy and because brain expresses only low amounts of the highly muscle-specific ClC-1 channel.

G. Pharmacology of ClC-1

Small organic acids have long been known to reduce the skeletal muscle Cl^- conductance, g_{Cl}. In particular, g_{Cl} is reduced by 9-anthracene-carboxylic acid (9-AC) (87, 618) and clofibric acid derivatives (144, 174). Both types of compounds have been confirmed to act directly on ClC-1 (33, 38, 807) with apparently different mechanism of function: 9-AC reduces the currents in a voltage-independent manner, whereas 2-(*p*-chlorophenoxy)propionic acid (CPP) leads to an apparent shift of the voltage dependence to more positive voltages (33). In qualitative agreement with its effect on skeletal muscle g_{Cl} (144), only the S(-) enantiomer

was effective (33). The reported small activating effect on g_{Cl} of the R(+) enantiomer (144, 174) is not seen in heterologously expressed ClC-1 (33, 675).

Using inside-out and outside-out patch-clamp recordings, both CPP and 9-AC were found to act directly on ClC-1 only when applied to the intracellular side of the membrane (672, 675), and 9-AC block was found to be voltage dependent similar to CPP-induced inhibition, however with a slow unblocking kinetics at positive voltages (672).

The relative specificity of channel block by 9-AC for ClC-1 versus ClC-0 and ClC-2 was experimentally exploited, e.g., to characterize heterodimers of ClC-0 with ClC-1 (897) and in a study of heteromeric channels between ClC-1 and ClC-2 (484), respectively. Furthermore, using a chimeric strategy and mutagenesis guided by the Ec-ClC-1 crystal structure, the putative binding sites of 9-AC and the CPP analogue CPA were found to be overlapping and close to the permeation pathway in a hydrophobic pocket (224). Lacking a ClC-1 crystal structure, however, the precise binding site is not clear at atomic detail. A modeling study of CPA binding to ClC-0 (569) identified superficial access binding modes by docking, and a deeper site in the pore by forced molecular dynamics (569). In the deep configuration, the negatively charged carboxylate moiety pointed to the gating glutamate (569) in agreement with strong effects of mutations of the gating glutamate on the apparent CPA affinity (224, 838). Several analogues of CPP, as well as niflumic acid, were found to inhibit ClC-1 in a similar manner, with adding a second phenoxy group resulting in a much more potent block (458–460).

The voltage-dependent inhibition of ClC-1 by CPP and CPP analogs is phenomenologically very similar to the action of intracellularly applied benzoate, hexanoate, and propionate (721). The mechanism by which these CPP analogs inhibit muscle-type CLC channels has been extensively studied in ClC-0, mostly using the simpler, nonchiral CPA. Using single-channel recordings, Pusch et al. (671) found that CPB (*p*-chloro-phenoxy-butyric acid) inhibits individual protopores of the double-barreled channel, inducing long closures consistent with a model in which CPB binds preferentially to closed channels in competition with Cl^-. Similarly, Accardi and Pusch (7) interpreted the voltage dependence of CPA/CPP block using a model in which CPA binds with high affinity to the closed state (of the fast gate) to act essentially as a gating modifier. Traverso and Pusch (838) found, in agreement with the mutagenesis study of Estévez (224), that the neutralization of the gating glutamate in the E166A mutant dramatically increased CPA affinity. They suggested that the E166A mutant can assume a conformation which resembles the closed state even though it is essentially locked open. CPA was proposed to bind to the closed conformation with rather high affinity, even though a simpler sequential binding model to a single open state could not be excluded (838).

These results show that the side chain of residues at position 166 have a significant steric influence on the affinity and permeability for CPA, even though the conduction of Cl^- is almost not affected. This "state-dependent" binding model was questioned by Chen and co-workers who found that other mutations of the gating glutamate, like E166Q or E166K, exhibited a very small affinity to CPA (954). They interpreted the effects of CPA on WT and mutated channel in a model with sequential binding of CPA to two binding sites, one close to the intracellular solution, and another one deep in the pore (954). In addition, Zhang et al. (954) proposed that CPA is aligned in the pore with its hydrophobic end oriented towards the gating glutamate, i.e., in the opposite orientation proposed by Moran et al. (569). In addition, Zhang and Chen (951) found that in the E166G mutant CPA can actually "punch" through the pore, when driven by large negative inside voltage. These results show that the side chain of residues at position 166 have a significant steric influence on the affinity and permeability for CPA, even though the conduction of Cl^- is hardly affected. In light of the crystal structure of the bovine ClC-K channel (628), which exhibits a very narrow pathway, it is rather surprising that molecules as large as CPA can permeate the ClC-0 pore. The result is however in agreement with the ability of intracellularly applied cysteine modifying reagents to modify the E166C mutant, in which the gating glutamate is replaced by a cysteine (955). In contrast, extracellularly applied cysteine modifying reagents are unable to affect this mutant (Pusch, unpublished result). It will be interesting to determine the precise binding of CPA and other small molecules in ClC-0 and ClC-1 at atomic resolution. Such studies could help to clarify if fast gating of these channels is associated with conformational changes beyond the movement of the side chain of E166.

In some cells including myotubes, the effect of drugs on ClC-1 currents is confounded by an (often Ca^{2+}-dependent) activation of PKC that may inhibit ClC-1 by phosphorylation (460, 653). For instance, all investigated statins inhibited ClC-1 by activating PKC, with only fenofibrate additionally blocking ClC-1 directly (653). Also niflumic acid, often used to inhibit Ca^{2+}-activated Cl^- channels (326) and which indeed acts on TMEM16A (104, 756) and TMEM16B (657), inhibits ClC-1 directly (42 μM) and indirectly through $[Ca^{2+}]_i$-dependent activation of PKC (460).

Unfortunately, we are still lacking ClC-1 inhibitors that display high affinity and specificity. While such drugs would be valuable for experimental studies in cells or animals, specific activators of ClC-1 might be useful to treat myotonia in those patients in which ClC-1 currents are not abolished, but reduced or shifted in their voltage dependence.

Sadly, no useful drug has emerged so far. The R(+) enantiomer of CPP increased muscle Cl^- conductance (144), but had no effect on heterologously expressed ClC-1 (33, 675). So far, only modulation of muscle Cl^- conductances by taurine (170, 171), insulin-like growth factor I (IGF1) (172), or PKC (173) appear to be feasible. However, no direct effect of taurine on ClC-1 expressed in *Xenopus* oocytes could be detected (Pusch, unpublished observation).

VI. ClC-2: A WIDELY EXPRESSED Cl^- CHANNEL INVOLVED IN VARIOUS PROCESSES

ClC-2 is a plasma membrane chloride channel that is found in cells of many, if not all, mammalian tissues (832). Macroscopic hyperpolarization-activated ClC-2-like currents have been described in many native cells including neurons in various brain regions (140, 256, 508, 702, 790, 797), sympathetic neurons (139), rod bipolar cells (221), astrocytes (239, 247, 346, 515, 516, 595) and oligodendrocytes (346), carotid chemoreceptors (643), trabecular meshwork cells (143), adrenal glomerulosa cells (246), hepatocytes (443), colon epithelial cells (109, 371), pancreatic acinar cells (105), salivary gland acinar (577, 629) and duct (197, 426, 709) cells, testicular Leydig and Sertoli cells (74), and erythrocytes (76, 361). Several studies used *Clcn2*$^{-/-}$ mice as controls to firmly establish that these currents are owed to ClC-2 (74, 246, 346, 361, 516, 577, 702, 709). *Clcn2*$^{-/-}$ mice also revealed that a prominent, cAMP-stimulated inwardly rectifying Cl^- current of choroid plexus cells (403), although reported to be reduced by anti-ClC-2 siRNA (404), is not mediated by ClC-2 (795). Less critical reviews focusing exclusively on ClC-2 and related diseases have been published recently (62, 875).

A. Properties of ClC-2

ClC-2 is a dimeric, "double-barreled" Cl^- channel with two pores and a single-channel conductance of ~3 pS (815, 834, 897) which remained unchanged when, in concatemeric channels, the neighboring subunit is from ClC-0 rather than from ClC-2 (897) **(FIGURE 2)**. It mediates macroscopic Cl^- currents that are slowly activated by hyperpolarization (832) **(FIGURE 7*A*)** that display the typical Cl > I selectivity of CLC channels. Hyperpolarization activation of ClC-2 depends on an NH_2-terminal cytoplasmic stretch which remained functional when transplanted to a cytoplasmic site between the two CBS domains (303), and an intracellular loop between helices J and K that was hypothesized to interact with the NH_2-teminal "inactivation domain" (399). Many mutations in either region lead to "constitutively open" ClC-2 channels **(FIGURE 7*B*)** that almost totally lacked gating relaxation and displayed much larger currents (303, 399). Much later, these regions turned out to be hotspots for human *CLCN2* mutations that cause primary aldosteronism by depolarizing aldosterone-producing adrenal glomerulosa cells through markedly increased efflux of Cl^- (246, 747). The effect of NH_2-terminal ClC-2 deletions or point mutations on gating is probably affected by a still unknown cytoplasmic factor because it is observed in two-electrode voltage-clamp measurements of *Xenopus* oocytes (303) or perforated patch measurements on transfected cells (856), but not in whole cell patch-clamp (856) or excised oocyte patches (674). The activation kinetics of ClC-2 also depends on the cell used for expression (629) and on the cholesterol content (344) and is slightly changed by intracellular ATP levels that most likely act by binding to its intracellular CBS domains (589, 815). Surprisingly, these CBS domains seem to be dispensable for ClC-2 channel function (280).

Akin to other CLC channels and transporters, the gating of ClC-2 depends on the concentrations of Cl^- and H^+. Raising the intracellular Cl^- concentration shifts the voltage dependence of ClC-2 to more positive potentials and thereby opens the channel (166, 588, 674, 730, 731), an effect that is likely to be physiologically important. At low $[Cl^-]_i$, ClC-2 gating is also influenced by extracellular Cl^- (730).

ClC-2 is strongly dependent on the extracellular pH in a biphasic manner: slightly acidic pH activates the channel, whereas stronger acidification blocks ClC-2 (36, 399). Activation occurs with an apparent Hill coefficient of 1, whereas block is more steeply dependent on the proton concentration with a Hill coefficient around 2 (36). Niemeyer et al. (587) identified histidine 532 at the extracellular, NH_2-terminal end of helix Q as the underlying proton sensor for acidification induced inhibition. Interestingly, mutants H532N and H532A were nonfunctional, whereas H532F lost acid induced inhibition (587). The analogous histidine (H497) mediates part of the inhibition of ClC-K channels by acidic pH (296). The mechanism underlying this inhibition is still unknown. In particular, it is unclear if protonation of this histidine residue results in the closure of the common gate. The respective histidine residue is conserved in ClC-0 and ClC-1, but its role in these channels is unknown.

The neutralization of the gating glutamate leads to an almost completely open phenotype as in ClC-0 and ClC-1 (588), with only some residual gating relaxations (178), suggesting that the gating glutamate is the key element of gating in ClC-2 and that basic gating mechanisms are conserved among these channels. The additional mutation H811A in the CBS-2 domain, the equivalent of which eliminated common gating in ClC-0 (223), resulted in a completely open phenotype (935). Further evidence for the presence of the two gating mechanisms in ClC-2, protopore gate and common gate, comes from the observation that mutat-

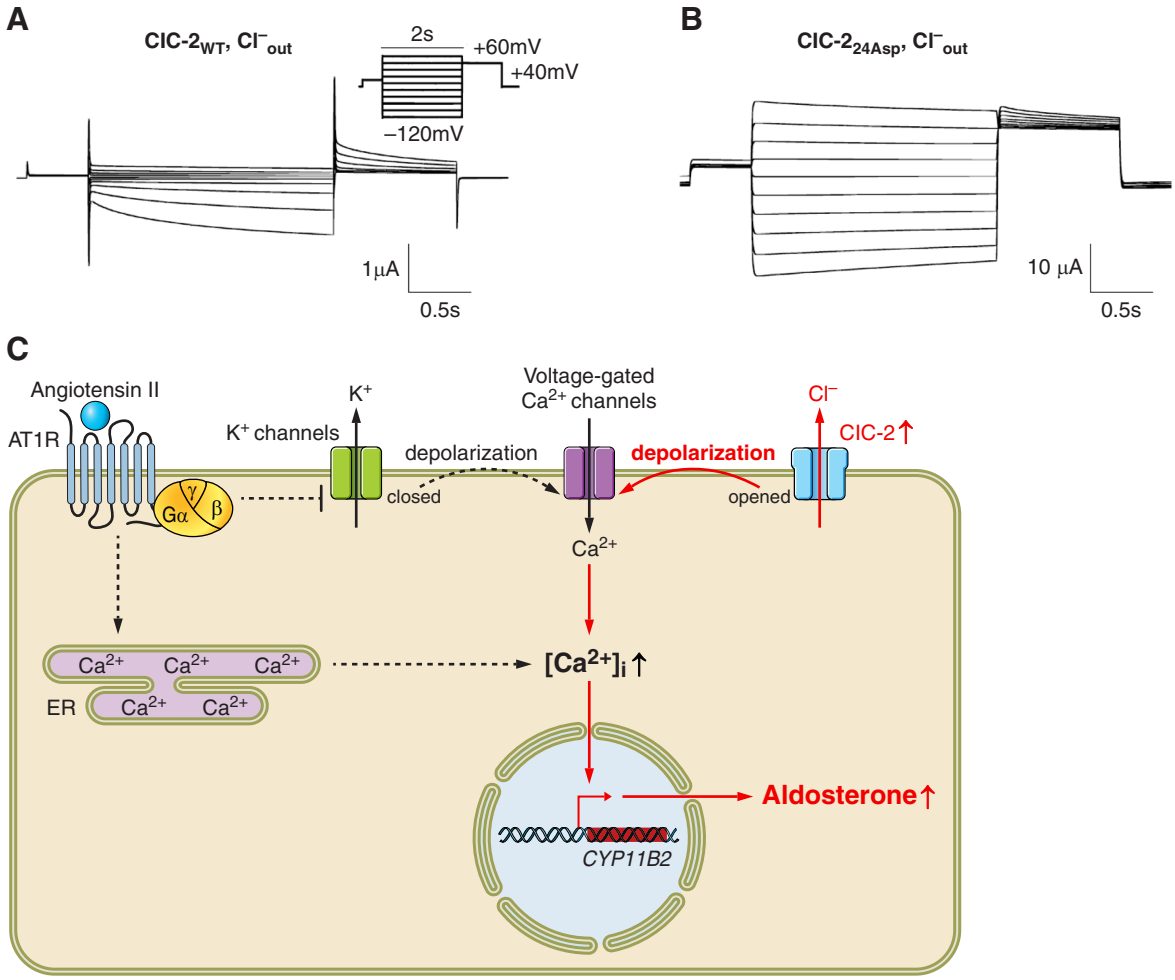

FIGURE 7. *CLCN2* gain-of-function mutations lead to primary aldosteronism. *A*: typical hyperpolarization-activated currents of ClC-2 in the *Xenopus* oocyte expression system. Currents slowly activate upon hyperpolarization beyond approximately −60 mV, leading to inward rectification of steady-state currents. *B*: currents from the G24D mutant identified in a patient with primary aldosteronism (246). It affects a residue in an amino-terminal "inactivation domain" previously identified to be crucial for the activation of ClC-2 by hyperpolarization and cell swelling (303, 399). It results in a large increase of ClC-2 currents that then almost totally lack voltage-dependent gating. *C*: model for the mechanism by which activating *CLCN2* mutations lead to hyperaldosteronism. In normal adrenal glomerulosa cells, binding of angiotensin II to its G protein-coupled receptor leads to an increase of IP_3 which releases Ca^{2+} from the ER, as well as to an inhibition of plasma membrane K^+ channels that largely determine the resting potential of these cells (794). This inhibition leads to a depolarization, which opens voltage-dependent Ca^{2+} channels, leading to a further increase of cytosolic Ca^{2+}. A rise in extracellular K^+ concentration can also directly depolarize glomerulosa cells. The large chloride currents observed with activating *CLCN2* mutations identified in patients with aldosteronism (246, 747) lead to constitutive depolarization of glomerulosa cells, Ca^{2+} influx, and increased aldosterone production by increased transcription of aldosterone synthase (red arrows). [Adapted from Fernandes-Rosa et al. (246).]

ing cysteine 256 (equivalent to C212 in ClC-0) to alanine led to a quite large fraction of constitutively open channels and to reduced block by extracellular Cd^{2+} (178, 971). Furthermore, in WT ClC-2, activation time constants of both processes were highly temperature sensitive, suggesting that in ClC-2 the two gates appear to be strongly coupled as in ClC-1 (971).

In contrast to ClC-0 and ClC-1, extracellular Cl^- and intracellular protons (731) have little effect on ClC-2 gating, which is instead mostly controlled by voltage, extracellular pH, and intracellular Cl^- (36, 399, 588, 674). The activation by mild acidic pH is most likely mediated by the protonation of the gating glutamate of ClC-2 (587). However, a major question is if the primary, voltage-dependent event, driving the displacement of the gating glutamate from its blocking position is a movement of a Cl^- from the inside, pushing the glutamate side towards the outside, or a H^+, protonating the gating glutamate from the outside. Niemeyer et al. (587) found that the apparent pK of acidification activation was voltage dependent with an apparent electrical distance from the outside of 0.62, favoring the idea that voltage-dependent protonation followed by allosteric stabilization by a Cl^- underlies gating of ClC-2. In

contrast, detailed studies from the Arreola group favor the idea that a Cl^-, coming from the inside, displaces the negatively charged gating glutamate, which is then stabilized by voltage-independent protonation from the outside in the open configurations (166, 730, 731). A strong argument of Arreola and colleagues was that they could open ClC-2 channels even at extracellular pH 10, which appears impossible if protonation is a prerequisite for channel opening (730, 731). Interestingly, also several intracellularly applied, impermeant anions are able to favor channel opening (166). Overall, these experiments indeed strongly favor the idea that ClC-2 is opened by intracellular Cl^-. Nevertheless, it might be insightful to perform detailed kinetic analysis in a simplified system, for example, with channels harboring mutations that eliminate slow gating in addition to the H532F mutant, allowing to extract opening and closing rate constants over large voltage ranges, similar to what has been done for ClC-0 (128, 963).

ClC-2 can also be activated by osmotic cell swelling (303, 399). This process involves the same intracellular structures that are important for the activation by hyperpolarization (303, 399). Native bona fide ClC-2 currents were increased by osmotic cell swelling in parotid acinar cells (577), but the volume regulation of these cells did not differ in *Clcn2*$^{-/-}$ mice. Although Bergmann glia appears to be slightly swollen in *Clcn2*$^{-/-}$ mice (346) and though insect cells heterologously overexpressing ClC-2 appear to display accelerated regulatory volume decrease (923), there is currently no convincing evidence that native ClC-2 plays a significant role in cell volume regulation. This contrasts with the volume-regulated anion channel VRAC that is clearly involved in regulatory volume decrease (386). It should again be made clear that the inwardly rectifying ClC-2 is distinct (303) from the slightly outwardly rectifying VRAC, which is now known to be composed of LRRC8 heteromers (821, 865).

Besides modulation by Cl^-, H^+, and ATP, other pathways may influence or regulate ClC-2 activity. Several reports suggest that ClC-2 may be the direct or indirect target of quite a few different kinases (271, 276, 352, 417, 619, 630, 887), but most of these studies need to be replicated, and their biological relevance remains unclear. The same holds true for the reported interactions of ClC-2 with cereblon (347), Hsp90 (345), and the dynein motor complex (192). In contrast, the interaction of ClC-2 with the adhesion molecule GlialCAM (also known as HepaCAM) appears firmly established. As discussed below, it changes the subcellular localization of ClC-2 and its biophysical properties (98, 346, 394, 395).

B. Loss of ClC-2 Leads to Male Infertility, Blindness, and Leukodystrophy

Disruption of *Clcn2* in mice leads to male infertility and blindness (74) as well as to slowly developing leukodystrophy, a degeneration of brain white matter (68). These phenotypes were reproduced in independently generated ClC-2 KO mice (150, 577) and in a chemically induced mouse mutant in which a stop codon truncates the ClC-2 protein within the transmembrane part (212). Moreover, *Clcn2* disruption decreased intestinal Cl^- absorption (111, 939).

Initial screening of 150 leukodystrophy patients (68) and of 18 patients with megalencephalic leukoencephalopathy with subcortical cysts (746) gave negative results, but *CLCN2* mutations (often resulting in stop codons on both alleles) were later identified in leukoencephalopathy patients who variably presented also with ataxia and visual disturbances (187, 289, 886) or paroxysmal dyskinesia (323, 944). A *CLCN2* mutation associated with leukodystrophy, electroretinogram abnormalities, and male infertility due to azoospermia has also been described (193). Human and mouse phenotypes of ClC-2 deficiency are not identical, but show significant overlap.

Clcn2$^{-/-}$ mice display severe testicular degeneration and azoospermia (74). Testes histology is normal during the first postnatal week, but seminiferous tubules of ClC-2-deficient mice fail to develop their normal lumen during their postnatal development. Germ cells are lost during the first four postnatal weeks after which tubules are filled with abnormal Sertoli cells. In the absence of changes in sex hormones, the testicular degeneration was suggested to result from defective transepithelial transport by Sertoli cells (74). These cells form the blood-testis barrier and "nurse" the developing germ cells by, for instance, regulating the ionic environment of spermatids and spermatocytes, providing nutrients, and phagocytosing residual cytoplasm from spermatids. Intriguingly, ClC-2 is concentrated in patches at contacts between Sertoli cells (74). Whereas a superficially similar patchy localization of ClC-2 at astrocytic contacts is mediated by the cell adhesion protein GlialCAM (346), the mechanism underlying ClC-2 clustering at Sertoli cell contacts remains unknown.

The blindness of *Clcn2*$^{-/-}$ mice ensues from an early postnatal degeneration of the photoreceptors, which eventually entails a complete degeneration of the retina (74). Again, this phenotype was tentatively attributed to impaired ion transport by "nursing cells," in this case the retinal pigment epithelium (RPE) (74). These cells form the blood-retinal barrier, regulate the ionic environment of photoreceptors, remove metabolites and supply nutrients, and phagocytose photoreceptor outer segments. Impaired ion transport by the RPE of *Clcn2*$^{-/-}$ mice was supported by reduced transepithelial currents in Ussing chamber experiments, with the caveat that the degeneration might already have changed the structural integrity of the RPE (74). *Clcn2*$^{-/-}$ RPE cells showed extended microvilli even before the loss of photoreceptors, and electroretinograms from heterozygous *Clcn2*$^{+/-}$ mice (which lack retinal degeneration) revealed

moderately changed RPE responses (212). Hence, both the testicular and retinal degeneration were suggested to result from impaired control of the extracellular environment by nursing epithelial cells (74). The transport of lactate by both the RPE and Sertoli cells requires an efficient regulation of extracellular pH in the narrow clefts between these nursing cells and photoreceptors and germ cells, respectively. It was therefore hypothesized that this regulation involves an interplay between Cl^-/HCO_3^- exchangers and the (pH_o-sensitive) ClC-2 Cl^- channel (74).

C. Gain-of-Function CLCN2 Mutations Lead to Aldosteronism

Gain-of-function mutations in the *CLCN2* gene were recently found to result in primary aldosteronism (246, 747), a condition in which dysregulated, constitutive production of aldosterone by adrenal glomerulosa cells entails severe hypertension and hypokalemia (245, 794). Gratifyingly, several of the identified human mutations (246, 747) change amino acids in the NH_2-terminal "inactivation domain" of ClC-2 that had been identified previously by structure-function analysis (303). One mutation affects a residue in the linker between helices J and K (747), a region previously postulated to interact with the NH_2-terminal inactivation domain (399). These mutations, like those previously engineered in the above-mentioned structure-function studies (303, 399), largely abolish the voltage-dependent gating of ClC-2 and significantly increase Cl^- currents **(FIGURE 7*B*)** (246, 747). This gain of function agrees with the dominant effect of the mutations that in patients are present in a heterozygous state. Because cytoplasmic chloride concentration in glomerulosa cells is higher than predicted by the Cl^- equilibrium potential, expression of these ClC-2 mutants depolarized adrenocortical H295R-S2 cells (246) and led to an induction aldosterone synthase and increased aldosterone production (246, 747). Experiments with Ca^{2+} channel inhibitors strongly suggested that the increase in aldosterone synthesis is mediated by an increase of cytosolic Ca^{2+} due to an opening voltage-gated Ca^{2+} channels (246) **(FIGURE 7*C*)**. It is currently unclear whether the "opening" of ClC-2 by these mutations entails pathological changes in other tissues or cells and whether WT ClC-2 influences aldosterone production under physiological conditions. Since the resting membrane potential of glomerulosa cells is very close to the K^+ equilibrium potential (794), however, a loss of ClC-2 is unlikely to significantly hyperpolarize these cells. No changes in blood pressure were reported for *Clcn2*$^{-/-}$ mice (74, 577) nor for patients with loss-of-function mutations in *CLCN2* (187, 289, 886), but this issue has not been investigated in detail.

D. ClC-2 in Epithelia

ClC-2 was suggested to play a role in Cl^- secretion in lung surface epithelia (66, 67, 574, 762) and in the intestine (158, 318, 565) and was also proposed to be able to compensate for the loss of CFTR Cl^- channels in cystic fibrosis. This hypothesis, however, requires that ClC-2 is present in apical membranes, an assumption that is most likely wrong.

The localization of ClC-2 to either the apical or basolateral membranes of epithelial cells was a matter of considerable controversy because of the lack of specific, *knockout* controlled antibodies. Initially ClC-2 was reported to reside in the apical membranes of lung surface epithelia (66, 475, 574) and at tight junction complexes of ileal surface epithelia (318). The latter labeling superficially resembles the KO-controlled dotlike ClC-2 staining of testicular Sertoli cells (74). However, it is now firmly established that ClC-2 is expressed at the basolateral membrane of intestinal epithelia (jejunum and colon) (109, 110, 475, 641) (Zdebik and Jentsch, unpublished data) and salivary gland ducts (709). Several of these results were controlled by the absence of staining in *Clcn2*$^{-/-}$ tissue (641, 709) (Zdebik and Jentsch, unpublished data). Moreover, when transfected into polarized epithelial cell lines like MDCK, ClC-2 was sorted to basolateral membranes (167, 641). Initially a dileucine motif in the second intracellular CBS domain was suggested to mediate basolateral sorting (641), but a more recent study (167) demonstrates that rather a dileucine motif in the first CBS domain interacts with AP-1 adaptors and is crucial for the basolateral sorting of ClC-2. These data suggest that ClC-2 may universally localize to basolateral membranes, with the likely exception of choroid plexus and retinal pigment epithelium in which normally basolateral proteins like the Na^+-K^+-ATPase are targeted to apical membranes.

Functional data also support a basolateral localization of ClC-2. Whereas there was no effect of *Clcn2*-disruption on the secretion of saliva (709), currents across colonic epithelia investigated in Ussing chambers showed that cAMP-stimulated Cl^- secretion was increased in *Clcn2*$^{-/-}$ mice (939), indicating that, in contrast to apical cAMP-activated CFTR, basolateral ClC-2 mediates Cl^- reabsorption. Moreover, the early lethality of *Cftr*$^{\Delta F508/\Delta F508}$ mice, that likely results from intestinal obstruction as a consequence of decreased fluid secretion, was ameliorated rather than exacerbated by the additional disruption of *Clcn2* (939). The role of ClC-2 in colonic Cl^- reabsorption rather than secretion was confirmed in another study that used a different *Clcn2*$^{-/-}$ strain (111). A basolateral localization of ClC-2 is bolstered by functional studies in which apical membranes of colon surface epithelia were permeabilized (110). Finally, immunohistochemistry and electrophysiology localized ClC-2 to the surface epithelium that is involved in salt reabsorption, rather than to crypts that coexpress CFTR and NKCC1 and are the sites of intestinal Cl^- secretion (109–111, 318, 371).

In spite of the well-established basolateral localization of ClC-2 and its role in intestinal Cl^- reabsorption, a drug,

lubiprostone, has been widely claimed to ameliorate obstipation by specifically opening apical ClC-2 channels in the intestine (25, 117, 158). However, the assertion that lubiprostone is a specific activator of ClC-2 is based on a publication by Cuppoletti and co-workers that reported effects on linear, time-independent currents that differ markedly from ClC-2 currents (158). When tested at the same concentration (1 μM) on typical, slowly activating inwardly rectifying currents obtained from heterologously expressed ClC-2, however, lubiprostone had no effect (599). Lubiprostone was also reported to activate a small-conductance, "ClC-2-like" channel in *Xenopus* A6 cells, but the gating kinetics of those channels (41) appeared slower than those reported for mammalian ClC-2 in other studies (815, 834, 897). Lubiprostone activated CFTR, but not ClC-2, when coexpressed with the prostanoid E_4 receptor (599). Several studies showed that lubiprostone, a bicyclic fatty acid derived from prostaglandin E_1, acts by stimulating prostanoid receptors (15, 48, 117, 159, 376). The effect on intestinal Cl^- secretion may occur by stimulating cAMP-dependent CFTR (29, 64, 599), although CFTR-independent actions were also reported (169, 376). Since ClC-2 has a role in intestinal Cl^- reabsorption rather than Cl^- secretion, the beneficial effect of lubiprostone on obstipation cannot be explained by an opening of ClC-2 (255, 384). If lubiprostone activates intestinal ClC-2 channels, it would cause obstipation rather than alleviating it.

The effect of lubiprostone on the recovery of the intestinal mucosal barrier after ischemia led Blikslager and co-workers to postulate a role of ClC-2 in this process (561). They further supported this notion by experiments with *Clcn2*$^{-/-}$ mice (398, 591). These results await replication by other laboratories.

ClC-2 was also speculated to be the Cl^- channel expressed in apical and tubulovesicular membranes of gastric parietal cells, where it is thought to be involved in gastric HCl secretion (517). However, the $Cl^- > I^-$ selectivity of ClC-2 (275, 399, 832) and its 3 pS single-channel conductance (815, 834, 897) differs from the $I^- > Cl^-$ selectivity and 7 pS conductance of Cl^- channels reconstituted from bona fide acid-transporting membranes from gastric mucosa (157). ClC-2 is weakly expressed in stomach as indicated by Northern (351, 832) and Western blots (590; but see Ref. 351). Immunohistochemistry seemed to suggest prominent ClC-2 expression in parietal cells (771). However, the labeling lacked essential KO controls and was much stronger and broader compared with the sparse dotlike fluorescence later reported by the same group (590). Although KO-controlled ClC-2 immunostaining prominently labeled ClC-2 in the colon and duodenum, it failed to detect ClC-2 in the stomach (641). Most importantly, *Clcn2* deletion did not affect histamine-induced gastric acid secretion (74). In contrast, Blikslager, Cuppoletti and colleagues more recently reported impaired gastric acid secretion in different *Clcn2*$^{-/-}$ mice (590). These mice, however, showed changes in gastric morphology, including a loss of parietal cells and H^+-K^+-ATPase (590), observations not made by others (641). Hence, there is no convincing evidence that ClC-2 is the apical parietal cell Cl^- channel that, together with the H^+-K^+-ATPase, is responsible for gastric HCl secretion.

E. ClC-2 in the Nervous System and Interaction With GlialCAM

Being almost ubiquitously expressed, ClC-2 has been detected in neurons, astrocytes, and oligodendrocytes using electrophysiology (139, 221, 239, 247, 256, 346, 508, 515, 516, 595, 702, 797) and immunohistochemistry (68, 187, 346, 777). ClC-2 has been localized to cell bodies and neurites of hippocampal neurons (777), prominently on Bergmann glia (68, 346), and was found in clusters at astrocytic endfeet contacting brain capillaries and at contacts between astrocytes and oligodendrocytes (68, 187, 346, 777). These results have been controlled by absence of staining in *Clcn2*$^{-/-}$ mice (68, 346). Disruption of *Clcn2* in mice led to slowly developing widespread vacuolization in the white matter of the brain and the spinal cord (68). Vacuolization was particularly evident in cerebellum and was associated with an upregulation of inflammation markers and with a disruption of the blood-brain barrier (68). Fluid-filled spaces appeared between myelin sheaths of central, but not peripheral neurons. Neurons appeared normal and, except for a decrease in nerve conduction velocity in the central auditory pathway, no neurological abnormalities were noticed (68). More recently, mild neuronal degeneration has been observed in old *Clcn2*$^{-/-}$ mice which also displayed mild abnormalities in electrocorticographic recordings (150). However, no spontaneous epilepsy nor a reduction of seizure thresholds were observed (68, 150). In contrast, various and variable neurological abnormalities, including ataxia, spasticity, and visual disturbances, have been found in patients with homozygous inactivating *CLCN2* mutations (187, 193, 323). Human *CLCN2*-related leukoencephalopathy is characterized by characteristic signs of white matter edema in MRT imaging (187).

Akin to the hypothesis brought forward to explain the testicular and retinal degeneration, the leukodystrophy caused by loss of ClC-2 might result from impaired regulation of the extracellular space (68), in this case by the astrocytic-oligodendrocytic syncytium. Extracellular potassium, which is released from neurons during electrical activity, is taken up by astrocytes and equilibrated with the blood through astrocytic endfeet in a process dubbed "potassium siphoning." This is important as in the narrow clefts surrounding neurons extracellular K^+ could otherwise easily reach concentrations sufficiently high to depolarize and excite neurons. Similarly, ClC-2 may serve to buffer extracellular chloride at GABAergic synapses (777) and guarantee

net electroneutral uptake of K^+ and Cl^- through independent, parallel K^+ and Cl^- channels (68). Indeed, ClC-2 is coexpressed with key components involved in K^+ siphoning such as the K^+ channel Kir4.1 (KCNJ10), aquaporin 4, and the gap junction proteins connexin 47 (Cx47) and Cx32 at astrocytic endfeet and astrocyte-oligodendrocyte contacts (90, 418, 579). Disruption of Kir4.1 and double-KO of Cx32 and Cx47 led to myelin vacuolization (538, 539, 579) resembling that of *Clcn2*$^{-/-}$ mice. In optic nerves, this vacuolization could be prevented by inhibiting its electrical activity with tetrodotoxin (539). The fact that optic nerves lacked vacuolization in *Clcn2*$^{-/-}$ mice [which are blind (74)] indirectly bolsters the hypothesis that glial ClC-2 functions in buffering extracellular K^+ and Cl^- concentrations (68).

In glia, the abundance of ClC-2 and its subcellular localization depend on the cell adhesion molecule GlialCAM (346) which physically binds ClC-2 (395). Although also called HepaCAM because of its downregulation in hepatocellular carcinoma (137, 562, 563), GlialCAM is mainly found in brain where its expression is restricted to astrocytes and oligodendrocytes (240). Mutations in GlialCAM (483) and of its protein interaction partner MLC1 (451) led to megalencephalic leukoencephalopathy with subcortical cysts (MLC), another form of leukodystrophy. Heterologous expression showed that GlialCAM localizes both MLC1 and ClC-2 to cell-cell contacts (395, 483) **(FIGURE 8)**. Indicative of homophilic GlialCAM interactions *in trans*, this localization requires the presence of GlialCAM in both cells (346). In *Glialcam*$^{-/-}$ mice, the loss of Glialcam mislocalizes and destabilizes Mlc1 and ClC-2, and rather surprisingly also the loss of Mlc1 (in *Mlc1*$^{-/-}$ mice) destabilizes and mislocalizes GlialCAM and ClC-2 (88, 204, 346), suggesting a complex formed by all three proteins.

GlialCAM not only affects the subcellular localization of ClC-2, but also changes its biophysical properties. Heterologous coexpression increases ClC-2 current amplitudes and converts its slowly activating, inwardly rectifying currents to almost linear, time-independent currents (395) **(FIGURE 8*E*)** by an effect on the slow ClC-2 gate (394). When comparing WT with *Glialcam*$^{-/-}$ mice, a similar effect on ClC-2 currents was observed in oligodendrocytes, but surprisingly not in Bergmann glia (346). The similarities in the leukodystrophies of *Clcn2*$^{-/-}$, *Glialcam*$^{-/-}$, and *Mlc1*$^{-/-}$ mice (346) suggest that this pathology may be in part due to the loss of ClC-2 currents and resulting consequences for ion homeostasis. However, the additional disruption of *Glialcam* worsened the white matter vacuolization of *Clcn2*$^{-/-}$ mice (346). Hence, the loss of Glialcam likely has additional detrimental effects, possibly because of the loss and mislocalization of Mlc1 (100, 346) or other binding partners (919).

Disease-causing mutations in *GLIALCAM* interfere with its binding to ClC-2 and Mlc1 (31, 32, 395, 483), and GlialCAM regions required for the interaction with ClC-2 and MLC1 have been mapped (98). It was found that the extracellular domain of GlialCAM is necessary for cell junction targeting and for mediating interactions with itself or with MLC1 and ClC-2 (98). The COOH terminus is also necessary for proper targeting to cell-cell junctions, but is not needed for the biochemical interaction. Interestingly, the first three amino acids of the transmembrane segment of GlialCAM are essential for the activation of ClC-2 currents

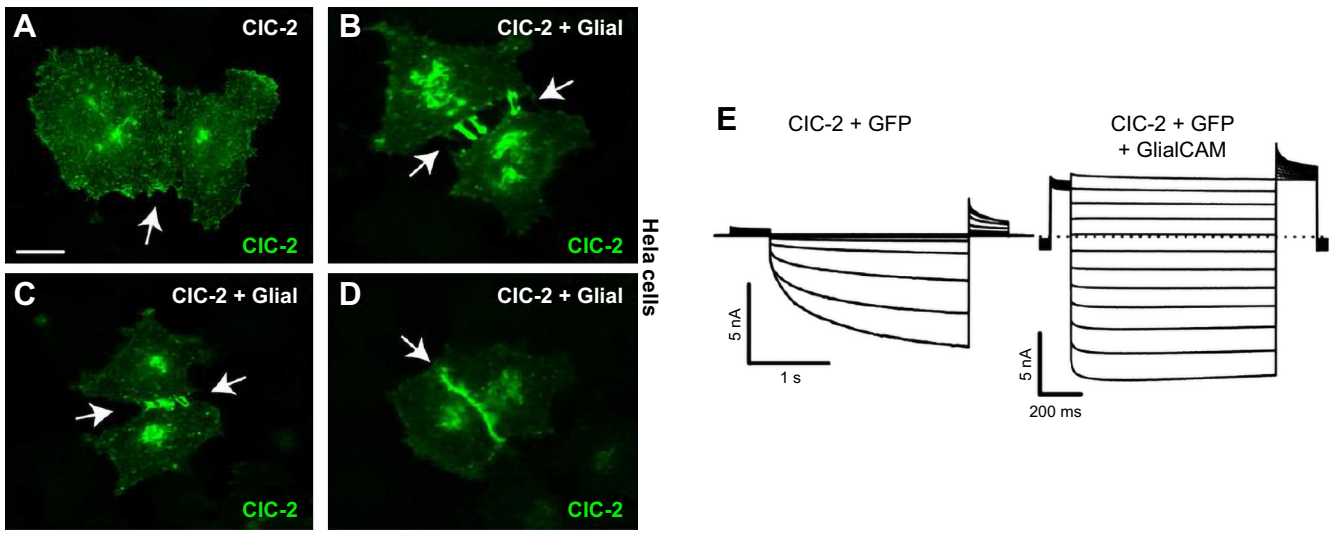

FIGURE 8. Clustering of ClC-2 at cell junctions and change of rectification properties of ClC-2 currents by GlialCAM in heterologous expression systems. *A*: in transiently transfected HeLa cells, ClC-2 is diffusely localized to the plasma membrane. Upon coexpression of GlialCAM, the channel is localized at long (*B*) or short (*C*) cell contact processes, or in extensive contact regions (*D*) (see arrows). *E*: in the absence of GlialCAM, ClC-2 currents activate slowly at negative voltages (*left*) but are almost constitutively active at all voltages in transfected HEK cells (*right*). [From Jeworutzki et al. (395).]

but are not involved in the clustering (98). It has been proposed that in astrocytes a ternary complex between ClC-2, GlialCAM, and MLC1 forms only upon exposure to high extracellular potassium concentrations (785). However, the physiological importance and the underlying mechanism remain obscure. The stoichiometry of the ClC-2/GlialCAM complex and the regions of the channel involved in the interaction are still unknown.

GlialCAM has been suggested as a ClC-2 auxiliary "β-subunit" (395). However, in contrast to barttin, the β-subunit of ClC-K channels (222), and Ostm1, the β-subunit of ClC-7 (445), it is not specific for this CLC isoform. In heterologous expression, GlialCAM also modifies currents of ClC-0, ClC-1, and ClC-K and clusters them at cell-cell contacts (394). The fact that GlialCAM interacts with ClC-Ka/barttin suggests that GlialCAM and barttin subunits have nonoverlapping interaction regions. Since GlialCAM also clusters and stabilizes MLC1 (483) and Cx43 (919), its interaction with transmembrane proteins seems quite promiscuous and hence its loss of function might cause leukodystrophy via several pathways.

In most adult neurons, $[Cl^-]_i$ is below electrochemical equilibrium to enable hyperpolarizing influx of Cl^- through inhibitory $GABA_A$- or glycine-receptor Cl^- channels. Likewise, the presence of a partially constitutively open Cl^- channel like ClC-2 may dampen neuronal excitability by providing hyperpolarizing and shunting currents. It is therefore conceivable that disruption of ClC-2 might lead to epilepsy. Intriguingly, linkage analysis identified a locus for idiopathic generalized epilepsy to 3q26, the chromosomal region that harbors the *CLCN2* gene (732). However, *Clcn2*$^{-/-}$ mice display neither spontaneous epilepsy nor reduced seizure threshold (68, 74). A widely cited paper asserting that *CLCN2* mutations underlie different forms of epilepsy in humans appears to be fraudulent and has been retracted (328). Even though there are some reports of *CLCN2* variants in epileptic patients (160, 225, 726), there is no convincing evidence that *CLCN2* mutations cause human epilepsy (68, 586, 589, 812).

ClC-2 may also influence neuronal $[Cl^-]_i$. In turn, ClC-2 activity is strongly dependent on $[Cl^-]_i$ (588, 674, 730). In contrast to the neuronal K^+Cl^- cotransporter KCC2, the main player in establishing the low $[Cl^-]_i$ of adult neurons (362, 704), a Cl^- channel such as ClC-2 can lower $[Cl^-]_i$ only down to its electrochemical equilibrium, as experimentally demonstrated by transfection of ClC-2 into dorsal root ganglia neurons whose $[Cl^-]_i$ is normally above equilibrium (798). Owing to lower $[Cl^-]_i$, transfected neurons displayed hyperpolarizing rather than depolarizing GABA responses. ClC-2 might also lower neuronal $[Cl^-]_i$ when it is elevated by intense GABAergic activity (256, 702), although mathematical modeling suggests that this does not occur under physiological conditions (692). However, the model by Ratté and Prescott (692) appears of limited value in that it did neither take into account the fundamental activity of the Na^+/K^+ pump, nor the $[Cl^-]_i$ dependence of ClC-2.

Two groups studied the role of ClC-2 in neurons using hippocampal slices from WT and *Clcn2*$^{-/-}$ mice (256, 702). Stein and co-workers (702) recorded substantial, typical ClC-2 currents from CA1 pyramidal cells and found rather surprisingly that ClC-2 contributes ~40% to their resting conductance. When lacking ClC-2, CA1 cells were intrinsically hyperexcitable, but this did not result in increased basal synaptic transmission in field recordings and unexpectedly led to decreased input/output relations. These may be explained by increased feed-forward inhibition by hyperexcitable interneurons (702). Földy et al. (256) reported differential effects of postsynaptic ClC-2 at inhibitory basket cell-pyramidal cell synapses, with ClC-2 proposed to lower cytoplasmic Cl^- specifically at fast-spiking synapses where intense activation of $GABA_A$ receptors may lead to an increase in $[Cl^-]_i$.

F. Pharmacology of ClC-2

ClC-2 is only weakly sensitive to classical Cl^- channel blockers like DIDS or 9-AC (139, 675, 832) as well as by Zn^{2+} and Cd^{2+} (139, 971). Using the differential sensitivity of ClC-1 and ClC-2 to 9-AC and clofibrates, and employing a chimeric strategy, Estévez et al. (224) found that by the single amino acid change T518S, ClC-2 became 8-fold more sensitive to 9-AC, while the opposite mutation in ClC-1 (S537T) decreased 9-AC sensitivity ~40-fold. The residue is located between helices O and P in the above-described putative hydrophobic binding pocket. The same mutation also dramatically increased affinity for CPA in ClC-2 (224). As for ClC-1, these compounds act from the intracellular side (224).

Thompson et al. reported that a component of the *Leiurus quinquestriatus* scorpion venom moderately inhibited ClC-2 from the extracellular side in a voltage-dependent manner (833). Later, a peptide from the venom, called GaTx2, was isolated that inhibited ClC-2 with a surprisingly high apparent affinity of 20 pM with no effect on other CLCs or GABA receptor Cl^- channels, but the same moderate effect (~60% inhibition) (834). Unfortunately, the toxin has not been used or independently verified in follow-up studies.

As discussed above, the evidence for activation of ClC-2 by lubiprostone, a drug used to treat chronic constipation (25), is highly controversial. In summary, no specific or high-affinity small molecule ligands exist for ClC-2, and the GatTx2 toxin has still to prove its usefulness.

VII. ClC-Ka/Kb-BARTTIN CHANNELS: HIGHLY CELL-SPECIFIC Cl^- CHANNELS MUTATED IN CERTAIN FORMS OF KIDNEY DISEASE AND DEAFNESS

Human ClC-Ka and -Kb, or rodent ClC-K1 and -K2 (10, 415, 845), are two highly homologous epithelial Cl^- channels that need the ancillary β-subunit barttin (encoded by the *BSND* gene), a small protein with two transmembrane domains (65), for functional expression at the plasma membrane (222). Both ClC-K isoforms and barttin are expressed in a highly tissue-specific pattern in nephron segments and epithelial cells of the cochlea and the vestibular organ. The nearly ohmic voltage dependence of ClC-K/barttin channels is well suited for the transepithelial Cl^- transport in the nephron and for recycling Cl^- to support K^+ secretion and voltage generation in the inner ear.

Disruption of mouse ClC-K1 (532) entails a severe renal concentration defect (nephrogenic diabetes insipidus), whereas loss of mouse ClC-K2 (302, 336) or human ClC-Kb (780) cause severe renal salt loss, which in humans is called Bartter syndrome type III. Since barttin disruption abolishes the plasma membrane ion transport of both CLC isoforms, it entails an even more severe renal phenotype and additionally leads to deafness in both mice (699) and humans (in Bartter syndrome type IV) (65). The same severe phenotype is observed in the rare patients with disruption of both *CLCNKA* and *CLCNKB* channel genes (601, 748).

A. Basic Properties of ClC-K/Barttin Proteins and Transcriptional Regulation

ClC-K proteins have 687 amino acids and display the transmembrane topology and cytoplasmic CBS domains typical for eukaryotic CLC proteins. They are *N*-glycosylated in the extracellular loop between helices L and M (415). The crystal structure of the cytoplasmic CBS domains from human ClC-Ka was obtained at 1.6 Å resolution (526). Contrasting with ClC-5 (542) and ClC-1 (57), no evidence for these domains to bind ATP was found (526). A recent cryo-electron microscopical study reveals the structure of a bovine ClC-K channel at ~3.9 Å resolution (628). It highlights the rather small differences in the pore structures between CLC $2Cl^-/H^+$ exchangers and Cl^- channels and will allow detailed structure-function analysis of CLC channel pores. A unique structural feature of ClC-K proteins is the lack of a "gating glutamate" (211) which is replaced by valine (in ClC-K1, -Ka and -Kb) or leucine (in ClC-K2) (415).

The human *CLCNKA* and *CLCNKB* genes, which encode ClC-Ka and ClC-Kb, respectively, are located in close proximity (separated by ~10 kb intervening sequence) on human chromosome 1p36.13. This close proximity and the ~90% identity at the amino acid level suggest that they have arisen by a recent gene duplication. The two rodent isoforms are also ~90% identical to each other, but only 80% identical to the human proteins. Based on homology, it was therefore impossible to decide on the correspondence of human and rodent isoforms and the nomenclature -Ka, -Kb and -K1, -K2 was adopted for the human and rodent isoforms, respectively (415) [the K was introduced by Uchida and colleagues (845) to highlight their prominent expression in kidney]. Expression patterns and functional data later indicated that ClC-K1 and -K2 correspond to ClC-Ka and -Kb, respectively. Promoters of *Clcnk* genes and relevant transcription factors have been analyzed in detail (686, 844, 846, 848), and mice driving the EGFP reporter gene under the control of the human *CLCNKB* promoter have been generated and analyzed (422, 513).

Renal transcription of ClC-K channels appears to be regulated by osmolarity and/or NaCl concentration. ClC-K1 is upregulated by water deprivation and hyperosmolarity (59, 845, 853). Experiments with renal cell lines suggested that such an upregulation of ClC-K1 and barttin might be cell-autonomous (59). Conversely, ClC-K1 and barttin are downregulated by diuretic (furosemide)-induced salt loss (911). The ClC-K2 mRNA was moderately decreased under high-salt diet (862), which is reminiscent of the transcriptional regulation of OmClC-K from tiliapia fish by changes from fresh to salt water (556).

B. Localization of ClC-K/Barttin Channels

Mammalian ClC-K proteins appear to be exclusively expressed in the kidney and the inner ear, a pattern exactly mirrored by that of their β-subunit barttin (222). The renal expression pattern differs substantially between the -K1 and -K2 isoforms. Early studies aimed at determining their segment-specific expression by RT-PCR of manually dissected nephron segments were in part plagued by mRNA contamination and lack of linearity (415, 845, 853, 868), and immunohistochemistry in many cases cannot distinguish between the two isoforms because of the difficulty in obtaining isoform-specific antibodies against these highly homologous proteins (222, 336, 421, 853, 908). However, one ClC-K1 antibody seems specific for this isoform (420, 847), and the ClC-K1/K2 antibody described by Kieferle et al. (415) might label predominantly ClC-K2 in the mouse kidney (336). Renal ClC-K2 expression has also been investigated by in situ hybridization (931). *Knockout* controlled immunohistochemistry (336, 421), and *CLCNKB* promoter-driven reporter gene expression (422) now gives a clear picture of the expression of either isoform along the nephron that fits to (patho-)physiological data.

In the kidney, immunohistochemistry initially detected ClC-K1 exclusively in the thin ascending limb (tAL) of Henle's loop, the nephron segment with the highest Cl^- permeability. In this segment, the channel is expressed in

both basolateral and apical membranes (847). The specificity of labeling was confirmed using *Clcnk1*$^{-/-}$ mice (532). In vitro perfusion of the tAL revealed a loss of transepithelial Cl^- permeability in the KO (532). However, also the medullary thick ascending limb (mTAL) appears to express significant amounts of ClC-K1 in their basolateral membranes, as suggested by labeling of *Clcnk2*$^{-/-}$ kidney sections with a ClC-K1/K2 antibody (336). One might hypothesize that the additional mTAL expression of -K1 occurs in compensation for the disruption of *Clcnk2*. However, the finding that furosemide (which, like *Clcnk2* disruption, inhibits salt absorption in the TAL) rather decreased ClC-K1 expression (911) weakens this hypothesis. The detection of basolateral ~40 pS Cl^- channels in the cortical thick ascending limb (cTAL) (633) might suggest some presence of ClC-K1 [which display 40 pS conductances (441)] in that segment where it has not been detected by immunohistochemistry.

Unlike ClC-K1, ClC-K2 is prominently expressed in basolateral membranes of the cTAL, the distal convoluted tubule (DCT), and α- and β-intercalated cells of the connecting tubule (CNT) and collecting duct (222, 336, 421). These results, which were obtained by immunohistochemistry with different ClC-K1/K2-reactive antibodies, have been ascertained using both *Clcnk1*$^{-/-}$ (421) and *Clcnk2*$^{-/-}$ (336) mice. This localization of ClC-K2 is further supported by RT-PCR of microdissected tubules (862) and the disappearance in *Clcnk2*$^{-/-}$ mice of a ~10pS Cl^- channel from basolateral membranes of TAL, DCT, and CNT/CCD intercalated cells (336). Human ClC-Kb displays an identical expression pattern as revealed by transgenic mice expressing EGFP under the control of the human *CLCNKB* promoter (422).

Until recently, the only confirmed extra-renal site of ClC-K expression (and that of its β-subunit barttin) was the inner ear **(FIGURE 9)**. Recent work detected barttin in basolateral membranes of salivary gland duct cells (774), strongly suggesting the presence of ClC-K/barttin channels also in this epithelium. In the inner ear, both ClC-K isoforms are expressed in basolateral membranes of K^+ secreting epithelial cells, i.e., of the marginal cells in the cochlear stria vascularis **(FIGURE 9)** and of dark cells in the vestibular organ (222, 422, 699, 725). The widespread expression of ClC-K in the cochlea reported by Qu et al. (682) is questionable because it has not been observed by others and relies on an antibody that has not been tested in *knockout* animals. Whereas immunohistochemistry could not prove the strial presence of both isoforms because it used ClC-K1/K2 antibodies (222, 725), both ClC-K1 and -K2 mRNAs were detected in the cochlea (222). Patch-clamp analysis revealed the presence of a Cl^- channel in strial marginal cells which displayed the Ca^{2+} and pH sensitivity of ClC-K (26). Re-

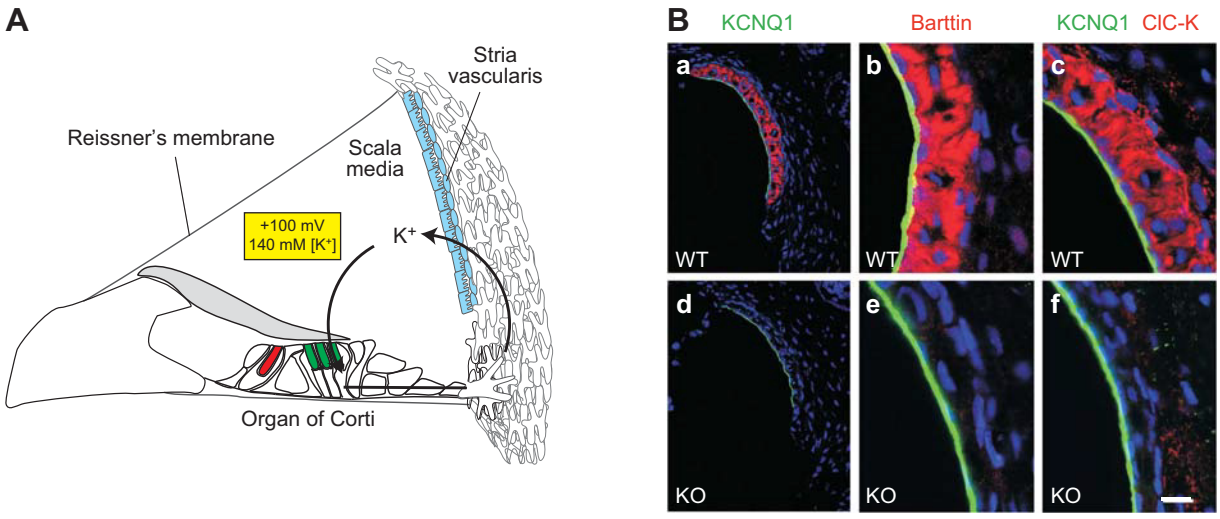

FIGURE 9. Function of ClC-K/barttin channels in the cochlea. *A*: model for K^+ recycling in the inner ear. Activation of outer (green) and inner (red) sensory hair cells by sound opens ciliar mechanosensitive cation channels leading to hair cell depolarization via K^+ influx driven by the high K^+ concentration in the endolymph and the large voltage gradient between the endolymph and the hair cell cytoplasm (100 mV). The composition of the endolymph and the positive extracellular voltage are established by the stria vascularis, a highly vascularized epithelial layer composed of primarily three epithelial cell types (marginal, intermediate, and basal cells) (colored in blue). K^+ released by hair cell at their basal end is shuttled to the stria via a system of gap junctions (884), taken up by marginal cells by the basolateral Na^+-K^+-$2Cl^-$ cotransporter NKCC1 and extruded through apical KCNQ1/KCNE1 K^+ channels into the endolymph. Chloride ions needed by the NKCC1 cotransporter are recycled by ClC-K1/Ka-barttin and ClCK-2/Kb-barttin channels at the basolateral membrane. *B*: immunofluorescence labeling of stria vascularis sections from WT and inner ear-specific barttin *knockout* mice with antibodies against KCNQ1 (green), barttin (*a*, *b*, *d*, *e*; red), and ClC-K (*c*, *f*; red). It demonstrates the colocalization of ClC-K with barttin in basolateral membranes of marginal cells, contrasting with the apical localization of KCNQ1 K^+ channels. Nuclei are stained in blue. [From Rickheit et al. (699).]

porter mice suggest the presence of ClC-Kb (-K2) (422) and RT-PCR the expression of ClC-K1 in the stria (26). Perhaps the most convincing evidence for the presence of both ClC-K isoforms in stria vascularis comes from genetics: only disruption of both isoforms, or of the common β-subunit barttin, leads to deafness in Bartter syndrome IV (65, 601, 699, 748).

The renal and inner ear localization of the β-subunit barttin has been studied by in situ hybridization (65) and immunohistochemistry (222, 699). In both organs, its localization matches perfectly those of the α-subunits ClC-K1 and ClC-K2 **(FIGURE 9)**. In kidney, *Clcnk1* and *Bsnd* mRNAs are upregulated in parallel upon dehydration (59), suggesting similar transcriptional control. Barttin may be useful as histochemical marker for certain types of renal (773) and salivary gland (774) tumors.

C. Interactions of ClC-K α-Subunits With Their β-Subunit Barttin

Upon heterologous expression, only rodent ClC-K1, but not ClC-K2 or human ClC-Ka and -Kb give plasma membrane currents by themselves (845, 847, 869). Site-directed mutagenesis proved that the observed currents are indeed mediated by ClC-K1 (869). For instance, the V166E mutant which, as we now know, inserted a "gating glutamate" (211), drastically changed the voltage dependence of currents and thereby led to an activation by hyperpolarization (869). The currents initially ascribed to ClC-K2 and to a variant with a deletion of transmembrane domains (10) are most likely endogenous to the expression system. The failure to functionally express these channels was surprising since immunohistochemistry (847, 853) and the role of ClC-Kb in Bartter syndrome (780) strongly indicated that they mediate plasma membrane ion transport. Analysis of chimeras between ClC-K1 and ClC-Kb narrowed down a ClC-K1 region that was sufficient to allow plasma membrane currents without a β-subunit (roughly helices N-R) (869).

The mystery surrounding the lack of plasma membrane currents upon overexpression of most ClC-K isoforms was lifted shortly after Hildebrandt and colleagues (65) used positional cloning to identify *BSND*, the gene encoding barttin, as underlying Bartter syndrome type IV (444). Consistent with the renal and hearing phenotypes of Bartter IV, mouse barttin was localized to relevant nephron segments and the cochlear stria vascularis by in situ hybridization (65). Barttin, which lacks homology to other proteins, is a 320-amino acid protein (in humans) which displays two transmembrane domains. Both the short NH_2 terminus and the longer COOH terminus are cytosolic (222). The renal phenotype of Bartter IV, though somewhat more severe than in *CLCNKB*-related Bartter III, suggested barttin as a candidate subunit of ClC-K channels. Indeed, coexpressing ClC-K1 with barttin enhanced currents >10-fold, and coexpression with ClC-Ka or ClC-Kb elicited plasma membrane currents that could not be detected without this ancillary subunit (222, 868). Other CLC channels or transporters such as ClC-1 or ClC-5 did not interact with barttin upon coexpression (222, 868). Coimmunoprecipitation experiments using overexpressing cells indicated that barttin directly binds ClC-K proteins (329, 868). Binding may occur through ClC-K helices B and J which, as expected, are located at the periphery of the channel (822). The cytoplasmic COOH terminus of barttin could be deleted substantially without losing the effect on ClC-K currents, but the extent of tolerated deletions appears to depend on the expression system (222, 754). The main mechanism by which barttin facilitates plasma membrane currents is an increased surface expression of ClC-K proteins which are otherwise stuck in the endoplasmic reticulum or Golgi (222, 329, 441, 754, 868). Akin to other membrane proteins [e.g., ClC-7 (445)], the correct localization of ClC-K proteins appears to enhance their stability. Mice lacking barttin in the inner ear (699) or expressing instead the Bartter IV-associated R8L mutant (598) had dramatically reduced ClC-K levels. Also in vitro ClC-K was stabilized by barttin (329). In addition to boosting ClC-K plasma membrane currents by increasing surface expression, barttin can change current properties, e.g., the sensitivity of ClC-K1 to extracellular calcium ($[Ca^{2+}]_o$) (868). The transmembrane part of barttin may act as a chaperone for the transport to the plasma membrane, whereas a short cytoplasmic stretch, which needs to be tethered to the membrane, might influence properties of ClC-K currents (754). Detailed analysis of more mutants indicates, however, that also transmembrane residues influence current properties (910). Moreover, barttin is palmitoylated at two cysteine residues shortly after the second transmembrane domain (804). Barttin mutants in which both cysteines were replaced by serine were fully competent in bringing ClC-K proteins to the plasma membrane, but failed to stimulate currents. It is, however, premature to conclude that this failure is owed to a loss of palmitoylation because an effect of the mutation per se could not be excluded. It should be stressed again that barttin is not required for intrinsic ClC-K channel activity. This is not only evident from currents elicited by rodent ClC-K1 without barttin, but also from recent experiments with purified ClC-K proteins. While bovine ClC-K needs barttin for plasma membrane insertion and hence plasma membrane currents, it mediates Cl^- transport also without barttin when reconstituted into lipid bilayers (628).

The cytoplasmic tail of barttin displays a sequence (PQPPYVRL) that contains a tyrosine-based consensus site for endocytosis (YxxL) (71) and bears weak resemblance to WW domain-interacting "PY" motifs (214, 614). Binding of WW domain-containing ubiquitin ligases leads to ubiquitination and internalization of, e.g., the ENaC Na^+ channel (799) or the $2Cl^-/H^+$ exchanger ClC-5 (355, 759).

Compatible with either mechanism, disruption of this site by the Y98A mutation increased ClC-Ka/barttin and ClC-Kb/barttin currents about twofold (222) and augmented their presence in the plasma membrane (329), creating a tool which is now widely used to boost ClC-K/barttin currents (368, 441, 465, 528, 934). The Nedd4–2 ubiquitin ligase was reported to mediate ClC-K/barttin downregulation (217), but since dominant negative forms of WW-domain containing ubiquitin ligases failed to have an effect (Jentsch laboratory, unpublished results), the PPYVRL motif in barttin may rather function as a tyrosine-based, AP-adaptor interacting internalization signal.

D. Biophysical Properties of ClC-K/Barttin Channels

Currents from both ClC-Ka/barttin and ClC-Kb/barttin, although differing in detail, show little gating relaxations and do not display strong rectification (222). The small gating relaxations of ClC-Ka and ClC-Kb expressed in *Xenopus* oocytes show an inverse voltage dependence: ClC-Ka activates at negative voltages, whereas ClC-Kb activates at positive voltages (222, 463, 648). One structural difference underlying this behavior has been spotted to an aspartic acid at the end of helix B (D68). The side chain of the corresponding D54 of EcClC-1 projects into the extracellular vestibule in EcClC-1 (210), and mutating the corresponding aspartate in ClC-0 and ClC-1 dramatically alters common gating (233, 490). ClC-Ka and rat ClC-K1 carry an asparagine at position 68, and the ClC-Kb D68N mutant shows a gating phenotype, which is very similar to that of ClC-Ka, activating at negative voltages (648). The same residue is also important for the binding of several extracellularly acting small molecule ClC-K blockers (648).

The absence of a "gating glutamate" largely eliminates the protopore gate (249, 441) which in part confers voltage dependence to other CLC channels (211). Evolution may have selected for the absence of a gating glutamate to enable constitutive channel activity over a broad voltage range as required for transepithelial transport. They display a typical $Cl > Br > I$ permeability sequence (222, 868, 869), but the conductance of Br^- is higher than that of Cl^- in ClC-K1 without barttin (845, 869). Similar to ClC-2, ClC-K channels behave quite differently when expressed in mammalian cell lines, compared with *Xenopus* oocytes (222, 229, 295, 368, 441, 648, 754). In oocytes, the open probability of ClC-K/barttin channels is very small, as estimated by noise analysis and single-channel recordings (293, 295, 296, 441). In contrast, when expressed in HEK cells, the open probability is very high (249, 441). The reason underlying this difference is unknown, but most likely independent of the cholesterol content of the cell membrane (368). L'Hoste et al. (441) found that mouse ClC-K1/barttin showed time-dependent gating in cell-attached patches but not in whole cell recordings or inside-out patches and suggested that some intracellular factor is necessary to maintain the voltage dependence.

ClC-K1 (847, 869) as well as ClC-Ka/barttin and ClC-Kb/barttin (222, 868) are activated by extracellular Ca^{2+} in the millimolar range, a feature of unknown physiological significance. The sensitivity of ClC-K1 to $[Ca^{2+}]_o$ is modulated by barttin. In its presence currents reach maximal activation around physiological values of $[Ca^{2+}]_o$, whereas currents of ClC-K1 alone continue to increase when $[Ca^{2+}]_o$ is further raised from 7 to 12 mM (868). In a mutagenic screen, Gradogna et al. (293) identified two acidic residues, E261 and D278, that reduced Ca^{2+}-mediated activation when mutated singly, and completely abolished Ca^{2+} sensitivity when both were mutated in the double mutant E261Q/D278N. Interestingly, these residues are localized in the loop connecting helices I and J, a relatively long loop that traverses the whole extracellular surface, relatively close to the dimer interface in EcClC-1 (210). The corresponding loop is not resolved in the CmClC crystal structure (242) and neither in the bovine ClC-K structure (628). Even more interesting is that, based on the Ec-ClC-1 structure, E261 from one subunit is physically close to D278 from the neighboring subunit, suggesting that these residues form two symmetrical, intersubunit low-affinity Ca^{2+} binding sites (293). Further investigation of the binding site, using also a homology model of ClC-Ka, revealed the contribution of two other residues (E258 and E281) that are probably involved in the binding site, both also being located within the I-J loop (294). Zn^{2+} block of ClC-K channels was unaffected by these I-J lop mutations, showing that the inhibitory Zn^{2+} binding site, which is probably conserved among ClC-0, ClC-1, ClC-2 and ClC-K channels, is unrelated to the activating Ca^{2+} binding site of ClC-Ks. Furthermore, Ca^{2+} sensitivity could be conferred to ClC-0 by transplanting the I-J loop. However, the ClC-0 construct with the transplanted loop exhibited a profoundly inwardly rectifying phenotype, suggesting that the loop has a large effect on the common gate (294). Surprisingly, a Bartter III-associated mutant of ClC-Kb (R538P) in the linker between the transmembrane part and the CBS domain abolished the Ca^{2+} sensitivity of ClC-Kb/barttin, but not of ClC-Ka/barttin, by an unknown mechanism (528). Other disease-causing *CLCNKB* mutations that change the Ca^{2+} sensitivity affect still other residues (R351W (934) and V170M (28), suggesting indirect effects by conformational changes.

ClC-K1, ClC-Ka/barttin, and ClC-Kb/barttin currents are also inhibited by extracellular acidification in the range between pH 8 to 6 (222, 847, 868, 869). The responsible residue has been mapped to extracellular histidine H497 (293) which is homologous to the histidine (H532) involved in the block of ClC-2 by extracellular protons (587). ClC-K channels are also blocked by strongly alkaline pH (pH 8–11), an effect mapped to lysine 165 in the extracellular

vestibule of the channel (296). The sensitivity of ClC-K2/barttin to both intra- and extracellular pH may play a role in the regulation of Cl^-/HCO_3^- exchange and NaCl reabsorption in β-intercalated cells of the distal nephron (658, 907).

In spite of being ~90% identical, ClC-K1/barttin and ClC-K2/barttin channels surprisingly appear to have rather different single-channel conductances. The directly measured single-channel conductance of heterologously expressed (rodent) ClC-K1 is ~40 pS (441) or ~34 pS (249), similar to native Cl^- channels previously reported for the cortical thick ascending limb (633). Human ClC-Ka/barttin conductance amounts to 18–20 pS by noise analysis (804, 962) or 26 pS by single-channel recordings (696). In contrast, ClC-K2/barttin displays a single-channel conductance of ~10 pS as indicated by the lack of ~8 and ~11 pS channels in the basolateral membranes of the cortical thick ascending limb (cTAL) and of intercalated cells of the connecting tubule (CNT) and cortical collecting duct (CCD) in *Clcnk2*$^{-/-}$ mice (336). Such 10 pS channels have already been observed previously in these segments (593, 594, 658, 936). Patch-clamp studies suggest that the channel activity of bona fide ClC-K2 channels native to the CCD is acutely enhanced or decreased by IGF1 and insulin, respectively (936).

However, these "single-channel" conductances in part reflect the combined conductance of both protopores of double-barelled channels. Rare "half-conductance" states were observed with mouse ClC-K1/barttin (441) and apparently more often in rClC-1 without barttin (249), suggesting that these states represent the "true" single-channel (protopore) conductance of ClC-K1. Presumably these half-conductance states are rarely observed because ClC-K proteins lack the gating glutamate which is crucial, albeit not absolutely required, for protopore gating of ClC-0 (211). The ~40 pS single-channel conductance of ClC-K1 likely represents the combined conductance of two pores that are gated together by the common gate. Indeed, introduction of a "gating" glutamate with the V166E mutation not only changes the voltage dependence of rClC-K1 (869), but results in ~20 pS mClC-K1/barttin channels apparently gated by an introduced protopore gate (441). It is not entirely clear whether single-channel conductances reported for other ClC-K channels represent single or combined protopore conductances. While the absence of the gating glutamate favors the second possibility, the ~20 pS conductance of hClC-Ka/barttin (804, 962) was suggested to represent the protopore conductance (249). Individual residues responsible for the differences in the single-channel conductances between the ClC-K isoforms have not yet been identified. However, we speculate that it might be due to the residue at the position of the gating glutamate found in all other mammalian CLCs. ClC-K1 displays a valine, and ClC-K2 a leucine at this position (415). The bulkier leucine side chain may lead to the observed smaller conductance of the ClC-K2 pore. Although ClC-K1 and -K2 are likely to heteromerize upon coexpression, double-barreled channels displaying two different single-channel conductances [as observed with coexpression of ClC-0 and ClC-1 or -2 (897)] have not yet been reported.

Barttin has no significant effect on the single-channel conductance of ClC-K1 (249, 441), but Fahlke and co-workers reported that barttin drastically changed the voltage dependence of the ClC-K1 V166E mutant and increased its single-channel conductance from ~9 to ~20 pS (754). However, these latter findings could not be reproduced by Teulon and colleagues (441).

E. Roles of ClC-K/Barttin Channels in Physiology and Pathology

The physiological roles of ClC-K/barttin channels are evident from the pathologies observed upon their disruption in mice or mutations in human genetic disease. Loss of ClC-K/barttin function leads to diverse, severe renal phenotypes that are sometimes associated with sensorineuronal deafness. Renal roles of ClC-K channels were the subject of several recent reviews (27, 229, 432, 937).

In addition to the well-established roles of *CLCNK* and *BSND* mutations in monogenic disorders of the kidney and the inner ear, less convincing genetic association studies suggest contributions of *CLCNKA* and *CLCNKB* polymorphisms to other pathologies. A common *CLCNKB* polymorphism (381) has been associated with high blood pressure in human populations (382, 778), but could not be replicated in other studies (118, 238, 425, 796). Moreover, this polymorphism (T481S) increased ClC-Kb/barttin currents upon expression in *Xenopus* oocytes (381), but not in HEK cells (778). Noncoding SNPs in *CLCNKA* were associated with salt-sensitive hypertension (45), and *CLCNKB* variants were suggested to underlie differences in hearing thresholds (268). Moreover, a nonsynonymous coding *CLCNKA* polymorphism has been linked with heart failure (101). The corresponding R38G exchange, which reduced ClC-Ka/barttin currents by ~50%, was speculated to operate via the renin-angiotensin axis, whereas a subsequent study of another cohort rather found an association of the polymorphism with glomerular filtration rate without providing a mechanistic explanation (829).

1. ClC-K1/barttin: a crucial role in concentrating urine

By ensuring the hyperosmolarity of the kidney medulla (16), ClC-K1/barttin is crucial for the concentration of urine (532). The high osmolarity of kidney medulla is needed to generate an osmotic gradient in the medullary collecting duct to allow passive reabsorption of water

through vasopressin-regulated aquaporin2 (AQP2) water channels (244). This high osmolarity is generated by the countercurrent system embodied by the loop of Henle. To perform its function, it needs, as we now know from *Clcnk1*$^{-/-}$ mice (16, 532), the high ClC-K1/barttin-mediated Cl^- permeability of both apical and basolateral membranes of the tAL (532, 847).

2. ClC-K2/barttin channels are crucial for renal salt reabsorption

Transepithelial transport in the TAL, a major site of renal salt absorption, is well understood and supported by human mutations that underlie various forms of renal salt loss. Powered by the sodium gradient that is generated by the basolateral Na^+-K^+-ATPase, the apical Na^+-K^+-2Cl cotransporter NKCC2 (SLC12A1), which is mutated in Bartter syndrome type I (781), takes up Na^+ and Cl^- from the primary urine. Na^+ is pumped across the basolateral membrane by the Na^+-K^+-ATPase and Cl^- exits passively across the same membrane through ClC-Kb/barttin Cl^- channels [with *CLCNKB* and *BSND* mutated in Bartter III (780) and IV (65), respectively]. Potassium ions cotransported by the apical NKCC transporter must be recycled across the apical membrane, a process mediated by ROMK (Kir1.1, KCNJ1) channels. This process is essential for NaCl reabsorption as revealed by mutations in *KCNJ1* that cause Bartter syndrome II (782).

Pathogenic mutations include large deletions as well as nonsense and missense mutations (780). Several deletions of *CLCNKB* sequence resulted from unequal crossing over of the neighboring genes. Interestingly, one such event predicts a fusion protein between ClC-Ka and ClC-Kb which is under the control of the *CLCNKA* promoter, highlighting the importance of a correct expression pattern along the nephron (780). Following the original report (780), many more *CLCNKB* mutations were found in Bartter syndrome (17, 28, 85, 134, 272, 273, 322, 411, 427, 607, 708, 768, 823, 934, 942).

Obviously, deletions or nonsense mutations in *CLCNKB* lead to a loss of channel function. Many of the *CLCNKB* missense mutations affect surface expression (411), leading to a reduction of plasma membrane currents. Although located at different positions (P124L, V170M, R351W, R538P), several mutants affect the response of ClC-Kb/Barttin to external pH and Ca^{2+} (28, 528, 934), but it has not been established that this change explains the pathogenicity of these mutations. Some mutations were identified in patients with mild forms of the disease (17, 28), but symptoms can markedly vary even with patients carrying the same mutations (707, 708). The phenotype of *CLCNKB*-related Bartter syndrome is highly variable (427). However, recent studies found that the reduction of ClC-Kb/barttin currents of *CLCNKB* mutants expressed in HEK cells correlates with the clinical severity of renal disease (131, 768).

Whereas *Clcnk1*$^{-/-}$ (532) and *Bsnd1*$^{-/-}$ mice (699) were reported in 1999 and 2008, respectively, it took another eight years for two independent *Clcnk2*$^{-/-}$ mouse lines to be published (302, 336). Both mouse models display the symptoms typical for Bartter III such as renal salt loss, hypokalemia, metabolic alkalosis, and increase of prostaglandin E_2. They also displayed hypertrophy of the juxtaglomerular apparatus and proliferation of renin-producing cells (302, 336). The mouse strains seem to differ in the sensitivity to drugs inhibiting the apical cation-chloride cotransporters of the TAL (furosemide, acting on NKCC2) and the DCT (thiazides, inhibiting NCC). Whereas Hennings et al. (336) report that the sensitivity to furosemide is abolished and that to thiazides reduced, Grill et al. (302) state a reduction of furosemide sensitivity and abolishment of thiazide sensitivity. This apparent discrepancy might be owed to the use of different drug concentrations or other differences in experimental design. In any case, these experiments clearly indicate crucial roles of ClC-K2/barttin in both the TAL and the DCT. By using ClC-K1/K2 antibodies in *Clcnk2*$^{-/-}$ mice, Hennings et al. (336) further show that ClC-K1 expression extends from the tAL to include the mTAL. Their patch-clamp experiments on cTAL cells and CNT/CCD intercalated cells revealed the disappearance in *Clcnk2*$^{-/-}$ mice of a ~10 pS channel (336), confirming that this previously described channel (593, 594, 658, 936) is encoded by *Clcnk2*.

3. Loss of barttin, or of both ClC-K1 and ClC-K2, entails deafness and severe renal salt loss

Since the surface expression of ClC-K ion-conducting α-subunits depends on the β-subunit barttin (222, 868), disruption of the *BSND* gene leads to an almost complete loss of both ClC-Ka and ClC-Kb channel activity. Therefore, the renal phenotype of Bartter IV patients is more severe than with a loss of *CLCNKA* (nephrogenic diabetes insipidus) or *CLCNKB* (Bartter III), except when a *BSND* mutation elicits only a partial loss of function (696, 769). Likewise, constitutive *Bsnd*$^{-/-}$ mice die within a few days after birth due to severe salt loss and dehydration (699), whereas *Clcnk1*$^{-/-}$ mice (532) and *Clcnk2*$^{-/-}$ mice (302, 336) survive with the renal phenotypes described above.

In addition to the severe renal phenotype, Bartter IV patients (65, 444) and *Bsnd*$^{-/-}$ mice (699) display congenital deafness. The inner ear reacts more sensitively to a reduction of barttin function than the kidney, as revealed by nonsyndromic hearing loss with mild *BSND* mutations (696, 769). As shown by in situ hybridization (65) and immunohistochemistry (222, 699), barttin localizes to the basolateral membranes of two types of K^+-secreting epithelial cells: dark cells of the vestibular organ and marginal cells of the stria vascularis **(FIGURE 9)**. This highly vascularized multilayered epithelium is found in the lateral wall of the scala media that contains the sensory organ of Corti. By secreting K^+ and generating a positive potential in the scala

media, the stria generates an appropriate electrochemical potassium gradient to drive depolarizing K^+ currents through mechanosensitive channels of sensory hair cells (940) **(FIGURE 9*A*)**. The passive apical uptake of K^+ through mechanosensitive channels is matched by an equally passive basal efflux from hair cells mainly through KCNQ4 (Kv7.4) K^+ channels (413, 436). This is possible because the base of hair cells is exposed to normal extracellular fluid. This purely passive K^+ movement drastically lowers the need for metabolic energy in these sensory cells. The energy necessary for ion transport is provided by the "power station" of the stria vascularis. If it fails, deafness ensues.

Like the transport model for the TAL (see above), the model for potassium secretion by marginal cells of the stria vascularis is strongly supported by genetic evidence. Its feasibility has been tested by measuring intrastrial ion concentrations and by mathematical modeling (592, 684, 685). Potassium is secreted across the apical membrane through the KCNQ1(Kv7.1)/KCNE1 K^+ channel. Both disruption of the α-subunit KCNQ1 (108, 448, 581) and of the β-subunit KCNE1 (758, 858) entail deafness in mice and humans. Potassium is taken up across the highly infolded basolateral membrane of marginal cells by the combined action of the Na^+-K^+-ATPase and the Na^+-K^+-$2Cl^-$-cotransporter NKCC1 [disruption of which leads to deafness in mice (182, 198, 253)]. Akin to the need for K^+ recycling of the apical NKCC2 in the TAL, NKCC1 needs recycling of Cl^- across the basolateral membrane of marginal cells. This is accomplished by ClC-Ka/barttin and ClC-Kb/barttin channels which operate in parallel. Since deafness is not observed with single disruptions of either *CLCNKA* or *CLCNKB* (or their mouse orthologs), the function of either channel is sufficient for strial function. Only loss of both channels, either by a loss of function of their common β-subunit barttin (65, 699), or in rare patients by mutations in both channels (601, 748), impairs Cl^- recycling to a degree that causes deafness.

The impact of barttin on hearing has been studied in detail in mice with inner ear-specific *Bsnd* disruption (699). Similar to the congenital deafness observed with Bartter IV patients, these mice displayed a severe hearing loss that was already fully developed at the normal onset of hearing. Unexpectedly, disruption of barttin did not decrease the high K^+ concentration in the scala media, but drastically reduced the endocochlear potential. This suggested the presence of another Cl^- channel in marginal cells which is barely sufficient for strial K^+ secretion, but not for generating the highly positive (~+100 mV) endocochlear potential. The collapse of this potential sufficed to impair the function of sensory outer hair cells which later also degenerated, without, however, compromising hearing further. Importantly, ClC-K proteins could no longer be observed by immunohistochemistry in the cochlea or vestibular organ, demonstrating that in vivo the stability of the ClC-K α-subunit depends on its β-subunit barttin. This excludes that ClC-K1, which is not strictly dependent on barttin in heterologous expression systems, mitigates symptoms in mice. Consistent with the expression of ClC-K/barttin in dark cells, subtle vestibular symptoms were also observed (699).

Two additional *Bsnd* mouse models were described recently: a *knock in* mouse carrying the R8L mutation found in Bartter IV patients and, obtained as an intermediate step in its generation, a mouse expressing this mutant at very low levels (a hypomorph) (598). Whereas hypomorphic mice showed Bartter-like symptoms [but less severe than $Bsnd^{-/-}$ mice (699)], $Bsnd^{R8L/R8L}$ mice had a surprisingly mild phenotype which became apparent only under low salt diet (598). They also displayed a subtle hearing loss (597). Importantly, mutant R8L barttin and ClC-K immunoreactivity were shifted from the plasma membrane to the cytosol of kidney epithelial cells (598), consistent with the trafficking effect observed in cell culture (329). In proof-of-principle experiments, treatment with an Hsp90 inhibitor slightly rescued the plasma membrane localization of R8L mutant barttin and of ClC-K in $Bsnd^{R8L/R8L}$ mice, corrected their metabolic alkalosis, ameliorated hypokalemia, and slightly amended the hearing loss (597).

Many, if not most, pathogenic *BSND* mutations, like the R8L mutation (65) later studied in *knock in* mice (598), affect ClC-K function by decreasing the plasma membrane residence of the channel (329, 377, 696). Some *BSND* mutations, like G47R, seem to lead to a mild phenotype (555, 556), but this is not always the case (627). Of note, one particular mutation (I12T) underlies nonsyndromic deafness, i.e., without significant renal abnormalities, in four different pedigrees (696). Another *BSND* mutation (V33L) was associated with nonsyndromic hearing loss in another family (769). Both mutants markedly reduce, but do not abolish, ClC-K/barttin currents in heterologous expression owing to reduced transport to the plasma membrane (696, 825), suggesting that the inner ear reacts more sensitively than the kidney to a reduction in ClC-K/barttin function.

BSND mutations might cause disease not only because they impair the transport of ClC-K α-subunits to the cell surface (329), but also by modulating the function of plasma membrane inserted ClC-K channels (377). However, it may be difficult to extrapolate cell culture studies to the in vivo situation. For instance, using heterologous expression, Fahlke and co-workers (377) reported that several pathogenic Barttin mutants including R8L reached the plasma membrane but failed to activate ClC-K currents. However, as mentioned above, $Bsnd^{R8L/R8L}$ *knock in* mice revealed that in vivo R8L mutant Barttin is largely retained intracellularly, resulting in a drastic overall decrease of ClC-K/barttin expression levels (598).

F. Pharmacology of ClC-K Channels

Before the molecular identification of ClC-K channels, Wangemann et al. (885) screened hundreds of compounds for their ability to reduce the basolateral Cl^- conductance of the thick ascending limb of Henle's loop (TAL), and identified NPPB as one of the most potent compounds with an apparent affinity of ~0.1 μM. However, subsequent studies on heterologously expressed ClC-K channels found only a weak block of rat and mouse ClC-K1 by this compound (441, 465). So far, no functional data have been published for rat or mouse ClC-K2 channels, which are presumably underlying the basolateral Cl^- conductance in the TAL, and the effect of NPPB on human ClC-Kb has not been reported in the literature. Screening several classical Cl^- channel blockers and novel compounds, Liantonio and co-workers (458, 465) identified derivatives of CPP, in particular a bisphenoxy compound and 3-phenyl-CPP, as rather potent inhibitors of ClC-K channels with affinities around 100 μM for rat ClC-K1 and human ClC-Ka. Interestingly, human ClC-Kb was much less sensitive to 3-phenyl-CPP and also to DIDS, a nonspecific anion channel blocker (648). The reason for this different pharmacological profile could be nailed down mostly to residues in the extracellular vestibule, which are negatively charged in the less sensitive ClC-Kb and neutral in ClC-Ka: D/N68 and E/G72 (648). These results strongly suggest that the blockers are inhibiting ClC-K channels by directly binding to the external pore entry, in agreement with dependence of the affinity of the extracellular Cl^- concentration (465). Matulef et al. (533) found that polythiourea derivatives of DIDS, created by DIDS hydrolysis in aqueous solutions, bind to the same site with rather high affinity. Interestingly, the D68 residue was also found to be important for the gating of ClC-K channels (648), as in ClC-1 (233) and ClC-0 (490). The same residue also affects gating relaxations in the Cl^-/H^+ antiporter ClC-5 (180).

Subsequently, even higher affinity benzofuran derivative blockers were identified with IC_{50} values <10 μM (462, 464). Surprisingly, these compounds were practically equally effective on ClC-Ka and ClC-Kb. Two of these compounds have been found to slightly increase urine volume and to slightly reduce systolic blood pressure, without affecting electrolyte balance, in agreement with the presumed effect on kidney ClC-K channels (461, 462). These studies support the hypothesis that ClC-K channel inhibitors might be interesting alternative diuretics (257). However, the specificity of these compounds with respect to other targets, such as potassium channels or NKCC/KCC cotransporters, chloride-bicarbonate exchangers, or also regulatory proteins like WNK kinases, remains to be determined. Recently, Louet et al. (486) used virtual screening, docking compounds on a homology model of human ClC-Kb based on the bovine ClC-K structure to explore novel ClC-K ligands, using RT-93, one of the benzofuran derivative with highest affinity (464), as a reference point. However, testing ~40 compounds resulting from the screening did not reveal any substance with higher affinity than RT-93 (486). Somewhat surprisingly, despite a very high sequence identity between bovine and human ClC-Kb, several helices in the model appeared to be oriented in significantly different directions compared with the experimental structure (486). Another disconcerting result was that the mutant D68N, which affects a residue that is critically involved in binding of various inhibitors (648), was reported to not express functional currents (486), in contrast to the robust currents shown by Picollo et al. (648). Recently, testing FDA approved drugs for which Bartter syndrome like side effects had been reported, the angiotension receptor 1 (AT1) blocker valsartan was found to rather specifically inhibit ClC-Ka (IC_{50} ~20 μM) but less so ClC-Kb (IC_{50} >100 μM) (370). The difference in binding affinity suggests that the blocker binds to the same site as 3-phenyl-CPP (648), as also confirmed by docking studies (370). A surprising finding was that niflumic acid (NFA), a common Cl^- channel blocker, actually potentiated currents of human (but not rat) ClC-K channels expressed in *Xenopus* oocytes (463). For ClC-Ka the effect was biphasic with concentrations below 1 mM resulting in channel activation, whereas larger concentrations blocked the channel. In contrast, ClC-Kb currents were augmented at all concentrations with an up to fourfold potentiation (463). Interestingly, the chemically highly similar flufenamic acid (FFA) only led to channel block (463), an effect that could be pinpointed to the nonplanarity of NFA compared with the more rigid planar structure of FFA (464). The NFA binding site is probably different from the 3-phenyl-CPP blocking binding site in that mutations that affect 3-phenyl-CPP block only slightly affected potentiation and NFA potentiation was independent of the extracellular Cl^- concentration (463, 647). However, a scanning mutagenesis study could not unequivocally identify the NFA binding site (962). More recently, two amino acids at the beginning of the I-J loop, close to the Ca^{2+} binding site, were shown to have a dramatic influence on NFA activation when mutated (295): In ClC-Ka, the mutation F256A dramatically augmented NFA-mediated activation with almost 50-fold maximal activation. In contrast, the N257A mutation completely locked the channel open, probably by activation of the common gate, and introduced a high-affinity NFA-mediated block with an IC_{50} of ~1 μM (295). While these effects are dramatic, the molecular mechanisms underlying the complex interaction of ClC-K channels with NFA are still unclear. Furthermore, Imbrici et al. (368) found that NFA has practically no activating effect on ClC-K channels expressed in HEK cells, probably because their open probability is constitutively high in these cells and cannot be increased further. Benzofuran blockers were equally effective in the two systems (368). The reason for the difference of the properties in the two expression systems is unclear.

VIII. VESICULAR $2Cl^-/H^+$ EXCHANGERS

For a long time, ClC-3 through ClC-7 were considered to be Cl^- channels like ClC-0 and ClC-1, ClC-2, and ClC-K channels. Although predominently localized on endosomes, ClC-4 and ClC-5 yielded plasma membrane currents upon heterologous expression and ion substitution experiments showed that these currents depend on the anion concentration. However, their extreme outward rectification precluded the determination of reversal potentials. Therefore, the coupling of anion movement to proton countertransport was missed until the discovery of $2Cl^-/H^+$ exchange in reconstituted EcClC-1 (5) prompted direct investigation of proton transport of ClC-4 and ClC-5 by two groups (651, 742). We now know that all vesicular CLCs, ClC-3 through ClC-7, function as Cl^-/H^+-exchangers.

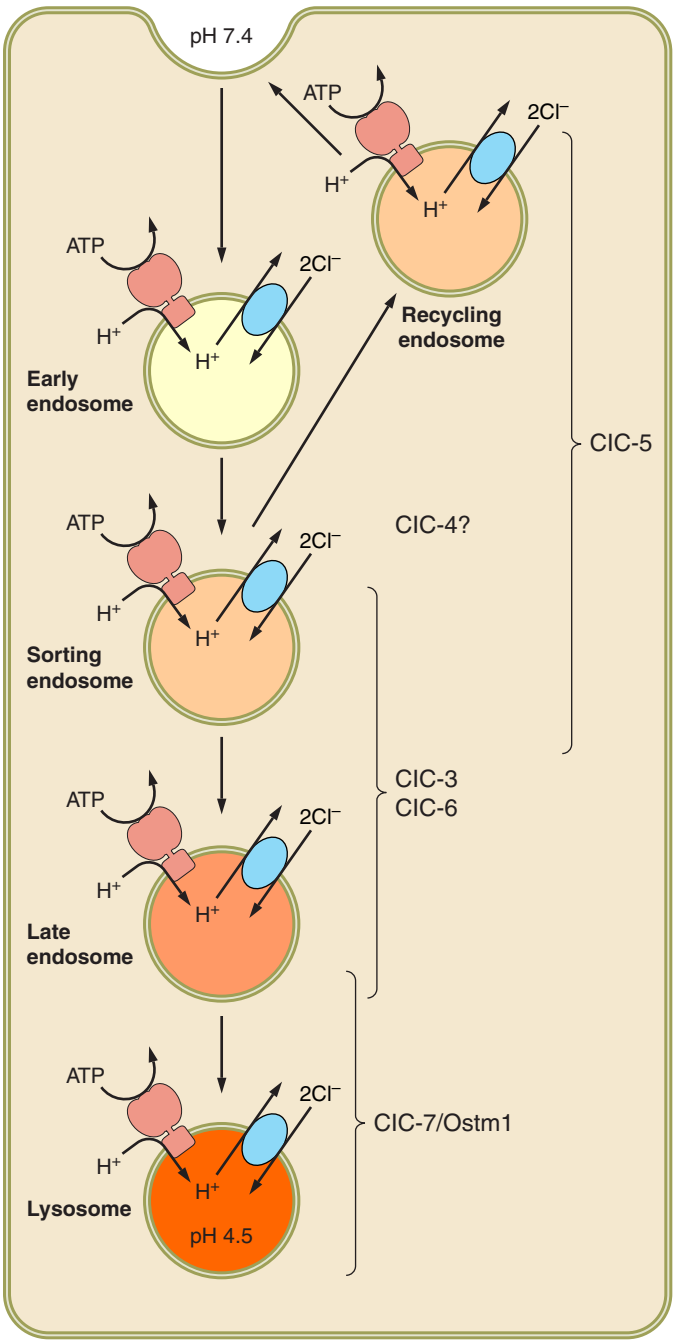

Vesicular CLCs are believed to assist the acidification of intracellular vesicles by electrically shunting the currents of the vesicular H^+-ATPase **(FIGURE 10)**. Such a shunt is not only possible with chloride channels, but also with the highly electrogenic $2Cl^-/H^+$ exchangers, even though one proton exits from the vesicle during one transport cycle. For electroneutrality, the three negative charges transferred by $2Cl^-/H^+$ exchange have to be compensated for by three H^+ pumped by the ATPase; hence, out of three protons, only one leaves the vesicle in this oversimplified model. Rather surprisingly, model calculations (372, 896) show that $2Cl^-/H^+$ exchange would achieve, together with the proton pump, a more acidic vesicular pH than a simple Cl^- conductance. This can be attributed to a more inside-negative voltage obtained with an exchanger (896). In addition to a potential impact on luminal pH and luminal voltage, $2Cl^-/H^+$ exchange will also raise the vesicular Cl^- concentration. The large transmembrane H^+ gradient of inside-acidic vesicles will raise luminal $[Cl^-]$ above the levels obtained with a shunting Cl^- channel.

As discussed for the individual vesicular CLCs below, the expected changes in luminal pH and $[Cl^-]$ were indeed observed in some of the *knockout* mouse models, which have been obtained for all mammalian vesicular CLCs. However, it remains unclear how these changes, and which ones, lead to the often severe pathologies of mice or human patients lacking functional vesicular CLCs. The strong outward rectification of ClC-3 through ClC-7 in heterologous expression at the plasma membrane poses another serious problem. Although model calculations predict a lumen-negative potential when $2Cl^-/H^+$ exchangers operate in parallel with a proton pump (372, 896), endosomes/lysosomes

FIGURE 10. Approximate subcellular distribution of CLC $2Cl^-/H^+$ exchangers in the endosomal-lysosomal system. Vesicular CLCs are differentially localized on various endosomal and lysosomal compartments, where they are coexpressed with V-type H^+-ATPases. The currents of these highly electrogenic CLC exchangers may help in the acidification of these compartments by neutralizing currents of the proton pumps, as has been shown for ClC-3 (325) and ClC-5 (308, 600). However, no change in lysosomal pH is observed upon loss of ClC-7/Ostm1 (407, 445, 896), probably owing to the presence of cation conductances in lysosomes (803). Proton-driven Cl^- transport is predicted to increase vesicular Cl^- concentration (383), as experimentally verified for ClC-7 using mouse models (896). The conversion of ClC-5 and ClC-7 into pure Cl^- conductors by point mutations in *knock in* mice demonstrated that the exchange activity of vesicular CLC is biologically important (600, 896). This suggested that an increase of luminal Cl^- concentration has an important, though unknown, function in endosomes and lysosomes. CLCs of early and recycling endosomes, such as ClC-5 and possibly ClC-4, might be found to a small extent also at the plasma membrane. However, their extreme outward rectification seems to exclude that they transport ions across that membrane.

are generally assumed to be inside positive. No methods are currently available to quantitatively measure this voltage. One may hypothesize that these CLCs display a different voltage dependence when present in intracellular membranes, possibly owing to different lipid composition or posttranslational modification. Moreover, the voltage across endolysosomal membranes may show short excursion to negative voltages, for instance, due to the opening of Ca^{2+} channels. The biological role of vesicular CLCs may only be sufficiently understood once our picture of vesicular ion homeostasis in general is more complete.

IX. ClC-3: A WIDELY EXPRESSED, MAINLY ENDOSOMAL Cl^-/H^+ EXCHANGER

ClC-3 (73, 410) is a widely, possibly even ubiquitously, expressed member of the second homology branch of the CLC family. Like its close homologues ClC-4 and ClC-5, ClC-3 is very predominantly expressed in membranes of the endolysosomal system (810). It may also be present on synaptic vesicles (729, 810) and synaptic-like microvesicles (SLMVs) (523, 729). Some ClC-3 splice variants may partially reach the plasma membrane upon heterologous overexpression (317, 609).

Like its close congeners ClC-4 and ClC-5, ClC-3 is a strongly outwardly rectifying, electrogenic $2Cl^-/H^+$ exchanger (316, 651), although the stoichiometry of coupling has not yet been firmly established. Due to the difficulty of expressing ClC-3 at the plasma membrane, even upon heterologous overexpression, and owing to the apparently small transport rates of ClC-3 (316), many different, endogenous plasma membrane anion currents have been erroneously attributed to ClC-3 (153, 203, 360, 409, 410, 529, 554, 877, 881). This confusion has led to a large and still expanding body of literature purporting roles of ClC-3 in cell volume regulation (203, 342), apoptosis (306, 945), cell cycle regulation (152, 320, 520), cell migration (154, 279, 311), cardiac function (77, 454, 921, 922), vasculature (279, 506, 960), and cancer (153, 348, 871), among others. These publications will not be covered here.

Like other vesicular $2Cl^-/H^+$-antiporters, ClC-3 may assist in the acidification of endosomes and other compartments by shunting the electrical current of the vesicular V-type H^+-ATPase (325, 610, 810, 930). ClC-3 may also change the vesicular voltage or lead to luminal chloride accumulation, as directly shown for the lysosomal $2Cl^-/H^+$-exchanger ClC-7 (895, 896). These parameters may impinge on various vesicular functions, including vesicle budding, fusion and trafficking, and secondary active transport of ions and organic compounds across their limiting membranes.

Important biological functions of ClC-3 are indeed indicated by the severe phenotype of ClC-3 KO mice which eventually completely lose their hippocampus **(FIGURE 11)** and show severe retinal degeneration (810). The neurodegeneration of these mice is not restricted to the hippocampus and *Clcn3*$^{-/-}$ mice appear systemically sick (194, 608, 810, 930). The mechanistic link between a loss of ClC-3 and the resulting pathology, however, remains obscure. So far, no human pathology has been attributed to mutations in *CLCN3*.

A. Basic Properties of ClC-3

ClC-3 migrates as a broad 95- to 155-kDa band in SDS PAGE (751, 810). Its size and migration behavior depend on apparently tissue-specific *N*-linked glycosylation (751) and the specific splice variant (317, 604, 609). These variants can add 58 amino acids to the NH_2 terminus, or 42 amino acids to the COOH terminus of the shortest 760-residue-long ClC-3a protein (317). Interestingly, a COOH-terminal variant (originally named ClC-3b) that replaces a short part of the ClC-3 COOH terminus and adds a PDZ binding domain (604), was alternatively suggested to interact with EBP50 to yield plasma membrane localization (604) or with GOPC to yield Golgi localization (286). NH_2-terminal splice variants, which are differentially expressed across tissues (317), appear to change the subcellular localization of ClC-3 with ClC-3c reported to be localized to recycling rather than late endosomes (317). No differences in the biophysical transport properties of these splice variants were found (317, 609).

ClC-3 may form heteromers with its close relatives ClC-4 and ClC-5, but not with ClC-6 or ClC-7 (820). ClC-3 interacts with clathrin through an NH_2-terminal dileucine

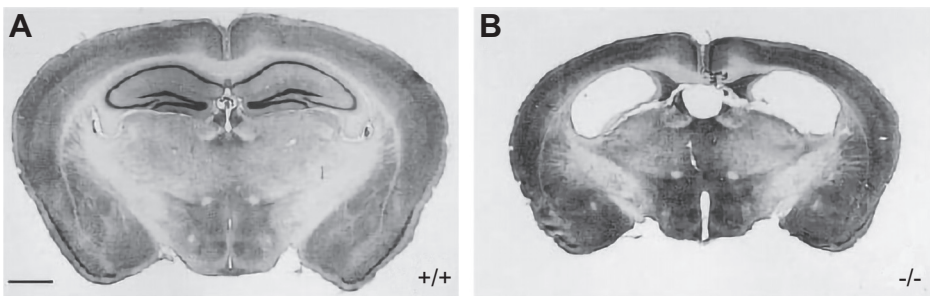

FIGURE 11. Loss of hippocampus in *Clcn3*$^{-/-}$ mice. Nissl-stained frontal sections of adult WT (*A*) and *Clcn3*$^{-/-}$ (*B*) mice illustrate the almost complete degeneration of the hippocampal formation caused by the lack of ClC-3. [From Stobrawa et al. (810).]

cluster (801, 958). Mutating this and other NH_2-terminal motifs leads to slightly increased plasma membrane expression that facilitates the biophysical analysis of ClC-3 (316, 317, 958). In contrast to clathrin binding, the purported ClC-3 protein interactions with postsynaptic glutamate receptors and PSD-95 (881) or with CaMKII (153) should be viewed critically.

B. Ion Transport by ClC-3

ClC-3 is a strongly outwardly rectifying, electrogenic $2Cl^-/H^+$ exchanger with biophysical properties that closely resemble those of its close homologues ClC-4 and ClC-5 which yield larger plasma membrane currents (269, 808). Upon overexpression, ClC-3 yields strongly outwardly rectifying currents that are clearly different from background only at voltages more positive than +20 mV (316, 317, 456, 457, 531, 609, 651), display a $Cl^- > I^-$ conductance sequence (456, 531, 609), and are reduced by extracellular acidification (531). ClC-3 currents activate and deactivate almost instantaneously upon voltage steps. Rigorous experiments showed that ClC-3 currents depend neither on intracellular nor extracellular Ca^{2+} (609). Not only the strong rectification, ion selectivity, and pH dependence fit to the other vesicular CLCs, but importantly, also the effect of neutralizing mutations of the crucial "gating glutamate" of ClC-3 that abolish the strong current rectification and result in an almost ohmic anion conductance (457, 531, 609) just as observed for ClC-4 and ClC-5 (269, 651, 742), ClC-6 (576), and ClC-7 (453).

Even though the more recent studies used ClC-3 splice variants or mutants which increased plasma membrane expression without detectably changing current properties (316, 317, 609, 958), ClC-3 plasma membrane currents are low and several groups were unable to detect novel currents upon ClC-3 overexpression (269, 902). It therefore remains difficult to directly show that ClC-3 is a Cl^-/H^+ exchanger. The strong rectification and almost complete absence of tail currents precludes measurements of reversal potentials as a function of chloride and proton concentrations (609) [which were possible for the slowly gating ClC-7 (453) and a ClC-5 mutant (180)]. One report (316), however, showed small voltage-dependent pH_i changes with ClC-3 expressing cells that are expected for a Cl^-/H^+ exchanger.

In summary, there is no reasonable doubt that ClC-3 is a Cl^-/H^+ exchanger which may affect the ion homeostasis of intracellular vesicles. However, ClC-3 transport activity may be low compared with ClC-4 and ClC-5, even when corrected for the extent of plasma membrane expression (316). It was therefore suggested that the biological role of ClC-3 consists of providing increased membrane capacitance (which differed between splice variants) by performing "nontransporting cycles" (316). These authors speculated that increased endosomal capacitance may facilitate the acidification of intracellular compartments by "buffering" the electric charge transported by the vesicular H^+-ATPase, rather than by providing an ionic countercurrent. The model calculation used to demonstrate the feasibility of this concept, however, is based on the buffer capacity of pure water (316), which is orders of magnitude lower than that of endosomes or the cytoplasm. Therefore, a significant contribution of ClC-3 capacitance to endosomal acidification seems excluded.

C. Currents Erroneously Ascribed to ClC-3

The field of ClC-3 research has been plagued by the fact that many different plasma membrane currents, which were probably endogenous to the expression system, have been mistakenly attributed to ClC-3. ClC-3 was first suggested to mediate time-independent, slightly outwardly rectifying currents that were strongly inhibited by PKC (410), but the same group later reported incongruent strongly rectifying single-channel currents (100–140 pS at positive potentials) that were directly inhibited by cytosolic Ca^{2+} (409). In contrast, others proposed that ClC-3 mediates outwardly rectifying anion currents with an $I^- > Cl^-$ halide selectivity that are activated by cytosolic Ca^{2+} through Ca^{2+}/calmodulin-dependent protein kinase (CaMKII) (153, 237, 279, 360, 554, 706, 881). However, the single channels ascribed to CaMKII-activated ClC-3 in hippocampal neurons (881) look suspiciously similar to ClC-2 (815, 834, 897). ClC-3 KO mice displayed unchanged Ca^{2+}-activated Cl^- currents in salivary glands (37), and currents from overexpressed ClC-3 are Ca^{2+} independent (609).

ClC-3 had also been suggested (203, 342, 397) to encode the ubiquitously expressed volume-regulated anion channel VRAC. This channel is slowly activated by hypotonic cell swelling and displays a $I^- > Cl^-$ permeability and outward rectification (635). This notion was even supported by changed characteristics upon ClC-3 mutagenesis (202, 203, 575) and, although disproven, is still popular with some groups (311, 454, 871, 960). Three independent *Clcn3* KO mouse models (194, 810, 930) revealed that typical $I_{Cl,vol}$ VRAC currents are unchanged in hepatocytes and pancreatic epithelial cells (810), salivary gland cells (36), cardiomyocytes (291, 876, 926), and osteoclasts (610). The long search for the proteins constituting VRAC, which had yielded more than 10 "candidates" including ClC-3 (634), finally came to an end when two independent genome-wide siRNA screens identified LRRC8A as an indispensable VRAC subunit (681, 865). This subunit needs to assemble with other LRRC8 isoforms to form functional VRAC channels (865), which, depending on their subunit composition, also conduct various organic compounds (499, 662).

Another probably ubiquitously expressed anion channel, the acid-stimulated outward rectifier ASOR (103), most likely underlies the currents ascribed to "uncoupling" of

ClC-3 Cl^-/H^+ exchange at strongly acidic external pH (529). ASOR probably also underlies the acid-activated currents ascribed to ClC-4 in skeletal muscle (408) and acid-activated currents observed upon ClC-7 expression in *Xenopus* oocytes (195). ASOR, however, is definitely distinct from ClC-3 (609, 737) and LRRC8/VRAC channels (736). Moreover, a ClC-3 splice variant has been suggested to mediate CFTR-regulated outwardly rectifying Cl^- currents at the plasma membrane (604). For completeness, it should be mentioned that currents reported for a long NH_2-terminal variant of ClC-3 rather resemble swelling-activated VRAC/LRRC8 currents (772) and that strongly outwardly rectifying currents reported by Lamb et al. (531) show atypical slow activation by depolarization.

D. Localization of ClC-3

ClC-3 may be expressed in all mammalian tissues and cells. Northern blots found pronounced ClC-3 expression, for instance, in tissues as diverse as brain and kidney (73, 410, 810), results that were confirmed by Western blots (751). KO-controlled immunohistochemistry detected salient ClC-3 expression in neuroendocrine cells such as those of the posterior pituitary, pancreatic islets, and chromaffin cells of the adrenal medulla (523).

1. ClC-3 resides on late endosomes

ClC-3 is very predominantly expressed on intracellular vesicles (523, 729, 810). The identification of these vesicles by immunohistochemistry in native tissues has often been plagued by poor sensitivity and cross-reactivity of antibodies and a lack of controls in the form of tissue from *Clcn3*$^{-/-}$ mice. Subcellular fractionation by gradient centrifugation of liver membranes revealed that ClC-3 partially copurifies with lamp-1, a marker of late endosomes and lysosomes, and with rab4, an endosomal marker protein (810). The "purest" lysosomal fractions (from brain), as identified by the presence of cathepsin D, however, did not contain ClC-3, but rather ClC-7 and small amounts of ClC-6 (663), suggesting a predominantly late endosomal rather than lysosomal localization of ClC-3. Interestingly, ClC-3 (and ClC-6) shifted to lysosomal fraction upon disruption of ClC-7 (663).

A few *knockout* controlled immunolocalization studies of native tissues and cells also showed a late endosomal localization of ClC-3. Native ClC-3 colocalized with lamp-2 in cultured osteoclasts (610). Endosomal compartments of renal proximal tubules, which display particularly high rates of endocytosis, are nicely layered within the cell. In these cells, immunofluorescence localized ClC-3-positive vesicles below the apical brush border (523) between more apical ClC-5-containing (early) endosomes and more basal ClC-7-containing vesicles (mostly lysosomes) (888). KO-controlled immunohistochemistry (IHC) also revealed prominent ClC-3-positive vesicles in epithelial cells of the epididymis, somata of CA3 hippocampal neurons, various neuroendocrine cells, and hepatocytes (523).

Upon transfection, epitope-tagged ClC-3 also resides, at least partially, in vesicles positive for lamp-1 (316, 317, 457, 810, 820, 901), lamp-2 and cathepsin D (457), and the late endosomal rab7 (317), but also with the early endosomal marker EEA1 (820). A ClC-3 splice variant (ClC-3c) rather localized to rab11- and transferrin receptor-positive recycling endosomes (and partially to the plasma membrane) (317), and ClC-3-overexpressing vesicles were accessible to endocytosed transferrin (729). Inferring native subcellular localization from heterologous expression, however, is particularly problematic with ClC-3 because it artificially generates remarkably large vesicles with lysosome-like properties (317, 457). The generation of these vesicles depends on the transport properties of ClC-3 because it does not occur with the E224A mutant (457) that abolishes ClC-3's voltage dependence (457, 531, 609) and that most likely converts it from a $2Cl^-/H^+$ exchanger into a pure Cl^- conductance [as shown for ClC-4 and −5 (651, 742)]. Collectively, these results provide overwhelming evidence for a (most likely late) endosomal localization of ClC-3.

2. Evidence for presence of ClC-3 on synaptic vesicles and synaptic-like microvesicles

Additionally, there is considerable evidence that ClC-3 is expressed on synaptic vesicles (SVs) (523, 729, 810), although the extent and functional relevance of this localization has been questioned (745). Likewise, ClC-3 has been localized by subcellular fractionation to synaptic-like microvesicles (SLMVs) in neuroendocrine cells (523, 729). In contrast, the postulated localization of ClC-3 to insulin-containing large dense-core secretory vesicles (LDCVs) (44, 188, 455), which was based in part on IHC that lacked *Clcn3*$^{-/-}$ controls, is not convincing (390, 523). A presence of ClC-3 on SVs/SLMVs, and absence on LDCVs, fits to the difference in biogenesis between SVs/SLMVs and dense core vesicles (290). Whereas the former are largely generated from endosomal intermediates (133, 729), secretory dense-core vesicles rather form directly from the *trans*-Golgi network (TGN) (416).

ClC-3 was present in a highly purified preparation of synaptic vesicles and was detected in both immuno-isolated GABAergic and glutamatergic vesicles (810). In the retina, KO-controlled IHC showed intense labeling for ClC-3 in the outer and inner plexiform layers (OPL and IPL, respectively) which contain the majority of retinal synapses (810) and where it (but only partially) overlapped with the SV marker synaptophysin (523). KO-controlled IHC of mouse brain revealed punctate/vesicular staining for ClC-3 in cell bodies and neurites of CA3 hippocampal neurons. In neu-

rites of the dentate gyrus, it partially colocalized with synaptophysin (523).

ClC-3 was present in synaptophysin-positive fractions upon fractionation of brain membranes using various protocols (523, 729). In both chromaffin cells and the INS-1 pancreatic β-cell line, ClC-3 copurified with synaptophysin, but not with secretogranins or carboxypeptidase E as markers for secretory dense-core vesicles (523). The latter finding was supported by IHC of INS-1 cells showing differential vesicular distribution of ClC-3 and insulin (523). Trafficking of ClC-3 (and the zinc transporter ZnT3) to bona fide SVs and SLMVs in brain and PC12 cells depended on the adaptor complex AP3 (729), although ClC-3 appears not to bind AP3 directly (801). Functional data also seemed to indicate a presence of ClC-3 on SVs/SLMVs (729, 810): disruption of ClC-3 inhibited the ATP-dependent acidification of SV-enriched vesicles fractions (810) and cotargeting of ZnT3 and ClC-3 SLMV-like fractions increased intravesicular Zn accumulation (729). Both results were interpreted in terms of an anion conductance of ClC-3 which neutralizes the electrical charge transferred by the H^+-ATPase or the zinc transporter, respectively. However, for unknown reasons, expression of the glutamate transporter vGlut1 is strongly decreased in SVs of *Clcn3*$^{-/-}$ mice (810). Since vGlut1 is now known to also mediate a Cl^- conductance, this secondary loss, and not directly a loss of ClC-3 on SVs, may explain the impaired SV acidification in *Clcn3*$^{-/-}$ mice (745). Another concern was raised by quantitative Western blots of purified SVs that seemed to indicate that only a very small fraction of SVs contains ClC-3 (745). However, the ClC-3 quantification used by Schenck et al. (745) has to be viewed with caution as it was based on a calibration of ClC-3 antibodies which used a COOH-terminal epitope tag located close to the epitope on the native channel, the recognition of which might have been affected. A low abundance of ClC-3 on SVs is, on the other hand, consistent with the absence of ClC-3 in the published proteome of purified synaptic vesicles (824), although some other bona fide SV membrane proteins were also missed in that work. As discussed below, effects of *Clcn3* disruption on synaptic transmission are controversial. Although we believe that there are very good arguments for the presence of ClC-3 on SVs/SLMVs, more work is needed to convincingly demonstrate a role of ClC-3 in these important organelles.

E. Pathology From ClC-3 Disruption and Possible Physiological Roles

Disruption of *Clcn3* in mice entails severe neurodegeneration that, after a few months, leads to a conspicuous absence of the hippocampus **(FIGURE 11)** and includes early blindness (810). These observations were reproduced in two other *Clcn3*$^{-/-}$ mouse models (194, 930). Neurodegeneration is also observed in several other brain regions including the cortex (194, 608, 810, 930). Nonetheless, *Clcn3*$^{-/-}$ mice, depending on the genetic background, survive for many months. Uchida and colleagues found some signs for lysosomal storage disease of the neuronal ceroid lipofuscinosis type in their mice (930) and that is accelerated by ischemia (608). However, lysosomal storage is much less pronounced in *Clcn3*$^{-/-}$ than in *Clcn6*$^{-/-}$ or *Clcn7*$^{-/-}$ mice (429, 663, 668). Lamb and co-workers (194) reported a preferential predeliction for the GABAergic system. In accord with their neurodegeneration, *Clcn3*$^{-/-}$ mice showed impaired motor coordination in rotarod tests, but could learn to improve their skills (810). The exact mechanism leading to neurodegeneration remains unclear and is difficult to ascertain like in other forms of neurodegeneration. It seems, however, likely that the pathology is a consequence of impaired vesicular trafficking or function.

Further functional analysis of *Clcn3*$^{-/-}$ mice therefore focused on the possible roles of ClC-3 in endosomes, synaptic, and other types of vesicles. The underlying hypothesis is that ClC-3, being possibly a Cl^- channel or, as we now know, an electrogenic $2Cl^-/H^+$ exchanger, would support their luminal acidification by supplying countercurrents for the vesicular H^+-ATPase. Indeed, endosomal acidification and concomitant Cl^- accumulation was impaired in hepatocytes from *Clcn3*$^{-/-}$ versus WT mice, and ClC-3 transfected CHO cells showed more acidic endosomal pH (325). Based on less reliable acridine orange staining, overexpression of ClC-3 also seemed to decrease vesicular pH (and increase drug resistance) in HEK293 and BON cells (901), and lysosensor staining suggested that intracellular vesicles of *Clcn3*$^{-/-}$ osteoclasts were less acidic than those in the WT (610). A role of ClC-3 in endocytosis, however, has not yet been demonstrated. Although ClC-3 is prominently expressed in apical endosomes of renal proximal tubules (523), proximal tubular endocytosis of luminal proteins was not affected in *Clcn3*$^{-/-}$ mice (700). This contrasts with the strong reduction of proximal tubular endocytosis upon disruption of ClC-5 (661, 700).

Much work has focused on possible roles of ClC-3 in synaptic vesicles (314, 695, 745, 810), but it is fair to say that no definitive conclusions are possible to date. As mentioned above, the impaired acidification of synaptic vesicles of *Clcn3*$^{-/-}$ mice that was observed by Stobrawa et al. (810) might be owed to the loss of vGlut1 on SVs (810) because vGlut1 is now known to also provide a Cl^- conductance (745). The impaired acidification of bona fide inhibitory synaptic vesicles reported by Nelson and co-workers (695) is based to a large extent on a so-called "rat KO model" in which vesicles fractions enriched for inhibitory SVs were depleted for ClC-3-containing vesicles using antibodies coupled to magnetic beads. Of course, the resulting vesicle population is distinct from inhibitory SVs disrupted for *Clcn3*. ClC-3 might affect the loading of neurotransmitters

into SVs since the respective vesicular uptake transporters are differentially driven by pH or voltage gradients, which are expected to be increased and decreased, respectively, by the presence of ClC-3. Vesicular uptake of glutamate depends on the voltage rather than pH. Consistent with a role of ClC-3 in SV glutamate uptake, a slight increase in miniature synaptic currents (postsynaptic currents in response to presynaptic exocytosis of single synaptic vesicles, reflecting in part their glutamate content) was observed in hippocampal slice preparations of *Clcn3*$^{-/-}$ mice (810). However, even though these data were obtained before an onset of conspicuous degeneration, degenerative changes, which may include altered densities or localization of postsynaptic glutamate receptors, cannot be excluded. Miniature excitatory postsynaptic currents and action-potential induced excitatory potentials were also enhanced when comparing *Clcn3*$^{-/-}$ to WT neurons in culture (314). These authors also reported an increase in the volume of SVs from *Clcn3*$^{-/-}$ mice (314). Miniature inhibitory synaptic currents were unchanged in slice preparations of *Clcn3*$^{-/-}$ mice in one study (810), but reduced in another report (695). Together with a report claiming that ClC-3 is only expressed on a very minor fraction of SVs (745), these contradictory results do not yet allow to unambiguously establish a role of ClC-3 in SVs.

Disruption of *Clcn3* impairs the exocytosis of large dense-core vesicles (188, 455, 523). This is probably an indirect effect because, as discussed above, IHC and subcellular fractionation revealed that ClC-3 is strongly expressed on SMLVs rather than on LDCVs, as observed both in chromaffin and β-cells (523). Moreover, the reported localization of ClC-3 to insulin granules (44, 188, 455) is not convincing (390). Exocytosis of catecholamine-containing LDCVs, as determined by capacitance changes or amperometry upon depolarization or intracellular Ca^{2+} release, was decreased in chromaffin cells from *Clcn3*$^{-/-}$ mice (523). These mice also displayed reduced serum insulin levels (523). However, this decrease may be owed to an indirect systemic effect, since *Clcn3*$^{-/-}$ are lean and have altered levels of other hormones such as leptin (523). A variable decrease in resting serum insulin concentration or insulin secretion from pancreatic islets was observed in two other studies (188, 455) which differ in several aspects (390). Given the systemic sickness and changed metabolism of *Clcn3*$^{-/-}$ mice, pancreatic β-cell specific disruption seems appropriate to better characterize the role of ClC-3 in insulin secretion (390).

ClC-3 has also been localized to lamp-2-positive compartments in mouse osteoclasts (610). The acidity of these compartments seemed reduced in *Clcn3*$^{-/-}$ osteoclasts that were moderately impaired in their bone-degrading capacity as determined using in vitro pit assays (610). This effect was much less pronounced compared with *Clcn7*$^{-/-}$ osteoclasts (429). In contrast to ClC-3, ClC-7 also localizes to the acid-secreting ruffled border and its disruption causes severe osteopetrosis (429).

ClC-3 was also proposed to be present on secretory vesicles and phagosomes (vacuoles) of polymorphonuclear leukocytes, but the subcellular fractionation supporting this localization lacks essential controls for endosomes (570). Based on this assumed localization and the effect of (nonspecific) inhibitors, the authors suggested that ClC-3 provides a countercurrent for the phagosomal NADPH oxidase that is necessary for reactive oxygen species (ROS) generation in the oxidative burst. Indeed, ROS production appeared to be reduced in *Clcn3*$^{-/-}$ neutrophils (570, 571). The idea that ClC-3 neutralizes currents of the NAPDH oxidase in phagosomes is attractive, as the oxidase current, in contrast to the current of vesicular H^+-ATPase, will render the compartment inside-negative (cytoplasmic positive) and thus open the strongly outwardly rectifying ClC-3 Cl^-/H^+ exchanger. The same group also suggested that ClC-3 is important for NADPH-oxidase function in smooth muscle cells, with an important effect on their migration (136), and that the activation of VRAC channels by tumor necrosis factor-α requires ClC-3-dependent ROS production (530). However, a more recent study found no change in vacuolar pH, nor in respiratory burst in neutrophils from *Clcn3*$^{-/-}$ mice (260). The hypothesis that ClC-3 supports NADPH oxidase function should therefore be viewed with due caution until other groups provide convincing evidence for this notion.

X. ClC-4: A VESICULAR Cl^-/H^+ EXCHANGER WITH SLOWLY EMERGING ROLES

ClC-4 is a close homologue of ClC-3 and ClC-5 and is found in many tissues, including prominent expression in brain (389, 852). Like its homologues, ClC-4 is a strongly outwardly rectifying $2Cl^-/H^+$ exchanger (651, 742) and probably resides on endosomes (566, 820), although its heterologous overexpression can target it to the endoplasmic reticulum (611) and partially to the plasma membrane where it can be studied functionally (269). Its biological function may be related to the ion homeostasis, including acidification, of endosomes (566, 567). Although no obvious phenotype has been detected in *Clcn4*$^{-/-}$ mice (700), it is now clear from exome sequencing that mutations in human *CLCN4* underlie particular forms of *X*-linked mental retardation (359, 620) sometimes associated with epileptic seizures (857).

The *CLCN4* gene localizes to the human X-chromosome (Xp22.2). While also present on the X-chromosome in the wild Mediterranean mouse *Mus spretus*, *Clcn4* is surprisingly located on autosomal chromosome 7 in the laboratory mouse *Mus musculus* (621, 713). This unusual situation, which contravenes "Ohno's law" (215), is of genetic inter-

est (11, 585, 621). Crossing both mouse species can give mice lacking *Clcn4* (11, 621). Like *Clcn4*$^{-/-}$ mice later generated in laboratory mice (700), *Clcn4*$^{-}$ mice resulting from such crosses lack obvious phenotypes except for infertility that is not ClC-4-related (11, 567, 621).

A. Basic Properties of ClC-4

Human full-length ClC-4 has 760 residues, but there may be shorter ClC-4 isoforms starting at later initiation sites and thus losing some of the NH_2-terminal residues. The NCBI-listed human short isoform 2 (NP_001243873), however, lacks essential parts of the protein (the first transmembrane helix B) and is predicted to be nonfunctional. The ClC-4 protein is ~80% identical to ClC-3 or ClC-5. It can interact with either of these proteins, but not with ClC-6 or ClC-7, and may therefore form functional ClC-3/4 or ClC-4/-5 heteromeric Cl^-/H^+ exchangers (315, 566, 820). The NH_2 terminus of ClC-4 interacts with clathrin, but this binding appeared weaker than that observed with ClC-3 and ClC-5 (801).

Upon overexpression in *Xenopus* oocytes or in mammalian cells, a small portion of ClC-4 can reach the plasma membrane, thereby enabling its biophysical characterization. Like ClC-3 and ClC-5, ClC-4 yields strongly outwardly rectifying currents with a $NO_3^- > Cl^- > I^-$ conductance sequence (269). These currents, which are significant only at cytoplasmic potentials more positive than ~+20 mV, are inhibited by extracellular acidification. Like the other vesicular CLC proteins, ClC-4 is a Cl^-/H^+ exchanger (651, 742), and neutralization of its "gating glutamate" by mutating it to alanine abolishes its rectification (269) and converts it into a pure Cl^- conductance (651, 742). At first, a 3-pS single-channel conductance was ascribed to ClC-4 (855), but noise analysis later indicated that ClC-4 displays much smaller single-channel amplitudes (~0.1 pS) (334). These are similar to those later obtained for ClC-5 (~0.45 pS) and which likely represent the gating of the $2Cl^-/H^+$ exchange process (941).

Currents mediated by ClC-4 expressed in oocytes are inhibited by extracellular Zn^{2+} and Cd^{2+} with an apparent affinity around 50 μM (613). However, the inhibition is not complete even at very high concentrations. The uncoupled gating glutamate mutation E224A was insensitive to Zn^{2+}, suggesting that the cation binding interferes with the transport process. Mutating H493, which is located at the extracellular end of helix N, slightly reduced Zn^{2+} sensitivity (613). If, however, this residue is part of the binding site is unknown.

The acid-activated currents with an $I^- > Cl^-$ selectivity ascribed to skeletal muscle ClC-4 (408) probably rather reflect activity of the widely expressed acid-activated ASOR channel (103).

B. Localization of ClC-4

ClC-4 is expressed in many tissues, including brain, skeletal muscle, liver, kidney, intestine, and heart (389, 408, 564, 611, 852). There may be differences in the expression pattern between rodents and humans, but published Northern blots display disconcerting variability (11, 389, 408, 852). Part of the variability of tissue expression pattern may be owed to the different chromosomal localization and gene structure in rat and wild mice versus laboratory mouse strains (11, 585). In any case, ClC-4 is prominently found in brain, with particular high expression in pyramidal cells and dentate gyrus of the hippocampus (11, 810) and the Purkinje cell layer of the cerebellum (810).

Although we favor the notion that ClC-4 resides on endosomes, there is currently no consensus on its native localization. This is largely owed to the lack of specific antibodies that work well in IHC with native tissues and cells, and to the lack of KO controls in several publications. Additionally, antibody cross-reactivity to ClC-3 and ClC-5 because of the high degree of homology between these transporter proteins must be addressed (374, 500, 523, 661). In IHC that lacked KO controls, Bear and co-workers (564) described ClC-4 in apical brush-border membrane of intestinal epithelia, where it seemed to colocalize with CFTR, and additionally in intracellular EEA1- and transferrin-positive endosomal compartments. These authors also found ClC-4 in subapical vesicles of renal proximal tubules (566), resembling the localization of ClC-5 (661) and ClC-3 (523). Upon overexpression in HEK293 cells, epitope-tagged ClC-4 was targeted to endosomal structures where it colocalized with ClC-3 and partially with ClC-5 with which it might form heteromers (820). As described below, an endosomal localization seems to be supported by a few functional studies (566, 567). However, immunofluorescence and cell fractionation studies by Sardini and colleagues (611) suggested that ClC-4 rather localizes to the endoplasmic and sarcoplasmic reticulum when overexpressed either in HEK cells or in vivo in skeletal muscle fibers [where native ClC-4 appears highly expressed (611, 852)]. This localization seemed to be supported by fractionation of brain membranes where ClC-4 overlapped with the ER marker SERCA2. Unfortunately, these experiments are not conclusive because subcellular fractions were not tested for endosomal marker proteins (611). Nonetheless, the authors identified an NH_2-terminal motif in ClC-4 that apparently directs ClC-4 specifically to the ER (611).

C. Possible Physiological Roles of ClC-4

The physiological role of ClC-4 remains largely enigmatic. Even if the questionable localization of ClC-4 to the intestinal brush-border membrane (564) were correct, the strong outward rectification of ClC-4 (269) would preclude the postulated role in transepithelial transport (564). On the

other hand, ClC-4 might have a role in endocytosis similar to that of ClC-5 (661). Indeed, Bear and co-workers reported reduced endosomal acidification and altered transferrin trafficking upon siRNA-mediated downregulation of ClC-4 (566), followed by a similar study on *Clcn4*$^{-}$ fibroblasts obtained by crossing *Mus spretus* with *Mus musculus* (567). However, their conclusion that ClC-4 is essential for transferrin endocytosis appears to conflict with the apparently normal renal endocytosis in *Clcn4*$^{-/-}$ mice (700). Wang and Weinman (879) hypothesized that ClC-4 is important for neutralizing currents of the Cu^{2+}-ATPase in the hepatic secretory pathway to explain their observation of increased copper loading of ceruloplasmin upon ClC-4 overexpression. However, this issue was not pursued further, and unpublished work from the Jentsch laboratory found unchanged ceruloplasmin oxidase activity in liver extracts from *Clcn4*$^{-/-}$ mice (802). To add to the confusion, it has been reported that overexpression of ClC-4 might contribute to tumor cell migration and metastasis (373), to osteogenesis in an osteoprogenitor cell line (873), and to nerve growth factor-induced neurite outgrowth (363). It remains unclear how ClC-4 might exert these effects.

D. ClC-4 in Human Disease

Considering the likely effect of ClC-4 on endosomal ion homeostasis, and taking into account that disruption of ClC-5 leads to X-linked Dent's disease (an inherited kidney stone disorder) (481) by impairing renal proximal tubular endocytosis (661), several groups sequenced the *CLCN4* gene in patients with unclear forms of Dent's disease. No mutations were found (494, 836, 916). This agrees with the finding that, unlike *Clcn5*$^{y/-}$ mice (661), *Clcn4*$^{-/-}$ mice do not show proteinuria (700). The disruption of both *Clcn4* and *Clcn5* did not exacerbate the impairment of endocytosis caused by *Clcn5* disruption (700).

Unexpectedly, human genetics rather revealed an important, but poorly understood, role of ClC-4 in the brain. So far, two frameshifting mutations and >10 missense mutations in *CLCN4* have been found in patients with mental retardation that was variably associated with behavior and seizure disorders as well as some facial abnormalities (359, 620, 857). Although mostly seen in males (359, 857) (who carry only one copy of the affected X-chromosome), less severe disease symptoms were also observed in heterozygous females (620) (expected to express mutated and WT ClC-4 in a mosaic manner). When expressed in *Xenopus* oocytes, the majority of the disease-associated missense mutations reduced or abolished the outwardly rectifying ClC-4 exchange currents (359, 620, 857). Of note, most of the missense mutations lie close to the interface of the two subunits of the ClC-4 protein (620).

It remains unclear how ClC-4 loss-of-function mutations might cause these disease phenotypes. Hu et al. (359) reported an impaired neurite branching of cultured hippocampal neurons upon *Clcn4* knockdown with shRNA, and a similar, but less pronounced effect was observed with neurons from *Clcn4*$^{-/-}$ mice. Although this observation is consistent with a previous report (363), effects on neurite branching might be nonspecific and can currently not be mechanistically linked to a loss of ClC-4. Moreover, no obvious morphological changes were observed in the brain of *Clcn4*$^{-/-}$ mice which neither showed obvious learning deficits (Stuhlmann and Jentsch, unpublished).

XI. ClC-5: A KIDNEY-SPECIFIC Cl^-/H^+ ANTIPORTER INVOLVED IN RENAL ENDOCYTOSIS

ClC-5 was identified independently by homology cloning (808) and by positional cloning as the gene being affected in Dent's disease patients (251, 252). Dent's disease, a renal Fanconi syndrome, is an X-linked renal tubular disorder characterized by low-molecular-weight proteinuria (LMWP), associated with hypercalciuria, nephrocalcinosis, and nephrolithiasis (kidney stones) (481, 743). The human *CLCN5* gene is located on Xp11.22 and the gene is X-linked also in rodents. ClC-5 shares ~80% sequence identity with ClC-3 and ClC-4. The protein is composed of 746 amino acids and has a calculated molecular mass of 83 kDa. It is glycosylated at Asn408 (401), a highly conserved glycosylation site in CLC proteins.

ClC-5 is one of the best studied members of the mammalian CLC transporters. The $2Cl^-/H^+$ antiporter is predominantly expressed in the kidney, where its transport activity in the endosomal membrane is essential for receptor-mediated and fluid-phase endocytosis, and the endocytosis of apical plasma membrane proteins, in the proximal tubule. Functional properties have been extensively studied in heterologous expression systems.

A. Basic Properties

Even though in vivo ClC-5 is mostly localized in endosomes, it reaches the plasma membrane in a significant amount in heterologous expression systems, and its functional properties can be studied using conventional electrophysiological techniques. A striking feature of ClC-5-mediated currents is their extreme outward rectification (corresponding to an inward movement of chloride) with currents being measurable only for voltages >20 mV (269, 808). Upon steps to positive voltages, a large proportion of the current activates instantaneously (as judged by the time resolution of the patch-clamp technique), followed by a further increase with millisecond kinetics (269, 808, 941, 966, 967). Surprisingly, no inward tail currents can be resolved upon subsequent steps to a negative voltage (269). Importantly, the strong rectification of ClC-5 is preserved

under a broad range of intracellular and extracellular pH and Cl^- concentration values (787). These properties make it practically impossible to determine the reversal potential of ClC-5-mediated currents. Based on the magnitude of outward currents, a "conductivity sequence" of $SCN^- > NO_3^- > Cl^- > Br^- > I^-$ was determined (269, 808, 941). These general properties of human and rat ClC-5 are qualitatively very similar in the species homologues from *Xenopus laevis* (559), pig (199), mouse (740), and guinea pig (148).

After the landmark discovery that the bacterial EcClC-1 is a secondary-active $2Cl^-/H^+$ antiporter and not a passive Cl^- channel as previously assumed (5), two independent studies, using different methods to detect local H^+ concentration changes, showed that also ClC-4 and ClC-5 are coupled chloride/proton antiporters (651, 742). As in EcClC-1, the "gating glutamate" is essential for proton transport (651, 742). Neutralization of the gating glutamate by mutation to alanine converts ClC-4 and ClC-5 to passive Cl^- conductors (651, 742) that show an almost linear current-voltage relationship, i.e., that permit inward currents that are not seen for the respective WT proteins (269, 651, 742). In addition, currents mediated by the gating glutamate mutant are completely time independent, i.e., lack the millisecond time scale kinetics seen for WT ClC-5. Using concatemers of WT and gating glutamate mutations it could be demonstrated that coupled Cl^-/H^+ transport is carried out by the individual subunits of the homodimeric protein (941). The transport stoichiometry of ClC-5 was determined as $2Cl^-:1H^+$ using a quantitative fluorescence transport assay (966). However, similar to what has been described for the bacterial EcClC-1, polyatomic anions like SCN^- and NO_3^- lead to a partial (in the case of NO_3^-) or almost complete (in the case of SCN^-) uncoupling of Cl^- and H^+ transport, i.e., these anions are transported without or with less countertransport of protons (941). Interestingly, almost completely coupled $2NO_3^-/1H^+$ transport could be introduced into ClC-5 by mutating a highly conserved serine residue to a proline (60, 966), as found in the plant At-ClC-a transporter that performs coupled $2NO_3^-/1H^+$ transport (164), demonstrating the importance of the "central" anion binding site for the ion selectivity of CLC proteins. However, also mutations of the highly conserved lysine residue K210, which is localized in the extracellular pore entrance, slightly affected anion selectivity (179).

Intracellular protons are assumed to access the transport pathway via the so-called proton glutamate that is localized "off-pore," relatively close to the dimer interface (1). Mutating the proton glutamate in EcClC-1 led to a loss of H^+ transport, but Cl^- transport was fully preserved, similar to neutralizing mutations of the gating glutamate (9). Surprisingly, analogous mutations of the proton glutamate in ClC-4 and ClC-5 to alanine or glutamine completely abolished transport, even that of the uncoupling polyatomic SCN^- or NO_3^- anions (941). Interestingly, transport was retained if the proton glutamate was replaced by the titratable residues Asp, His, and Tyr, but not by Arg (941). Additional neutralization of the gating glutamate restored Cl^- transport but not H^+ transport (941).

While the proton glutamate mutant E268A does not exhibit steady-state transport, Smith and Lippiat (788) found that upon voltage steps the mutant shows prominent "pre-steady-state" or "transient" currents. Such transient currents can be observed in response to voltage steps in a variety of electrogenic transporters, such as GABA transporters, or cistine transporters (132, 714). In these transporters, the transient currents are particularly evident in the absence of one of the substrates and generally reflect a combination of voltage-dependent binding of a charged cotransported substrate (e.g., sodium ions/protons) and conformational changes, associated with the partial completion of the transport cycle. Careful analysis of these transient currents can provide insights into some steps of the mechanism of transport. Full completion of the transport cycle is impeded by the absence of an obligatory substrate. However, a combination of transient currents and steady transport currents is possible if the initial rearrangement of states caused by the voltage step is faster than the overall turnover.

The fact that the transient currents in ClC-5 have been observed in the proton glutamate mutant E268A (788) suggests that a full transport cycle is inhibited because no protons can be supplied from the intracellular solution. Smith and Lippiat (788) suggested that the transient currents mainly reflect the voltage-dependent movement of an intrinsic "voltage sensor" of the protein and that anions "modulate" this voltage dependence. Zifarelli et al. (961) could exclude H^+ movement to be significantly involved in the generation of the transient currents. However, a detailed analysis of the Cl^- dependence suggested that the movement of extracellular Cl^- into the transporter contributes to the transient currents (961). The results could be well described by a three-state model predicting that, upon a step to a positive voltage, the first events in the transport cycle are the movement of the gating glutamate from S_{ext} to S_{cen}, accompanied by a movement of a Cl^- from S_{cen} to the inside, which is then followed by the binding of an extracellular Cl^- to S_{ext} (961). The direct involvement of the gating glutamate in the generation of the transient currents was further supported by analyzing the E211D mutant, in which the gating glutamate is substituted by an aspartic acid, which differs from a glutamate only by the lack of a single CH_2 group. The E211D mutant showed no steady transport activity (961), similar to the analogous mutations in CmClC and EcClC-1 (243). Interestingly however, the E211D mutant displayed transient currents even with the proton glutamate being intact. The E211D transient currents were significantly smaller in magnitude, shifted to more negative voltages compared with those of the E268A

mutant, and were almost independent of extracellular Cl^- (961). These results strongly support the idea that the transient currents indeed reflect a movement of the gating glutamate in addition to Cl^- movements.

The voltage dependence of the transient currents of the proton glutamate mutant E268A is characterized by a voltage of half-maximal activation beyond 100 mV (961). Grieschat and Alekov (301) found that in the context of the mutation K210R, in which the lysine next to the gating glutamate is mutated to arginine, the voltage dependence of the transient currents is shifted to more negative voltages. This leftward shift parallels the much less pronounced outward rectification of the currents mediated by the K210R mutation (179) and suggests that the outward rectification of ClC-5 and the activation of the transient currents by positive voltages reflect the same underlying voltage-dependent process, i.e., the displacement of the gating glutamate. The two components of the charge-voltage relationship described by Grieschat and Alekov (301) confirm the three-state model proposed by Zifarelli et al. (961). However, the use of capacitance measurements to quantify the charge displacement (301) does not provide an accurate measurement if the kinetics of the charge movement are too slow to follow the stimulating sine wave. Thus the quantitative aspects of the work of Grieschat and Alekov (301) are questionable.

Interestingly, ClC-3, when targeted to the plasma membrane by mutation of NH_2-terminal sorting motifs, exhibits relatively large transient currents, even without mutating the proton glutamate (316). These authors even proposed that the transient currents could contribute to the charge compensation in vesicular acidification. This is however extremely unlikely since each CLC transporter would contribute only maximally three elementary charges. In fact, in the model proposed by Guzman et al. (316), the buffer capacity of the vesicular lumen was not taken into account, completely invalidating this hypothesis.

For ClC-4 and ClC-5, it was unclear if the extreme outward rectification reflects "instantaneous," transport-related rectification or a fast gating process because no inward tail currents could be detected that would reflect a deactivation of the gating process (180, 269, 808). However, a certain degree of current relaxation is visible for ClC-5 and ClC-4, which has been exploited to perform nonstationary noise analysis to estimate the single transporter turnover rate, resulting in surprisingly large numbers in the order of 10^5 s^{-1} (612, 941, 966, 967). Several mutations of ClC-5 led to significant kinetic alterations of these relaxations, suggesting the presence of a gating mechanism (269). More recently, a point mutant (D76H) of ClC-5 was identified that showed reduced "instantaneous" currents, slowed activation kinetics, and inwardly directed Cl^-/H^+ exchange currents at acidic extracellular pH (180), demonstrating for the first time unambiguously the presence of a gating process in ClC-5 that at least partially underlies the strong outward rectification. However, the interdependence of gating and permeation that plagues the biophysics of CLC channels is even worse for CLC transporters, and so far, we have no good understanding of the gating process in ClC-5.

The dependence of endo/lysosomal transporters on pH is physiologically important because the luminal pH is acidic. ClC-5 is inhibited by acidic extracellular pH (269), in a manner that is compatible with a voltage-dependent binding from the extracellular solution (649). The dependence of transport on intracellular pH has been studied in inside-out macro-patches (966). Macroscopic currents increased at acidic pH with an almost voltage-independent apparent p*K* of ~7. Interestingly, at least for pH≤7.3, the single-transporter turnover estimated by noise analysis did not depend on pH, suggesting that pH_i mostly affects the gating process of ClC-5 (966). These results also suggest that H^+ entry into the transporter from the cytosol is not rate-limiting in the turnover of the WT protein.

Like all mammalian CLCs, the COOH terminus of each ClC-5 monomer harbors two CBS domains. Wellhauser and co-workers provided biochemical evidence that isolated COOH-terminal fragments of the ClC-5 Cl^-/H^+ antiporter bind ATP and other nucleotides (898), and small-angle X-ray scattering indicated a compactation of the CBS domains upon ATP binding (899). The two full-length structures of CBS domain containing CLC proteins, i.e., that of the red alga *Cyanidioschyzon merolae* CmClC Cl^-/H^+ antiporter (242) and that of the bovine ClC-K channel (628), had no nucleotide bound in the CBS domain. Yet, the isolated ClC-5 COOH terminus could be crystallized only in the presence of nucleotides, and an ATP or ADP molecule was found in the crystal structure sandwiched in the cleft between CBS1 and CBS2, making contacts with the protein almost exclusively with the adenine moiety (542). This kind of interaction is consistent with the equal high micromolar binding affinity of AMP, ADP, and AMP demonstrated by biochemical binding studies (542). Functional effects of nucleotide regulation have been studied in ClC-5 using the inside-out patch-clamp technique (967). Adenine nucleotides (ATP, ADP, AMP) increased currents mediated by the human ClC-5 Cl^-/H^+ antiporter almost twofold (967). The effect of nucleotides on the currents could be well described by an allosteric model in which nucleotide binding stabilizes an active, transporting conformation, with apparent binding affinities of 0.9 mM for the inactive state and 0.4 mM for the active state (967). Mutagenesis studies guided by the crystal structure of the ClC-5 CBS domain/ATP complex (542) are overall in agreement with the conclusion that the crystal structure faithfully reflects nucleotide binding in the full-length proteins in that mutants Y617A and D727A were insensitive to nucleotides,

but otherwise had functional properties that were similar to those of WT ClC-5 (967).

B. Transcriptional Regulation

In general, the transcriptional regulation of ClC-5 in humans is little understood. The 5′ regions of mouse and human genes encoding ClC-5 are complex and not fully conserved between the two species (252, 261, 330, 481, 837), rendering an extrapolation of mouse data to humans difficult. However, Tanaka et al. (826) found that the transcription factor HNF1α (homeodomain-containing hepatocyte nuclear factor 1α), which is predominantly expressed in the proximal tubule, activates expression of mouse and human ClC-5 encoding genes, whose 5′ UTRs contain several predicted HNF1α binding sites. In HNF1α-null mice, expression of *Clcn5* was reduced in the proximal tubule but not in the collecting duct (826), where the closely related factor HNF1β might play an important role. HNF1α-null mice show LMWP (831), caused by a downregulation of the expression of the genes encoding cubulin and megalin (831), and probably by an indirect reduction of cubulin and megalin in the brush-border membrane due to reduced endocytic recycling caused by a reduced ClC-5 expression, as seen in ClC-5 KO mice (see below).

Interestingly, intron 3 of the human *CLCN5* gene harbors several microRNAs that play a role in lymphocytic leukemia (715). In chronic lymphocytic leukemia cells, interleukin-4 caused an upregulation of *CLCN5* and a consequent induction of the expression of the miR-362, miR-500a, miR-502, and miR-532 genes (715). A possible role of ClC-5 in this tumorigenic process is unexplored.

C. Localization of ClC-5 and Interacting Proteins

In the adult rat, ClC-5 mRNA is found most abundantly in the kidney but also in intestine, thyroid, and to a smaller extent also in brain, liver, lung, and testis (808, 850, 854). With the use of in situ hybridization, mRNA was localized in cortical medullary ray and outer medullary tubule epithelial cells (500). In the kidney, ClC-5 is expressed as early as E13.5 in mice and at 12 wk of gestation in humans, i.e., at times when glomerular filtration starts (401). Interestingly, in the mouse embryo, ClC-5 mRNA is found not only in the kidney but also abundantly in other absorptive epithelia and even in skeletal muscle (826).

In a landmark study, Günther et al. (307) precisely localized the ClC-5 protein in several segments of the kidney tubule. In the proximal tubule, ClC-5 was found predominantly below the brush border, colocalizing with the H^+-ATPase (307), which is present in the membrane of endosomes. In agreement with the localization of ClC-5 in the endosomal membrane, ClC-5 also colocalized with internalized proteins early after uptake (307). As ClC-5 was believed to be a Cl^- channel, these results led to the hypothesis that ClC-5 plays a role in endocytosis by providing a shunting Cl^- conductance to allow efficient endosomal acidification by the H^+-ATPase (307). In addition to the proximal tubule (PT), ClC-5 protein was found in intercalated cells but not in principal cells of the collecting duct (307). Intercalated cells are most important for acid/base homeostasis. In acid-secreting α-intercalated cells, ClC-5 again colocalized with the H^+-ATPase in apical, submembranous vesicles (307). In acid-resorbing β-intercalated cells, ClC-5 was seen in the apical cytoplasm, whereas the H^+-ATPase localized in the basolateral part of the cells (307). The expression of ClC-5 in PT and in the collecting duct was confirmed in independent studies (190, 603, 728), and additional expression in the thick ascending limb of Henle's loop was found (190).

Mechanisms involved in the membrane stability and subcellular targeting of ClC-5 are still little understood. The intracellular COOH-terminal region between the two CBS domains contains the amino acid sequence PLPPY, which is a putative "PY-motif" (660), and which is not conserved in the highly homologous ClC-3 and ClC-4. In vitro a ClC-5-derived peptide containing this sequence bound to fragments from the WW domain containing proteins WWP1 and WWP2 (660). In support of a role of the PY motif in ubiquitin-mediated degradation, in the heterologous *Xenopus* oocyte expression systems, currents mediated by ClC-5 were doubled by mutation of the motif or by overexpression of a dominant-negative mutant of the WWP2 ubiquitin ligase (759). In addition, stimulation of endocytosis by coexpression of rab5 mutants decreased currents of WT ClC-5, but not ClC-5 with a mutated PY motif, and inhibiting endocytosis had the inverse effect (759). Similar results were obtained in oocytes with the Nedd4.2, but not with the Nedd4, WW domain containing ubiquitin ligase, although both proteins bound to ClC-5 (355). In opossum kidney (OK) cells, a PT cell model that expresses ClC-5 (735), ClC-5 biochemically interacted with other WW- and HECT-domain containing proteins, Nedd4 or Nedd4–2 (355). Knocking down Nedd4–2 activity in OK cells reduced albumin uptake, but it is not clear if ClC-5 was involved in this effect (355). Despite the in vitro evidence, the physiological role of the PY motif is still unclear as no effect on ClC-5 protein abundance or localization, or on proximal tubular endocytosis, was observed in a *knock in* mouse model in which the PY motif was disrupted (700). The possibility that heteromerization with the homologous ClC-3 or ClC-4 proteins could have masked a phenotype in this *knock in* model was excluded by showing that the combination of a disrupted PY motif in ClC-5 with knocking out ClC-3 or ClC-4 did not induce low-molecular-weight proteinurea or defective PT endocytosis (700).

Several other proteins have been described to interact with ClC-5 and to be involved in the regulation of the transporter. For example, the actin depolymerizing protein clofilin was detected in a yeast-two-hybrid screen (357). However, the possible role of this interaction is obscure. The sodium hydrogen exchanger regulatory factors NHERF-1 and NHERF-2 and other PDZ domain containing scaffolding proteins are involved in the regulation of various transport processes in the PT (155). The PDZ2 domain of NHERF-2 was found to interact with ClC-5 (354) and silencing NHERF-2 in OK cells slightly reduced, and silencing of NHERF-1 slightly increased ClC-5 surface expression (354). The significance of these findings is unclear. Neither NHERF-1 nor NHERF-2 *knockout* mice showed LMWP (156), a hallmark of ClC-5 dysfunction. Again using yeast-two-hybrid screening, the KIF3B protein was reported to interact with a bait consisting of a COOH-terminal fragment of ClC-5 and the interaction was confirmed by pull-down and immunoprecipitation (693). KIF3B is a component of a heterotrimeric kinesin 2 microtubule-associated motor protein complex including also KIF3A and KAP3. Among other functions, kinesin-2 has been implicated in bidirectional transport of vesicles and organelles associated with both the secretory and endocytic pathways, moving towards the plus end of microtubules (753). Consistent with the idea that KIF3B containing kinesin 2 motors are involved in the regulation of ClC-5 in the plasma membrane, various maneuvers of up- and downregulation of KIF3B in HEK cells overexpressing ClC-5 or in polarized OK cells expressing ClC-5 endogenously resulted in the relatively small but predicted changes in ClC-5-mediated ionic currents and surface expression (693). However, effects resulting from the overexpression or suppression of a single subunit of a heterotrimeric complex are difficult to interpret, and indirect effects on ClC-5 by a broad effect on intracellular trafficking are likely. Specificity should be demonstrated in future experiments by identification and subsequent modification of the KIF3B binding site on the ClC-5 protein.

Surprisingly, using a GST-fusion protein pulldown assay, neither of the above-mentioned proteins was identified as a binding partner of ClC-5 (447). Instead, the cytosolic aspartyl aminopeptidase DNPEP was pulled down and direct interaction was confirmed by coimmunoprecipitation in vitro and in rat kidney lysates (447). DNPEP overexpression in OK cells induced small effects on albumin endocytosis and ClC-5 plasma membrane expression (447). The overall physiological relevance of this interaction remains to be established.

D. Dent's Disease Mechanism Revealed by Knockout Mouse Models

ClC-5 gained particular interest after it was shown that defects in the *CLCN5* gene are underlying Dent's disease (251, 252, 481). Dent's disease (OMIM no. 300009), a type of renal Fanconi syndrome, refers to a group of closely related, previously distinctly defined X-linked diseases associated with malfunctions of the proximal tubule, including X-linked recessive nephrolithiasis, X-linked hypercalciuric hypophosphatemic rickets, and idiopathic LMWP with hypercalciuria and nephrocalcinosis (184, 191, 666, 744). The most common symptom present in practically all patients is LMWP, which is also seen in many female carriers (191). However, LMWP is clinically not the most important symptom. Patients often exhibit hyperphosphaturia and hypercalciuria which can result in rickets, nephrocalcinosis, and kidney stones, which can lead to progressive kidney failure (743, 915). Most male patients exhibit hypercalciuria, two-thirds present with nephrocalcinosis, and about half of them develop kidney stones (112), the most relevant clinical symptom of the disease.

More recently, a certain genetic variability of Dent's disease has emerged. In fact, only ~60% of patients with Dent's disease carry mutations in *CLCN5*. In ~15% of patients, mutations were found in the X-chromosomal *OCRL1* gene (349). Dent's disease associated with *OCRL1* mutations is now termed Dent's disease 2 (175). *OCRL1* encodes a phosphatidylinositol-4,5-bisphosphate [$PI(4,5)P_2$] 5-phosphatase which hydrolyzes the signaling lipid $PI(4,5)P_2$ in several cellular compartments (350, 956). OCRL1 is a membrane-associated protein localized to the Golgi apparatus and early endosomes (950), but also to lysosomes (168). The precise function of OCRL1 is not clear, but there is some evidence that the phosphatase is involved in endocytic megalin recycling through the effect of $PI(4,5)P_2$ levels on actin polymerization (859). Previously, *OCRL1* mutations had been exclusively associated with the oculocerebrorenal syndrome of Lowe, which is characterized by congenital cataracts, severe mental retardation, and renal defects similar to Dent's disease (39, 488). However, some *OCRL1* mutations cause renal defects typical of Dent's disease without other pathological manifestations (350). It is not clear why certain OCRL1 mutations only cause the renal symptoms and not the full spectrum of symptoms characteristic for Lowe syndrome. It has been suggested that the difference may be related to the presence of OCRL1 splice variants and that some mutations only affect a limited number of variants (775). The lack of *CLCN5* or *OCRL1* mutations in patients with Dent's disease suggests that at least one additional gene is associated with the disease (350, 916).

For simplicity, hereafter we will refer to Dent's disease as the subtype caused by *CLCN5* mutations. Many Dent's disease causing mutations cause a severe or total loss of function of the protein (see below). For such mutations, affected males will have a complete loss of ClC-5 function, while female carriers will have a loss of function in approximately one-half of cells due to X-chromosome inactiva-

tion. Two independent *knockout* mouse lines have been created to investigate the mechanisms underlying Dent's disease (661, 878). The lines showed some interesting differences and for simplicity will be designated as the Jentsch mouse (661) and the Guggino mouse (878), respectively. Both lines were viable, had normal growth, and were fertile. No gross anatomical changes were seen in either except that a small number of Guggino ClC-5^{-} mice had deformities of the dorsal spine and backward growth of teeth but not osteopenia or rickets (878). Both KO lines showed prominent LMWP with an elevated loss of vitamin D binding protein (661, 878), retinol binding protein, PTH, injected beta2-microglobulin (661) **(FIGURE 12, *A–C*)** and Clara cell protein (878). Both mice exhibited polyuria and phosphaturia and the Guggino mouse had also glycosuria and aminoaciduria (which was not tested in the Jentsch mouse). Surprisingly, the Jentsch mouse did not exhibit hypercalciurea or nephrolithiasis, while the Guggino mouse had a more than doubled urine Ca^{2+} concentration and microscopic calcium deposits were found in the corticomedullary junction. Possible reasons for this difference will be discussed below. Another mouse model in which ClC-5 was partially reduced with a ribozyme approach showed neither proteinurea nor phosphaturia and will not be discussed further (501).

The LMWP in the KO mouse models was caused by a defective receptor-mediated endocytosis process in the PT

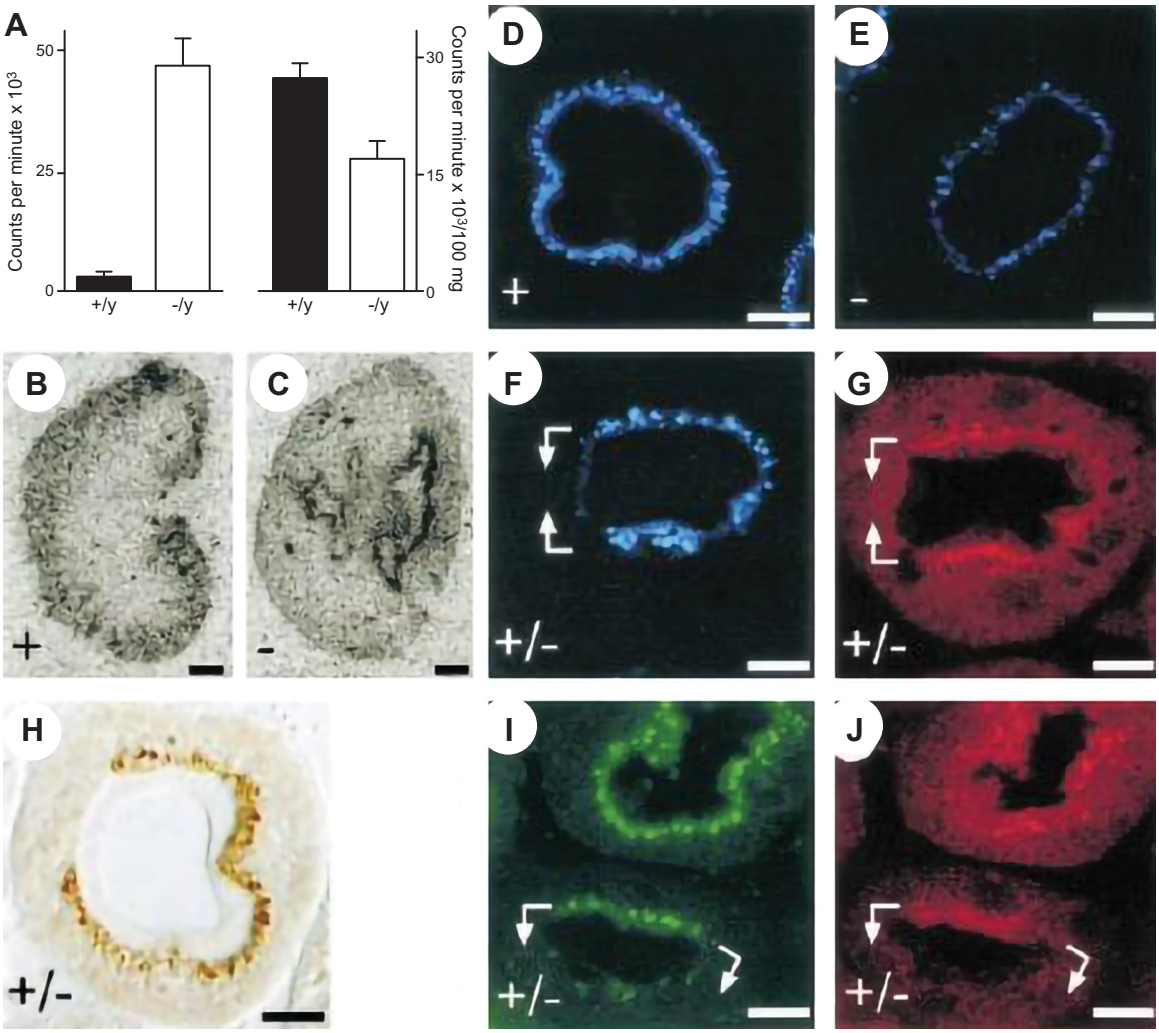

FIGURE 12. Role of ClC-5 in proximal tubule endocytosis. *A*: amounts of injected radioactive β2-microglobulin lost in the urine (*left*) or retained in the kidney (*right*) in WT mice and male mice lacking ClC-5. *B* and *C*: autoradiographs of kidneys 7 min after injection of radioactive β2-microglobulin show that the small protein had accumulated in the cortex, which consist mostly of proximal tubules, in WT kidneys, but is found in deeper, probably pelvic regions in ClC-5^{-} kidneys. *D–F*: endocytosis of fluorescently labeled β-lactoglobulin (in blue) is severely impaired in *Clcn5*$^{-}$ proximal tubules (*E*) compared with WT (*D*). Heterozygous *Clcn5*$^{+/-}$ females (*F*), which express normal ClC-5 levels in some cells and lack ClC-5 in others, display normal endocytosis in exactly those cells that do express ClC-5, as highlighted by antibody staining (*G*, red). *H*: reduced receptor-mediated uptake of horseradish peroxidase only in some cells in a heterozygous *Clcn5*$^{+/-}$ female. *I* and *J*: fluid-phase endocytosis of FITC-labeled dextran (*I*, red) is impaired only in ClC-5 lacking cells (ClC-5 stained in red in *J*) in a heterozygous *Clcn5*$^{+/-}$ female. [From Piwon et al. (661).]

(661, 878). Injected horseradish peroxidase was poorly endocytosed **(FIGURE 12*H*)** and was detected in distal segments in the Guggino mouse (878), and the accumulation of injected fluorescently labeled lactoglobulin accumulated in vesicles below the PT brush border was drastically reduced in the Jentsch mouse (661). In addition, Piwon et al. (661) exploited the fact that heterozygous female mice are mosaic *knockouts* because due to random X-chromosome inactivation about half of cells are ClC-5 *knockout*, whereas the other half express normal levels of ClC-5 **(FIGURE 12)**. Detecting fluorescent lactoglobulin at the single-cell level and costaining with ClC-5 antibodies, they could show that the defective receptor-mediated endocytosis is seen only in the ClC-5$^-$ cells, i.e., it is a cell-autonomous defect (661) **(FIGURE 12)**. Very similar results were seen with FITC-dextran, a marker of fluid-phase endocytosis (661) **(FIGURE 12)**.

An important finding was that megalin, the apical receptor for endocytosis of a broad range of luminal proteins which partially overlaps in localization with ClC-5 in WT mice (661), was significantly reduced in ClC-5$^-$ PT cells (661). Normally megalin is recycled to the plasma membrane after discharging its endocytosed cargo in the endosomal lumen, and the observed reduction of megalin in ClC-5$^-$ most likely reflects a defect in this recycling step. Later studies confirmed the reduction of megalin at the electron microscopic levels and additionally demonstrated that also the apical coreceptor cubilin is drastically reduced in the brush border in the PT of ClC-5$^-$ KO mice (135). The localization or abundance of the H^+-ATPase was affected neither in the PT nor in α-intercalated cells in the collecting duct (661).

Piwon et al. (661) further studied in great detail the mechanisms of phosphate and calcium regulation in the ClC-5$^-$ mouse. A large proportion of phosphate is reabsorbed by the apical Na-phosphate cotransporter Napi2 (also known as NaPi-2a or Npt2, encoded by the human SLC34A1 gene) (52). Napi2 is known to be regulated by endocytosis in PT, in response to parathyroid hormone (PTH). On a normal diet, WT mice showed an intense staining for Napi2 in the brush border, which was significantly reduced in ClC-5$^-$ mice (661). This is a priori surprising if ClC-5$^-$ mice have a defect in endocytosis. Importantly, with the use of mosaic female *Clcn5*$^{+/-}$ mice, it was found that the reduction of Napi2 was not a cell autonomous effect (661). In fact, Piwon et al. (661) convincingly demonstrated that the Napi2 downregulation was secondarily caused by a defective endocytosis of the peptide hormone PTH that induces Napi2 endocytosis. The reduced Napi-2 expression most likely underlies the hyperphosphaturia seen in the *knockout* mice. Under a reduced phosphate diet, which is known to stimulate Napi2 expression (573), the presence of Napi2 was normalized in *Clcn5*$^-$ mice (661). To directly test the effect of PTH, the hormone was injected and kidney tissue was fixed at various time-points. Fifteen minutes after PTH injection, Napi2 was internalized in a cell-autonomous manner in WT but not in ClC-5$^-$ mice, while 1 h after injection Napi2 was internalized also in the *knockout*. Hence, its endocytosis is reduced but not fully abolished (661). These results show that defective PTH uptake resulting in excessive Napi2 internalization underlies hyperphospaturia in Dent's disease.

Another transporter found to be disregulated in ClC-5$^-$ mice was the Na^+/H^+ exchanger NHE3, which is involved in Na and bicarbonate, and consequently, also water reabsorption. As Napi2, NHE3 is regulated by PTH-induced endocytosis. As found for Napi2, on a normal diet, NHE3 was internalized in a non-cell autonomous manner in ClC-5$^-$ mice, and dietary phosphate deprivation led to an increased plasma membrane expression (661). Similar to the observations made for Napi2, PTH-induced endocytosis of NHE3 was markedly slowed, but not abolished in ClC-5$^-$ mice. The decreased activity of NHE3 may contribute to increased volume of urine seen in both KO models (661, 878). The decreased protein abundance of NHE3 in ClC-5$^-$ mice was recently confirmed using transport activity measurements in kidney slices from the Guggino mouse (473). Acute dexamethasone stimulation, which is believed to augment NHE3 surface expression via exocytosis, increased NHE3 less in ClC-5$^-$ mice compared with WT mice (473). Further experiments in OK cells, in which endogenous ClC-5 was partially knocked-down by short hairpin RNA, suggested that PTH-induced endocytosis of NHE3 was not significantly impaired by ClC-5 knock-down (473), in contrast to in vivo experiments with *Clcn5*$^-$ mice (661). However, the earliest time point at which endocytosis was assessed was 20 min after addition of PTH, such that a slowing of endocytosis might not have been detected. Acute dexamethasone treatment led to a significantly smaller increase in NHE3 surface expression in OK cells in which ClC-5 had been knocked down, suggesting the possibility that ClC-5 is important for the exocytotic plasma membrane insertion of NHE3 (473). Contrasting with the decrease of megalin, Napi-2 and NHE3 in the apical membrane of PT cell lacking ClC-5, aquaporin 1 (AQP1) expression was reported to be rather increased in apical (but not basolateral) membranes of those cells (664). These results are in general agreement with the idea that ClC-5 is not only important for endocytosis but also for the recycling of endosomes (385), which in fact most likely underlies the decrease of megalin in the brush border (661).

Reabsorption of Ca^{2+} in the kidney occurs via paracellular and transcellular pathways that most likely do not directly involve ClC-5 as an endosomal protein. Thus the hypercalciuria seen in many Dent's disease patients and in the Guggino mouse and the phenotypic differences between the two ClC-5$^-$ lines are most likely explained by a slightly different balance in the handling of calciotropic hormones and their effects in the kidney, as indeed strongly suggested by the investigations of Piwon et al. (661). It has to be remembered

that the proximal tubule is the major site in the body for the enzymatic conversion of 25(OH)-vitamin D_3 to the active form 1,25$(OH)_2$-vitamin D_3, a reaction performed by the mitochondrial α-hydroxylase, which is upregulated by PTH. Various effects of reduced endocytosis in the PT with opposite outcomes have to be considered. First, increased PTH should upregulate α-hydroxylase, as indeed observed (308). This should stimulate the conversion of 25(OH)-vitamin D_3 to 1,25$(OH)_2$-vitamin D_3 in the PT, leading to increased intestinal Ca^{2+} absorption. Also the urinary loss of phosphate could increase 1,25$(OH)_2$-vitamin D_3 as seen in *Npt2*$^{+/-}$ mice with a heterozygous loss of Napi2 (52). Indeed, increased 1,25$(OH)_2$-vitamin D_3 concentrations are seen in Dent's disease patients (743). On the other hand, the reduced endocytosis of vitamin D binding protein leads to urinary loss of vitamin D, i.e., a decreased availability of the precursor in the PT. In fact, both forms of vitamin D_3 were decreased in the serum, with the ratio 1,25$(OH)_2$-vitamin D/25(OH)-vitamin D being slightly increased (308, 661). Thus a delicate balance between the supply of the precursor and the stimulation of the hydroxylase by PTH likely determines the presence or absence of hypercalciuria as seen in the Guggino mouse versus the Jentsch mouse and may underlie the phenotypic variability in Dent's disease patients. In addition, alterations in the Ca^{2+} homeostasis of bone, another important vitamin D target organ, have to be considered. Indeed, an analysis of the Ca^{2+} handling in the Guggino mouse suggested that their hypercalciuria is of bone and renal origin instead of being caused by increased intestinal Ca^{2+} absorption (779). Especially the finding that the KO mice have elevated bone turnover markers points to a use of their bone Ca^{2+} stores.

Overall, the systemic effects induced by the dysfunction of ClC-5 show that the endocytosis of small proteins in the PT does not primarily serve to recover amino acids but has an important role in the control of hormone effects via their carrier proteins. An additional example regards retinol and its binding protein, which is lost in the urine in ClC-5$^-$ mice (661). This may underlie the upregulation or retinol target genes seen in ClC-5$^-$ mice (525) and may be the cause of night blindness reported in three Indian boys with Dent's disease and mutations in *CLCN5* (765). Gailly et al. (278), using RT-PCR on cells from ClC-5$^-$ PT, found increased expression of various proteins linked to oxidative stress and an induction of type III carbonic anhydrase (CAIII). The role of CAIII in Dent's disease, however, remains elusive. More generally, 720 genes involved in various physiological processes are differentially expressed in ClC-5$^-$ mice (914).

More recently, glomerular pathology, in particular focal glomerulosclerosis, focal interstitial fibrosis, interstitial lymphocyte infiltration, and tubular damage, has been described in a considerable fraction of patients with Dent's disease (147, 270, 880). While glomerulosclerosis is of clear pathological relevance, it remains to be understood if it was caused secondary to the tubular phenotype or directly by ClC-5 dysfunction in glomerular cells, where the protein is expressed at a very small level (307).

E. The Function of ClC-5 as a 2 Cl^-/H^+ Antiporter in Proximal Tubule Endocytosis and Recycling

Assuming that ClC-5 is a passive Cl^- channel like ClC-0 and ClC-1, the most parsimonious explanation of the phenotype of Dent's disease, was that ClC-5 enables efficient endosomal acidification by providing an anion conductance necessary to neutralize the build-up of luminal positive charge by the V-type H^+-ATPase (307, 661). This notion was bolstered by the colocalization of ClC-5 with the H^+-ATPase (307). The electrophysiological properties of ClC-5 did not provide any reason to doubt this hypothesis (269, 808). In agreement with this proposition, the rate of ATP-induced acidification of cortical endosomes from *Clcn5*$^-$ mice was significantly slowed compared with WT (308, 600). In agreement with Cl^- playing an important role in ClC-5-dependent endocytosis, Wang et al. (882) found that replacement of Cl^- by the impermeable gluconate reduced receptor-mediated and fluid-phase endocytosis in cultured PT cells from WT mice to the same level as in bafilomycin-treated cells (284) and as in cells from *Clcn5*$^-$ mice. The residual endocytotic activity seen in cells from *Clcn5*$^-$ mice or in bafilomycin-treated cells could be further reduced by the NHE3 inhibitor S3226 (882). *Nhe3*$^{-/-}$ mice display moderate proteinuria (285), but the precise role of NHE3 in PT endocytosis remains to be established. As expected, re-expression of WT ClC-5 but not of ClC-5 carrying Dent's disease mutations restored endocytosis in cells from *Clcn5*$^-$ mice (882).

After the discovery that the bacterial EcClC-1 is a transporter and not a channel (5), the properties of ClC-5 were reassessed, and it was established that also ClC-5 is a secondary active transporter that exchanges 2 Cl^- for 1 H^+ (651, 742, 966). This finding forced a revision of the physiological role of ClC-5, because the transport of protons directly impinges on endosomal pH. In this respect, a major unresolved question regards the direction of transport. The finding that ClC-5, like the other vesicular CLCs, shows extreme outward rectification is often interpreted as meaning that these transporters can only mediate transport of Cl^- out of the lumen and protons into the endosomal lumen. However, if the voltage dependence of the transporter is independent of the ion gradients, appropriate Cl^- and H^+ gradients would allow also net transport in the opposite direction if the cytoplasmic potential is positive enough. On the other hand, Smith and Lippiat (787) reported shifts in the voltage dependence of ClC-5 with changes in pH and [Cl^-] that conspire to only allow Cl^- transport into the cytosol. This would mean that ClC-5 directly contributes to endosomal acidification (742), but in a manner that would

actually exacerbate positive charge accumulation that should oppose sustained endosomal acidification. In line with such a hypothesis, Smith and Lippiat (787) found that overexpression of WT ClC-5 in HEK cells induced a component of endosomal acidification that could not be inhibited by the H^+-ATPase blocker bafilomycin (787). This component was not seen after overexpression of mutants that are unable to transport protons, i.e., the uncoupled, passively Cl^- transporting gating glutamate mutant or the nontransporting proton glutamate mutant (787). Furthermore, in OK cells, which endogenously express ClC-5, a bafilomycin-independent component of endosomal acidification could be significantly reduced by knocking down ClC-5 expression (787). However, even though a direct contribution of ClC-5 to endosomal acidification cannot be safely ruled out as our knowledge of the native transport properties of endosomes is very limited, a few basic considerations render the hypothesis rather unlikely. Assuming that an endosome has to lower the pH from an initial value of 7.4 by at least 1.5 pH units, and assuming a pH buffer capacity around 30 mM/pH unit, a total of 45 mM H^+ have to be pumped into the lumen corresponding to ~90 mM equivalent Cl^- to be pumped out assuming a 2:1 Cl^-/H^+ antiport stoichiometry. This figure, i.e., 90 mM Cl^-, is above the initial value of Cl^- which was measured to be <20 mM in endosomes after endocytic uptake (792). In fact, Sonawane et al. (792) found that endosomal Cl^- concentration increased during the acidification process, in contrast to the decrease predicted by Smith and Lippiat (787). Even ignoring this aspect, the total amount of charge to be neutralized amounts to 135 mM, which, based on the available ion species, can be realistically accomplished only by an outward movement of Na^+. Even with the assumption of the existence of an endosomal Na^+ channel, the overall process would lead to a dramatic reduction of endosomal osmolarity and consequent shrinkage, which is not observed experimentally.

Important insight into to the role of ClC-5 was obtained by the study of mice in which ClC-5 carried a mutation of the gating glutamate that uncouples Cl^- and H^+ transport rendering ClC-5 a pure anion conductance (600). Endosomes prepared from mice carrying this uncoupling mutation (ClC-5^{unc}) exhibited practically normal ATP-dependent acidification, but, surprisingly, endocytosis was severely impaired and the mice displayed a similar phenotype compared with ClC-5- mice KO (600). ClC-5^{unc} mice even showed hypercalciuria and hyperphosphaturia (600). In agreement with these results from a mouse model, recently, Dent's disease patients were shown to carry the uncoupling mutation E211Q (738, 764). These results show that defective endocytosis in Dent's disease is not (or not only) the result of reduced ATP-driven acidification but is critically dependent on the coupling between Cl^- and H^+ transport (600). In fact, conceptually, a major difference between a passively shunting Cl^- conductance and a secondary active Cl^-/H^+ antiport mechanism is that due to the strict transport coupling, the equilibrium values of the luminal Cl^- concentration, the luminal pH, and the endosomal membrane potential are intrinsically linked. This implies the somewhat counterintuitive result that $2Cl^-/1H^+$ antiporter can sustain a more acidic luminal pH value compared with a passive Cl^- conductance as shown in model calculations under simplifying assumptions (372, 896), even though acidification requires more metabolic energy because H^+ are partially "wasted." In these calculations, the endosomal membrane potential reached rather negative (inside) potentials. A prediction of the antiport mechanism of ClC-5 (and all other intracellular CLCs) is that the luminal Cl^- concentration is increased above the cytosolic Cl^- concentration due to the pH gradient. In fact, based on the result from the *Clcn5*^{unc} mice and similar *Clcn7*^{unc} mice, Jentsch and colleagues proposed that this is the major function of endo/lysosomal CLCs (600, 896), implying that a high endosomal Cl^- concentration is essential for endocytosis. In ClC-7^{unc} mice, a decreased lysosomal Cl^- concentration could be measured using a ratiometric fluorescent Cl^- sensor (896).

F. Phenotype of Dent's Disease Mutations

A micro-deletion of <515 kb on Xp11.22 containing the *CLCN5* gene led to the identification of ClC-5 as the causative gene of Dent's disease (251, 252) and showed that a complete loss of function leads to the typical Dent's disease phenotype. Subsequently, the first single-point mutations including nonsense, missense, and donor splice site mutations were identified in Dent's disease kindreds (481). Partial or complete loss of function was confirmed for four missense mutations in heterologous expression systems (481).

Up to now, more than 190 *CLCN5* sequence variants are known to cause Dent's disease, including large deletions, promoter mutations, splice site mutations, frameshift mutations, and missense and nonsense mutations (519, 680). Most missense mutations that have been studied in heterologous expression systems lead to a lack of functional expression of the protein at the plasma membrane (161, 487, 680, 764, 802). The missense mutations are found all over the protein with a slight tendency to cluster at the dimer interface (487, 789, 917). If such mutations act by destabilizing biochemically or functionally the dimeric proteins, as seen, e.g., for several myotonia-causing mutations in the muscle ClC-1 channel (670), is unknown.

Only a relatively small number of mutations have been characterized at the functional level, mostly in heterologous expression systems. Practically all mutations exhibit reduced or abolished ion transport ability at the plasma membrane. A limited number of mutations showed alterations of biophysical gating processes (21). In most cases, the loss of

function is caused by impaired surface expression due to ER retention or altered redistribution between early and late endosomes (487, 519, 680). Surface expression is an indirect manner to assay ClC-5 function, whose physiological role is performed in the endosomal membrane. In this respect, a surprising finding was that two mutants (G57V and R280P) showed reduced surface expression, but unaltered (G57V) or even enhanced (R280P) endosomal acidification (789). However, results obtained in overexpressing heterologous systems have to be interpreted cautiously. A more physiological system was established by Gorvin et al. (292) who obtained conditionally immortalized proximal-tubular epithelial cell lines (ciPTEC) from patients with Dent's disease and studied the process of endocytosis. With this approach it was shown that all mutations studied reduced receptor-mediated endocytosis as expected (292). Interestingly, in one of the mutant cell lines (harboring the 30:insH mutation), endosomal pH was unaltered compared with WT cells, suggesting that the mechanism by which ClC-5 mutations lead to Dent's disease is not necessarily linked to defective endosomal acidification (292). Such patient-derived cell lines offer the opportunity to perform pharmacological tests aimed at correcting the functional defect.

G. Role of ClC-5 in Other Organs

In addition to kidney, ClC-5 is significantly expressed in intestine, thyroid, and to a small extent also in liver and brain (148, 808, 850, 854). In the liver, no defect of endocytosis of asialofetuin could be detected in ClC-5^{-} mice (661). In the intestine, with the use of immunofluorescence, it was found that ClC-5 is concentrated in the cytoplasm above the nuclei of enterocytes and colon cells (854). Ulcerative colitis, one of the major forms of inflammatory bowel disease, is often associated with defects in intestinal ion and water transport, and Alex et al. (23) reported an increased susceptibility to dextran sulfide sodium induced colitis in *Clcn5*$^{-}$ mice. However, whether this was associated with altered intestinal fluid and salt handling was not investigated. Thus the physiological role of ClC-5 in the intestine remains essentially unknown. An altered immune response at the basis of the increased susceptibility to colitis would be consistent with microarray data from intestine showing differences in genes implicated in the immune system (525).

The quite significant expression of ClC-5 in the thyroid (524, 850) led to the suggestion that it might be involved in the megalin-mediated endocytosis of iodinated thyroglobulin from the follicular lumen, similar to megalin-mediated endocytosis in the kidney. Consistent with a role of ClC-5 in the thyroid, the Guggino *Clcn5*$^{-}$ mice indeed show a thyroid phenotype with mice developing a goiter, i.e., an increased size of the thyroid gland, at 5 mo of age (850), whereas this was not observed in the Jentsch mouse (524). Importantly, both mouse models had normal levels of thyroid hormones and normal endocytosis, and no reduction in megalin was seen in the thyroid of Jentsch mice (524). The goiter of the Guggino mouse was associated with a reduced expression of the apical I^{-}/Cl^{-} exchanger pendrin involved in apical I^{-} efflux (850). However, the mechanistic link to ClC-5 dysfunction is not resolved (258).

H. Pharmacology of ClC-5

Several classical Cl^{-} channel blockers including DIDS, 9-AC, NPPB, DPC (diphenylamine-2-carboxylate), NFA, and CPP have been tested on ClC-5, but none of these has any appreciable effect (675, 808). The only small molecule compound reported to reduce ClC-5 is RT-93 with a reported IC_{50} value of ~200 μM (464). This low affinity and the hydrophobic nature of RT-93 render this compound rather useless for practical applications. High-affinity ligands are of considerable interest in particular as experimental tools to interfere acutely with ClC-5 function in physiological experiments. From a therapeutic perspective, "correctors" that help to reduce mutation-induced misfolding could help in a significant number of patients.

XII. ClC-6: A LATE ENDOSOMAL Cl^{-}/H^{+} EXCHANGER OF NEURONS

Together with ClC-7, ClC-6 forms the third branch of the mammalian CLC gene family (79). In spite of a wide expression of the *CLCN6* mRNA across many human tissues (79), the ClC-6 protein appears to be rather specific for the nervous system (663). ClC-6 resides predominantly on late endosomes (663) and mediates voltage-dependent electrogenic Cl^{-}/H^{+} exchange (576) like the other vesicular CLC proteins. Disruption of *Clcn6* entails a peculiar form of neuronal lysosomal storage disease in mice that resembles mild forms of neuronal ceroid lipofuscinosis (663) **(FIGURE 13)** and is distinct from that observed with a loss of *Clcn7* (407, 668). As yet, no convincing disease-causing mutations have been identified in human patients. ClC-6 is one of the less studied mammalian CLCs.

A. Basic Properties of ClC-6

ClC-6 is a glycosylated (366) ~97 kDa protein of 869 amino acids that shares ~45% sequence identity with ClC-7 (79, 663) with which it forms an own branch of the gene family. In contrast to members of the second CLC family branch (ClC-3 through ClC-5), which could be coimmunoprecipitated and may form heteromeric transporters (820), ClC-6 appears not to interact with ClC-7, nor with other CLCs (820). Both the NH_2 and the COOH terminus of ClC-6 can bind to the adaptor complex AP3 (801). Several *CLCN6* splice variants have been identified by RT-PCR from a human cell line (213), but their significance is questionable as they predict severely truncated, nonfunctional proteins.

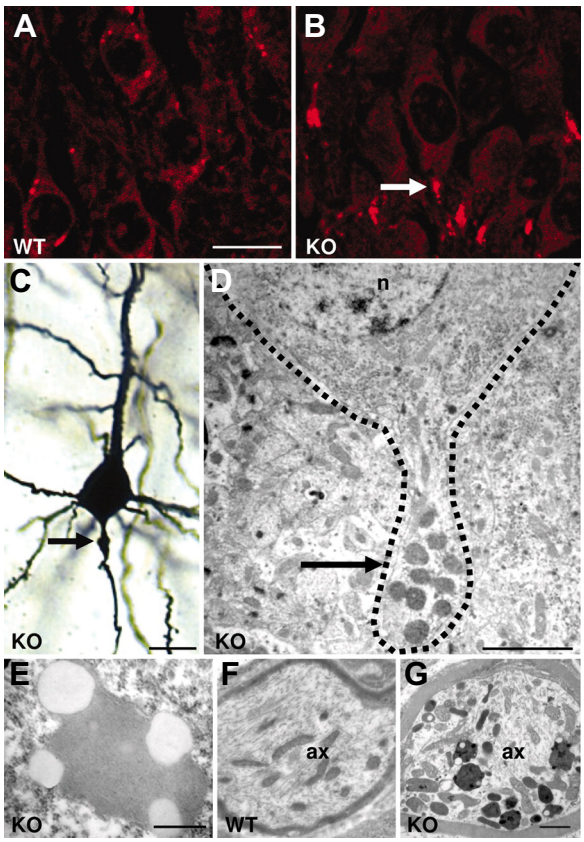

FIGURE 13. Storage material and axonal swelling in *Clcn6*$^{-/-}$ mice. *A* and *B*: autofluorescence, reflecting the presence of lysosomal storage material, in hippocampal sections reveals the accumulation of storage material in 3-mo-old *Clcn6*$^{-/-}$ mice (*B*) compared with WT littermates (*A*) and localization in the initial axon segment (arrow). *C*: Golgi staining shows proximal axonal swelling in cortical neurons from *Clcn6*$^{-/-}$ mice (6 mo). *D*: electron microscopy picture showing similar swelling of a hippocampal axon because of material accumulation (arrow). The plasma membrane of the neuron is highlighted by a dashed line; n, nucleus. *E*: presence of lipofuscin-like lipopigment associated with lipid droplets in a cortical neuron of a *Clcn6*$^{-/-}$ mouse. *F* and *G*: presence of storage material in DRG axons ClC-6 knockout (*G*) but not in WT (*F*). [From Poët et al. (663).]

For more than 10 years, attempts to determine the transport properties of ClC-6 were unsuccessful (79, 92) because of its targeting to endosomes. Mutating AP3-binding sites and other consensus sorting motifs failed to bring sufficient amounts of ClC-6 to the plasma membrane (801), but for unknown reasons fusion of GFP to the NH_2 terminus of ClC-6 finally allowed a small fraction of ClC-6 to reach the outer membrane (576). GFP-ClC-6 mediates small, strongly outwardly rectifying currents in CHO cells (576) which lack significant ClC-5 expression (808) and display minimal Cl^-/H^+ exchange background activity. These currents activated almost instantaneously upon depolarization, were inhibited by extracellular acidification, and displayed the $NO_3^- > Cl^- > I^-$ conductance sequence that is typical for mammalian CLC exchangers (576). Cl^-/H^+ exchange activity could be ascertained by voltage-dependent changes of pH_i in GFP-ClC-6 expressing *Xenopus* oocytes (576). Like in other mammalian CLC exchangers, mutations in the gating glutamate of GFP-ClC-6 abolished proton coupling and converted ClC-6 to an almost ohmic anion conductance. This conductance could be increased threefold by mutating a Cl^- coordinating tyrosine (576) which is thought to represent an internal gate in the *E. coli* exchanger EcClC-1 (378). As further proof for ClC-6 mediating these rather small currents, mutating the Cl^- coordinating serine to proline increased its preference for NO_3^-, just as observed in ClC-4 and -5 (60, 966), ClC-0 (60), and EcClC-1 (650). Although expression levels did not allow to determine the stoichiometry of Cl^-/H^+ coupling, there is little doubt that ClC-6 is a $2Cl^-/H^+$ exchanger with transport properties that strongly resemble those of ClC-4 and ClC-5.

B. Localization of ClC-6

Although Northern blots (79) and NCBI expression databases show a nearly ubiquitous expression of ClC-6 transcripts, Western blots revealed that the ClC-6 protein was expressed in brain, but not in liver, kidney, and heart (663). Immunohistochemistry detected ClC-6 in the hippocampus and all cortical layers of adult mice (663), and in situ hybridization of mouse P0 embryos revealed strong signals in brain, spinal cord, trigeminal and dorsal root ganglia and the eye (663). In situ hybridization of adult mouse tissue sections (414) found impressive *Clcn6* signals in the testis and in epithelial cells of the lung, trachea, pancreas, and intestine, but failed to detect *Clcn6* transcripts in the brain. The reason for the discrepancy between the wide mRNA and restricted protein expression is unclear. It seems possible that it involves tissue-specific translational control, or rather a neuron-specific interaction partner that stabilizes the ClC-6 protein.

Like all other vesicular CLC proteins, ClC-6 is found on vesicles of the endolysosomal system (663). *Knockout* controlled IHC revealed that native ClC-6 partially overlapped with the late endosomal/lysosomal marker lamp-1 in somata of cortical, thalamic, and dorsal root ganglia neurons (663). When brain membranes were fractioned on Percoll gradient, ClC-6 partially comigrated with ClC-3 and ClC-7, and, less than ClC-7, with the lysosomal enzyme cathepsin D (663). In *Clcn7*$^{-/-}$ brain, ClC-6 shifted partially to the lysosomal fractions (663). ClC-6 could functionally complement the *gef1* phenotype of yeast (414) which results from disruption of the single *S. cerevisiae* CLC Gef1p (299), a protein located in the yeast Golgi and prevacuole (81, 760). In conclusion, native ClC-6 resides in late endosomes, partially overlapping with late endosomal ClC-3 and with late endosomal/lysosomal ClC-7.

Consistent with a late endosomal localization, native ClC-6 also co-localized with lamp-1, but not with EEA1 or the transferrin receptor in the human neuroblastoma cell line

SH-SY5Y (366). However, when overexpressed in the same cell line or in HeLa or COS cells [where the authors had previously found an ER localization (91)], ClC-6 was rather found in early or recycling endosomes as indicated by colocalization with EEA1 and transferrin receptors, respectively (366). Upon expression in HEK cells, ClC-6 partially colocalized with EEA1 and lamp-1 (820). The colocalization of ClC-6 with the transferrin receptor in transfected HeLa cells could not be changed by mutating a confirmed AP3-binding site, even when done in combination with mutations in several other putative sorting signals (801). In contrast, mutating a stretch of basic amino acids in the ClC-6 NH_2 terminus that is involved in the incorporation of ClC-6 into detergent-resistant membranes shifted ClC-6 into a "later," ClC-7 positive compartment (366), but the biological significance of this finding is unclear. In spite of the uncertainties concerning the mechanisms of ClC-6 sorting (801), it seems obvious that native ClC-6 resides predominantly in late endosomal compartments.

C. Possible Physiological Roles of ClC-6 and Involvement in Pathologies

The loss of ClC-6 leads to moderate lysosomal storage in neurons (663) **(FIGURE 13)**, but the mechanism underlying this pathology and the precise physiological role of ClC-6 remain unknown. Most likely, ClC-6 is involved in the ion homeostasis, possibly including pH regulation, of late endosomes. Measurements of lysosomal pH of cultured hippocampal neurons with ratiometric dyes indicated that this parameter is not changed by *Clcn6* disruption (663). In contrast to similar negative results for lysosomal ClC-7 (407, 445), however, these results may just reflect the fact that ClC-6 has its major role in late endosomes, and not lysosomes, into which the indicator had been chased after endocytosis.

Clcn6$^{-/-}$ mice are viable, fertile, and lack an immediately obvious phenotype (663). However, they display lysosomal storage in neurons that develops over the first few months after birth. Autofluorescence is seen in initial axon segments that are often ballooned and contain storage material positive for lysosomal proteins such as lamp-1, cathepsin D, and ClC-7 **(FIGURE 13)**. It was also labeled with antibodies against subunit c of the mitochondrial ATPase which is a marker for neuronal ceroid lipofuscinosis (NCL). The relatively mild pathology, localization of storage material to initial axon segments, and virtual absence of neurodegeneration markedly differ from the severe lysosomal storage and neurodegeneration observed with a loss of ClC-7 or its β-subunit Ostm1 (407, 445, 668). The strong accumulation of storage material in dorsal root ganglia neurons (see **FIGURE 13**) probably explains the reduced pain sensitivity of *Clcn6*$^{-/-}$ mice in tail flick assays (663). In addition, *Clcn6*$^{-/-}$ mice displayed mild cognitive abnormalities (663).

The phenotype of *Clcn6*$^{-/-}$ mice prompted Poët et al. (663) to search patients with mild forms of NCL for *CLCN6* mutations. This included patients with Kuf's disease who typically accumulate storage materials in initial axon segments (61). However, although 2 of 75 patients displayed heterozygous *CLCN6* missense variants, no convincing disease-causing mutations were found (663).

In inconclusive studies, *CLCN6* sequence variants were identified in patients with epilepsy (883, 927), but the Glu178Ala *CLCN6* variant reported by Wang et al. (883) is questionable as there is no Glu178 in ClC-6. Sequence variants in the *CLCN6* gene were also linked to lower blood pressure levels (932) and to coronary heart disease (949). These results need confirmation in other cohorts.

XIII. ClC-7: A LYSOSOMAL Cl^-/H^+ ANTIPORTER MUTATED IN OSTEOPETROSIS AND NEURODEGENERATION

ClC-7 is a 89-kDa protein with 803 amino acids in rat (805 amino acids in humans) that is ubiquitously expressed (79). It conforms to the overall CLC structure with a large transmembrane domain and two COOH-terminal CBS domains, even though the stretch between the CBS1 and CBS2 domains is shorter compared with the other CLCs. Together with ClC-6, with which it shares ~45% sequence identity, it forms the third branch of mammalian CLCs (79). It has only low sequence similarity with the other mammalian CLC-proteins but is rather closely related to the plant homologues At-ClCa-d (335, 428, 510). ClC-7 is strictly associated with the 1 TMD protein Ostm1 (445) and the protein complex functions as a $2Cl^-/H^+$ antiporter in lysosomes and in the ruffled border of osteoclasts (298, 407, 429, 445, 453, 802, 888). ClC-7 lacks any *N*-glycosylation site, while Ostm1 is heavily glycosylated (79, 445), a property which could be important for protein stability in the acidic, protease-rich lysosomal lumen. Mutations in the genes encoding ClC-7 and Ostm1 cause osteopetrosis and neurodegeneration (116, 429). In the ruffled border of osteoclasts, ClC-7/Ostm1 is most likely essential for the acidification of the resorption lacuna (the sealed extracellular space contacting the bone) and consequent osteoclast-mediated bone resorption (429). In lysosomes, the $2Cl^-/H^+$ antiporter might be important for the regulation of the luminal Cl^- concentration (896).

A. Localization and Transcriptional Regulation of ClC-7

ClC-7 mRNA is expressed in practically all tissues examined, and expression starts early in development being detectable already at embryonic day 7 (79). With the use of in situ hybridization, high *Clcn7* mRNA expression was

found in brain, eye, spinal cord, dorsal root ganglion, and trigeminal ganglion in mouse embryos (429) and in various CNS neurons, hepatocytes, kidney outer medulla, lung, pancreas, and testis in adult mice (414). These sites of expression were confirmed by studies of ClC-7 KO mice in which β-galactosidase was expressed under the control of the endogenous *Clcn7* promoter (429). X-gal staining in these mice further revealed expression in osteoclasts, lens, retinal pigment epithelium, and cells of the neuroretina (429), as well as in all regions of the adult kidney (888). With the use of antibodies that had been controlled on *knockout* tissue, immunohistochemical staining demonstrated the presence of ClC-7 in neurons (407), in microglia, and in cortical kidney segments including the proximal tubule (888).

Regarding the subcellular localization, ClC-7 shows a high degree of overlap with the late endosomal/lysosomal marker lamp-1 in all reported cell types, including mouse fibroblasts (429), hippocampal neurons (407), and proximal tubule cells (888). Immunoelectron microscopy confirmed the lysosomal localization in cortical neurons (407). The lysosomal localization of ClC-7 was also shown by subcellular fractionation of brain (429, 663) and subsequently of liver and HeLa cells (298). Cell fractionation showed that ClC-7 is the only lysosome-resident CLC (298, 663). In the brain of *Clcn7*$^{-/-}$ mice, ClC-3 and ClC-6 are partially shifted into the lysosomal fractions (663). Collectively, these studies provide overwhelming evidence for a lysosomal localization of ClC-7 in most tissues, but additional localization to late endosomes or phagosomes is likely. In quiescent cultured microglia, ClC-7 and Ostm1 are predominantly found in the ER but can be shifted to lysosomes by treatment with macrophage colony-stimulating factor (514). The subcellular localization of ClC-7/Ostm1 in microglia in situ remains to be determined.

ClC-7 is targeted to lysosomes also in heterologous expression systems (445, 801, 820). Stauber and Jentsch (801) found that both the NH_2 and the COOH terminus of ClC-7 interacted with members of the adaptor protein complex (AP) and identified regions of amino acid residues in the NH_2 terminus that mediated this binding. In addition, the NH_2 terminus also pulled down members of the Golgi-localized, γ-ear-containing, Arf-binding (GGA) family (801). Mutating the leucine residues of the putative GGA binding motif (DDELL^{69}) indeed abolished the interaction with GGA proteins, but did not affect AP binding. Conversely, mutating the two leucine residues of the potential AP binding (DE)XXXL(LI) motif EAAPLL^{24} to alanine abolished pulldown of APs but not of GGAs (801). Interestingly, in chimeric constructs, the NH_2 terminus of ClC-7 was sufficient to target the plasma membrane channel ClC-0 to lysosomes. However, the combined disruption of the two above-mentioned leucine-based sorting motifs in the context of the chimera did not abolish lysosomal targeting (801). An additional putative AP binding (DE)XXX-L(LI) consensus motif (EETPLL^{37}) was then found to be critical for lysosomal targeting of the chimera. In the full-length ClC-7 protein, mutating the leucines of the two AP motifs to alanines (L23A, L24A, L36A, L37A) was sufficient to redirect ClC-7 and also the ClC-7/Ostm1 complex partially to the plasma membrane (801). This construct is also called ClC-7^{PM} and has been used for extensive electrophysiological characterization of ClC-7/Ostm1-mediated currents and for the functional characterization of osteopetrosis-causing mutations (453).

In osteoclasts, ClC-7 is not only present in lysosomes, but also in the ruffled border, a specialized plasma membrane region that is sealed on the bone surface defining the sites where osteoclasts reabsorb the bone material (429). The delivery of ClC-7 and the V-type ATPase to the ruffled border occurs via lysosomal exocytosis, which also delivers acid hydrolases to the so-called "resorption lacuna" or "extracellular lysosome."

Transcriptional regulation of ClC-7 and Ostm1 is little understood. A putative promoter fragment of mouse *Clcn7* showed a high G/C content and lacked apparent TATA boxes, consistent with an ubiquitous expression pattern as seen for many housekeeping genes (428). In addition, two "E-boxes" were identified in the promoter region (428). In osteoclasts, the genes encoding ClC-7 and Ostm1 are both regulated by the transcription factor microphthalmia, which controls several genes in osteoclast function (536).

Pattern discovery analysis on 96 known lysosomal genes led to the identification of a palindromic 10-bp promoter motif that was enriched in 68 of the 96 genes and included *CLCN7* but not *OSTM1* (733). This motif is recognized by the TFEB transcription factor that appears to act as a master regulator of lysosome biogenesis (733).

B. Ostm1 Is an Obligatory ClC-7 β-Subunit

Ostm1 was identified (116) as the gene mutated in the spontaneous mouse mutant "grey lethal" (*gl*) (304). Grey lethal mice exhibit severe osteopetrosis characterized by defective osteoclast maturation and function and die at 3–4 wk of age (689). A further characteristic of *gl* mice is a gray coat color in an *agouti* background, being caused by a malfunction of pigment forming granules in melanocytes (304). The genetic defect underlying the *gl* phenotype was found to be a 460-bp insertion in the gene encoding the Ostm1 protein (116). Ostm1 RNA was found to be widely expressed in osteoclasts, brain, kidney, spleen, thymus, testis, heart, liver, and primary osteoblasts and in fetal tissues at E12.5 (116, 445). The open reading frame encodes 338 amino acids with a single predicted transmembrane domain. Evolutionary, Ostm1 homologues are found in multicellular animals like *C. elegans* but not in yeast (116, 622). The lack

of an Ostm1 homologue in yeast may underlie the finding that ClC-7 could not functionally complement the yeast CLC (414). The importance of Ostm1 in humans was confirmed by the finding that a mutation in the *OSTM1* gene at a donor splice site caused recessive osteopetrosis in an Italian patient (116), followed by the identification of additional mutations in other patients (624, 690).

However, the function of Ostm1 and the mechanisms leading to osteopetrosis were completely unclear until Lange et al. (445) discovered that Ostm1 is an essential β-subunit of ClC-7. The two proteins could be coimmunoprecipitated from brain tissue and colocalized in late endosomes and lysosomes in mouse fibroblasts (445). Immunohistochemistry showed colocalization also in neuronal cell bodies in lysosomal structures and in osteoclasts in the ruffled border (445). In the absence of ClC-7, Ostm1 showed an ER-like distribution in transfected cells, and Ostm1 staining was very weak in *Clcn7*$^{-/-}$ mice, suggesting that association with ClC-7 is needed for Ostm1 protein stability (445). Conversely, staining of ClC-7 was greatly reduced in *gl* mice (445). Importantly, the transcript levels of *Clcn7* were unchanged in *gl* mice and those of *Ostm1* were unchanged in *Clcn7*$^{-/-}$ mice (445).

These data firmly established that Ostm1 serves as an essential β-subunit of ClC-7 and that the two proteins mutually stabilize each other. Lysosomal targeting of Ostm1 is fully dependent on ClC-7 with Ostm1 "following" the α-subunit (801). The interdependence of the two proteins is also reflected in the very similar phenotype of the respective *knockout* models. For example, *Clcn7*$^{-/-}$ mice have gray fur in an *agouti* background, and retinal and hippocampal neurodegeneration was detected in *gl* mice (445). It closely resembles the neurodegenerative phenotype of *Clcn7*$^{-/-}$ mice (407, 668, 888).

Lange et al. (445) also obtained important information on the biochemical properties of Ostm1. The authors firmly established the topology of the protein as a type I transmembrane protein with extracellular, highly glycosylated NH_2 terminus and a short cytoplasmic COOH terminus mice. In addition, the protein bears a proteolytic cleavage site in the NH_2 terminus. The fragments created by the cleavage are probably kept together by disulfide bonds (445). The topology was fully confirmed in a later study (622). However, the results concerning subcellular localization and putative protein interaction partners of that study (622) are questionable because most experiments were performed overexpressing Ostm1 in the absence of ClC-7, a condition known to destabilize the protein (445). The established topology of Ostm1 ruled out a previous hypothesis according to which Ostm1 is a RING finger containing cytosolic ubiquitin ligase (250). Another report suggested a role of Ostm1 in Wnt/β-catenin signaling (241), but experiments with *Clcn7*$^{-/-}$ and *Ostm1*$^{-/-}$ fibroblasts and melanocytes contradicted this notion (895).

C. General Biophysical Properties of ClC-7/Ostm1-Mediated Transport

Due to its strict intracellular localization, functional characterization of ClC-7 using standard electrophysiological techniques had not been possible for a long time (79, 407, 429, 445). An antiporter instead of channel function was suspected because ClC-7 carries a "proton-glutamate" (E312) as other CLC exchangers (9, 383, 941). A first characterization of endogenous lysosome Cl^-/H^+ antiport activity was performed on native lysosomes prepared from rat liver (298). Using sophisticated flux measurements, Graves et al. (298) showed that the major endogenous lysosomal Cl^- transporting pathway has $2Cl^-/H^+$ antiport characteristic, with a typical CLC anion preference of $NO_3^- > Cl^- \geq Br^- > I^-$. Since ClC-7 is the only lysosomal CLC protein (407, 429, 888) and because ClC-7 was the only CLC that copurified with the lysosomal preparation (298), the transport activity was likely mediated by ClC-7. This notion was ascertained by Weinert et al. (896) who studied the response of luminal pH to Cl^- gradients with lysosomal preparation from WT and *Clcn7*$^{-/-}$ mice. Interestingly, transport activity was enhanced in acidic pH (298) similar to the bacterial EcClC-1 (5).

A breakthrough allowing functional analysis of ClC-7 came from a systematic study by Stauber and Jentsch (801) who discovered that NH_2-terminal leucine-based sorting motifs are critically involved in the lysosomal targeting of ClC-7. They found that mutating four leucine residues (L23, L24, L36, L37) to alanines resulted in partial membrane localization of the protein (see above). Using this "ClC-7^{PM}" variant, Leisle et al. (453) performed a detailed electrophysiological characterization of heterologously expressed ClC-7. Importantly, Ostm1 "followed" ClC-7 (801), being colocalized with ClC-7^{PM} at the plasma membrane (801). Interestingly, the NH_2 terminus of Ostm1 was not essential for colocalization of the two proteins but, together with the transmembrane domain, it was required for functional activity, while the COOH terminus could be exchanged by that of the CD4 protein (453). In voltage-clamp experiments in *Xenopus* oocytes as well as in transfected mammalian cells, ClC-7^{PM}/Ostm1-mediated currents slowly activated at positive membrane potentials with kinetics in the seconds range. These currents deactivated with a time constant of the order of hundreds of milliseconds upon repolarization to negative voltages (453). Currents of rat and human ClC-7 clones were indistinguishable. The very slow activation of ClC-7^{PM}/Ostm1-mediated currents at positive voltages clearly reflects a "gating" phenomenon, i.e., a conformational change of the protein from an inactive, nontransporting state to an actively transporting state. In agreement with this interpretation, gating kinetics showed a rel-

atively large temperature dependence characterized by a Q_{10} of ~3 (453). Activation kinetics were so slow and activation occurred at such positive voltages that no true equilibrium could be achieved. Measuring currents from the "fast" mutant R762Q (see below), and using classical protocols to assess steady-state voltage dependence, a voltage of half-maximal activation of ~80 mV and an apparent gating valence of 1.3 was determined (453). The mechanism of the gating of ClC-7 is little understood. It appears to involve both the transmembrane part as well as the cytoplasmic CBS domains because mutations in both regions strongly affected gating kinetics (453), suggesting that the gate could bear similarity to the common gate of CLC channels that depends of both subunits of the homodimer. This hypothesis was tested by Ludwig et al. (493) using a clever coexpression approach that exploited the transport-deficient proton glutamate mutant E312A. Currents mediated by WT ClC-7^{PM}/Ostm1 were accelerated by coexpression with gate-accelerating mutations in the background of E312A, and conversely, fast mutants were slowed down upon coexpression with the transport-deficient E312A demonstrating that the nontransporting subunit influences the speed of the conformational change of gating (493). Such a dominant acceleration of gating may underlie the dominance of several gate-accelerating osteopetrotic mutations (453).

The currents mediated by ClC-7^{PM}/Ostm1 showed a $Cl^- > Br^- > NO_3^- > I^-$ conductivity sequence. Similar as for all mammalian CLCs, iodide was less conductive, but somewhat surprisingly also NO_3^- was conducted less efficiently than Cl^-. This contrasts with ClC-4 and ClC-5 exchangers (941, 966, 967) and with what had been reported for endogenous lysosomal flux activity (298). Mutating the highly conserved pore serine 202 to proline, as found in the plant At-ClC-a NO_3^-/H^+ antiporter (164), greatly enhanced NO_3^- conductance of ClC-7^{PM}/Ostm1 (453), similar to what had been described for ClC-5 (60, 966), and demonstrating that the fundamental mechanisms of ion selectivity and transport coupling are conserved in ClC-7. The presence of inward tail currents allowed Leisle et al. (453) to determine the transport stoichiometry by measuring the reversal potential upon changing pH and Cl^- concentration. They consistently found a $2Cl^-/1H^+$ stoichiometry when changing both ion species (453). Proton transport was also directly detected by fluorometrically measuring intracellular pH changes upon current stimulation (453). As for ClC-5 (269, 649), ClC-7^{PM}/Ostm1-mediated outward currents were slowed down, and their magnitude was decreased by acidic extracellular pH (453). Such inhibition is possibly of physiological relevance as the lysosomal luminal pH is highly acidic. In this respect, it is interesting to note that the endogenous lysosomal Cl^-/H^+ antiport was actually enhanced by acidic pH (298). Furthermore, the activity of heterologously expressed ClC-7^{PM}/Ostm1 was very low at negative or slightly positive membrane potentials (453). For these reasons, it will be interesting to characterize the voltage- and pH-dependent biophysical properties of ClC-7/Ostm1 in their native membrane environment.

The functional properties of ClC-7^{PM}/Ostm1 are very different from those of acid-induced anion currents reported in Sertoli cells (40), acid-induced currents in ClC-7 expressing oocytes (195), or acid-induced currents in mouse osteoclasts (606). The anion currents reported in these studies are most likely unrelated to ClC-7. Indeed, Capurro et al. (103) found that acid-induced anion currents are neither mediated by members of the TMEM16 family nor by ClC-3 or ClC-7.

D. Gating of ClC-7 and Osteopetrosis

The gating of ClC-7 is likely of physiological relevance because several osteopetrosis mutations led to a significantly accelerated gating kinetics (453). Human mutations with accelerated gating include residues in the transmembrane part, some of which in regions close to the dimer interface, and several residues in the cytosolic CBS domains (453). Accelerated activation kinetics is, a priori, a gain of function, at least at positive voltages. However, osteopetrosis is clearly due to a loss or reduction of function of ClC-7/Ostm1 as demonstrated by the presence of disease-causing deletion and truncation mutations (e.g., Refs. 181, 429) and missense mutations that reduce functional expression (453). It cannot be excluded that the gating phenotype seen with ClC-7^{PM}/Ostm1 in heterologous expression is an epiphenomenon and that the mutations induce, for example, a reduction of protein expression in vivo. This has indeed been described for the gate-accelerating mutation R762Q, for which less protein was found in Western blots from patient-derived fibroblasts (429). However, detailed in vivo studies are difficult to perform for human mutations. Recently, a cattle model of osteopetrosis shed light on this issue (734). Animals carrying the Y750Q mutation (affecting a conserved tyrosine in CBS2) had severe osteopetrosis and blindness that was associated with high perinatal lethality. Importantly, the mutations did not affect protein abundance and preserved lysosomal localization (734). In the background of the plasma membrane targeted ClC-7^{PM}/Ostm1, the mutation significant accelerated gating kinetics (734), which was thus the only detectable functional effect of the mutation.

E. ClC-7, Bone Resorption, and Osteopetrosis

The importance of ClC-7 for osteoclast-mediated bone resorption was revealed by the phenotype of ClC-7 KO mice that displayed severe osteopetrosis, a disease characterized by dense and fragile bones (429). Even though ClC-7 is expressed early in the embryo (429), birth rate of *knockout*

pups was Mendelian, and heterozygous mice were at first undistinguishable from WT. Later, *Clcn7*$^{-/-}$ mice were smaller, their teeth failed to erupt, and they died after 6–7 wk even if fed a liquid diet (429). Analysis of bones of *Clcn7*$^{-/-}$ mice revealed shortened long bones, absence of bone marrow cavity, disorganized trabecular structure, fibrosis, and absence of a regular corticalis, while osteoblast-mediated bone apposition rate was unaltered (429).

Osteopetrosis in *Clcn7*$^{-/-}$ mice is not caused by a lack of osteoclasts but by their inability to reabsorb calcified bone, as shown by the inability of in vitro differentiated cultured osteoclasts to excavate pits on dentin substrate, even though the H^+-ATPase was normally expressed in osteoclasts (429, 580). In addition, osteoclasts were abnormally large in *Clcn7*$^{-/-}$ mice (429, 580). Importantly, no resorption lacuna was formed by *Clcn7*$^{-/-}$ osteoclasts in culture even though the osteoclasts firmly attached to bone and osteoclast from *Clcn7*$^{-/-}$ are able to degrade decalcified bone (580).

The inability to resorb dentin was associated with an apparent inability to acidify the resorption lacuna as assayed by acridine orange fluorescence (429). However, as no clear resorption lacuna was actually formed by *knockout* osteoclasts, it is difficult to distinguish an acidification defect from a maturation defect of the ruffled membrane. Indeed, the intracellular punctate pattern of acridine orange fluorescence, reflecting likely acidic lysosomes of the osteoclasts, was preserved in *Clcn7*$^{-/-}$ mice, suggesting that lysosomal acidification was not affected (429), in agreement with quantitative measurements of lysosomal pH in cultured neurons (407) and fibroblasts of *Clcn7*$^{-/-}$ mice (445, 896).

The critical role played by ClC-7 in bone resorption was confirmed by the finding that *CLCN7* mutations cause osteopetrosis in a significant number of patients (429, 791). The first mutations were found in a compound heterozygous patient who carried a nonsense (Q555X) mutation on one allele and a missense (R762Q) mutation on the other allele (429). No RNA was detected for the Q555X transcript. Interestingly, no ClC-7 protein was found in patient-derived fibroblasts, suggesting that the R762Q mutation, which alters a charged residue in CBS2, leads to protein instability (429). However, large currents of the R762Q mutant in the background of plasma membrane redirected ClC-7 construct could be measured in heterologous expression, and the mutant displayed faster gating kinetics (453).

Osteoclast-rich autosomal recessive osteopetrosis had been previously associated with mutations in the a3 subunit of the H^+-ATPase (266, 430). It is also one of the symptoms in carbonic anhydrase deficiency syndrome (786). However, while the phenotypes caused by these genetic defects are overlapping, symptoms and treatment options differ in detail and are clinically important (46). Since the defective osteoclasts are of hematopoietic origin, bone marrow transplantation can often be curative (791). However, the severe neurological symptoms associated with homozygous *CLCN7* loss-of-function mutations will not be corrected by this treatment.

Over the years, a large number of osteopetrosis-causing *CLCN7* mutations have been identified (70, 141, 183, 429, 442, 623, 659, 791, 943, 959). Osteopetrosis caused by *CLCN7* mutations is classified as infantile malignant *CLCN7*-related recessive osteopetrosis (ARO), intermediate autosomal osteopetrosis (IAO), and autosomal dominant osteopetrosis type II (ADOII, Albers-Schönberg disease) (141, 791). The recessive forms of the disease are generally much more severe with clinical symptoms that include fractures, poor growth, optic nerve compression, absence of the bone marrow cavity resulting in anemia and thrombocytopenia, dental abnormalities, and various other secondary symptoms (791). Children with ARO rarely survive to adulthood. Onset of the dominant form of osteopetrosis is in late childhood or adolescence and symptoms are much milder. The dominant inheritance of certain *CLCN7* mutations is most likely caused by a dominant negative effect of the mutated allele on the dimeric complex, similar to what is occurring in dominant myotonia congenita (679). Among the dominant mutations, several lead to a faster gating kinetics, including L213F (453, 867), R286Q (267, 453), P619L (453, 644), Y7050Q (in cattle) (734), and R762L (453, 867). Since the gating of ClC-7 involves both subunits of the dimeric transporter (493), it is tempting to speculate that in many cases the dominant imposition of accelerated gating on ClC-7 dimers underlies the dominant inheritance pattern. In principle, a dominant negative effect may also be observed if a mutated subunit impairs the trafficking of both mutant/mutant and mutant/WT ClC-7 dimers.

A different mechanism of dominance underlies the G215R mutation (141). Osteoclasts derived from patients carrying this mutation could degrade bone only to 10–20% of the level in controls (337). In vitro, the mutation led to a retention of the protein in the ER, being, however, functional in a supported bilayer assay (757). The equivalent mouse mutation G213R was used to generate a mouse model of dominant osteopetrosis (19). Homozygous G213R *knock in* mice showed severe osteopetrosis and in general a phenotype similar to *Clcn7*$^{-/-}$ mice (19). Heterozygous mice had only a very mild phenotype without neurological symptoms that was highly variable depending on the genetic background, but structural bone parameters were significantly altered and a higher number of osteoclasts were observed (19, 20). In a proof-of-principle gene therapeutic approach, treatment of heterozygous G213R *knock in* mice by repeated intravenous injection of conjugated G213R specific small interfering RNA led to a significant amelioration of

various disease markers (102). However, the mechanism underlying the dominant inheritance of the G215R mutations remains unknown. The G213R *knock in* mouse model has also been used to test pharmacological interventions indicating that interferon-gamma, but not calcitriol might be helpful in dominant osteopetrosis (18). Another more recent mouse model for dominant osteopetrosis carrying the ClC-7 F318L mutation (94) displays a similar phenotype. Crossing these mice with the G213R mice to generate double-heterozygous *Clcn7*$^{F318L/G213R}$ mice showed that the mutant alleles do not complement each other and likely result in loss of function (94).

The impact of disease-causing *CLCN7* or *OSTM1* mutations on osteoclast function can be studied in patient-derived, in vitro differentiated osteoclasts using resorption assays. These showed reduced osteoclast activity in all cases (129, 337, 338, 819). Interestingly, for several missense mutations (associated with recessive or dominant osteopetrosis), no reduction of ClC-7 protein abundance or localization was found, suggesting that these mutations affect the ion transport properties of the transporter (819). A notable exception were osteoclasts from a heterozygous patient carrying the P470L and the R762Q mutations, which showed significantly reduced ClC-7 protein expression (819). To obtain insight into the phenotypic variability, Supanchart et al. (819) analyzed several transgenic mouse lines that expressed TRAP promoter-driven ClC-7 in a *Clcn7*$^{-/-}$ background to different levels, and estimated that a reduction of ClC-7 activity by 70–80% impaired osteoclast resorption capability to a degree seen in dominant osteopetrosis. Furthermore, it was found that ClC-7 is not critically involved in gastric acid secretion, in agreement with the absence of osteopetrorickets in patients with mutations in *CLCN7* (819).

Teeth of *Clcn7*$^{-/-}$ mice do not erupt due to the severe osteopetrosis (429). Impaired tooth eruption as well as root and enamel formation were also reported for patients with *CLCN7*-related osteopetrosis (924). Two groups (309, 900) studied the role of ClC-7 on teeth formation in more detail, using *Clcn7*$^{-/-}$ mice of Kornak et al. (429). They concluded that ClC-7 is crucial for tooth eruption and root development by enabling osteoclasts to remove craniofacial bone, with only minor effect or no effect on dentin mineral density and enamel, respectively. In contrast, changes in enamel were observed in another study using local application of *Clcn7* siRNA in mice (874).

Clcn7$^{-/-}$ mice not only show osteopetrosis, but also severe neurological defects and blindness, which will be discussed below. A common symptom also seen in non-*CLCN7*-associated osteopetrosis is visual impairment caused by compression of the optic nerve by osteopetrotic narrowing of the optical canal (809). Several lines of evidence show that the retinal degeneration of *Clcn7*$^{-/-}$ mice is nevertheless a primary defect caused by photoreceptor degeneration. First, the number of retinal ganglion cells, the first cell type affected by optic nerve compression, is not reduced at 4 wk of age (429). Second, "curing" osteopetrosis of *Clcn7*$^{-/-}$ mice by expression of ClC-7 under the TRAP promoter did not prevent retinal degeneration (407).

All reported human *OSTM1* mutations predict a truncated protein (116, 341, 521, 624, 683, 690, 793). As expected from the phenotype of *gl* mice (116), targeted *Ostm1*$^{-/-}$ mice (632) and the role of Ostm1 as ClC-7 β-subunit (445), patients carrying such mutations on both alleles exhibit severe osteopetrosis with strong neurological symptoms that cannot be cured by bone marrow transplantation (615).

F. Role of ClC-7 in Lysosomes in Neurons and in the Renal Proximal Tubule

Kasper et al. (407) and Wartosch et al. (888) studied in detail the mechanisms underlying neurodegeneration in ClC-7-deficient mice. First, using a lacZ fusion protein under the control of the endogenous ClC-7 promoter, expression was found in practically all neuronal cell types and in glia (407). Immunostaining revealed punctate patterns in neuronal cell bodies in almost perfect colocalization with the lysosomal marker lamp-1 (407). Loss of ClC-7 led to widespread neurodegeneration that was most evident in the CA3 region of the hippocampus (407). It was associated with the appearance of electron-dense osmiophilic material in hippocampal and cortical neurons at P40 with ultrastructural characteristics of lysosomal storage disease of the neuronal ceroid lipofuscinosis (NCL) type (407). In agreement with NCL, autofluorescent punctae were observed in *Clcn7*$^{-/-}$ brains as early as P20. Storage material was also seen in the kidney proximal tubule (407). Somewhat surprisingly, the abundance and the in vitro activity in lysates of several tested lysosomal enzymes was markedly increased in *Clcn7*$^{-/-}$ mice (407), possibly reflecting a compensatory increase of enzymes that are, however, to a large degree inactive in vivo because of their localization in storage material. In fibroblasts, however, the in vivo activity of the β-hexosaminidase and tripeptidyl peptidase I (TPP1) was unchanged. No neurodegenerative symptoms were observed in parallel experiments of osteosclerotic *oc/oc* mice that lack the a3 subunit of the V-type ATPase, demonstrating that the neurodegeneration of *Clcn7*$^{-/-}$ mice was not secondary to osteopetrosis (407). Further proof that the neurodegeneration and osteopetrosis are independent outcomes was obtained by investiging *Clcn7*$^{-/-}$ mice that transgenically expressed ClC-7 under the control of the tartrate-resistant acid phosphatase (TRAP) promoter, which is nearly exclusively active in osteoclasts and macrophages (761). These mice had no osteopetrosis but lived only ~3 wk longer than *Clcn7*$^{-/-}$ mice and had severe retinal and CNS degeneration similar to the full *knockout* (407). Similarly,

ClC-7 targeted mice which expressed an alternate ClC-7 transcript in bone exhibited neurodegeneration but no osteopetrosis (688). Very similar neurodegeneration was also seen in *gl* mice (339, 445, 668), most likely reflecting the decrease of ClC-7 protein caused by the absence of Ostm1 (445, 888). Surprisingly, osteopetrosis of *gl* mice was not cured by transgenic, TRAP promoter-driven expression of Ostm1 (631). Transgenic Ostm1 expression in myeloid progenitors using a construct containing PU.1 regulatory sequences could instead rescue the bone phenotype (631). This suggested that Ostm1 has additional functions beyond stabilization of the ClC-7 protein in the osteoclast lineage or in other hematopoietic cell types indirectly affecting osteoclast function (631). However, in the transgenic TRAP promoter Ostm1 expressing *gl* mice, the expression of Ostm1 protein in osteoclasts was not ascertained to be of the same level as in WT mice (631).

ClC-7, like other CLC proteins, had been proposed to provide a shunting conductance to allow efficient lysosomal acidification by the H^+-ATPase (392). However, using a ratiometric, dextrane-coupled lysosomally targeted pH indicator, the average lysosomal pH was unchanged in lysosomes of cultured neurons and fibroblasts from KO compared with WT mice (407, 445, 895, 896). In contrast, lysosomal Cl^- concentration was significantly decreased (896). A role of ClC-7 in neutralizing the currents of the NADPH-oxidase in the phagocytic vacuole of neutrophils has also been excluded (260).

The severe phenotype and early death of *Clcn7*$^{-/-}$ and *gl* mice provide severe obstacles in studying the mechanisms underlying the observed neurodegeneration. These problems were overcome by Wartosch et al. (888), who developed and studied mouse models that allowed to follow neurodegeneration and lysosomal biology in long lived mice. In the first model, floxed *Clcn7* was specifically disrupted in hippocampal and forebrain structures of the cortex, sparing parvalbumin-positive interneurons (888). These mice lived to the same age as WT without osteopetrosis or change in size. However, some behavioral abnormalities became apparent at 4–5 mo of age (888). There was a massive loss of cortical neurons that was confined to regions that did not express ClC-7. Neurodegeneration started in the CA3 region of the hippocampus as in constitutive *Clcn7*$^{-/-}$ mice, showing that neurodegeneration occurs in a cell-autonomous manner (888). At 1.5 yr of age, the cortex and the hippocampus had almost disappeared (888). The distribution of the late endosomal/lysosomal marker lamp-1 was more diffuse in neurons from constitutive *Clcn7*$^{-/-}$ mice and in ClC-7-lacking neurons from the forebrain specific knockout (888). The neurodegeneration was associated with typical features of NCL such as the presence of storage material in the somata of cortical neurons at P37. Astrogliosis and activation of microglia, which is also seen in constitutive *Clcn7*$^{-/-}$ mice (407, 668) and which is a typical feature of NCL and other neurodegenerative pathologies, was restricted to those brain regions where ClC-7 had been disrupted (888). As the EMX1 promoter used to drive Cre expression in the forebrain-specific KO is not active in astrocytes and microglia, this result strongly suggests that astrogliosis and microglia activation represent a secondary response to the primary neurodegeneration.

To investigate in more detail the role of ClC-7 in lysosomal biology, Wartosch et al. (888) concentrated on the kidney as a model for endocytosis and lysosomal dysfunction. ClC-7 was found to be highly expressed in all parts of the kidney, colocalizing with Ostm1 and lamp-1, and large amounts of lysosomal storage material and of the autophagy marker LC3-II were seen in proximal tubular cells (PTCs) of *Clcn7*$^{-/-}$ and *gl* mice (888). It is not clear if the accumulation of LC3-II reflects increased autophagy or reduced degradation. Lamp-1-positive structures were enlarged and distributed more broadly in PTCs from *Clcn7*$^{-/-}$ mice, resembling somewhat the pattern seen in neurons (888). The morphology of ClC-3-positive late endosomes or ClC-5-positive early endosomes was unchanged. In vivo pulse-chase endocytosis experiments revealed that the enlarged lysosomal structures are connected to the endocytic system (888). Crossing the floxed *Clcn7* mice with mice expressing Cre recombinase in renal cortex led to a mosaic disruption of ClC-7 in PTC, allowing the comparison of endocytosis in ClC-7-expressing and *Clcn7*$^{-/-}$ PTCs side by side (888) **(FIGURE 14)**. In essence, it was found that in *Clcn7*$^{-/-}$ PTCs, endocytosis per se is not affected, endocytosed material is delivered to the enlarged lamp-1 positive vesicles, but degradation is significantly slowed (888). Importantly, the enlargement of the lysosomal structures probably does not depend on an accumulation of endocytic cargo because it was not abolished by additional disruption of ClC-5 that greatly diminished endocytosis (888).

G. Role of ClC-7 as a Lysosomal Cl^-/H^+ Antiporter

Early on, endosomal and lysosomal CLC proteins had been proposed to function as Cl^- channels that provide a charge compensating conductance necessary for the efficient luminal acidification by the electrogenic H^+-ATPase (307, 392). Indeed, ATP-dependent acidification of renal cortical endosomes is significantly slowed in ClC-5 *knockout* mice (308, 600). Surprisingly, and conflicting with the idea that ClC-7/Ostm1 is essential for lysosomal acidification, pH was normal in lysosomes of cells from *Clcn7*$^{-/-}$ and *Ostm1*$^{-/-}$ mice (407, 445, 896). The report by Graves et al. (298) that siRNA-mediated downregulation of ClC-7 leads to an alkalinization of lysosomes in HeLa cells needs to be interpreted with caution, because their assay was based on a nonratiometric fluorescent dye and on poorly effective siRNAs. Working with permeabilized cells and ratiometric

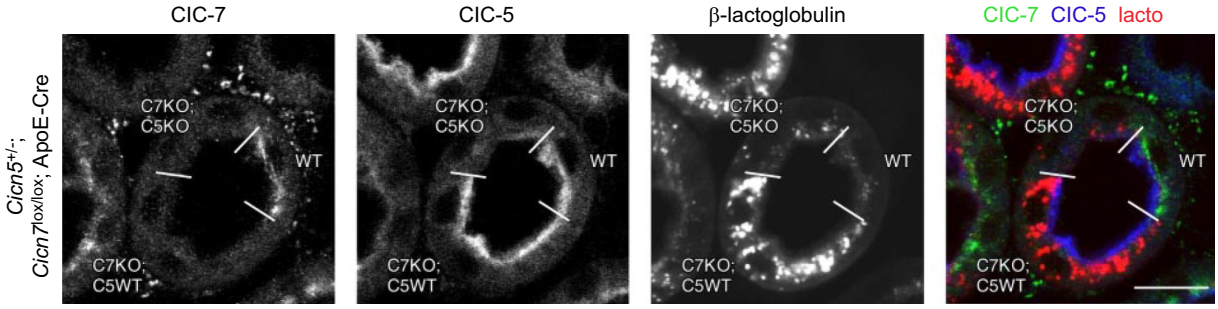

FIGURE 14. Localization and functional role of ClC-5 and ClC-7 in renal proximal tubules. Confocal light microscopical image of proximal tubules from a female *Clcn5*$^{+/-}$;*Clcn7*$^{lox/lox}$;ApoE-Cre mouse that had been injected intravenously 1 h before fixation with fluorescently labeled β-lactoglobulin (red in *right panel*) to reveal the fate of proteins that pass the glomerular filter. Sections were stained with antibodies against ClC-7 and ClC-5 (green and blue, respectively, in *right panel*). Because ClC-5 is encoded on the X-chromosome, which shows random inactivation in females, some cells of the proximal tubule shown in the center express ClC-5, whereas others do not. The *Clcn7* gene was also disrupted in a mosaic manner by using "floxed" *Clcn7*$^{lox/lox}$ mice and ApoE-Cre mice which leads to incomplete, random *Clcn7* disruption in proximal tubular cells (888). Hence, endocytosis and degradation of proteins can be compared side by side in the same tubule as a function of all combinations of expression of ClC-5 and ClC-7. One hour after injection of β-lactoglobulin, the protein is only seen in cells lacking ClC-7, highlighting its role in lysosomal protein degradation. At that time point, β-lactoglobulin has already been degraded in WT cells. Impairment of apical endocytosis by ClC-5 disruption (661) prevents its accumulation in cells lacking ClC-7. Note that in proximal tubular cells early endosomal ClC-5 is located more apically than lysosomal ClC-7, consistent with the high rate of apical endocytosis in the cells. [From Wartosch et al. (888).]

measurements of lysosomal pH, Steinberg et al. (803) found that cations contribute in a significant manner to support lysosomal acidification. Different results have also been reported for cultured microglia in which full lysosomal acidification could only be achieved if ClC-7/Ostm1 had been upregulated by treatment with macrophage colony-stimulating factor (514). As primary cultures of microglia do not always faithfully reflect the in vivo situation (509), it will be important to confirm these results, for example, in brain slices or using a conditional *knockout* model. The same caution should be maintained interpreting recent results reporting a reduction of Ostm1 expression and an alkalinization of lysosomal pH in cultured microglia treated with Alzheimer's disease-related Aβ peptides (312).

A clearly diminished acidification in *Clcn7*$^{-/-}$ mice has been observed for the osteoclastic resorption lacuna (429). It might be that the highly specialized acid-secreting ruffled border, in contrast to lysosomes, lacks a parallel cation conductance. Alternatively and more likely, the lack of ClC-7 interferes with vesicular trafficking and the buildup of the acid-secreting ruffled border by exocytic insertion of lysosomal membranes. Indeed, electron microscopy shows that the ruffled border of *Clcn7*$^{-/-}$ osteoclasts in situ is underdeveloped (429, 895).

The interpretation of the role of ClC-7 in lysosomal biology changed significantly after it had become likely (383) and later established that ClC-7 is not a Cl^- channel, but a coupled $2Cl^-/1H^+$ antiporter (298, 453, 896). Intuitively, such a transport mode might not seem well suited to provide a Cl^--based shunting permeability for the H^+-ATPase as the required inward movement of Cl^- into the lumen is accompanied by an outward movement of protons, leading thus to a waste of pumped protons, increasing thereby the metabolic expense of the acidification process. However, model calculations show that under certain conditions the presence of a $2Cl^-/1H^-$ exchanger results in a more acidic luminal pH compared with the presence of a Cl^- conductance (372, 522, 896). Under these conditions, the voltage across the lysosomal membrane would become negative inside, a situation that would be actually in harmony with the strongly outwardly rectifying electrophysiological phenotype of CLC exchangers. However, little is known about the actual voltage across endo/lysosomal membranes.

The physiological relevance of the $2Cl^-/1H^-$ exchange mechanism for lysosomal and osteoclast biology was tested using a *knock in* mouse model in which the gating glutamate neutralizing E245A mutation was introduced into the *Clcn7* gene (896). The equivalent mutation abolishes H^+ transport in bacterial and plant CLCs (5, 60) and in ClC-4 and ClC-5 (651, 742), converting the transporters to uncoupled and voltage-independent Cl^- conductances, as later verified directly for ClC-7 (453). Similar to *Clcn7*$^{-/-}$ mice, the so-called *Clcn7*$^{unc/unc}$ (for "uncoupled") mice had a severe phenotype with growth retardation and they died within 5 wk (896). ClC-7 was normally expressed in lysosomes and also the abundance and localization of Ostm1 were unchanged (896). Similar to mice lacking ClC-7 (888) or Ostm1 (445), *Clcn7*$^{unc/unc}$ mice developed retinal degeneration and lysosomal storage disease associated with neurodegeneration and signs of NCL (896). Mice also developed osteopetrosis (896), which was, however, less severe compared with *Clcn7*$^{-/-}$ (429) or *gl* (116) mice. Interestingly, on an *agouti* background the fur was brownish in

Clcn7$^{unc/unc}$ mice as in WT mice (896) and not gray as in *gl* (116) or in *Clcn7*$^{-/-}$ mice (445). The less severe osteopetrosis was associated with a slightly more developed ruffled border and improved osteoclast function in a pit assay (896) compared with cells from *Clcn7*$^{-/-}$ mice (429).

Lysosomal pH measurements in cells from WT, *Clcn7*$^{-/-}$ and *Clnc7*$^{unc/unc}$ cells and application of a proton ionophore indicated that lysosomes must have a sizeable cation conductance and that the luminal Cl^- concentration in *Clcn7*$^{unc/unc}$ mice is lower than in WT lysosomes (896). In agreement with a large cation conductance, ATP-driven lysosomal acidification was similar in all genotypes (896). A lower lysosomal Cl^- concentration was directly confirmed using a ratiometric lysosomal targeted Cl^- sensor, although the saturation of this sensor at high Cl concentrations required a preincubation of cells in Cl^--depleted medium (896).

Clearly, the physiological roles of endo/lysosomal CLC exchangers are far from being understood. The simple idea of a Cl^- shunting conductance certainly does not hold true. Indeed, if ClC-7 were the only or rate-limiting pathway to shunt the H^+-ATPase, its *knockout* would be expected to be embryonically lethal. Based on the combined results from the various mouse models, Jentsch and co-workers proposed the hypothesis that the major role of ClC-7 (and of other endo/lysosomal CLCs) is not to provide a shunting conductance for efficient acidification, but to exploit the pH gradient created by the H^+-ATPase to increase the luminal Cl^- concentration (383, 600, 800, 896). Surprisingly, lysosomal chloride concentrations were recently found to be reduced in *C. elegans* and mammalian cell models of several lysosomal storage diseases unrelated to primary defects in lysosomal Cl^- transport (115), raising questions about the underlying mechanism. It is not clear why a high Cl^- concentration could be important. In principle, a chloride gradient across the lysosomal membrane could be used by (unknown) secondary active transporters. Furthermore, several degradative enzymes, like e.g., cathepsin C, are directly regulated by Cl^- (138). The slower degradation in ClC-7-deficient PTCs (888) would be consistent with this hypothesis. However, the enlargement of lysosomal structures in PTCs was independent of endocytic cargo (888). Interestingly, the enlarged structures were enriched for the late endosomal marker lysobisphosphatidic acid (LBPA), raising the possibility of defective endosomal-lysosomal trafficking (888). A trafficking effect could also underlie the underdevelopment of the ruffled border in osteoclasts. However, it is unknown if luminal Cl^- concentration affects endosomal-lysosomal trafficking. The Cl^- concentration, and consequently also the membrane voltage, might affect fusion and fission of organelles, which have been proposed to be associated with the release of luminal Ca^{2+}. In this respect, it is interesting to note that an endosomal Ca^{2+} channel has been reported to be regulated by luminal Cl^- (727).

Additional, ion transport-independent roles for ClC-7/Ostm1 are suggested by the phenotype of a ClC-7 *knock in* mouse model in which the transport deficient "proton-glutamate" mutation had been introduced (895). The proton glutamate is essential for the shuttling of intracellular protons to the gating glutamate (9, 468) and its mutation to alanine or glutamine abolishes Cl^- and H^+ transport activity in ClC-7 (453) as it does in ClC-4 and ClC-5 (941). As expected for a nonfunctional mutant, the *Clcn7*$^{td/td}$ (transport deficient) *knock in* mice exhibited an osteopetrosis phenotype that was as severe as that of *Clcn7*$^{-/-}$ mice (895). Surprisingly however, fur color in an *agouti* background was not affected (895), suggesting that the relevant activity of ClC-7/Ostm1 in melanocytes was maintained. This led to the suggestion that ClC-7/Ostm1 might have functions beyond its transport activity, for example, by directly interacting with other proteins. However, it cannot be fully excluded that some residual transport activity, not detectable in heterologous expression systems, is maintained in the proton glutamate mutant (895), as is the case in the bacterial EcClC-1, which exhibits uncoupled Cl^- transport (9).

H. Pharmacology of ClC-7

ClC-7 has been suggested as a target for the treatment of osteoporosis since its activity in osteoclasts is essential for bone resorption. Schaller et al. (741) reported that the compound NS3736 inhibits acidification in resorption compartments and osteoclastic resorption in vitro and prevented bone loss in a rat model of osteoporosis. Analogues of NS3736 have similar effects (406). However, it remains to be shown that these compounds act directly on ClC-7. Several classical Cl^- channel blockers and inhibitors of ClC-K channels have been tested on the open "gating glutamate" mutation E245A. However, none of these compounds showed inhibitory activity with an EC-50 below 0.5 mM (938).

XIV. CLCs IN OTHER ORGANISMS

CLCs have been studied in various model organisms like yeast, *C. elegans*, zebrafish (642), *Drosophila* (849), and plants (335). We will restrict the review on those organisms which have been investigated in more detail, i.e., yeast, *C. elegans*, and *Arabidopsis*.

A. Yeast

The yeast (*Saccharomyces cerevisae*) genome encodes a single ScCLC also called Gef1p because it was identified as one of the genes underlying the GEF (glycerol/ethanol, Fe-re-

quiring) phenotype (299), which is characterized by a loss of high-affinity iron uptake, reduced resistance to toxic cations, and sensitivity to alkaline pH (281, 282, 299, 760). Gef1p has been implicated in Cl^- transport in a late secretory compartment where Cl^- is needed for the maturation of the Fet3p multi-copper oxidase (163). A unique feature of this CLC protein is a proteolytic processing in the secretory pathway in the first extracellular loop (866). So far, Gef1p is not functionally expressed in heterologous systems. Based on the presence of the proton glutamate, Gef1 is probably an anion/H^+ exchanger and not a channel. Accordingly, the uncoupling mutation of the gating glutamate, E230A, could not complement the GEF phenotype and resulted in the acidification of the Gef1-containing compartment (81). Furthermore, the GEF phenotype can be easily complemented by CLC antiporter homologues such as ClC-6 (414) or the fish OmClC-3 and OmClC-5 (558), but not by ClC-0 (B. Schwappach, personal communication). However, ClC-2 was reported to rescue the GEF phenotype when overexpressed together with Kha1p (254), a putative yeast cation/H^+-exchanger that colocalized with ClC-2 in the same Golgi to prevacuolar compartments that normally express the yeast CLC protein. Interestingly, similar to the role of Gef1, mammalian ClC-4 has been implicated in cellular copper/iron transport (567, 879). However, it is unclear if the underlying mechanisms are similar, and the effects of ClC-4 on liver copper metabolism have been questioned (see above).

B. Plants

Anion transport in plants is important for many physiological processes including nutrient uptake, salt stress, turgor/osmoregulation, stomatal opening, and photosynthesis (for reviews, see Refs. 42, 165, 433, 965). The first plant CLC homologues have been identified in *Arabidopsis thaliana* (335) and in tobacco (498), and genome sequencing revealed their presence in all investigated plant species. Most information has been obtained for CLCs from the model flowering plant *Arabidopsis*, and we will restrict the present review to these. The *Arabidopsis* genome encodes seven members called AtClC-a through AtClC-g. They can be phylogenetically grouped into two classes (502): AtClC-a to -d and AtClC-g form one group, which is relatively closely related to the bacterial EcClC-1, whereas AtClC-e and -f have very low similarity with EcClC-1 or mammalian CLCs even in the key ion binding regions (502). Direct functional data are available only for AtClC-a and AtClC-b (see below), and most information has been obtained from *knockout*, GUS reporter and protein/RNA localization studies. None of the AtCLCs is expressed in the plasma membrane. AtClC-a, -b, -c, and -g are localized to the vacuolar (tonoplast) membrane (164, 584, 863, 893). AtCLC-d is found in the *trans*-Golgi network co-localizing with a V-type ATPase (864). Also AtClC-f is localized to the Golgi (527), and both Golgi localized isoforms are able to complement the yeast Gef1 phenotype (527, 864). AtClC-e is localized to thylakoid membranes in the chloroplast (527), where its absence affects the proton-motive force (340).

After the initial finding that the loss of AtClC-a function reduces the capacity to accumulate NO_3^- by 50% (283), in a landmark paper De Angeli et al. (164) discovered that AtClC-a is a vacuolar $2NO_3^-/1H^+$ antiporter using patch-clamp recordings on isolated vacuoles from WT and AtClC-a *knockout* plants. The preference for NO_3^- over Cl^- was unprecedented for CLC proteins and was later pinpointed to the presence of a proline residue in the selectivity filter (60, 863, 893, 966). Physiologically, AtClC-a is assumed to accumulate NO_3^- in vacuoles, exploiting the proton gradient (164, 165). More recently, Wege et al. (892) discovered that AtClC-a activity is regulated by the OST1 protein kinase via phosphorylation of Thr-38 in response to abscisic acid (ABA) stimulation and proposed that the transporter is also able to release NO_3^- from the vacuole in stomatal guard cells. Like AtClC-a, also the highly homologous AtClC-b carries a proline residue in the selectivity filter and is a vacuolar NO_3^-/H^+ exchanger, as demonstrated by heterologous expression in *Xenopus* oocytes (863). However, knocking out AtClC-b had not detectable phenotype (863). Interestingly, Carpaneto et al. (106) recently discovered that endogenous AtClC-a-mediated vacuolar currents are inhibited by the low-abundance signaling lipid phosphatidylinositol-3,5-bisphosphate [$PI(3,5)P_2$] and that the inhibition resulted in enhanced vacuolar acidification. It will be interesting to identify the binding site of $PI(3,5)P_2$ in AtClC-a and to find out if other CLC proteins are modulated by phosphoinositides.

The other two vacuolar AtCLCs, AtClC-c and AtClC-g, which are ~60% homologous to each other, carry a serine residue in the selectivity filter and are thus probably Cl^-/H^+ exchangers. Both AtClC-c and AtClC-g are involved in salt tolerance (400, 584) and AtClC-c is additionally important for stomatal opening (400). There are still many open questions regarding the functional properties of most plant CLCs and their precise physiological role remains to be determined.

C. *Caenorhabditis elegans*

The nematode *Caenorhabditis elegans* is a widely used simple model organism which has a number of experimental advantages compared with more complex organisms (82). Its genome encodes six different CLCs, called CeClC-1 to -6 (755). CeClC-1 to -4 are similar to mammalian plasma membrane CLC channels, but no clear correspondences can be identified. CeClC-5 is distantly related to mammalian ClC-3 to -5, whereas CeClC-6 falls in the same class as human ClC-6 and ClC-7. The nematode has no homologue of the accessory proteins barttin, Ostm1, or GlialCAM. CeClC-4 shows a rather specific expression in the large

H-shaped excretory cell, coexpressing with CeClC-3, which has, however, a relatively broad expression in neurons, muscle, and epithelia (755). Also CeClC-2 is broadly expressed in several neurons, intestinal cells, and vulval muscle (755). CeClC-5 is ubiquitously expressed (578), whereas CeClC-6 is predominantly neuronal (578) and appears to be specifically expressed in two GABAergic RME neurons (63). Functional electrophysiological data are available for CeClC-1, -2, and -3 (578, 755). All three isoforms exhibit strongly inwardly rectifying currents with some similarity to mammalian ClC-2 when expressed in *Xenopus* oocytes or mammalian cell lines (578, 755). Very recently, CeClC-1 has been reported to be permeable to HCO_3^- and to contribute to the pH homeostasis in amphid sheath glia (297). However, due to the extreme inward rectification of currents mediated by CeClC-1, reliable reversal potential measurements are difficult to obtain using standard current-voltage pulse protocols, as employed by Grant et al. (297). Specific tail current protocols with careful leak subtraction are necessary to accurately obtain reversal potential measurements from channels whose steady-state open probability is very low in the voltage range of the expected reversal potential.

The CeClC-3 channel has been studied in most detail. Two predominant splice variants, called CeClC-3a and CeClC-3b, have been described. They differ at their NH_2 terminus and in the COOH terminus, mostly regarding the loop between CBS1 and CBS2, and the part downstream of CBS2, including the last residues of the CBS2 domain (162, 185). CeClC-3b exhibits simple inwardly rectifying currents similar to mammalian ClC-2, albeit with faster kinetics (578). Gating of the CeClC-3a splice variant is more complex with an additional gating process induced by "conditioning" pulses to positive voltages (185, 331, 755). Interestingly, exchanging parts of CBS2 between the two isoforms could interchange the gating phenotypes, suggesting that the differences reflect properties of the common gate (162).

In general, *C. elegans* cells are difficult to assess with electrophysiological recording techniques. A notable exception are oocytes that can be released from the animals. Using this approach, Rutledge et al. (716) discovered that *C. elegans* oocytes exhibit swelling-activated inwardly rectifying Cl^- currents carried by CeClC-3. The physiological signal for channel activation is the induction of oocyte meiotic maturation, and the current was proposed to modulate ovulatory contractions of gap junction-coupled gonadal sheath cells (716). Swelling-induced activation does not appear to be direct but rather mediated by the action of type CeCLC-7-α or -β phosphatases (717). The kinase underlying the corresponding phosphorylation was identified as the GCK-3 kinase, a member of the Ste20 family of kinases that are involved in osmosensing in mammals (186). Denton et al. (186) found that GCK-3 directly binds to the channel and that heterologous coexpression reduced currents. Regulation in vivo was shown by GCK-3 knockdown (186). The specific sites phosphorylated by GCK-3 were identified as S742 and S747 in the CBS1-CBS2 linker (235). The single mutants S742E and S747E were still regulated by volume and phosphorylation, whereas the double mutant was constitutively active (557). The CBS1-CBS2 linker is unstructured, and the mechanism underlying the gating effects of phosphorylation/dephosphorylation was described as a "catch and fish" mechanism (816). The phosphorylation effects on external Zn^{2+} block described by Yamada et al. (925) are consistent with an involvement of the common gate in these regulatory processes, and in general agreement with the close apposition of the COOH terminus with the membrane domain as seen in the CmClC crystal structure (242). In addition to the well-studied role of CeClC-3 in oocytes, Branicky et al. (80) found that the channel modulates electrical activity of HSN neurons which control egg laying.

In summary, while the role of CeClC-3b is relatively well understood in oocytes, in general the physiological roles of CLC proteins in *C. elegans* remain largely unexplored.

XV. SUMMARY AND OUTLOOK

The molecular identification of ClC-0 (393), the apparently "strange" double-barreled channel form *Torpedo* electrical organ (905), led to the identification of a gene family of Cl^- channels and Cl^-/H^+ exchangers with members in all phyla. Human genetic diseases and mouse models yielded many, and often very surprising, insights into their diverse physiological functions. Other model organisms such as yeast, *C. elegans*, and *Arabidopis* revealed roles in other phyla. Structure-function analysis, first limited to biophysical analysis of mutants but now firmly based on several crystal and cryo-EM structures, revealed fascinating insights into the mechanism of ion transport that is strikingly different from those of Kv-related cation channels. The presence of anion channels and cation/anion exchangers within the same gene family is particularly intriguing.

Although the field has come of age, we expect that exciting discoveries on the biological roles of CLC proteins will continue to be made, as suggested by the only recent discovery of activating *CLCN2* mutations in primary aldosteronism (246, 747). Many physiological aspects remain enigmatic, in particular concerning the roles of CLC $2Cl^-/H^+$ exchangers in the endosomal-lysosomal pathway, synaptic and possibly other types of vesicles. Key aspects of their structure-function relationship remain poorly understood, as exemplified by the common gating of both ion translocation pathways, the roles of CBS domains, and the mechanism underlying the strong influence of NH_2-terminal residues on ClC-2 gating. Very little is known about the interaction between CLCs and their accessory subunits, including the interaction stoichiometry. Furthermore, the reg-

ulation of CLC proteins by posttranslational modifications needs to be ascertained and put on a more solid basis. Also, the functional properties of endo/lysosomal CLC exchangers have yet to be explored in their native endomembrane environment. Finally, CLC proteins remain interesting putative targets for pharmacological interventions in a variety of pathological conditions, but so far no useful high-affinity blockers or activators have been identified. CLC channels and transporters will remain an exciting research field.

ACKNOWLEDGMENTS

We thank Giovanni Zifarelli and Norma Nitschke for helpful comments on the manuscript.

Address for reprint requests and other correspondence: T. J. Jentsch, Leibniz-Forschungsinstitut für Molekulare Pharmakologie and Max-Delbrück-Centrum für Molekulare Medizin, 13125 Berlin, Germany (e-mail: jentsch@fmp-berlin.de) or M. Pusch, Istituto di Biofisica, Consiglio Nazionale delle Ricerche, Genova, Italy (e-mail: michael.pusch@ge.ibf.cnr.it).

GRANTS

Funding by European Research Council Advanced Grant 294435 "Cytovolion," the Deutsche Forschungsgemeinschaft (SFB 740 and Exc257 "Neurocure"), and the Leibniz Association (SAW-2014-FMP-2 359) to T. J. Jentsch is gratefully acknowledged.

DISCLOSURES

No conflicts of interest, financial or otherwise, are declared by the authors.

REFERENCES

1. Accardi A. Structure and gating of CLC channels and exchangers. *J Physiol* 593: 4129–4138, 2015. doi:10.1113/JP270575.

2. Accardi A, Ferrera L, Pusch M. Drastic reduction of the slow gate of human muscle chloride channel (ClC-1) by mutation C277S. *J Physiol* 534: 745–752, 2001. doi:10.1111/j.1469-7793.2001.00745.x.

3. Accardi A, Kolmakova-Partensky L, Williams C, Miller C. Ionic currents mediated by a prokaryotic homologue of CLC Cl^- channels. *J Gen Physiol* 123: 109–119, 2004. doi:10.1085/jgp.200308935.

4. Accardi A, Lobet S, Williams C, Miller C, Dutzler R. Synergism between halide binding and proton transport in a CLC-type exchanger. *J Mol Biol* 362: 691–699, 2006. doi:10.1016/j.jmb.2006.07.081.

5. Accardi A, Miller C. Secondary active transport mediated by a prokaryotic homologue of ClC Cl^- channels. *Nature* 427: 803–807, 2004. doi:10.1038/nature02314.

6. Accardi A, Picollo A. CLC channels and transporters: proteins with borderline personalities. *Biochim Biophys Acta* 1798: 1457–1464, 2010. doi:10.1016/j.bbamem.2010.02.022.

7. Accardi A, Pusch M. Conformational changes in the pore of CLC-0. *J Gen Physiol* 122: 277–293, 2003. doi:10.1085/jgp.200308834.

8. Accardi A, Pusch M. Fast and slow gating relaxations in the muscle chloride channel CLC-1. *J Gen Physiol* 116: 433–444, 2000. doi:10.1085/jgp.116.3.433.

9. Accardi A, Walden M, Nguitragool W, Jayaram H, Williams C, Miller C. Separate ion pathways in a Cl^-/H^+ exchanger. *J Gen Physiol* 126: 563–570, 2005. doi:10.1085/jgp.200509417.

10. Adachi S, Uchida S, Ito H, Hata M, Hiroe M, Marumo F, Sasaki S. Two isoforms of a chloride channel predominantly expressed in thick ascending limb of Henle's loop and collecting ducts of rat kidney. *J Biol Chem* 269: 17677–17683, 1994.

11. Adler DA, Rugarli EI, Lingenfelter PA, Tsuchiya K, Poslinski D, Liggitt HD, Chapman VM, Elliott RW, Ballabio A, Disteche CM. Evidence of evolutionary up-regulation of the single active X chromosome in mammals based on *Clc4* expression levels in *Mus spretus* and *Mus musculus*. *Proc Natl Acad Sci USA* 94: 9244–9248, 1997. doi:10.1073/pnas.94.17.9244.

12. Adrian RH. Internal chloride concentration and chloride efflux of frog muscle. *J Physiol* 156: 623–632, 1961. doi:10.1113/jphysiol.1961.sp006698.

13. Adrian RH, Bryant SH. On the repetitive discharge in myotonic muscle fibres. *J Physiol* 240: 505–515, 1974. doi:10.1113/jphysiol.1974.sp010620.

14. Adrian RH, Freygang WH. The potassium and chloride conductance of frog muscle membrane. *J Physiol* 163: 61–103, 1962. doi:10.1113/jphysiol.1962.sp006959.

15. Akiba Y, Kaunitz JD. May the truth be with you: lubiprostone as EP receptor agonist/ClC-2 internalizing "inhibitor". *Dig Dis Sci* 57: 2740–2742, 2012. doi:10.1007/s10620-012-2410-2.

16. Akizuki N, Uchida S, Sasaki S, Marumo F. Impaired solute accumulation in inner medulla of *Clcnk1*$^{-/-}$ mice kidney. *Am J Physiol Renal Physiol* 280: F79–F87, 2001. doi:10.1152/ajprenal.2001.280.1.F79.

17. Al-Shibli A, Yusuf M, Abounajab I, Willems PJ. Mixed Bartter-Gitelman syndrome: an inbred family with a heterogeneous phenotype expression of a novel variant in the *CLCNKB* gene. *Springerplus* 3: 96, 2014. doi:10.1186/2193-1801-3-96.

18. Alam I, Gray AK, Acton D, Gerard-O'Riley RL, Reilly AM, Econs MJ. Interferon Gamma, but not Calcitriol Improves the Osteopetrotic Phenotypes in ADO2 Mice. *J Bone Miner Res* 30: 2005–2013, 2015. doi:10.1002/jbmr.2545.

19. Alam I, Gray AK, Chu K, Ichikawa S, Mohammad KS, Capannolo M, Capulli M, Maurizi A, Muraca M, Teti A, Econs MJ, Del Fattore A. Generation of the first autosomal dominant osteopetrosis type II (ADO2) disease models. *Bone* 59: 66–75, 2014. doi:10.1016/j.bone.2013.10.021.

20. Alam I, McQueen AK, Acton D, Reilly AM, Gerard-O'Riley RL, Oakes DK, Kasipathi C, Huffer A, Wright WB, Econs MJ. Phenotypic severity of autosomal dominant osteopetrosis type II (ADO2) mice on different genetic backgrounds recapitulates the features of human disease. *Bone* 94: 34–41, 2017. doi:10.1016/j.bone.2016.10.016.

21. Alekov AK. Mutations associated with Dent's disease affect gating and voltage dependence of the human anion/proton exchanger ClC-5. *Front Physiol* 6: 159, 2015. doi:10.3389/fphys.2015.00159.

22. Alekov AK, Fahlke C. Channel-like slippage modes in the human anion/proton exchanger ClC-4. *J Gen Physiol* 133: 485–496, 2009. doi:10.1085/jgp.200810155.

23. Alex P, Ye M, Zachos NC, Sipes J, Nguyen T, Suhodrev M, Gonzales L, Arora Z, Zhang T, Centola M, Guggino SE, Li X. *Clcn5* knockout mice exhibit novel immunomodulatory effects and are more susceptible to dextran sulfate sodium-induced colitis. *J Immunol* 184: 3988–3996, 2010. doi:10.4049/jimmunol.0901657.

24. Alper SL. The band 3-related anion exchanger (AE) gene family. *Annu Rev Physiol* 53: 549–564, 1991. doi:10.1146/annurev.ph.53.030191.003001.

25. Ambizas EM, Ginzburg R. Lubiprostone: a chloride channel activator for treatment of chronic constipation. *Ann Pharmacother* 41: 957–964, 2007. doi:10.1345/aph.1K047.

26. Ando M, Takeuchi S. mRNA encoding 'ClC-K1, a kidney Cl^--channel' is expressed in marginal cells of the stria vascularis of rat cochlea: its possible contribution to Cl^- currents. *Neurosci Lett* 284: 171–174, 2000. doi:10.1016/S0304-3940(00)01021-1.

27. Andrini O, Keck M, Briones R, Lourdel S, Vargas-Poussou R, Teulon J. ClC-K chloride channels: emerging pathophysiology of Bartter syndrome type 3. *Am J Physiol Renal Physiol* 308: F1324–F1334, 2015. doi:10.1152/ajprenal.00004.2015.

28. Andrini O, Keck M, L'Hoste S, Briones R, Mansour-Hendili L, Grand T, Sepúlveda FV, Blanchard A, Lourdel S, Vargas-Poussou R, Teulon J. *CLCNKB* mutations causing mild

Bartter syndrome profoundly alter the pH and Ca^{2+} dependence of ClC-Kb channels. *Pflugers Arch* 466: 1713–1723, 2014. doi:10.1007/s00424-013-1401-2.

29. Ao M, Venkatasubramanian J, Boonkaewwan C, Ganesan N, Syed A, Benya RV, Rao MC. Lubiprostone activates Cl^- secretion via cAMP signaling and increases membrane CFTR in the human colon carcinoma cell line, T84. *Dig Dis Sci* 56: 339–351, 2011. doi:10.1007/s10620-010-1495-8.

30. Argenzio E, Moolenaar WH. Emerging biological roles of Cl^- intracellular channel proteins. *J Cell Sci* 129: 4165–4174, 2016. doi:10.1242/jcs.189795.

31. Arnedo T, Aiello C, Jeworutzki E, Dentici ML, Uziel G, Simonati A, Pusch M, Bertini E, Estévez R. Expanding the spectrum of megalencephalic leukoencephalopathy with subcortical cysts in two patients with GLIALCAM mutations. *Neurogenetics* 15: 41–48, 2014. doi:10.1007/s10048-013-0381-x.

32. Arnedo T, López-Hernández T, Jeworutzki E, Capdevila-Nortes X, Sirisi S, Pusch M, Estévez R. Functional analyses of mutations in *HEPACAM* causing megalencephalic leukoencephalopathy. *Hum Mutat* 35: 1175–1178, 2014. doi:10.1002/humu.22622.

33. Aromataris EC, Astill DS, Rychkov GY, Bryant SH, Bretag AH, Roberts ML. Modulation of the gating of ClC-1 by *S*-(-) 2-(4-chlorophenoxy) propionic acid. *Br J Pharmacol* 126: 1375–1382, 1999. doi:10.1038/sj.bjp.0702459.

34. Aromataris EC, Rychkov GY. ClC-1 chloride channel: matching its properties to a role in skeletal muscle. *Clin Exp Pharmacol Physiol* 33: 1118–1123, 2006. doi:10.1111/j.1440-1681.2006.04502.x.

35. Aromataris EC, Rychkov GY, Bennetts B, Hughes BP, Bretag AH, Roberts ML. Fast and slow gating of CLC-1: differential effects of 2-(4-chlorophenoxy) propionic acid and dominant negative mutations. *Mol Pharmacol* 60: 200–208, 2001. doi:10.1124/mol.60.1.200.

36. Arreola J, Begenisich T, Melvin JE. Conformation-dependent regulation of inward rectifier chloride channel gating by extracellular protons. *J Physiol* 541: 103–112, 2002. doi:10.1113/jphysiol.2002.016485.

37. Arreola J, Begenisich T, Nehrke K, Nguyen HV, Park K, Richardson L, Yang B, Schutte BC, Lamb FS, Melvin JE. Secretion and cell volume regulation by salivary acinar cells from mice lacking expression of the *Clcn3* Cl^- channel gene. *J Physiol* 545: 207–216, 2002. doi:10.1113/jphysiol.2002.021980.

38. Astill DS, Rychkov G, Clarke JD, Hughes BP, Roberts ML, Bretag AH. Characteristics of skeletal muscle chloride channel C1C-1 and point mutant R304E expressed in Sf-9 insect cells. *Biochim Biophys Acta* 1280: 178–186, 1996. doi:10.1016/0005-2736(95)00281-2.

39. Attree O, Olivos IM, Okabe I, Bailey LC, Nelson DL, Lewis RA, McInnes RR, Nussbaum RL. The Lowe's oculocerebrorenal syndrome gene encodes a protein highly homologous to inositol polyphosphate-5-phosphatase. *Nature* 358: 239–242, 1992. doi:10.1038/358239a0.

40. Auzanneau C, Thoreau V, Kitzis A, Becq F. A novel voltage-dependent chloride current activated by extracellular acidic pH in cultured rat Sertoli cells. *J Biol Chem* 278: 19230–19236, 2003. doi:10.1074/jbc.M301096200.

41. Bao HF, Liu L, Self J, Duke BJ, Ueno R, Eaton DC. A synthetic prostone activates apical chloride channels in A6 epithelial cells. *Am J Physiol Gastrointest Liver Physiol* 295: G234–G251, 2008. doi:10.1152/ajpgi.00366.2007.

42. Barbier-Brygoo H, Vinauger M, Colcombet J, Ephritikhine G, Frachisse J, Maurel C. Anion channels in higher plants: functional characterization, molecular structure and physiological role. *Biochim Biophys Acta* 1465: 199–218, 2000. doi:10.1016/S0005-2736(00)00139-5.

43. Bardouille C, Vullhorst D, Jockusch H. Expression of chloride channel 1 mRNA in cultured myogenic cells: a marker of myotube maturation. *FEBS Lett* 396: 177–180, 1996. doi:10.1016/0014-5793(96)01098-8.

44. Barg S, Huang P, Eliasson L, Nelson DJ, Obermüller S, Rorsman P, Thévenod F, Renström E. Priming of insulin granules for exocytosis by granular Cl^- uptake and acidification. *J Cell Sci* 114: 2145–2154, 2001.

45. Barlassina C, Dal Fiume C, Lanzani C, Manunta P, Guffanti G, Ruello A, Bianchi G, Del Vecchio L, Macciardi F, Cusi D. Common genetic variants and haplotypes in renal *CLCNKA* gene are associated to salt-sensitive hypertension. *Hum Mol Genet* 16: 1630–1638, 2007. doi:10.1093/hmg/ddm112.

46. Barvencik F, Kurth I, Koehne T, Stauber T, Zustin J, Tsiakas K, Ludwig CF, Beil FT, Pestka JM, Hahn M, Santer R, Supanchart C, Kornak U, Del Fattore A, Jentsch TJ, Teti A, Schulz A, Schinke T, Amling M. *CLCN7* and *TCIRG1* mutations differentially affect bone matrix mineralization in osteopetrotic individuals. *J Bone Miner Res* 29: 982–991, 2014. doi:10.1002/jbmr.2100.

47. Basilio D, Noack K, Picollo A, Accardi A. Conformational changes required for H^+/Cl^- exchange mediated by a CLC transporter. *Nat Struct Mol Biol* 21: 456–463, 2014. doi:10.1038/nsmb.2814.

48. Bassil AK, Borman RA, Jarvie EM, McArthur-Wilson RJ, Thangiah R, Sung EZ, Lee K, Sanger GJ. Activation of prostaglandin EP receptors by lubiprostone in rat and human stomach and colon. *Br J Pharmacol* 154: 126–135, 2008. doi:10.1038/bjp.2008.84.

49. Bateman A. The structure of a domain common to archaebacteria and the homocystinuria disease protein. *Trends Biochem Sci* 22: 12–13, 1997. doi:10.1016/S0968-0004(96)30046-7.

50. Bauer CK, Steinmeyer K, Schwarz JR, Jentsch TJ. Completely functional double-barreled chloride channel expressed from a single *Torpedo* cDNA. *Proc Natl Acad Sci USA* 88: 11052–11056, 1991. doi:10.1073/pnas.88.24.11052.

51. Beck CL, Fahlke C, George AL Jr. Molecular basis for decreased muscle chloride conductance in the myotonic goat. *Proc Natl Acad Sci USA* 93: 11248–11252, 1996. doi:10.1073/pnas.93.20.11248.

52. Beck L, Karaplis AC, Amizuka N, Hewson AS, Ozawa H, Tenenhouse HS. Targeted inactivation of Npt2 in mice leads to severe renal phosphate wasting, hypercalciuria, and skeletal abnormalities. *Proc Natl Acad Sci USA* 95: 5372–5377, 1998. doi:10.1073/pnas.95.9.5372.

53. Bell SP, Curran PK, Choi S, Mindell JA. Site-directed fluorescence studies of a prokaryotic ClC antiporter. *Biochemistry* 45: 6773–6782, 2006. doi:10.1021/bi0523815.

54. Bennetts B, Parker MW. Molecular determinants of common gating of a ClC chloride channel. *Nat Commun* 4: 2507, 2013. doi:10.1038/ncomms3507.

55. Bennetts B, Parker MW, Cromer BA. Inhibition of skeletal muscle ClC-1 chloride channels by low intracellular pH and ATP. *J Biol Chem* 282: 32780–32791, 2007. doi:10.1074/jbc.M703259200.

56. Bennetts B, Roberts ML, Bretag AH, Rychkov GY. Temperature dependence of human muscle ClC-1 chloride channel. *J Physiol* 535: 83–93, 2001. doi:10.1111/j.1469-7793.2001.t01-1-00083.x.

57. Bennetts B, Rychkov GY, Ng HL, Morton CJ, Stapleton D, Parker MW, Cromer BA. Cytoplasmic ATP-sensing domains regulate gating of skeletal muscle ClC-1 chloride channels. *J Biol Chem* 280: 32452–32458, 2005. doi:10.1074/jbc.M502890200.

58. Bennetts B, Yu Y, Chen TY, Parker MW. Intracellular β-nicotinamide adenine dinucleotide inhibits the skeletal muscle ClC-1 chloride channel. *J Biol Chem* 287: 25808–25820, 2012. doi:10.1074/jbc.M111.327551.

59. Bergler T, Stoelcker B, Jeblick R, Reinhold SW, Wolf K, Riegger GA, Krämer BK. High osmolality induces the kidney-specific chloride channel CLC-K1 by a serum and glucocorticoid-inducible kinase 1 MAPK pathway. *Kidney Int* 74: 1170–1177, 2008. doi:10.1038/ki.2008.312.

60. Bergsdorf EY, Zdebik AA, Jentsch TJ. Residues important for nitrate/proton coupling in plant and mammalian CLC transporters. *J Biol Chem* 284: 11184–11193, 2009. doi:10.1074/jbc.M901170200.

61. Berkovic SF, Carpenter S, Andermann F, Andermann E, Wolfe LS. Kufs' disease: a critical reappraisal. *Brain* 111: 27–62, 1988. doi:10.1093/brain/111.1.27.

62. Bi MM, Hong S, Zhou HY, Wang HW, Wang LN, Zheng YJ. Chloride channelopathies of ClC-2. *Int J Mol Sci* 15: 218–249, 2013. doi:10.3390/ijms15010218.

63. Bianchi L, Miller DM III, George AL Jr. Expression of a CIC chloride channel in *Caenorhabditis elegans* gamma-aminobutyric acid-ergic neurons. *Neurosci Lett* 299: 177–180, 2001. doi:10.1016/S0304-3940(01)01525-7.

64. Bijvelds MJ, Bot AG, Escher JC, De Jonge HR. Activation of intestinal Cl^- secretion by lubiprostone requires the cystic fibrosis transmembrane conductance regulator. *Gastroenterology* 137: 976–985, 2009. doi:10.1053/j.gastro.2009.05.037.

65. Birkenhäger R, Otto E, Schürmann MJ, Vollmer M, Ruf EM, Maier-Lutz I, Beekmann F, Fekete A, Omran H, Feldmann D, Milford DV, Jeck N, Konrad M, Landau D, Knoers NVAM, Antignac C, Sudbrak R, Kispert A, Hildebrandt F. Mutation of *BSND* causes

Bartter syndrome with sensorineural deafness and kidney failure. *Nat Genet* 29: 310–314, 2001. doi:10.1038/ng752.

66. Blaisdell CJ, Edmonds RD, Wang XT, Guggino S, Zeitlin PL. pH-regulated chloride secretion in fetal lung epithelia. *Am J Physiol Lung Cell Mol Physiol* 278: L1248–L1255, 2000. doi:10.1152/ajplung.2000.278.6.L1248.

67. Blaisdell CJ, Morales MM, Andrade AC, Bamford P, Wasicko M, Welling P. Inhibition of CLC-2 chloride channel expression interrupts expansion of fetal lung cysts. *Am J Physiol Lung Cell Mol Physiol* 286: L420–L426, 2004. doi:10.1152/ajplung.00113.2003.

68. Blanz J, Schweizer M, Auberson M, Maier H, Muenscher A, Hübner CA, Jentsch TJ. Leukoencephalopathy upon disruption of the chloride channel ClC-2. *J Neurosci* 27: 6581–6589, 2007. doi:10.1523/JNEUROSCI.0338-07.2007.

69. Boettger T, Hübner CA, Maier H, Rust MB, Beck FX, Jentsch TJ. Deafness and renal tubular acidosis in mice lacking the K-Cl co-transporter Kcc4. *Nature* 416: 874–878, 2002. doi:10.1038/416874a.

70. Bonapace G, Moricca MT, Talarico V, Graziano F, Pensabene L, Miniero R. Identification of two novel mutations on *CLCN7* gene in a patient with malignant ostopetrosis. *Ital J Pediatr* 40: 90, 2014. doi:10.1186/s13052-014-0090-6.

71. Bonifacino JS, Traub LM. Signals for sorting of transmembrane proteins to endosomes and lysosomes. *Annu Rev Biochem* 72: 395–447, 2003. doi:10.1146/annurev.biochem.72.121801.161800.

72. Borges AS, Barbosa JD, Resende LA, Mota LS, Amorim RM, Carvalho TL, Garcia JF, Oliveira-Filho JP, Oliveira CM, Souza JE, Winand NJ. Clinical and molecular study of a new form of hereditary myotonia in Murrah water buffalo. *Neuromuscul Disord* 23: 206–213, 2013. doi:10.1016/j.nmd.2012.11.008.

73. Borsani G, Rugarli EI, Taglialatela M, Wong C, Ballabio A. Characterization of a human and murine gene (*CLCN3*) sharing similarities to voltage-gated chloride channels and to a yeast integral membrane protein. *Genomics* 27: 131–141, 1995. doi:10.1006/geno.1995.1015.

74. Bösl MR, Stein V, Hübner C, Zdebik AA, Jordt SE, Mukhopadhyay AK, Davidoff MS, Holstein AF, Jentsch TJ. Male germ cells and photoreceptors, both dependent on close cell-cell interactions, degenerate upon ClC-2 Cl^- channel disruption. *EMBO J* 20: 1289–1299, 2001. doi:10.1093/emboj/20.6.1289.

75. Bothe MK, Mundhenk L, Kaup M, Weise C, Gruber AD. The murine goblet cell protein mCLCA3 is a zinc-dependent metalloprotease with autoproteolytic activity. *Mol Cells* 32: 535–541, 2011. doi:10.1007/s10059-011-0158-8.

76. Bouyer G, Egée S, Thomas SL. Toward a unifying model of malaria-induced channel activity. *Proc Natl Acad Sci USA* 104: 11044–11049, 2007. doi:10.1073/pnas.0704582104.

77. Bozeat ND, Xiang SY, Ye LL, Yao TY, Duan ML, Burkin DJ, Lamb FS, Duan DD. Activation of volume regulated chloride channels protects myocardium from ischemia/reperfusion damage in second-window ischemic preconditioning. *Cell Physiol Biochem* 28: 1265–1278, 2011. doi:10.1159/000335858.

78. Brammer AE, Stockbridge RB, Miller C. F^-/Cl^- selectivity in CLCF-type F^-/H^+ antiporters. *J Gen Physiol* 144: 129–136, 2014. doi:10.1085/jgp.201411225.

79. Brandt S, Jentsch TJ. ClC-6 and ClC-7 are two novel broadly expressed members of the CLC chloride channel family. *FEBS Lett* 377: 15–20, 1995. doi:10.1016/0014-5793(95)01298-2.

80. Branicky R, Miyazaki H, Strange K, Schafer WR. The voltage-gated anion channels encoded by clh-3 regulate egg laying in *C. elegans* by modulating motor neuron excitability. *J Neurosci* 34: 764–775, 2014. doi:10.1523/JNEUROSCI.3112-13.2014.

81. Braun NA, Morgan B, Dick TP, Schwappach B. The yeast CLC protein counteracts vesicular acidification during iron starvation. *J Cell Sci* 123: 2342–2350, 2010. doi:10.1242/jcs.068403.

82. Brenner S. The genetics of *Caenorhabditis elegans*. *Genetics* 77: 71–94, 1974.

83. Bretag AH. Muscle chloride channels. *Physiol Rev* 67: 618–724, 1987. doi:10.1152/physrev.1987.67.2.618.

84. Brinkmeier H, Jockusch H. Activators of protein kinase C induce myotonia by lowering chloride conductance in muscle. *Biochem Biophys Res Commun* 148: 1383–1389, 1987. doi:10.1016/S0006-291X(87)80285-1.

85. Brochard K, Boyer O, Blanchard A, Loirat C, Niaudet P, Macher MA, Deschenes G, Bensman A, Decramer S, Cochat P, Morin D, Broux F, Caillez M, Guyot C, Novo R, Jeunemaître X, Vargas-Poussou R. Phenotype-genotype correlation in antenatal and neonatal variants of Bartter syndrome. *Nephrol Dial Transplant* 24: 1455–1464, 2009. doi:10.1093/ndt/gfn689.

86. Brown GL, Harvey AM. Congenital myotonia in the goat. *Brain* 62: 341–363, 1939. doi:10.1093/brain/62.4.341.

87. Bryant SH, Morales-Aguilera A. Chloride conductance in normal and myotonic muscle fibres and the action of monocarboxylic aromatic acids. *J Physiol* 219: 367–383, 1971. doi:10.1113/jphysiol.1971.sp009667.

88. Bugiani M, Dubey M, Breur M, Postma NL, Dekker MP, Ter Braak T, Boschert U, Abbink TEM, Mansvelder HD, Min R, van Weering JRT, van der Knaap MS. Megalencephalic leukoencephalopathy with cysts: the *Glialcam*-null mouse model. *Ann Clin Transl Neurol* 4: 450–465, 2017. doi:10.1002/acn3.405.

89. Burgunder JM, Huifang S, Beguin P, Baur R, Eng CS, Seet RC, Lim EC, Ong BK, Hunziker W, Sigel E. Novel chloride channel mutations leading to mild myotonia among Chinese. *Neuromuscul Disord* 18: 633–640, 2008. doi:10.1016/j.nmd.2008.05.007.

90. Butt AM, Kalsi A. Inwardly rectifying potassium channels (Kir) in central nervous system glia: a special role for Kir4.1 in glial functions. *J Cell Mol Med* 10: 33–44, 2006. doi:10.1111/j.1582-4934.2006.tb00289.x.

91. Buyse G, Trouet D, Voets T, Missiaen L, Droogmans G, Nilius B, Eggermont J. Evidence for the intracellular location of chloride channel (ClC)-type proteins: co-localization of ClC-6a and ClC-6c with the sarco/endoplasmic-reticulum Ca^{2+} pump SERCA2b. *Biochem J* 330: 1015–1021, 1998. doi:10.1042/bj3301015.

92. Buyse G, Voets T, Tytgat J, De Greef C, Droogmans G, Nilius B, Eggermont J. Expression of human pICln and ClC-6 in *Xenopus* oocytes induces an identical endogenous chloride conductance. *J Biol Chem* 272: 3615–3621, 1997. doi:10.1074/jbc.272.6.3615.

93. Bykova EA, Zhang XD, Chen TY, Zheng J. Large movement in the C terminus of CLC-0 chloride channel during slow gating. *Nat Struct Mol Biol* 13: 1115–1119, 2006. doi:10.1038/nsmb1176.

94. Caetano-Lopes J, Lessard SG, Hann S, Espinoza K, Kang KS, Lim KE, Horan DJ, Noonan HR, Hu D, Baron R, Robling AG, Warman ML. $Clcn7^{F318L/+}$ as a new mouse model of Albers-Schönberg disease. *Bone* 105: 253–261, 2017. doi:10.1016/j.bone.2017.09.007.

95. Cahalan MD, Lewis RS. Functional roles of ion channels in lymphocytes. *Semin Immunol* 2: 107–117, 1990.

96. Camerino GM, Bouchè M, De Bellis M, Cannone M, Liantonio A, Musaraj K, Romano R, Smeriglio P, Madaro L, Giustino A, De Luca A, Desaphy JF, Camerino DC, Pierno S. Protein kinase C theta (PKCθ) modulates the ClC-1 chloride channel activity and skeletal muscle phenotype: a biophysical and gene expression study in mouse models lacking the PKCθ. *Pflugers Arch* 466: 2215–2228, 2014. doi:10.1007/s00424-014-1495-1.

97. Cannon SC. Channelopathies of skeletal muscle excitability. *Compr Physiol* 5: 761–790, 2015. doi:10.1002/cphy.c140062.

98. Capdevila-Nortes X, Jeworutzki E, Elorza-Vidal X, Barrallo-Gimeno A, Pusch M, Estévez R. Structural determinants of interaction, trafficking and function in the ClC-2/MLC1 subunit GlialCAM involved in leukodystrophy. *J Physiol* 593: 4165–4180, 2015. doi:10.1113/JP270467.

100. Capdevila-Nortes X, López-Hernández T, Apaja PM, López de Heredia M, Sirisi S, Callejo G, Arnedo T, Nunes V, Lukacs GL, Gasull X, Estévez R. Insights into MLC pathogenesis: GlialCAM is an MLC1 chaperone required for proper activation of volume-regulated anion currents. *Hum Mol Genet* 22: 4405–4416, 2013. doi:10.1093/hmg/ddt290.

101. Cappola TP, Matkovich SJ, Wang W, van Booven D, Li M, Wang X, Qu L, Sweitzer NK, Fang JC, Reilly MP, Hakonarson H, Nerbonne JM, Dorn GW II. Loss-of-function DNA sequence variant in the *CLCNKA* chloride channel implicates the cardio-renal axis in interindividual heart failure risk variation. *Proc Natl Acad Sci USA* 108: 2456–2461, 2011. doi:10.1073/pnas.1017494108.

102. Capulli M, Maurizi A, Ventura L, Rucci N, Teti A. Effective Small Interfering RNA Therapy to Treat *CLCN7*-dependent Autosomal Dominant Osteopetrosis Type 2. *Mol Ther Nucleic Acids* 4: e248, 2015. doi:10.1038/mtna.2015.21.

103. Capurro V, Gianotti A, Caci E, Ravazzolo R, Galietta LJ, Zegarra-Moran O. Functional analysis of acid-activated Cl^- channels: properties and mechanisms of regulation. *Biochim Biophys Acta* 1848, 1 Pt A: 105–114, 2015. doi:10.1016/j.bbamem.2014.10.008.

104. Caputo A, Caci E, Ferrera L, Pedemonte N, Barsanti C, Sondo E, Pfeffer U, Ravazzolo R, Zegarra-Moran O, Galietta LJ. TMEM16A, a membrane protein associated with calcium-dependent chloride channel activity. *Science* 322: 590–594, 2008. doi:10.1126/science.1163518.

105. Carew MA, Thorn P. Identification of ClC-2-like chloride currents in pig pancreatic acinar cells. *Pflugers Arch* 433: 84–90, 1996. doi:10.1007/s004240050252.

106. Carpaneto A, Boccaccio A, Lagostena L, Di Zanni E, Scholz-Starke J. The signaling lipid phosphatidylinositol-3,5-bisphosphate targets plant CLC-a anion/H^+ exchange activity. *EMBO Rep* 18: 1100–1107, 2017. doi:10.15252/embr.201643814.

107. Carr G, Simmons N, Sayer J. A role for CBS domain 2 in trafficking of chloride channel CLC-5. *Biochem Biophys Res Commun* 310: 600–605, 2003. doi:10.1016/j.bbrc.2003.09.057.

108. Casimiro MC, Knollmann BC, Ebert SN, Vary JC Jr, Greene AE, Franz MR, Grinberg A, Huang SP, Pfeifer K. Targeted disruption of the *Kcnq1* gene produces a mouse model of Jervell and Lange-Nielsen Syndrome. *Proc Natl Acad Sci USA* 98: 2526–2531, 2001. doi:10.1073/pnas.041398998.

109. Catalán M, Cornejo I, Figueroa CD, Niemeyer MI, Sepúlveda FV, Cid LP. ClC-2 in guinea pig colon: mRNA, immunolabeling, and functional evidence for surface epithelium localization. *Am J Physiol Gastrointest Liver Physiol* 283: G1004–G1013, 2002. doi:10.1152/ajpgi.00158.2002.

110. Catalán M, Niemeyer MI, Cid LP, Sepúlveda FV. Basolateral ClC-2 chloride channels in surface colon epithelium: regulation by a direct effect of intracellular chloride. *Gastroenterology* 126: 1104–1114, 2004. doi:10.1053/j.gastro.2004.01.010.

111. Catalán MA, Flores CA, González-Begne M, Zhang Y, Sepúlveda FV, Melvin JE. Severe defects in absorptive ion transport in distal colons of mice that lack ClC-2 channels. *Gastroenterology* 142: 346–354, 2012. doi:10.1053/j.gastro.2011.10.037.

112. Cebotaru V, Kaul S, Devuyst O, Cai H, Racusen L, Guggino WB, Guggino SE. High citrate diet delays progression of renal insufficiency in the ClC-5 knockout mouse model of Dent's disease. *Kidney Int* 68: 642–652, 2005. doi:10.1111/j.1523-1755.2005.00442.x.

113. Cederholm JM, Rychkov GY, Bagley CJ, Bretag AH. Inter-subunit communication and fast gate integrity are important for common gating in hClC-1. *Int J Biochem Cell Biol* 42: 1182–1188, 2010. doi:10.1016/j.biocel.2010.04.004.

114. Chadda R, Krishnamani V, Mersch K, Wong J, Brimberry M, Chadda A, Kolmakova-Partensky L, Friedman LJ, Gelles J, Robertson JL. The dimerization equilibrium of a ClC Cl^-/H^+ antiporter in lipid bilayers. *eLife* 5: e17438, 2016. doi:10.7554/eLife.17438.

115. Chakraborty K, Leung K, Krishnan Y. High lumenal chloride in the lysosome is critical for lysosome function. *eLife* 6: e28862, 2017. doi:10.7554/eLife.28862.

116. Chalhoub N, Benachenhou N, Rajapurohitam V, Pata M, Ferron M, Frattini A, Villa A, Vacher J. Grey-lethal mutation induces severe malignant autosomal recessive osteopetrosis in mouse and human. *Nat Med* 9: 399–406, 2003. doi:10.1038/nm842.

117. Chan WW, Mashimo H. Lubiprostone Increases Small Intestinal Smooth Muscle Contractions Through a Prostaglandin E Receptor 1 (EP1)-mediated Pathway. *J Neurogastroenterol Motil* 19: 312–318, 2013. doi:10.5056/jnm.2013.19.3.312.

118. Chang PY, Zhang XG, Su XL. Lack of association of variants of the renal salt reabsorption-related genes *SLC12A3* and *ClC-Kb* and hypertension in Mongolian and Han populations in Inner Mongolia. *Genet Mol Res* 10: 948–954, 2011. doi:10.4238/vol10-2gmr1165.

119. Charlet-B N, Savkur RS, Singh G, Philips AV, Grice EA, Cooper TA. Loss of the muscle-specific chloride channel in type 1 myotonic dystrophy due to misregulated alternative splicing. *Mol Cell* 10: 45–53, 2002. doi:10.1016/S1097-2765(02)00572-5.

120. Chen MF, Chen TY. Different fast-gate regulation by external Cl^- and H^+ of the muscle-type ClC chloride channels. *J Gen Physiol* 118: 23–32, 2001. doi:10.1085/jgp.118.1.23.

121. Chen MF, Chen TY. Side-chain charge effects and conductance determinants in the pore of ClC-0 chloride channels. *J Gen Physiol* 122: 133–145, 2003. doi:10.1085/jgp.200308844.

122. Chen MF, Niggeweg R, Iaizzo PA, Lehmann-Horn F, Jockusch H. Chloride conductance in mouse muscle is subject to post-transcriptional compensation of the functional Cl^- channel 1 gene dosage. *J Physiol* 504: 75–81, 1997. doi:10.1111/j.1469-7793.1997.075bf.x.

123. Chen TT, Klassen TL, Goldman AM, Marini C, Guerrini R, Noebels JL. Novel brain expression of ClC-1 chloride channels and enrichment of *CLCN1* variants in epilepsy. *Neurology* 80: 1078–1085, 2013. doi:10.1212/WNL.0b013e31828868e7.

124. Chen TY. Coupling gating with ion permeation in ClC channels. *Sci STKE* 2003: pe23, 2003. doi:10.1126/stke.2003.188.pe23.

125. Chen TY. Extracellular zinc ion inhibits ClC-0 chloride channels by facilitating slow gating. *J Gen Physiol* 112: 715–726, 1998. doi:10.1085/jgp.112.6.715.

126. Chen TY. Structure and function of clc channels. *Annu Rev Physiol* 67: 809–839, 2005. doi:10.1146/annurev.physiol.67.032003.153012.

127. Chen TY, Chen MF, Lin CW. Electrostatic control and chloride regulation of the fast gating of ClC-0 chloride channels. *J Gen Physiol* 122: 641–651, 2003. doi:10.1085/jgp.200308846.

128. Chen TY, Miller C. Nonequilibrium gating and voltage dependence of the ClC-0 Cl^- channel. *J Gen Physiol* 108: 237–250, 1996. doi:10.1085/jgp.108.4.237.

129. Chen X, Zhang K, Hock J, Wang C, Yu X. Enhanced but hypofunctional osteoclastogenesis in an autosomal dominant osteopetrosis type II case carrying a c.1856C>T mutation in *CLCN7*. *Bone Res* 4: 16035, 2016. doi:10.1038/boneres.2016.35.

130. Chenal C, Gunner MR. Two Cl Ions and a Glu Compete for a Helix Cage in the CLC Proton/Cl^- Antiporter. *Biophys J* 113: 1025–1036, 2017. doi:10.1016/j.bpj.2017.07.025.

131. Cheng CJ, Lo YF, Chen JC, Huang CL, Lin SH. Functional severity of *CLCNKB* mutations correlates with phenotypes in patients with classic Bartter's syndrome. *J Physiol* 595: 5573–5586, 2017. doi:10.1113/JP274344.

132. Cherubino F, Bertram S, Bossi E, Peres A. Pre-steady-state and reverse transport currents in the GABA transporter GAT1. *Am J Physiol Cell Physiol* 302: C1096–C1108, 2012. doi:10.1152/ajpcell.00268.2011.

133. Cheung G, Cousin MA. Adaptor protein complexes 1 and 3 are essential for generation of synaptic vesicles from activity-dependent bulk endosomes. *J Neurosci* 32: 6014–6023, 2012. doi:10.1523/JNEUROSCI.6305-11.2012.

134. Cho HW, Lee ST, Cho H, Cheong HI. A novel mutation of *CLCNKB* in a Korean patient of mixed phenotype of Bartter-Gitelman syndrome. *Korean J Pediatr* 59, Suppl 1: S103–S106, 2016. doi:10.3345/kjp.2016.59.11.S103.

135. Christensen EI, Devuyst O, Dom G, Nielsen R, Van der Smissen P, Verroust P, Leruth M, Guggino WB, Courtoy PJ. Loss of chloride channel ClC-5 impairs endocytosis by defective trafficking of megalin and cubilin in kidney proximal tubules. *Proc Natl Acad Sci USA* 100: 8472–8477, 2003. doi:10.1073/pnas.1432873100.

136. Chu X, Filali M, Stanic B, Takapoo M, Sheehan A, Bhalla R, Lamb FS, Miller FJ Jr. A critical role for chloride channel-3 (ClC-3) in smooth muscle cell activation and neointima formation. *Arterioscler Thromb Vasc Biol* 31: 345–351, 2011. doi:10.1161/ATVBAHA.110.217604.

137. Chung Moh M, Hoon Lee L, Shen S. Cloning and characterization of hepaCAM, a novel Ig-like cell adhesion molecule suppressed in human hepatocellular carcinoma. *J Hepatol* 42: 833–841, 2005. doi:10.1016/j.jhep.2005.01.025.

138. Cigić B, Pain RH. Location of the binding site for chloride ion activation of cathepsin C. *Eur J Biochem* 264: 944–951, 1999. doi:10.1046/j.1432-1327.1999.00697.x.

139. Clark S, Jordt SE, Jentsch TJ, Mathie A. Characterization of the hyperpolarization-activated chloride current in dissociated rat sympathetic neurons. *J Physiol* 506: 665–678, 1998. doi:10.1111/j.1469-7793.1998.665bv.x.

140. Clayton GH, Staley KJ, Wilcox CL, Owens GC, Smith RL. Developmental expression of ClC-2 in the rat nervous system. *Brain Res Dev Brain Res* 108: 307–318, 1998. doi:10.1016/S0165-3806(98)00045-5.

141. Cleiren E, Bénichou O, Van Hul E, Gram J, Bollerslev J, Singer FR, Beaverson K, Aledo A, Whyte MP, Yoneyama T, deVernejoul MC, Van Hul W. Albers-Schönberg disease

(autosomal dominant osteopetrosis, type II) results from mutations in the *ClCN7* chloride channel gene. *Hum Mol Genet* 10: 2861–2867, 2001. doi:10.1093/hmg/10.25.2861.

142. Cohen J, Schulten K. Mechanism of anionic conduction across ClC. *Biophys J* 86: 836–845, 2004. doi:10.1016/S0006-3495(04)74159-4.

143. Comes N, Abad E, Morales M, Borrás T, Gual A, Gasull X. Identification and functional characterization of ClC-2 chloride channels in trabecular meshwork cells. *Exp Eye Res* 83: 877–889, 2006. doi:10.1016/j.exer.2006.04.008.

144. Conte-Camerino D, Mambrini M, DeLuca A, Tricarico D, Bryant SH, Tortorella V, Bettoni G. Enantiomers of clofibric acid analogs have opposite actions on rat skeletal muscle chloride channels. *Pflugers Arch* 413: 105–107, 1988. doi:10.1007/BF00581238.

145. Conte Camerino D, De Luca A, Mambrini M, Vrbovà G. Membrane ionic conductances in normal and denervated skeletal muscle of the rat during development. *Pflugers Arch* 413: 568–570, 1989. doi:10.1007/BF00594192.

146. Coonan JR, Lamb GD. Effect of transverse-tubular chloride conductance on excitability in skinned skeletal muscle fibres of rat and toad. *J Physiol* 509: 551–564, 1998. doi:10.1111/j.1469-7793.1998.551bn.x.

147. Copelovitch L, Nash MA, Kaplan BS. Hypothesis: Dent disease is an underrecognized cause of focal glomerulosclerosis. *Clin J Am Soc Nephrol* 2: 914–918, 2007. doi:10.2215/CJN.00900207.

148. Cornejo I, Niemeyer MI, Sepúlveda FV, Cid LP. Cloning, cellular distribution and functional expression of small intestinal epithelium guinea pig ClC-5 chloride channel. *Biochim Biophys Acta* 1512: 367–374, 2001. doi:10.1016/S0005-2736(01)00331-5.

149. Corry B, O'Mara M, Chung SH. Conduction mechanisms of chloride ions in ClC-type channels. *Biophys J* 86: 846–860, 2004. doi:10.1016/S0006-3495(04)74160-0.

150. Cortez MA, Li C, Whitehead SN, Dhani SU, D'Antonio C, Huan LJ, Bennett SA, Snead OC III, Bear CE. Disruption of ClC-2 expression is associated with progressive neurodegeneration in aging mice. *Neuroscience* 167: 154–162, 2010. doi:10.1016/j.neuroscience.2010.01.042.

151. Cruz AJ, Castro A. Gitelman or Bartter type 3 syndrome? A case of distal convoluted tubulopathy caused by *CLCNKB* gene mutation. *BMJ Case Rep* 2013, jan22 1: bcr2012007929, 2013. doi:10.1136/bcr-2012-007929.

152. Cuddapah VA, Habela CW, Watkins S, Moore LS, Barclay TT, Sontheimer H. Kinase activation of ClC-3 accelerates cytoplasmic condensation during mitotic cell rounding. *Am J Physiol Cell Physiol* 302: C527–C538, 2012. doi:10.1152/ajpcell.00248.2011.

153. Cuddapah VA, Sontheimer H. Molecular interaction and functional regulation of ClC-3 by Ca^{2+}/calmodulin-dependent protein kinase II (CaMKII) in human malignant glioma. *J Biol Chem* 285: 11188–11196, 2010. doi:10.1074/jbc.M109.097675.

154. Cuddapah VA, Turner KL, Seifert S, Sontheimer H. Bradykinin-induced chemotaxis of human gliomas requires the activation of KCa3.1 and ClC-3. *J Neurosci* 33: 1427–1440, 2013. doi:10.1523/JNEUROSCI.3980-12.2013.

155. Cunningham R, Biswas R, Steplock D, Shenolikar S, Weinman E. Role of NHERF and scaffolding proteins in proximal tubule transport. *Urol Res* 38: 257–262, 2010. doi:10.1007/s00240-010-0294-1.

156. Cunningham R, Esmaili A, Brown E, Biswas RS, Murtazina R, Donowitz M, Dijkman HB, van der Vlag J, Hogema BM, De Jonge HR, Shenolikar S, Wade JB, Weinman EJ. Urine electrolyte, mineral, and protein excretion in NHERF-2 and NHERF-1 null mice. *Am J Physiol Renal Physiol* 294: F1001–F1007, 2008. doi:10.1152/ajprenal.00504.2007.

157. Cuppoletti J, Baker AM, Malinowska DH. Cl^- channels of the gastric parietal cell that are active at low pH. *Am J Physiol Cell Physiol* 264: C1609–C1618, 1993. doi:10.1152/ajpcell.1993.264.6.C1609.

158. Cuppoletti J, Malinowska DH, Tewari KP, Li QJ, Sherry AM, Patchen ML, Ueno R. SPI-0211 activates T84 cell chloride transport and recombinant human ClC-2 chloride currents. *Am J Physiol Cell Physiol* 287: C1173–C1183, 2004. doi:10.1152/ajpcell.00528.2003.

159. Cuthbert AW. Lubiprostone targets prostanoid EP_4 receptors in ovine airways. *Br J Pharmacol* 162: 508–520, 2011. doi:10.1111/j.1476-5381.2010.01058.x.

160. D'Agostino D, Bertelli M, Gallo S, Cecchin S, Albiero E, Garofalo PG, Gambardella A, St Hilaire JM, Kwiecinski H, Andermann E, Pandolfo M. Mutations and polymorphisms of the *CLCN2* gene in idiopathic epilepsy. *Neurology* 63: 1500–1502, 2004. doi:10.1212/01.WNL.0000142093.94998.1A.

161. D'Antonio C, Molinski S, Ahmadi S, Huan LJ, Wellhauser L, Bear CE. Conformational defects underlie proteasomal degradation of Dent's disease-causing mutants of ClC-5. *Biochem J* 452: 391–400, 2013. doi:10.1042/BJ20121848.

162. Dave S, Sheehan JH, Meiler J, Strange K. Unique gating properties of *C. elegans* ClC anion channel splice variants are determined by altered CBS domain conformation and the R-helix linker. *Channels (Austin)* 4: 289–301, 2010. doi:10.4161/chan.4.4.12445.

163. Davis-Kaplan SR, Askwith CC, Bengtzen AC, Radisky D, Kaplan J. Chloride is an allosteric effector of copper assembly for the yeast multicopper oxidase Fet3p: an unexpected role for intracellular chloride channels. *Proc Natl Acad Sci USA* 95: 13641–13645, 1998. doi:10.1073/pnas.95.23.13641.

164. De Angeli A, Monachello D, Ephritikhine G, Frachisse JM, Thomine S, Gambale F, Barbier-Brygoo H. The nitrate/proton antiporter AtCLCa mediates nitrate accumulation in plant vacuoles. *Nature* 442: 939–942, 2006. doi:10.1038/nature05013.

165. De Angeli A, Monachello D, Ephritikhine G, Frachisse JM, Thomine S, Gambale F, Barbier-Brygoo H. Review. CLC-mediated anion transport in plant cells. *Philos Trans R Soc Lond B Biol Sci* 364: 195–201, 2009. doi:10.1098/rstb.2008.0128.

166. De Jesús-Pérez JJ, Castro-Chong A, Shieh RC, Hernández-Carballo CY, De Santiago-Castillo JA, Arreola J. Gating the glutamate gate of CLC-2 chloride channel by pore occupancy. *J Gen Physiol* 147: 25–37, 2016. doi:10.1085/jgp.201511424.

167. De la Fuente-Ortega E, Gravotta D, Perez Bay A, Benedicto I, Carvajal-Gonzalez JM, Lehmann GL, Lagos CF, Rodríguez-Boulan E. Basolateral sorting of chloride channel 2 is mediated by interactions between a dileucine motif and the clathrin adaptor AP-1. *Mol Biol Cell* 26: 1728–1742, 2015. doi:10.1091/mbc.E15-01-0047.

168. De Leo MG, Staiano L, Vicinanza M, Luciani A, Carissimo A, Mutarelli M, Di Campli A, Polishchuk E, Di Tullio G, Morra V, Levtchenko E, Oltrabella F, Starborg T, Santoro M, Di Bernardo D, Devuyst O, Lowe M, Medina DL, Ballabio A, De Matteis MA. Autophagosome-lysosome fusion triggers a lysosomal response mediated by TLR9 and controlled by OCRL. *Nat Cell Biol* 18: 839–850, 2016. doi:10.1038/ncb3386.

169. De Lisle RC, Mueller R, Roach E. Lubiprostone ameliorates the cystic fibrosis mouse intestinal phenotype. *BMC Gastroenterol* 10: 107, 2010. doi:10.1186/1471-230X-10-107.

170. De Luca A, Pierno S, Camerino DC. Effect of taurine depletion on excitation-contraction coupling and Cl^- conductance of rat skeletal muscle. *Eur J Pharmacol* 296: 215–222, 1996. doi:10.1016/0014-2999(95)00702-4.

171. De Luca A, Pierno S, Camerino DC. Taurine: the appeal of a safe amino acid for skeletal muscle disorders. *J Transl Med* 13: 243, 2015. doi:10.1186/s12967-015-0610-1.

172. De Luca A, Pierno S, Liantonio A, Camerino C, Conte Camerino D. Phosphorylation and IGF-1-mediated dephosphorylation pathways control the activity and the pharmacological properties of skeletal muscle chloride channels. *Br J Pharmacol* 125: 477–482, 1998. doi:10.1038/sj.bjp.0702107.

173. De Luca A, Tricarico D, Pierno S, Conte Camerino D. Aging and chloride channel regulation in rat fast-twitch muscle fibres. *Pflugers Arch* 427: 80–85, 1994. doi:10.1007/BF00585945.

174. De Luca A, Tricarico D, Wagner R, Bryant SH, Tortorella V, Conte Camerino D. Opposite effects of enantiomers of clofibric acid derivative on rat skeletal muscle chloride conductance: antagonism studies and theoretical modeling of two different receptor site interactions. *J Pharmacol Exp Ther* 260: 364–368, 1992.

175. De Matteis MA, Staiano L, Emma F, Devuyst O. The 5-phosphatase OCRL in Lowe syndrome and Dent disease 2. *Nat Rev Nephrol* 13: 455–470, 2017. doi:10.1038/nrneph.2017.83.

176. De Paoli FV, Broch-Lips M, Pedersen TH, Nielsen OB. Relationship between membrane Cl^- conductance and contractile endurance in isolated rat muscles. *J Physiol* 591: 531–545, 2013. doi:10.1113/jphysiol.2012.243246.

177. De Paoli FV, Ørtenblad N, Pedersen TH, Jørgensen R, Nielsen OB. Lactate per se improves the excitability of depolarized rat skeletal muscle by reducing the Cl^- conductance. *J Physiol* 588: 4785–4794, 2010. doi:10.1113/jphysiol.2010.196568.

178. De Santiago JA, Nehrke K, Arreola J. Quantitative analysis of the voltage-dependent gating of mouse parotid ClC-2 chloride channel. *J Gen Physiol* 126: 591–603, 2005. doi:10.1085/jgp.200509310.

179. De Stefano S, Pusch M, Zifarelli G. Extracellular determinants of anion discrimination of the Cl^-/H^+ antiporter protein CLC-5. *J Biol Chem* 286: 44134–44144, 2011. doi:10.1074/jbc.M111.272815.

180. De Stefano S, Pusch M, Zifarelli G. A single point mutation reveals gating of the human ClC-5 Cl^-/H^+ antiporter. *J Physiol* 591: 5879–5893, 2013. doi:10.1113/jphysiol.2013.260240.

181. Del Fattore A, Peruzzi B, Rucci N, Recchia I, Cappariello A, Longo M, Fortunati D, Ballanti P, Iacobini M, Luciani M, Devito R, Pinto R, Caniglia M, Lanino E, Messina C, Cesaro S, Letizia C, Bianchini G, Fryssira H, Grabowski P, Shaw N, Bishop N, Hughes D, Kapur RP, Datta HK, Taranta A, Fornari R, Migliaccio S, Teti A. Clinical, genetic, and cellular analysis of 49 osteopetrotic patients: implications for diagnosis and treatment. *J Med Genet* 43: 315–325, 2006. doi:10.1136/jmg.2005.036673.

182. Delpire E, Lu J, England R, Dull C, Thorne T. Deafness and imbalance associated with inactivation of the secretory Na-K-2Cl co-transporter. *Nat Genet* 22: 192–195, 1999. doi:10.1038/9713.

183. Deng H, He D, Rong P, Xu H, Yuan L, Li L, Lu Q, Guo Y. Novel *CLCN7* mutation identified in a Han Chinese family with autosomal dominant osteopetrosis-2. *Mol Pain* 12: 1–7, 2016. doi:10.1177/1744806916652628.

184. Dent CE, Friedman M. Hypercalcuric Rickets Associated with Renal Tubular Damage. *Arch Dis Child* 39: 240–249, 1964. doi:10.1136/adc.39.205.240.

185. Denton J, Nehrke K, Rutledge E, Morrison R, Strange K. Alternative splicing of N- and C-termini of a *C. elegans* ClC channel alters gating and sensitivity to external Cl^- and H^+. *J Physiol* 555: 97–114, 2004. doi:10.1113/jphysiol.2003.053165.

186. Denton J, Nehrke K, Yin X, Morrison R, Strange K. GCK-3, a newly identified Ste20 kinase, binds to and regulates the activity of a cell cycle-dependent ClC anion channel. *J Gen Physiol* 125: 113–125, 2005. doi:10.1085/jgp.200409215.

187. Depienne C, Bugiani M, Dupuits C, Galanaud D, Touitou V, Postma N, van Berkel C, Polder E, Tollard E, Darios F, Brice A, de Die-Smulders CE, Vles JS, Vanderver A, Uziel G, Yalcinkaya C, Frints SG, Kalscheuer VM, Klooster J, Kamermans M, Abbink TE, Wolf NI, Sedel F, van der Knaap MS. Brain white matter oedema due to ClC-2 chloride channel deficiency: an observational analytical study. *Lancet Neurol* 12: 659–668, 2013. doi:10.1016/S1474-4422(13)70053-X.

188. Deriy LV, Gomez EA, Jacobson DA, Wang X, Hopson JA, Liu XY, Zhang G, Bindokas VP, Philipson LH, Nelson DJ. The granular chloride channel ClC-3 is permissive for insulin secretion. *Cell Metab* 10: 316–323, 2009. doi:10.1016/j.cmet.2009.08.012.

189. Desaphy JF, Gramegna G, Altamura C, Dinardo MM, Imbrici P, George AL Jr, Modoni A, Lomonaco M, Conte Camerino D. Functional characterization of ClC-1 mutations from patients affected by recessive myotonia congenita presenting with different clinical phenotypes. *Exp Neurol* 248: 530–540, 2013. doi:10.1016/j.expneurol.2013.07.018.

190. Devuyst O, Christie PT, Courtoy PJ, Beauwens R, Thakker RV. Intra-renal and subcellular distribution of the human chloride channel, CLC-5, reveals a pathophysiological basis for Dent's disease. *Hum Mol Genet* 8: 247–257, 1999. doi:10.1093/hmg/8.2.247.

191. Devuyst O, Thakker RV. Dent's disease. *Orphanet J Rare Dis* 5: 28, 2010. doi:10.1186/1750-1172-5-28.

192. Dhani SU, Mohammad-Panah R, Ahmed N, Ackerley C, Ramjeesingh M, Bear CE. Evidence for a functional interaction between the ClC-2 chloride channel and the retrograde motor dynein complex. *J Biol Chem* 278: 16262–16270, 2003. doi:10.1074/jbc.M209828200.

193. Di Bella D, Pareyson D, Savoiardo M, Farina L, Ciano C, Caldarazzo S, Sagnelli A, Bonato S, Nava S, Bresolin N, Tedeschi G, Taroni F, Salsano E. Subclinical leukodystrophy and infertility in a man with a novel homozygous *CLCN2* mutation. *Neurology* 83: 1217–1218, 2014. doi:10.1212/WNL.0000000000000812.

194. Dickerson LW, Bonthius DJ, Schutte BC, Yang B, Barna TJ, Bailey MC, Nehrke K, Williamson RA, Lamb FS. Altered GABAergic function accompanies hippocampal degeneration in mice lacking ClC-3 voltage-gated chloride channels. *Brain Res* 958: 227–250, 2002. doi:10.1016/S0006-8993(02)03519-9.

195. Diewald L, Rupp J, Dreger M, Hucho F, Gillen C, Nawrath H. Activation by acidic pH of CLC-7 expressed in oocytes from *Xenopus laevis*. *Biochem Biophys Res Commun* 291: 421–424, 2002. doi:10.1006/bbrc.2002.6462.

196. DiFranco M, Herrera A, Vergara JL. Chloride currents from the transverse tubular system in adult mammalian skeletal muscle fibers. *J Gen Physiol* 137: 21–41, 2011. doi:10.1085/jgp.201010496.

197. Dinudom A, Young JA, Cook DI. Na^+ and Cl^- conductances are controlled by cytosolic Cl^- concentration in the intralobular duct cells of mouse mandibular glands. *J Membr Biol* 135: 289–295, 1993. doi:10.1007/BF00211100.

198. Dixon MJ, Gazzard J, Chaudhry SS, Sampson N, Schulte BA, Steel KP. Mutation of the Na-K-Cl co-transporter gene *Slc12a2* results in deafness in mice. *Hum Mol Genet* 8: 1579–1584, 1999. doi:10.1093/hmg/8.8.1579.

199. Dowland LK, Luyckx VA, Enck AH, Leclercq B, Yu AS. Molecular cloning and characterization of an intracellular chloride channel in the proximal tubule cell line, LLC-PK1. *J Biol Chem* 275: 37765–37773, 2000. doi:10.1074/jbc.M004840200.

200. Doyle DA, Morais Cabral J, Pfuetzner RA, Kuo A, Gulbis JM, Cohen SL, Chait BT, MacKinnon R. The structure of the potassium channel: molecular basis of K^+ conduction and selectivity. *Science* 280: 69–77, 1998. doi:10.1126/science.280.5360.69.

201. Doyon N, Vinay L, Prescott SA, De Koninck Y. Chloride Regulation: A Dynamic Equilibrium Crucial for Synaptic Inhibition. *Neuron* 89: 1157–1172, 2016. doi:10.1016/j.neuron.2016.02.030.

202. Duan D, Cowley S, Horowitz B, Hume JR. A serine residue in ClC-3 links phosphorylation-dephosphorylation to chloride channel regulation by cell volume. *J Gen Physiol* 113: 57–70, 1999. doi:10.1085/jgp.113.1.57.

203. Duan D, Winter C, Cowley S, Hume JR, Horowitz B. Molecular identification of a volume-regulated chloride channel. *Nature* 390: 417–421, 1997. doi:10.1038/37151.

204. Dubey M, Bugiani M, Ridder MC, Postma NL, Brouwers E, Polder E, Jacobs JG, Baayen JC, Klooster J, Kamermans M, Aardse R, de Kock CP, Dekker MP, van Weering JR, Heine VM, Abbink TE, Scheper GC, Boor I, Lodder JC, Mansvelder HD, van der Knaap MS. Mice with megalencephalic leukoencephalopathy with cysts: a developmental angle. *Ann Neurol* 77: 114–131, 2015. doi:10.1002/ana.24307.

205. Duffield M, Rychkov G, Bretag A, Roberts M. Involvement of helices at the dimer interface in ClC-1 common gating. *J Gen Physiol* 121: 149–161, 2003. doi:10.1085/jgp.20028741.

206. Duffield MD, Rychkov GY, Bretag AH, Roberts ML. Zinc inhibits human ClC-1 muscle chloride channel by interacting with its common gating mechanism. *J Physiol* 568: 5–12, 2005. doi:10.1113/jphysiol.2005.091777.

207. Duran C, Thompson CH, Xiao Q, Hartzell HC. Chloride channels: often enigmatic, rarely predictable. *Annu Rev Physiol* 72: 95–121, 2010. doi:10.1146/annurev-physiol-021909-135811.

208. Dutka TL, Murphy RM, Stephenson DG, Lamb GD. Chloride conductance in the transverse tubular system of rat skeletal muscle fibres: importance in excitation-contraction coupling and fatigue. *J Physiol* 586: 875–887, 2008. doi:10.1113/jphysiol.2007.144667.

209. Dutzler R. The structural basis of ClC chloride channel function. *Trends Neurosci* 27: 315–320, 2004. doi:10.1016/j.tins.2004.04.001.

210. Dutzler R, Campbell EB, Cadene M, Chait BT, MacKinnon R. X-ray structure of a ClC chloride channel at 3.0 A reveals the molecular basis of anion selectivity. *Nature* 415: 287–294, 2002. doi:10.1038/415287a.

211. Dutzler R, Campbell EB, MacKinnon R. Gating the selectivity filter in ClC chloride channels. *Science* 300: 108–112, 2003. doi:10.1126/science.1082708.

212. Edwards MM, Marín de Evsikova C, Collin GB, Gifford E, Wu J, Hicks WL, Whiting C, Varvel NH, Maphis N, Lamb BT, Naggert JK, Nishina PM, Peachey NS. Photoreceptor degeneration, azoospermia, leukoencephalopathy, and abnormal RPE cell function in mice expressing an early stop mutation in *CLCN2*. *Invest Ophthalmol Vis Sci* 51: 3264–3272, 2010. doi:10.1167/iovs.09-4887.

213. Eggermont J, Buyse G, Voets T, Tytgat J, De Smedt H, Droogmans G, Nilius B. Alternative splicing of ClC-6 (a member of the ClC chloride-channel family) transcripts generates three truncated isoforms one of which, ClC-6c, is kidney-specific. *Biochem J* 325: 269–276, 1997. doi:10.1042/bj3250269.

214. Einbond A, Sudol M. Towards prediction of cognate complexes between the WW domain and proline-rich ligands. *FEBS Lett* 384: 1–8, 1996. doi:10.1016/0014-5793(96)00263-3.

215. Ellis NA. *Ecce* Ohno! *Nat Genet* 10: 373–375, 1995. doi:10.1038/ng0895-373.

216. Elvington SM, Liu CW, Maduke MC. Substrate-driven conformational changes in ClC-ec1 observed by fluorine NMR. *EMBO J* 28: 3090–3102, 2009. doi:10.1038/emboj.2009.259.

217. Embark HM, Böhmer C, Palmada M, Rajamanickam J, Wyatt AW, Wallisch S, Capasso G, Waldegger P, Seyberth HW, Waldegger S, Lang F. Regulation of CLC-Ka/barttin by the ubiquitin ligase Nedd4-2 and the serum- and glucocorticoid-dependent kinases. *Kidney Int* 66: 1918–1925, 2004. doi:10.1111/j.1523-1755.2004.00966.x.

218. Engh AM, Faraldo-Gómez JD, Maduke M. The mechanism of fast-gate opening in ClC-0. *J Gen Physiol* 130: 335–349, 2007. doi:10.1085/jgp.200709759.

219. Engh AM, Maduke M. Cysteine accessibility in ClC-0 supports conservation of the ClC intracellular vestibule. *J Gen Physiol* 125: 601–617, 2005. doi:10.1085/jgp.200509258.

220. Enríquez R, Adam V, Sirvent AE, García-García AB, Millán I, Amorós F. Gitelman syndrome due to p.A204T mutation in *CLCNKB* gene. *Int Urol Nephrol* 42: 1099–1102, 2010. doi:10.1007/s11255-010-9850-4.

221. Enz R, Ross BJ, Cutting GR. Expression of the voltage-gated chloride channel ClC-2 in rod bipolar cells of the rat retina. *J Neurosci* 19: 9841–9847, 1999. doi:10.1523/JNEUROSCI.19-22-09841.1999.

222. Estévez R, Boettger T, Stein V, Birkenhäger R, Otto E, Hildebrandt F, Jentsch TJ. Barttin is a Cl^- channel β-subunit crucial for renal Cl^- reabsorption and inner ear K^+ secretion. *Nature* 414: 558–561, 2001. doi:10.1038/35107099.

223. Estévez R, Pusch M, Ferrer-Costa C, Orozco M, Jentsch TJ. Functional and structural conservation of CBS domains from CLC chloride channels. *J Physiol* 557: 363–378, 2004. doi:10.1113/jphysiol.2003.058453.

224. Estévez R, Schroeder BC, Accardi A, Jentsch TJ, Pusch M. Conservation of chloride channel structure revealed by an inhibitor binding site in ClC-1. *Neuron* 38: 47–59, 2003. doi:10.1016/S0896-6273(03)00168-5.

225. Everett K, Chioza B, Aicardi J, Aschauer H, Brouwer O, Callenbach P, Covanis A, Dooley J, Dulac O, Durner M, Eeg-Olofsson O, Feucht M, Friis M, Guerrini R, Heils A, Kjeldsen M, Nabbout R, Sander T, Wirrell E, McKeigue P, Robinson R, Taske N, Gardiner M. Linkage and mutational analysis of *CLCN2* in childhood absence epilepsy. *Epilepsy Res* 75: 145–153, 2007. doi:10.1016/j.eplepsyres.2007.05.004.

226. Fahlke C. Chloride channels take center stage in a muscular drama. *J Gen Physiol* 137: 17–19, 2011. doi:10.1085/jgp.201010574.

227. Fahlke C, Beck CL, George AL Jr. A mutation in autosomal dominant myotonia congenita affects pore properties of the muscle chloride channel. *Proc Natl Acad Sci USA* 94: 2729–2734, 1997. doi:10.1073/pnas.94.6.2729.

228. Fahlke C, Desai RR, Gillani N, George AL Jr. Residues lining the inner pore vestibule of human muscle chloride channels. *J Biol Chem* 276: 1759–1765, 2001. doi:10.1074/jbc.M007649200.

229. Fahlke C, Fischer M. Physiology and pathophysiology of ClC-K/barttin channels. *Front Physiol* 1: 155, 2010. doi:10.3389/fphys.2010.00155.

230. Fahlke C, Knittle T, Gurnett CA, Campbell KP, George AL Jr. Subunit stoichiometry of human muscle chloride channels. *J Gen Physiol* 109: 93–104, 1997. doi:10.1085/jgp.109.1.93.

231. Fahlke C, Rhodes TH, Desai RR, George AL Jr. Pore stoichiometry of a voltage-gated chloride channel. *Nature* 394: 687–690, 1998. doi:10.1038/29319.

232. Fahlke C, Rosenbohm A, Mitrovic N, George AL Jr, Rüdel R. Mechanism of voltage-dependent gating in skeletal muscle chloride channels. *Biophys J* 71: 695–706, 1996. doi:10.1016/S0006-3495(96)79269-X.

233. Fahlke C, Rüdel R, Mitrovic N, Zhou M, George AL Jr. An aspartic acid residue important for voltage-dependent gating of human muscle chloride channels. *Neuron* 15: 463–472, 1995. doi:10.1016/0896-6273(95)90050-0.

234. Fahlke C, Yu HT, Beck CL, Rhodes TH, George AL Jr. Pore-forming segments in voltage-gated chloride channels. *Nature* 390: 529–532, 1997. doi:10.1038/37391.

235. Falin RA, Morrison R, Ham AJ, Strange K. Identification of regulatory phosphorylation sites in a cell volume- and Ste20 kinase-dependent ClC anion channel. *J Gen Physiol* 133: 29–42, 2009. doi:10.1085/jgp.200810080.

236. Faraldo-Gómez JD, Roux B. Electrostatics of ion stabilization in a ClC chloride channel homologue from *Escherichia coli*. *J Mol Biol* 339: 981–1000, 2004. doi:10.1016/j.jmb.2004.04.023.

237. Farmer LM, Le BN, Nelson DJ. CLC-3 chloride channels moderate long-term potentiation at Schaffer collateral-CA1 synapses. *J Physiol* 591: 1001–1015, 2013. doi:10.1113/jphysiol.2012.243485.

238. Fava C, Montagnana M, Almgren P, Rosberg L, Guidi GC, Berglund G, Melander O. The functional variant of the CLC-Kb channel T481S is not associated with blood pressure or hypertension in Swedes. *J Hypertens* 25: 111–116, 2007. doi:10.1097/HJH.0b013e3280103a5a.

239. Fava M, Ferroni S, Nobile M. Osmosensitivity of an inwardly rectifying chloride current revealed by whole-cell and perforated-patch recordings in cultured rat cortical astrocytes. *FEBS Lett* 492: 78–83, 2001. doi:10.1016/S0014-5793(01)02221-9.

240. Favre-Kontula L, Rolland A, Bernasconi L, Karmirantzou M, Power C, Antonsson B, Boschert U. GlialCAM, an immunoglobulin-like cell adhesion molecule is expressed in glial cells of the central nervous system. *Glia* 56: 633–645, 2008. doi:10.1002/glia.20640.

241. Feigin ME, Malbon CC. OSTM1 regulates β-catenin/Lef1 interaction and is required for Wnt/β-catenin signaling. *Cell Signal* 20: 949–957, 2008. doi:10.1016/j.cellsig.2008.01.009.

242. Feng L, Campbell EB, Hsiung Y, MacKinnon R. Structure of a eukaryotic CLC transporter defines an intermediate state in the transport cycle. *Science* 330: 635–641, 2010. doi:10.1126/science.1195230.

243. Feng L, Campbell EB, MacKinnon R. Molecular mechanism of proton transport in CLC Cl^-/H^+ exchange transporters. *Proc Natl Acad Sci USA* 109: 11699–11704, 2012. doi:10.1073/pnas.1205764109.

244. Fenton RA, Knepper MA. Mouse models and the urinary concentrating mechanism in the new millennium. *Physiol Rev* 87: 1083–1112, 2007. doi:10.1152/physrev.00053.2006.

245. Fernandes-Rosa FL, Boulkroun S, Zennaro MC. Somatic and inherited mutations in primary aldosteronism. *J Mol Endocrinol* 59: R47–R63, 2017. doi:10.1530/JME-17-0035.

246. Fernandes-Rosa FL, Daniil G, Orozco IJ, Göppner C, El Zein R, Jain V, Boulkroun S, Jeunemaitre X, Amar L, Lefebvre H, Schwarzmayr T, Strom TM, Jentsch TJ, Zennaro MC. A gain-of-function mutation in the *CLCN2* chloride channel gene causes primary aldosteronism. *Nat Genet* 50: 355–361, 2018. doi:10.1038/s41588-018-0053-8.

247. Ferroni S, Marchini C, Nobile M, Rapisarda C. Characterization of an inwardly rectifying chloride conductance expressed by cultured rat cortical astrocytes. *Glia* 21: 217–227, 1997. doi:10.1002/(SICI)1098-1136(199710)21:2<217::AID-GLIA5>3.0.CO;2-3.

248. Finnigan DF, Hanna WJ, Poma R, Bendall AJ. A novel mutation of the *CLCN1* gene associated with myotonia hereditaria in an Australian cattle dog. *J Vet Intern Med* 21: 458–463, 2007. doi:10.1111/j.1939-1676.2007.tb02990.x.

249. Fischer M, Janssen AG, Fahlke C. Barttin activates ClC-K channel function by modulating gating. *J Am Soc Nephrol* 21: 1281–1289, 2010. doi:10.1681/ASN.2009121274.

250. Fischer T, De Vries L, Meerloo T, Farquhar MG. Promotion of G α i3 subunit down-regulation by GIPN, a putative E3 ubiquitin ligase that interacts with RGS-GAIP. *Proc Natl Acad Sci USA* 100: 8270–8275, 2003. doi:10.1073/pnas.1432965100.

251. Fisher SE, Black GC, Lloyd SE, Hatchwell E, Wrong O, Thakker RV, Craig IW. Isolation and partial characterization of a chloride channel gene which is expressed in kidney and is a candidate for Dent's disease (an X-linked hereditary nephrolithiasis). *Hum Mol Genet* 3: 2053–2059, 1994.

252. Fisher SE, van Bakel I, Lloyd SE, Pearce SH, Thakker RV, Craig IW. Cloning and characterization of *CLCN5*, the human kidney chloride channel gene implicated in Dent disease (an X-linked hereditary nephrolithiasis). *Genomics* 29: 598–606, 1995. doi:10.1006/geno.1995.9960.

253. Flagella M, Clarke LL, Miller ML, Erway LC, Giannella RA, Andringa A, Gawenis LR, Kramer J, Duffy JJ, Doetschman T, Lorenz JN, Yamoah EN, Cardell EL, Shull GE. Mice

lacking the basolateral Na-K-2Cl cotransporter have impaired epithelial chloride secretion and are profoundly deaf. *J Biol Chem* 274: 26946–26955, 1999. doi:10.1074/jbc.274.38.26946.

254. Flis K, Hinzpeter A, Edelman A, Kurlandzka A. The functioning of mammalian ClC-2 chloride channel in *Saccharomyces cerevisiae* cells requires an increased level of Kha1p. *Biochem J* 390: 655–664, 2005. doi:10.1042/BJ20050480.

255. Flores CA. ClC-2 and intestinal chloride secretion. *Am J Physiol Gastrointest Liver Physiol* 311: G775, 2016. doi:10.1152/ajpgi.00310.2016.

256. Földy C, Lee SH, Morgan RJ, Soltesz I. Regulation of fast-spiking basket cell synapses by the chloride channel ClC-2. *Nat Neurosci* 13: 1047–1049, 2010. doi:10.1038/nn.2609.

257. Fong P. CLC-K channels: if the drug fits, use it. *EMBO Rep* 5: 565–566, 2004. doi:10.1038/sj.embor.7400168.

258. Fong P. Thyroid iodide efflux: a team effort? *J Physiol* 589: 5929–5939, 2011. doi:10.1113/jphysiol.2011.218594.

259. Fong P, Rehfeldt A, Jentsch TJ. Determinants of slow gating in ClC-0, the voltage-gated chloride channel of *Torpedo marmorata*. *Am J Physiol Cell Physiol* 274: C966–C973, 1998. doi:10.1152/ajpcell.1998.274.4.C966.

260. Foote JR, Behe P, Frampton M, Levine AP, Segal AW. An Exploration of Charge Compensating Ion Channels across the Phagocytic Vacuole of Neutrophils. *Front Pharmacol* 8: 94, 2017. doi:10.3389/fphar.2017.00094.

261. Forino M, Graziotto R, Tosetto E, Gambaro G, D'Angelo A, Anglani F. Identification of a novel splice site mutation of *CLCN5* gene and characterization of a new alternative 5′ UTR end of ClC-5 mRNA in human renal tissue and leukocytes. *J Hum Genet* 49: 53–60, 2004. doi:10.1007/s10038-003-0108-1.

262. Forrest LR. Structural Symmetry in Membrane Proteins. *Annu Rev Biophys* 44: 311–337, 2015. doi:10.1146/annurev-biophys-051013-023008.

263. Fox GQ, Richardson GP. The developmental morphology of *Torpedo marmorata*: electric organ–electrogenic phase. *J Comp Neurol* 185: 293–315, 1979. doi:10.1002/cne.901850205.

264. Fox GQ, Richardson GP. The developmental morphology of *Torpedo marmorata*: electric organ–myogenic phase. *J Comp Neurol* 179: 677–697, 1978. doi:10.1002/cne.901790313.

265. Fraser JA, Huang CL, Pedersen TH. Relationships between resting conductances, excitability, and t-system ionic homeostasis in skeletal muscle. *J Gen Physiol* 138: 95–116, 2011. doi:10.1085/jgp.201110617.

266. Frattini A, Orchard PJ, Sobacchi C, Giliani S, Abinun M, Mattsson JP, Keeling DJ, Andersson AK, Wallbrandt P, Zecca L, Notarangelo LD, Vezzoni P, Villa A. Defects in TCIRG1 subunit of the vacuolar proton pump are responsible for a subset of human autosomal recessive osteopetrosis. *Nat Genet* 25: 343–346, 2000. doi:10.1038/77131.

267. Frattini A, Pangrazio A, Susani L, Sobacchi C, Mirolo M, Abinun M, Andolina M, Flanagan A, Horwitz EM, Mihci E, Notarangelo LD, Ramenghi U, Teti A, Van Hove J, Vujic D, Young T, Albertini A, Orchard PJ, Vezzoni P, Villa A. Chloride channel *CICN7* mutations are responsible for severe recessive, dominant, and intermediate osteopetrosis. *J Bone Miner Res* 18: 1740–1747, 2003. doi:10.1359/jbmr.2003.18.10.1740.

268. Frey A, Lampert A, Waldegger S, Jeck N, Waldegger P, Artunc F, Seebohm G, Lang UE, Kupka S, Pfister M, Hoppe J, Gerloff C, Schaeffeler E, Schwab M, Lang F. Influence of gain of function epithelial chloride channel ClC-Kb mutation on hearing thresholds. *Hear Res* 214: 68–75, 2006. doi:10.1016/j.heares.2006.02.001.

269. Friedrich T, Breiderhoff T, Jentsch TJ. Mutational analysis demonstrates that ClC-4 and ClC-5 directly mediate plasma membrane currents. *J Biol Chem* 274: 896–902, 1999. doi:10.1074/jbc.274.2.896.

270. Frishberg Y, Dinour D, Belostotsky R, Becker-Cohen R, Rinat C, Feinstein S, Navon-Elkan P, Ben-Shalom E. Dent's disease manifesting as focal glomerulosclerosis: is it the tip of the iceberg? *Pediatr Nephrol* 24: 2369–2373, 2009. doi:10.1007/s00467-009-1299-2.

271. Fritsch J, Edelman A. Modulation of the hyperpolarization-activated Cl^- current in human intestinal T84 epithelial cells by phosphorylation. *J Physiol* 490: 115–128, 1996. doi:10.1113/jphysiol.1996.sp021130.

272. Fukuyama S, Hiramatsu M, Akagi M, Higa M, Ohta T. Novel mutations of the chloride channel Kb gene in two Japanese patients clinically diagnosed as Bartter syndrome with hypocalciuria. *J Clin Endocrinol Metab* 89: 5847–5850, 2004. doi:10.1210/jc.2004-0775.

273. Fukuyama S, Okudaira S, Yamazato S, Yamazato M, Ohta T. Analysis of renal tubular electrolyte transporter genes in seven patients with hypokalemic metabolic alkalosis. *Kidney Int* 64: 808–816, 2003. doi:10.1046/j.1523-1755.2003.00163.x.

274. Furman RE, Barchi RL. The pathophysiology of myotonia produced by aromatic carboxylic acids. *Ann Neurol* 4: 357–365, 1978. doi:10.1002/ana.410040411.

275. Furukawa T, Ogura T, Katayama Y, Hiraoka M. Characteristics of rabbit ClC-2 current expressed in *Xenopus* oocytes and its contribution to volume regulation. *Am J Physiol Cell Physiol* 274: C500–C512, 1998. doi:10.1152/ajpcell.1998.274.2.C500.

276. Furukawa T, Ogura T, Zheng YJ, Tsuchiya H, Nakaya H, Katayama Y, Inagaki N. Phosphorylation and functional regulation of ClC-2 chloride channels expressed in *Xenopus* oocytes by M cyclin-dependent protein kinase. *J Physiol* 540: 883–893, 2002. doi:10.1113/jphysiol.2001.016188.

277. Gadsby DC. Ion channels versus ion pumps: the principal difference, in principle. *Nat Rev Mol Cell Biol* 10: 344–352, 2009. doi:10.1038/nrm2668.

278. Gailly P, Jouret F, Martin D, Debaix H, Parreira KS, Nishita T, Blanchard A, Antignac C, Willnow TE, Courtoy PJ, Scheinman SJ, Christensen EI, Devuyst O. A novel renal carbonic anhydrase type III plays a role in proximal tubule dysfunction. *Kidney Int* 74: 52–61, 2008. doi:10.1038/sj.ki.5002794.

279. Ganapathi SB, Wei SG, Zaremba A, Lamb FS, Shears SB. Functional regulation of ClC-3 in the migration of vascular smooth muscle cells. *Hypertension* 61: 174–179, 2013. doi:10.1161/HYPERTENSIONAHA.112.194209.

280. García-Olivares J, Alekov A, Boroumand MR, Begemann B, Hidalgo P, Fahlke C. Gating of human ClC-2 chloride channels and regulation by carboxy-terminal domains. *J Physiol* 586: 5325–5336, 2008. doi:10.1113/jphysiol.2008.158097.

281. Gaxiola RA, Rao R, Sherman A, Grisafi P, Alper SL, Fink GR. The *Arabidopsis thaliana* proton transporters, AtNhx1 and Avp1, can function in cation detoxification in yeast. *Proc Natl Acad Sci USA* 96: 1480–1485, 1999. doi:10.1073/pnas.96.4.1480.

282. Gaxiola RA, Yuan DS, Klausner RD, Fink GR. The yeast CLC chloride channel functions in cation homeostasis. *Proc Natl Acad Sci USA* 95: 4046–4050, 1998. doi:10.1073/pnas.95.7.4046.

283. Geelen D, Lurin C, Bouchez D, Frachisse JM, Lelièvre F, Courtial B, Barbier-Brygoo H, Maurel C. Disruption of putative anion channel gene AtCLC-a in *Arabidopsis* suggests a role in the regulation of nitrate content. *Plant J* 21: 259–267, 2000. doi:10.1046/j.1365-313x.2000.00680.x.

284. Gekle M, Mildenberger S, Freudinger R, Silbernagl S. Endosomal alkalinization reduces J_{max} and K_m of albumin receptor-mediated endocytosis in OK cells. *Am J Physiol Renal Fluid Electrolyte Physiol* 268: F899–F906, 1995.

285. Gekle M, Völker K, Mildenberger S, Freudinger R, Shull GE, Wiemann M. NHE3 Na^+/H^+ exchanger supports proximal tubular protein reabsorption *in vivo*. *Am J Physiol Renal Physiol* 287: F469–F473, 2004. doi:10.1152/ajprenal.00059.2004.

286. Gentzsch M, Cui L, Mengos A, Chang XB, Chen JH, Riordan JR. The PDZ-binding chloride channel ClC-3B localizes to the Golgi and associates with cystic fibrosis transmembrane conductance regulator-interacting PDZ proteins. *J Biol Chem* 278: 6440–6449, 2003. doi:10.1074/jbc.M211050200.

287. George AL Jr, Sloan-Brown K, Fenichel GM, Mitchell GA, Spiegel R, Pascuzzi RM. Nonsense and missense mutations of the muscle chloride channel gene in patients with myotonia congenita. *Hum Mol Genet* 3: 2071–2072, 1994.

288. Gibson A, Lewis AP, Affleck K, Aitken AJ, Meldrum E, Thompson N. hCLCA1 and mCLCA3 are secreted non-integral membrane proteins and therefore are not ion channels. *J Biol Chem* 280: 27205–27212, 2005. doi:10.1074/jbc.M504654200.

289. Giorgio E, Vaula G, Benna P, Lo Buono N, Eandi CM, Dino D, Mancini C, Cavalieri S, Di Gregorio E, Pozzi E, Ferrero M, Giordana MT, Depienne C, Brusco A. A novel homozygous change of *CLCN2* (p.His590Pro) is associated with a subclinical form of leukoencephalopathy with ataxia (LKPAT). *J Neurol Neurosurg Psychiatry* 88: 894–896, 2017. doi:10.1136/jnnp-2016-315525.

290. Gondré-Lewis MC, Park JJ, Loh YP. Cellular mechanisms for the biogenesis and transport of synaptic and dense-core vesicles. *Int Rev Cell Mol Biol* 299: 27–115, 2012. doi:10.1016/B978-0-12-394310-1.00002-3.

291. Gong W, Xu H, Shimizu T, Morishima S, Tanabe S, Tachibe T, Uchida S, Sasaki S, Okada Y. ClC-3-independent, PKC-dependent activity of volume-sensitive Cl channel in mouse ventricular cardiomyocytes. *Cell Physiol Biochem* 14: 213–224, 2004. doi:10.1159/000080330.

292. Gorvin CM, Wilmer MJ, Piret SE, Harding B, van den Heuvel LP, Wrong O, Jat PS, Lippiat JD, Levtchenko EN, Thakker RV. Receptor-mediated endocytosis and endosomal acidification is impaired in proximal tubule epithelial cells of Dent disease patients. *Proc Natl Acad Sci USA* 110: 7014–7019, 2013. doi:10.1073/pnas.1302063110.

293. Gradogna A, Babini E, Picollo A, Pusch M. A regulatory calcium-binding site at the subunit interface of CLC-K kidney chloride channels. *J Gen Physiol* 136: 311–323, 2010. doi:10.1085/jgp.201010455.

294. Gradogna A, Fenollar-Ferrer C, Forrest LR, Pusch M. Dissecting a regulatory calcium-binding site of CLC-K kidney chloride channels. *J Gen Physiol* 140: 681–696, 2012. doi:10.1085/jgp.201210878.

295. Gradogna A, Imbrici P, Zifarelli G, Liantonio A, Camerino DC, Pusch M. I-J loop involvement in the pharmacological profile of CLC-K channels expressed in *Xenopus* oocytes. *Biochim Biophys Acta* 1838: 2745–2756, 2014. doi:10.1016/j.bbamem.2014.07.021.

296. Gradogna A, Pusch M. Alkaline pH block of CLC-K kidney chloride channels mediated by a pore lysine residue. *Biophys J* 105: 80–90, 2013. doi:10.1016/j.bpj.2013.05.044.

297. Grant J, Matthewman C, Bianchi L. A Novel Mechanism of pH Buffering in *C. elegans* Glia: Bicarbonate Transport via the Voltage-Gated ClC Cl^- Channel CLH-1. *J Neurosci* 35: 16377–16397, 2015. doi:10.1523/JNEUROSCI.3237-15.2015.

298. Graves AR, Curran PK, Smith CL, Mindell JA. The Cl^-/H^+ antiporter ClC-7 is the primary chloride permeation pathway in lysosomes. *Nature* 453: 788–792, 2008. doi:10.1038/nature06907.

299. Greene JR, Brown NH, DiDomenico BJ, Kaplan J, Eide DJ. The *GEF1* gene of *Saccharomyces cerevisiae* encodes an integral membrane protein; mutations in which have effects on respiration and iron-limited growth. *Mol Gen Genet* 241: 542–553, 1993. doi:10.1007/BF00279896.

300. Grenningloh G, Rienitz A, Schmitt B, Methfessel C, Zensen M, Beyreuther K, Gundelfinger ED, Betz H. The strychnine-binding subunit of the glycine receptor shows homology with nicotinic acetylcholine receptors. *Nature* 328: 215–220, 1987. doi:10.1038/328215a0.

301. Grieschat M, Alekov AK. Multiple discrete transitions underlie voltage-dependent activation in CLC Cl^-/H^+ antiporters. *Biophys J* 107: L13–L15, 2014. doi:10.1016/j.bpj.2014.07.063.

302. Grill A, Schießl IM, Gess B, Fremter K, Hammer A, Castrop H. Salt-losing nephropathy in mice with a null mutation of the *Clcnk2* gene. *Acta Physiol (Oxf)* 218: 198–211, 2016. doi:10.1111/apha.12755.

303. Gründer S, Thiemann A, Pusch M, Jentsch TJ. Regions involved in the opening of ClC-2 chloride channel by voltage and cell volume. *Nature* 360: 759–762, 1992. doi:10.1038/360759a0.

304. Grüneberg H. Grey-lethal, a new mutation in the house mouse. *J Hered* 27: 105–109, 1936. doi:10.1093/oxfordjournals.jhered.a104181.

305. Grunnet M, Jespersen T, Colding-Jørgensen E, Schwartz M, Klaerke DA, Vissing J, Olesen SP, Dunø M. Characterization of two new dominant ClC-1 channel mutations associated with myotonia. *Muscle Nerve* 28: 722–732, 2003. doi:10.1002/mus.10501.

306. Guan YY, Wang GL, Zhou JG. The ClC-3 Cl^- channel in cell volume regulation, proliferation and apoptosis in vascular smooth muscle cells. *Trends Pharmacol Sci* 27: 290–296, 2006. doi:10.1016/j.tips.2006.04.008.

307. Günther W, Lüchow A, Cluzeaud F, Vandewalle A, Jentsch TJ. ClC-5, the chloride channel mutated in Dent's disease, colocalizes with the proton pump in endocytotically active kidney cells. *Proc Natl Acad Sci USA* 95: 8075–8080, 1998. doi:10.1073/pnas.95.14.8075.

308. Günther W, Piwon N, Jentsch TJ. The ClC-5 chloride channel knock-out mouse: an animal model for Dent's disease. *Pflugers Arch* 445: 456–462, 2003. doi:10.1007/s00424-002-0950-6.

309. Guo J, Bervoets TJ, Henriksen K, Everts V, Bronckers AL. Null mutation of chloride channel 7 (*Clcn7*) impairs dental root formation but does not affect enamel mineralization. *Cell Tissue Res* 363: 361–370, 2016. doi:10.1007/s00441-015-2263-z.

310. Guo JH, Chen H, Ruan YC, Zhang XL, Zhang XH, Fok KL, Tsang LL, Yu MK, Huang WQ, Sun X, Chung YW, Jiang X, Sohma Y, Chan HC. Glucose-induced electrical activities and insulin secretion in pancreatic islet β-cells are modulated by CFTR. *Nat Commun* 5: 4420, 2014. doi:10.1038/ncomms5420.

311. Guo R, Pan F, Tian Y, Li H, Li S, Cao C. Down-Regulation of ClC-3 Expression Reduces Epidermal Stem Cell Migration by Inhibiting Volume-Activated Chloride Currents. *J Membr Biol* 249: 281–292, 2016. doi:10.1007/s00232-015-9867-9.

312. Guo X, Tang P, Chen L, Liu P, Hou C, Zhang X, Liu Y, Chong L, Li X, Li R. Amyloid β-Induced Redistribution of Transcriptional Factor EB and Lysosomal Dysfunction in Primary Microglial Cells. *Front Aging Neurosci* 9: 228, 2017. doi:10.3389/fnagi.2017.00228.

313. Gurnett CA, Kahl SD, Anderson RD, Campbell KP. Absence of the skeletal muscle sarcolemma chloride channel ClC-1 in myotonic mice. *J Biol Chem* 270: 9035–9038, 1995. doi:10.1074/jbc.270.16.9035.

314. Guzman RE, Alekov AK, Filippov M, Hegermann J, Fahlke C. Involvement of ClC-3 chloride/proton exchangers in controlling glutamatergic synaptic strength in cultured hippocampal neurons. *Front Cell Neurosci* 8: 143, 2014. doi:10.3389/fncel.2014.00143.

315. Guzman RE, Bungert-Plümke S, Franzen A, Fahlke C. Preferential association with ClC-3 permits sorting of ClC-4 into endosomal compartments. *J Biol Chem* 292: 19055–19065, 2017. doi:10.1074/jbc.M117.801951.

316. Guzman RE, Grieschat M, Fahlke C, Alekov AK. ClC-3 is an intracellular chloride/proton exchanger with large voltage-dependent nonlinear capacitance. *ACS Chem Neurosci* 4: 994–1003, 2013. doi:10.1021/cn400032z.

317. Guzmán RE, Miranda-Laferte E, Franzen A, Fahlke C. Neuronal ClC-3 Splice Variants Differ in Subcellular Localizations, but Mediate Identical Transport Functions. *J Biol Chem* 290: 25851–25862, 2015. doi:10.1074/jbc.M115.668186.

318. Gyömörey K, Yeger H, Ackerley C, Garami E, Bear CE. Expression of the chloride channel ClC-2 in the murine small intestine epithelium. *Am J Physiol Cell Physiol* 279: C1787–C1794, 2000. doi:10.1152/ajpcell.2000.279.6.C1787.

319. Ha K, Kim SY, Hong C, Myeong J, Shin JH, Kim DS, Jeon JH, So I. Electrophysiological characteristics of six mutations in hClC-1 of Korean patients with myotonia congenita. *Mol Cells* 37: 202–212, 2014. doi:10.14348/molcells.2014.2267.

320. Habela CW, Olsen ML, Sontheimer H. ClC3 is a critical regulator of the cell cycle in normal and malignant glial cells. *J Neurosci* 28: 9205–9217, 2008. doi:10.1523/JNEUROSCI.1897-08.2008.

321. Han W, Cheng RC, Maduke MC, Tajkhorshid E. Water access points and hydration pathways in CLC H^+/Cl^- transporters. *Proc Natl Acad Sci USA* 111: 1819–1824, 2014. doi:10.1073/pnas.1317890111.

322. Han Y, Lin Y, Sun Q, Wang S, Gao Y, Shao L. Mutation spectrum of Chinese patients with Bartter syndrome. *Oncotarget* 8: 101614–101622, 2017. doi:10.18632/oncotarget.21355.

323. Hanagasi HA, Bilgiç B, Abbink TE, Hanagasi F, Tüfekçioğlu Z, Gürvit H, Başak N, van der Knaap MS, Emre M. Secondary paroxysmal kinesigenic dyskinesia associated with *CLCN2* gene mutation. *Parkinsonism Relat Disord* 21: 544–546, 2015. doi:10.1016/j.parkreldis.2015.02.013.

324. Hanke W, Miller C. Single chloride channels from *Torpedo* electroplax. Activation by protons. *J Gen Physiol* 82: 25–45, 1983. doi:10.1085/jgp.82.1.25.

325. Hara-Chikuma M, Yang B, Sonawane ND, Sasaki S, Uchida S, Verkman AS. ClC-3 chloride channels facilitate endosomal acidification and chloride accumulation. *J Biol Chem* 280: 1241–1247, 2005. doi:10.1074/jbc.M407030200.

326. Hartzell C, Putzier I, Arreola J. Calcium-activated chloride channels. *Annu Rev Physiol* 67: 719–758, 2005. doi:10.1146/annurev.physiol.67.032003.154341.

327. Hartzell HC, Qu Z, Yu K, Xiao Q, Chien LT. Molecular physiology of bestrophins: multifunctional membrane proteins linked to best disease and other retinopathies. *Physiol Rev* 88: 639–672, 2008. doi:10.1152/physrev.00022.2007.

328. Haug K, Warnstedt M, Alekov AK, Sander T, Ramírez A, Poser B, Maljevic S, Hebeisen S, Kubisch C, Rebstock J, Horvath S, Hallmann K, Dullinger JS, Rau B, Haverkamp F, Beyenburg S, Schulz H, Janz D, Giese B, Müller-Newen G, Propping P, Elger CE, Fahlke C, Lerche H, Heils A. Retraction: Mutations in *CLCN2* encoding a voltage-gated chloride channel are associated with idiopathic generalized epilepsies. *Nat Genet* 41: 1043, 2009. doi:10.1038/ng0909-1043.

329. Hayama A, Rai T, Sasaki S, Uchida S. Molecular mechanisms of Bartter syndrome caused by mutations in the *BSND* gene. *Histochem Cell Biol* 119: 485–493, 2003. doi:10.1007/s00418-003-0535-2.

330. Hayama A, Uchida S, Sasaki S, Marumo F. Isolation and characterization of the human CLC-5 chloride channel gene promoter. *Gene* 261: 355–364, 2000. doi:10.1016/S0378-1119(00)00493-5.

331. He L, Denton J, Nehrke K, Strange K. Carboxy terminus splice variation alters ClC channel gating and extracellular cysteine reactivity. *Biophys J* 90: 3570–3581, 2006. doi:10.1529/biophysj.105.078295.

332. Hebeisen S, Biela A, Giese B, Müller-Newen G, Hidalgo P, Fahlke C. The role of the carboxyl terminus in ClC chloride channel function. *J Biol Chem* 279: 13140–13147, 2004. doi:10.1074/jbc.M312649200.

333. Hebeisen S, Fahlke C. Carboxy-terminal truncations modify the outer pore vestibule of muscle chloride channels. *Biophys J* 89: 1710–1720, 2005. doi:10.1529/biophysj.104.056093.

334. Hebeisen S, Heidtmann H, Cosmelli D, González C, Poser B, Latorre R, Alvarez O, Fahlke C. Anion permeation in human ClC-4 channels. *Biophys J* 84: 2306–2318, 2003. doi:10.1016/S0006-3495(03)75036-X.

335. Hechenberger M, Schwappach B, Fischer WN, Frommer WB, Jentsch TJ, Steinmeyer K. A family of putative chloride channels from *Arabidopsis* and functional complementation of a yeast strain with a *CLC* gene disruption. *J Biol Chem* 271: 33632–33638, 1996. doi:10.1074/jbc.271.52.33632.

336. Hennings JC, Andrini O, Picard N, Paulais M, Huebner AK, Cayuqueo IK, Bignon Y, Keck M, Cornière N, Böhm D, Jentsch TJ, Chambrey R, Teulon J, Hübner CA, Eladari D. The ClC-K2 Chloride Channel Is Critical for Salt Handling in the Distal Nephron. *J Am Soc Nephrol* 28: 209–217, 2017. doi:10.1681/ASN.2016010085.

337. Henriksen K, Gram J, Schaller S, Dahl BH, Dziegiel MH, Bollerslev J, Karsdal MA. Characterization of osteoclasts from patients harboring a G215R mutation in ClC-7 causing autosomal dominant osteopetrosis type II. *Am J Pathol* 164: 1537–1545, 2004. doi:10.1016/S0002-9440(10)63712-1.

338. Henriksen K, Sørensen MG, Nielsen RH, Gram J, Schaller S, Dziegiel MH, Everts V, Bollerslev J, Karsdal MA. Degradation of the organic phase of bone by osteoclasts: a secondary role for lysosomal acidification. *J Bone Miner Res* 21: 58–66, 2006. doi:10.1359/JBMR.050905.

339. Héraud C, Griffiths A, Pandruvada SN, Kilimann MW, Pata M, Vacher J. Severe neurodegeneration with impaired autophagy mechanism triggered by ostm1 deficiency. *J Biol Chem* 289: 13912–13925, 2014. doi:10.1074/jbc.M113.537233.

340. Herdean A, Nziengui H, Zsiros O, Solymosi K, Garab G, Lundin B, Spetea C. The Arabidopsis Thylakoid Chloride Channel AtCLCe Functions in Chloride Homeostasis and Regulation of Photosynthetic Electron Transport. *Front Plant Sci* 7: 115, 2016. doi:10.3389/fpls.2016.00115.

341. Herebian D, Alhaddad B, Seibt A, Schwarzmayr T, Danhauser K, Klee D, Harmsen S, Meitinger T, Strom TM, Schulz A, Mayatepek E, Haack TB, Distelmaier F. Coexisting variants in *OSTM1* and *MANEAL* cause a complex neurodegenerative disorder with NBIA-like brain abnormalities. *Eur J Hum Genet* 25: 1092–1095, 2017. doi:10.1038/ejhg.2017.96.

342. Hermoso M, Satterwhite CM, Andrade YN, Hidalgo J, Wilson SM, Horowitz B, Hume JR. ClC-3 is a fundamental molecular component of volume-sensitive outwardly rectifying Cl^- channels and volume regulation in HeLa cells and *Xenopus laevis* oocytes. *J Biol Chem* 277: 40066–40074, 2002. doi:10.1074/jbc.M205132200.

343. Hille B. *Ion Channels of Excitable Membranes*. Sunderland, MA: Sinauer, 2001.

344. Hinzpeter A, Fritsch J, Borot F, Trudel S, Vieu DL, Brouillard F, Baudouin-Legros M, Clain J, Edelman A, Ollero M. Membrane cholesterol content modulates ClC-2 gating and sensitivity to oxidative stress. *J Biol Chem* 282: 2423–2432, 2007. doi:10.1074/jbc.M608251200.

345. Hinzpeter A, Lipecka J, Brouillard F, Baudoin-Legros M, Dadlez M, Edelman A, Fritsch J. Association between Hsp90 and the ClC-2 chloride channel upregulates channel function. *Am J Physiol Cell Physiol* 290: C45–C56, 2006. doi:10.1152/ajpcell.00209.2005.

346. Hoegg-Beiler MB, Sirisi S, Orozco IJ, Ferrer I, Hohensee S, Auberson M, Gödde K, Vilches C, de Heredia ML, Nunes V, Estévez R, Jentsch TJ. Disrupting MLC1 and GlialCAM and ClC-2 interactions in leukodystrophy entails glial chloride channel dysfunction. *Nat Commun* 5: 3475, 2014. doi:10.1038/ncomms4475.

347. Hohberger B, Enz R. Cereblon is expressed in the retina and binds to voltage-gated chloride channels. *FEBS Lett* 583: 633–637, 2009. doi:10.1016/j.febslet.2009.01.018.

348. Hong S, Bi M, Wang L, Kang Z, Ling L, Zhao C. CLC-3 channels in cancer (review). *Oncol Rep* 33: 507–514, 2015. doi:10.3892/or.2014.3615.

349. Hoopes RR Jr, Raja KM, Koich A, Hueber P, Reid R, Knohl SJ, Scheinman SJ. Evidence for genetic heterogeneity in Dent's disease. *Kidney Int* 65: 1615–1620, 2004. doi:10.1111/j.1523-1755.2004.00571.x.

350. Hoopes RR Jr, Shrimpton AE, Knohl SJ, Hueber P, Hoppe B, Matyus J, Simckes A, Tasic V, Toenshoff B, Suchy SF, Nussbaum RL, Scheinman SJ. Dent Disease with mutations in OCRL1. *Am J Hum Genet* 76: 260–267, 2005. doi:10.1086/427887.

351. Hori K, Takahashi Y, Horikawa N, Furukawa T, Tsukada K, Takeguchi N, Sakai H. Is the ClC-2 chloride channel involved in the Cl^- secretory mechanism of gastric parietal cells? *FEBS Lett* 575: 105–108, 2004. doi:10.1016/j.febslet.2004.08.044.

352. Hosseinzadeh Z, Bhavsar SK, Lang F. Downregulation of ClC-2 by JAK2. *Cell Physiol Biochem* 29: 737–742, 2012. doi:10.1159/000178560.

353. Howery AE, Elvington S, Abraham SJ, Choi KH, Dworschak-Simpson S, Phillips S, Ryan CM, Sanford RL, Almqvist J, Tran K, Chew TA, Zachariae U, Andersen OS, Whitelegge J, Matulef K, Du Bois J, Maduke MC. A designed inhibitor of a CLC antiporter blocks function through a unique binding mode. *Chem Biol* 19: 1460–1470, 2012. doi:10.1016/j.chembiol.2012.09.017.

354. Hryciw DH, Ekberg J, Ferguson C, Lee A, Wang D, Parton RG, Pollock CA, Yun CC, Poronnik P. Regulation of albumin endocytosis by PSD95/Dlg/ZO-1 (PDZ) scaffolds. Interaction of Na^+-H^+ exchange regulatory factor-2 with ClC-5. *J Biol Chem* 281: 16068–16077, 2006. doi:10.1074/jbc.M512559200.

355. Hryciw DH, Ekberg J, Lee A, Lensink IL, Kumar S, Guggino WB, Cook DI, Pollock CA, Poronnik P. Nedd4-2 functionally interacts with ClC-5: involvement in constitutive albumin endocytosis in proximal tubule cells. *J Biol Chem* 279: 54996–55007, 2004. doi:10.1074/jbc.M411491200.

356. Hryciw DH, Rychkov GY, Hughes BP, Bretag AH. Relevance of the D13 region to the function of the skeletal muscle chloride channel, ClC-1. *J Biol Chem* 273: 4304–4307, 1998. doi:10.1074/jbc.273.8.4304.

357. Hryciw DH, Wang Y, Devuyst O, Pollock CA, Poronnik P, Guggino WB. Cofilin interacts with ClC-5 and regulates albumin uptake in proximal tubule cell lines. *J Biol Chem* 278: 40169–40176, 2003. doi:10.1074/jbc.M307890200.

358. Hsiao KM, Huang RY, Tang PH, Lin MJ. Functional study of CLC-1 mutants expressed in *Xenopus* oocytes reveals that a C-terminal region Thr891-Ser892-Thr893 is responsible for the effects of protein kinase C activator. *Cell Physiol Biochem* 25: 687–694, 2010. doi:10.1159/000315088.

359. Hu H, Haas SA, Chelly J, Van Esch H, Raynaud M, de Brouwer AP, Weinert S, Froyen G, Frints SG, Laumonnier F, Zemojtel T, Love MI, Richard H, Emde AK, Bienek M, Jensen C, Hambrock M, Fischer U, Langnick C, Feldkamp M, Wissink-Lindhout W, Lebrun N, Castelnau L, Rucci J, Montjean R, Dorseuil O, Billuart P, Stuhlmann T, Shaw M, Corbett MA, Gardner A, Willis-Owen S, Tan C, Friend KL, Belet S, van Roozendaal KE, Jimenez-Pocquet M, Moizard MP, Ronce N, Sun R, O'Keeffe S, Chenna R, van Bömmel A, Göke J, Hackett A, Field M, Christie L, Boyle J, Haan E, Nelson J, Turner G, Baynam G, Gillessen-Kaesbach G, Müller U, Steinberger D, Budny B, Badura-Stronka M, Latos-Bieleńska A, Ousager LB, Wieacker P, Rodríguez Criado G, Bondeson ML, Annerén G, Dufke A, Cohen M, Van Maldergem L, Vincent-Delorme C, Echenne B, Simon-Bouy B, Kleefstra T, Willemsen M, Fryns JP, Devriendt K, Ullmann R, Vingron M, Wrogemann K, Wienker TF, Tzschach A, van Bokhoven H, Gecz J, Jentsch TJ, Chen W, Ropers HH, Kalscheuer VM. X-exome sequencing of 405 unresolved families identifies seven novel intellectual disability genes. *Mol Psychiatry* 21: 133–148, 2016. doi:10.1038/mp.2014.193.

360. Huang P, Liu J, Di A, Robinson NC, Musch MW, Kaetzel MA, Nelson DJ. Regulation of human CLC-3 channels by multifunctional Ca^{2+}/calmodulin-dependent protein kinase. *J Biol Chem* 276: 20093–20100, 2001. doi:10.1074/jbc.M009376200.

361. Huber SM, Duranton C, Henke G, Van De Sand C, Heussler V, Shumilina E, Sandu CD, Tanneur V, Brand V, Kasinathan RS, Lang KS, Kremsner PG, Hübner CA, Rust MB, Dedek K, Jentsch TJ, Lang F. Plasmodium induces swelling-activated ClC-2 anion channels in the host erythrocyte. *J Biol Chem* 279: 41444–41452, 2004. doi:10.1074/jbc.M407618200.

362. Hübner CA, Stein V, Hermans-Borgmeyer I, Meyer T, Ballanyi K, Jentsch TJ. Disruption of KCC2 reveals an essential role of K-Cl cotransport already in early synaptic inhibition. *Neuron* 30: 515–524, 2001. doi:10.1016/S0896-6273(01)00297-5.

363. Hur J, Jeong HJ, Park J, Jeon S. Chloride channel 4 is required for nerve growth factor-induced TrkA signaling and neurite outgrowth in PC12 cells and cortical neurons. *Neuroscience* 253: 389–397, 2013. doi:10.1016/j.neuroscience.2013.09.003.

364. Hutter OF, Noble D. The chloride conductance of frog skeletal muscle. *J Physiol* 151: 89–102, 1960.

365. Ignoul S, Eggermont J. CBS domains: structure, function, and pathology in human proteins. *Am J Physiol Cell Physiol* 289: C1369–C1378, 2005. doi:10.1152/ajpcell.00282.2005.

366. Ignoul S, Simaels J, Hermans D, Annaert W, Eggermont J. Human ClC-6 is a late endosomal glycoprotein that associates with detergent-resistant lipid domains. *PLoS One* 2: e474, 2007. doi:10.1371/journal.pone.0000474.

367. Imbrici P, Altamura C, Pessia M, Mantegazza R, Desaphy JF, Camerino DC. ClC-1 chloride channels: state-of-the-art research and future challenges. *Front Cell Neurosci* 9: 156, 2015. doi:10.3389/fncel.2015.00156.

368. Imbrici P, Liantonio A, Gradogna A, Pusch M, Camerino DC. Targeting kidney CLC-K channels: pharmacological profile in a human cell line versus *Xenopus* oocytes. *Biochim Biophys Acta* 1838: 2484–2491, 2014. doi:10.1016/j.bbamem.2014.05.017.

369. Imbrici P, Maggi L, Mangiatordi GF, Dinardo MM, Altamura C, Brugnoni R, Alberga D, Pinter GL, Ricci G, Siciliano G, Micheli R, Annicchiarico G, Lattanzi G, Nicolotti O, Morandi L, Bernasconi P, Desaphy JF, Mantegazza R, Camerino DC. ClC-1 mutations in myotonia congenita patients: insights into molecular gating mechanisms and genotype-phenotype correlation. *J Physiol* 593: 4181–4199, 2015. doi:10.1113/JP270358.

370. Imbrici P, Tricarico D, Mangiatordi GF, Nicolotti O, Lograno MD, Conte D, Liantonio A. Pharmacovigilance database search discloses ClC-K channels as a novel target of the AT_1 receptor blockers valsartan and olmesartan. *Br J Pharmacol* 174: 1972–1983, 2017. doi:10.1111/bph.13794.

371. Inagaki A, Yamaguchi S, Takahashi-Iwanaga H, Iwanaga T, Ishikawa T. Functional characterization of a ClC-2-like Cl^- conductance in surface epithelial cells of rat rectal colon. *J Membr Biol* 235: 27–41, 2010. doi:10.1007/s00232-010-9253-6.

372. Ishida Y, Nayak S, Mindell JA, Grabe M. A model of lysosomal pH regulation. *J Gen Physiol* 141: 705–720, 2013. doi:10.1085/jgp.201210930.

373. Ishiguro T, Avila H, Lin SY, Nakamura T, Yamamoto M, Boyd DD. Gene trapping identifies chloride channel 4 as a novel inducer of colon cancer cell migration, invasion and metastases. *Br J Cancer* 102: 774–782, 2010. doi:10.1038/sj.bjc.6605536.

374. Isnard-Bagnis C, Da Silva N, Beaulieu V, Yu AS, Brown D, Breton S. Detection of ClC-3 and ClC-5 in epididymal epithelium: immunofluorescence and RT-PCR after LCM. *Am J Physiol Cell Physiol* 284: C220–C232, 2003. doi:10.1152/ajpcell.00374.2001.

375. Iyer R, Iverson TM, Accardi A, Miller C. A biological role for prokaryotic ClC chloride channels. *Nature* 419: 715–718, 2002. doi:10.1038/nature01000.

376. Jakab RL, Collaco AM, Ameen NA. Lubiprostone targets prostanoid signaling and promotes ion transporter trafficking, mucus exocytosis, and contractility. *Dig Dis Sci* 57: 2826–2845, 2012. doi:10.1007/s10620-012-2352-8.

377. Janssen AG, Scholl U, Domeyer C, Nothmann D, Leinenweber A, Fahlke C. Disease-causing dysfunctions of barttin in Bartter syndrome type IV. *J Am Soc Nephrol* 20: 145–153, 2009. doi:10.1681/ASN.2008010102.

378. Jayaram H, Accardi A, Wu F, Williams C, Miller C. Ion permeation through a Cl^--selective channel designed from a CLC Cl^-/H^+ exchanger. *Proc Natl Acad Sci USA* 105: 11194–11199, 2008. doi:10.1073/pnas.0804503105.

379. Jayaram H, Robertson JL, Wu F, Williams C, Miller C. Structure of a slow CLC Cl^-/H^+ antiporter from a cyanobacterium. *Biochemistry* 50: 788–794, 2011. doi:10.1021/bi1019258.

380. Jeck N, Konrad M, Peters M, Weber S, Bonzel KE, Seyberth HW. Mutations in the chloride channel gene, *CLCNKB*, leading to a mixed Bartter-Gitelman phenotype. *Pediatr Res* 48: 754–758, 2000. doi:10.1203/00006450-200012000-00009.

381. Jeck N, Waldegger P, Doroszewicz J, Seyberth H, Waldegger S. A common sequence variation of the *CLCNKB* gene strongly activates ClC-Kb chloride channel activity. *Kidney Int* 65: 190–197, 2004. doi:10.1111/j.1523-1755.2004.00363.x.

382. Jeck N, Waldegger S, Lampert A, Boehmer C, Waldegger P, Lang PA, Wissinger B, Friedrich B, Risler T, Moehle R, Lang UE, Zill P, Bondy B, Schaeffeler E, Asante-Poku S, Seyberth H, Schwab M, Lang F. Activating mutation of the renal epithelial chloride channel ClC-Kb predisposing to hypertension. *Hypertension* 43: 1175–1181, 2004. doi:10.1161/01.HYP.0000129824.12959.f0.

383. Jentsch TJ. Chloride and the endosomal-lysosomal pathway: emerging roles of CLC chloride transporters. *J Physiol* 578: 633–640, 2007. doi:10.1113/jphysiol.2006.124719.

384. Jentsch TJ. CLC chloride channels and transporters: from genes to protein structure, pathology and physiology. *Crit Rev Biochem Mol Biol* 43: 3–36, 2008. doi:10.1080/10409230701829110.

385. Jentsch TJ. Discovery of CLC transport proteins: cloning, structure, function and pathophysiology. *J Physiol* 593: 4091–4109, 2015. doi:10.1113/JP270043.

386. Jentsch TJ. VRACs and other ion channels and transporters in the regulation of cell volume and beyond. *Nat Rev Mol Cell Biol* 17: 293–307, 2016. doi:10.1038/nrm.2016.29.

387. Jentsch TJ, Friedrich T, Schriever A, Yamada H. The CLC chloride channel family. *Pflugers Arch* 437: 783–795, 1999. doi:10.1007/s004240050847.

388. Jentsch TJ, García AM, Lodish HF. Primary structure of a novel 4-acetamido-4′-isothiocyanostilbene-2,2′-disulphonic acid (SITS)-binding membrane protein highly expressed in *Torpedo californica* electroplax. *Biochem J* 261: 155–166, 1989. doi:10.1042/bj2610155.

389. Jentsch TJ, Günther W, Pusch M, Schwappach B. Properties of voltage-gated chloride channels of the ClC gene family. *J Physiol* 482, Suppl: 19S–25S, 1995. doi:10.1113/jphysiol.1995.sp020560.

390. Jentsch TJ, Maritzen T, Keating DJ, Zdebik AA, Thévenod F. ClC-3–a granular anion transporter involved in insulin secretion? *Cell Metab* 12: 307–308, 2010. doi:10.1016/j.cmet.2010.08.014.

391. Jentsch TJ, Poët M, Fuhrmann JC, Zdebik AA. Physiological functions of CLC Cl^- channels gleaned from human genetic disease and mouse models. *Annu Rev Physiol* 67: 779–807, 2005. doi:10.1146/annurev.physiol.67.032003.153245.

392. Jentsch TJ, Stein V, Weinreich F, Zdebik AA. Molecular structure and physiological function of chloride channels. *Physiol Rev* 82: 503–568, 2002. doi:10.1152/physrev.00029.2001.

393. Jentsch TJ, Steinmeyer K, Schwarz G. Primary structure of *Torpedo marmorata* chloride channel isolated by expression cloning in *Xenopus* oocytes. *Nature* 348: 510–514, 1990. doi:10.1038/348510a0.

394. Jeworutzki E, Lagostena L, Elorza-Vidal X, López-Hernández T, Estévez R, Pusch M. GlialCAM, a CLC-2 Cl^- channel subunit, activates the slow gate of CLC chloride channels. *Biophys J* 107: 1105–1116, 2014. doi:10.1016/j.bpj.2014.07.040.

395. Jeworutzki E, López-Hernández T, Capdevila-Nortes X, Sirisi S, Bengtsson L, Montolio M, Zifarelli G, Arnedo T, Müller CS, Schulte U, Nunes V, Martínez A, Jentsch TJ, Gasull X, Pusch M, Estévez R. GlialCAM, a protein defective in a leukodystrophy, serves as a ClC-2 Cl^- channel auxiliary subunit. *Neuron* 73: 951–961, 2012. doi:10.1016/j.neuron.2011.12.039.

396. Jiang T, Han W, Maduke M, Tajkhorshid E. Molecular Basis for Differential Anion Binding and Proton Coupling in the Cl^-/H^+ Exchanger ClC-ec1. *J Am Chem Soc* 138: 3066–3075, 2016. doi:10.1021/jacs.5b12062.

397. Jin NG, Kim JK, Yang DK, Cho SJ, Kim JM, Koh EJ, Jung HC, So I, Kim KW. Fundamental role of ClC-3 in volume-sensitive Cl^- channel function and cell volume regulation in AGS cells. *Am J Physiol Gastrointest Liver Physiol* 285: G938–G948, 2003. doi:10.1152/ajpgi.00470.2002.

398. Jin Y, Blikslager AT. ClC-2 regulation of intestinal barrier function: translation of basic science to therapeutic target. *Tissue Barriers* 3: e1105906, 2015. doi:10.1080/21688370.2015.1105906.

399. Jordt SE, Jentsch TJ. Molecular dissection of gating in the ClC-2 chloride channel. *EMBO J* 16: 1582–1592, 1997. doi:10.1093/emboj/16.7.1582.

400. Jossier M, Kroniewicz L, Dalmas F, Le Thiec D, Ephritikhine G, Thomine S, Barbier-Brygoo H, Vavasseur A, Filleur S, Leonhardt N. The *Arabidopsis* vacuolar anion transporter, AtCLCc, is involved in the regulation of stomatal movements and contributes to salt tolerance. *Plant J* 64: 563–576, 2010. doi:10.1111/j.1365-313X.2010.04352.x.

401. Jouret F, Igarashi T, Gofflot F, Wilson PD, Karet FE, Thakker RV, Devuyst O. Comparative ontogeny, processing, and segmental distribution of the renal chloride channel, ClC-5. *Kidney Int* 65: 198–208, 2004. doi:10.1111/j.1523-1755.2004.00360.x.

402. Jurkat-Rott K, Lerche H, Lehmann-Horn F. Skeletal muscle channelopathies. *J Neurol* 249: 1493–1502, 2002. doi:10.1007/s00415-002-0871-5.

403. Kajita H, Brown PD. Inhibition of the inward-rectifying Cl^- channel in rat choroid plexus by a decrease in extracellular pH. *J Physiol* 498: 703–707, 1997. doi:10.1113/jphysiol.1997.sp021894.

404. Kajita H, Omori K, Matsuda H. The chloride channel ClC-2 contributes to the inwardly rectifying Cl^- conductance in cultured porcine choroid plexus epithelial cells. *J Physiol* 523: 313–324, 2000. doi:10.1111/j.1469-7793.2000.t01-1-00313.x.

405. Kanadia RN, Johnstone KA, Mankodi A, Lungu C, Thornton CA, Esson D, Timmers AM, Hauswirth WW, Swanson MS. A muscleblind knockout model for myotonic dystrophy. *Science* 302: 1978–1980, 2003. doi:10.1126/science.1088583.

406. Karsdal MA, Henriksen K, Sørensen MG, Gram J, Schaller S, Dziegiel MH, Heegaard AM, Christophersen P, Martin TJ, Christiansen C, Bollerslev J. Acidification of the osteoclastic resorption compartment provides insight into the coupling of bone formation to bone resorption. *Am J Pathol* 166: 467–476, 2005. doi:10.1016/S0002-9440(10)62269-9.

407. Kasper D, Planells-Cases R, Fuhrmann JC, Scheel O, Zeitz O, Ruether K, Schmitt A, Poët M, Steinfeld R, Schweizer M, Kornak U, Jentsch TJ. Loss of the chloride channel ClC-7 leads to lysosomal storage disease and neurodegeneration. *EMBO J* 24: 1079–1091, 2005. doi:10.1038/sj.emboj.7600576.

408. Kawasaki M, Fukuma T, Yamauchi K, Sakamoto H, Marumo F, Sasaki S. Identification of an acid-activated Cl^- channel from human skeletal muscles. *Am J Physiol Cell Physiol* 277: C948–C954, 1999. doi:10.1152/ajpcell.1999.277.5.C948.

409. Kawasaki M, Suzuki M, Uchida S, Sasaki S, Marumo F. Stable and functional expression of the ClC-3 chloride channel in somatic cell lines. *Neuron* 14: 1285–1291, 1995. doi:10.1016/0896-6273(95)90275-9.

410. Kawasaki M, Uchida S, Monkawa T, Miyawaki A, Mikoshiba K, Marumo F, Sasaki S. Cloning and expression of a protein kinase C-regulated chloride channel abundantly expressed in rat brain neuronal cells. *Neuron* 12: 597–604, 1994. doi:10.1016/0896-6273(94)90215-1.

411. Keck M, Andrini O, Lahuna O, Burgos J, Cid LP, Sepúlveda FV, L'hoste S, Blanchard A, Vargas-Poussou R, Lourdel S, Teulon J. Novel *CLCNKB* mutations causing Bartter syndrome affect channel surface expression. *Hum Mutat* 34: 1269–1278, 2013. doi:10.1002/humu.22361.

412. Khantwal CM, Abraham SJ, Han W, Jiang T, Chavan TS, Cheng RC, Elvington SM, Liu CW, Mathews II, Stein RA, Mchaourab HS, Tajkhorshid E, Maduke M. Revealing an outward-facing open conformational state in a CLC Cl^-/H^+ exchange transporter. *eLife* 5: e11189, 2016. doi:10.7554/eLife.11189.

413. Kharkovets T, Dedek K, Maier H, Schweizer M, Khimich D, Nouvian R, Vardanyan V, Leuwer R, Moser T, Jentsch TJ. Mice with altered KCNQ4 K^+ channels implicate sensory outer hair cells in human progressive deafness. *EMBO J* 25: 642–652, 2006. doi:10.1038/sj.emboj.7600951.

414. Kida Y, Uchida S, Miyazaki H, Sasaki S, Marumo F. Localization of mouse CLC-6 and CLC-7 mRNA and their functional complementation of yeast CLC gene mutant. *Histochem Cell Biol* 115: 189–194, 2001.

415. Kieferle S, Fong P, Bens M, Vandewalle A, Jentsch TJ. Two highly homologous members of the ClC chloride channel family in both rat and human kidney. *Proc Natl Acad Sci USA* 91: 6943–6947, 1994. doi:10.1073/pnas.91.15.6943.

416. Kim T, Gondré-Lewis MC, Arnaoutova I, Loh YP. Dense-core secretory granule biogenesis. *Physiology (Bethesda)* 21: 124–133, 2006. doi:10.1152/physiol.00043.2005.

417. Klaus F, Laufer J, Czarkowski K, Strutz-Seebohm N, Seebohm G, Lang F. PIKfyve-dependent regulation of the Cl^- channel ClC-2. *Biochem Biophys Res Commun* 381: 407–411, 2009. doi:10.1016/j.bbrc.2009.02.053.

418. Kleopa KA, Orthmann JL, Enríquez A, Paul DL, Scherer SS. Unique distributions of the gap junction proteins connexin29, connexin32, and connexin47 in oligodendrocytes. *Glia* 47: 346–357, 2004. doi:10.1002/glia.20043.

419. Klocke R, Steinmeyer K, Jentsch TJ, Jockusch H. Role of innervation, excitability, and myogenic factors in the expression of the muscular chloride channel ClC-1. A study on normal and myotonic muscle. *J Biol Chem* 269: 27635–27639, 1994.

420. Kobayashi K, Uchida S, Mizutani S, Sasaki S, Marumo F. Developmental expression of CLC-K1 in the postnatal rat kidney. *Histochem Cell Biol* 116: 49–56, 2001.

421. Kobayashi K, Uchida S, Mizutani S, Sasaki S, Marumo F. Intrarenal and cellular localization of CLC-K2 protein in the mouse kidney. *J Am Soc Nephrol* 12: 1327–1334, 2001.

422. Kobayashi K, Uchida S, Okamura HO, Marumo F, Sasaki S. Human CLC-KB gene promoter drives the EGFP expression in the specific distal nephron segments and inner ear. *J Am Soc Nephrol* 13: 1992–1998, 2002. doi:10.1097/01.ASN.0000023434.47132.3D.

423. Koch MC, Steinmeyer K, Lorenz C, Ricker K, Wolf F, Otto M, Zoll B, Lehmann-Horn F, Grzeschik KH, Jentsch TJ. The skeletal muscle chloride channel in dominant and recessive human myotonia. *Science* 257: 797–800, 1992. doi:10.1126/science.1379744.

424. Koebis M, Kiyatake T, Yamaura H, Nagano K, Higashihara M, Sonoo M, Hayashi Y, Negishi Y, Endo-Takahashi Y, Yanagihara D, Matsuda R, Takahashi MP, Nishino I, Ishiura S. Ultrasound-enhanced delivery of morpholino with Bubble liposomes ameliorates the myotonia of myotonic dystrophy model mice. *Sci Rep* 3: 2242, 2013. doi:10.1038/srep02242.

425. Kokubo Y, Iwai N, Tago N, Inamoto N, Okayama A, Yamawaki H, Naraba H, Tomoike H. Association analysis between hypertension and *CYBA, CLCNKB*, and *KCNMB1* functional polymorphisms in the Japanese population–the Suita Study. *Circ J* 69: 138–142, 2005. doi:10.1253/circj.69.138.

426. Komwatana P, Dinudom A, Young JA, Cook DI. Characterization of the Cl^- conductance in the granular duct cells of mouse mandibular glands. *Pflugers Arch* 428: 641–647, 1994. doi:10.1007/BF00374588.

427. Konrad M, Vollmer M, Lemmink HH, van den Heuvel LP, Jeck N, Vargas-Poussou R, Lakings A, Ruf R, Deschênes G, Antignac C, Guay-Woodford L, Knoers NV, Seyberth HW, Feldmann D, Hildebrandt F. Mutations in the chloride channel gene *CLCNKB* as a cause of classic Bartter syndrome. *J Am Soc Nephrol* 11: 1449–1459, 2000.

428. Kornak U, Bösl MR, Kubisch C. Complete genomic structure of the *CLCN6* and *CLCN7* putative chloride channel genes. *Biochim Biophys Acta* 1447: 100–106, 1999. doi:10.1016/S0167-4781(99)00128-1.

429. Kornak U, Kasper D, Bösl MR, Kaiser E, Schweizer M, Schulz A, Friedrich W, Delling G, Jentsch TJ. Loss of the ClC-7 chloride channel leads to osteopetrosis in mice and man. *Cell* 104: 205–215, 2001. doi:10.1016/S0092-8674(01)00206-9.

430. Kornak U, Schulz A, Friedrich W, Uhlhaas S, Kremens B, Voit T, Hasan C, Bode U, Jentsch TJ, Kubisch C. Mutations in the a3 subunit of the vacuolar H^+-ATPase cause infantile malignant osteopetrosis. *Hum Mol Genet* 9: 2059–2063, 2000. doi:10.1093/hmg/9.13.2059.

431. Koulouridis E, Koulouridis I. Molecular pathophysiology of Bartter's and Gitelman's syndromes. *World J Pediatr* 11: 113–125, 2015. doi:10.1007/s12519-015-0016-4.

432. Krämer BK, Bergler T, Stoelcker B, Waldegger S. Mechanisms of Disease: the kidney-specific chloride channels ClCKA and ClCKB, the Barttin subunit, and their clinical relevance. *Nat Clin Pract Nephrol* 4: 38–46, 2008. doi:10.1038/ncpneph0689.

433. Krapp A, David LC, Chardin C, Girin T, Marmagne A, Leprince AS, Chaillou S, Ferrario-Méry S, Meyer C, Daniel-Vedele F. Nitrate transport and signalling in *Arabidopsis*. *J Exp Bot* 65: 789–798, 2014. doi:10.1093/jxb/eru001.

434. Kuang Z, Mahankali U, Beck TL. Proton pathways and H^+/Cl^- stoichiometry in bacterial chloride transporters. *Proteins* 68: 26–33, 2007. doi:10.1002/prot.21441.

435. Kubisch C, Schmidt-Rose T, Fontaine B, Bretag AH, Jentsch TJ. ClC-1 chloride channel mutations in myotonia congenita: variable penetrance of mutations shifting the voltage dependence. *Hum Mol Genet* 7: 1753–1760, 1998. doi:10.1093/hmg/7.11.1753.

436. Kubisch C, Schroeder BC, Friedrich T, Lütjohann B, El-Amraoui A, Marlin S, Petit C, Jentsch TJ. KCNQ4, a novel potassium channel expressed in sensory outer hair cells, is mutated in dominant deafness. *Cell* 96: 437–446, 1999. doi:10.1016/S0092-8674(00)80556-5.

437. Kuchenbecker M, Schu B, Kürz L, Rüdel R. Topology of the human skeletal muscle chloride channel hClC-1 probed with hydrophilic epitope insertion. *Pflugers Arch* 443: 280–288, 2001. doi:10.1007/s004240100688.

438. Kürz L, Wagner S, George AL Jr, Rüdel R. Probing the major skeletal muscle chloride channel with Zn^{2+} and other sulfhydryl-reactive compounds. *Pflugers Arch* 433: 357–363, 1997.

439. Kürz LL, Klink H, Jakob I, Kuchenbecker M, Benz S, Lehmann-Horn F, Rüdel R. Identification of three cysteines as targets for the Zn^{2+} blockade of the human skeletal muscle chloride channel. *J Biol Chem* 274: 11687–11692, 1999. doi:10.1074/jbc.274.17.11687.

440. Kwieciński H, Lehmann-Horn F, Rüdel R. Drug-induced myotonia in human intercostal muscle. *Muscle Nerve* 11: 576–581, 1988. doi:10.1002/mus.880110609.

441. L'Hoste S, Diakov A, Andrini O, Genete M, Pinelli L, Grand T, Keck M, Paulais M, Beck L, Korbmacher C, Teulon J, Lourdel S. Characterization of the mouse ClC-K1/Barttin chloride channel. *Biochim Biophys Acta* 1828: 2399–2409, 2013. doi:10.1016/j.bbamem.2013.06.012.

442. Lam CW, Tong SF, Wong K, Luo YF, Tang HY, Ha SY, Chan MH. DNA-based diagnosis of malignant osteopetrosis by whole-genome scan using a single-nucleotide polymorphism microarray: standardization of molecular investigations of genetic diseases due to consanguinity. *J Hum Genet* 52: 98–101, 2007. doi:10.1007/s10038-006-0075-4.

443. Lan WZ, Abbas H, Lam HD, Lemay AM, Hill CE. Contribution of a time-dependent and hyperpolarization-activated chloride conductance to currents of resting and hypotonically shocked rat hepatocytes. *Am J Physiol Gastrointest Liver Physiol* 288: G221–G229, 2005. doi:10.1152/ajpgi.00226.2004.

444. Landau D, Shalev H, Ohaly M, Carmi R. Infantile variant of Bartter syndrome and sensorineural deafness: a new autosomal recessive disorder. *Am J Med Genet* 59: 454–459, 1995. doi:10.1002/ajmg.1320590411.

445. Lange PF, Wartosch L, Jentsch TJ, Fuhrmann JC. ClC-7 requires Ostm1 as a β-subunit to support bone resorption and lysosomal function. *Nature* 440: 220–223, 2006. doi:10.1038/nature04535.

446. Last NB, Miller C. Functional Monomerization of a ClC-Type Fluoride Transporter. *J Mol Biol* 427: 3607–3612, 2015. doi:10.1016/j.jmb.2015.09.027.

447. Lee A, Slattery C, Nikolic-Paterson DJ, Hryciw DH, Wilk S, Wilk E, Zhang Y, Valova VA, Robinson PJ, Kelly DJ, Poronnik P. Chloride channel ClC-5 binds to aspartyl aminopeptidase to regulate renal albumin endocytosis. *Am J Physiol Renal Physiol* 308: F784–F792, 2015. doi:10.1152/ajprenal.00322.2014.

448. Lee MP, Ravenel JD, Hu RJ, Lustig LR, Tomaselli G, Berger RD, Brandenburg SA, Litzi TJ, Bunton TE, Limb C, Francis H, Gorelikow M, Gu H, Washington K, Argani P, Goldenring JR, Coffey RJ, Feinberg AP. Targeted disruption of the *Kvlqt1* gene causes deafness and gastric hyperplasia in mice. *J Clin Invest* 106: 1447–1455, 2000. doi:10.1172/JCI10897.

449. Lee S, Mayes HB, Swanson JM, Voth GA. The Origin of Coupled Chloride and Proton Transport in a Cl^-/H^+ Antiporter. *J Am Chem Soc* 138: 14923–14930, 2016. doi:10.1021/jacs.6b06683.

450. Lee TT, Zhang XD, Chuang CC, Chen JJ, Chen YA, Chen SC, Chen TY, Tang CY. Myotonia congenita mutation enhances the degradation of human CLC-1 chloride channels. *PLoS One* 8: e55930, 2013. doi:10.1371/journal.pone.0055930.

451. Leegwater PA, Yuan BQ, van der Steen J, Mulders J, Könst AA, Boor PK, Mejaski-Bosnjak V, van der Maarel SM, Frants RR, Oudejans CB, Schutgens RB, Pronk JC, van der Knaap MS. Mutations of *MLC1* (KIAA0027), encoding a putative membrane protein, cause megalencephalic leukoencephalopathy with subcortical cysts. *Am J Hum Genet* 68: 831–838, 2001. doi:10.1086/319519.

452. Lehmann-Horn F, Mailänder V, Heine R, George AL. Myotonia levior is a chloride channel disorder. *Hum Mol Genet* 4: 1397–1402, 1995. doi:10.1093/hmg/4.8.1397.

453. Leisle L, Ludwig CF, Wagner FA, Jentsch TJ, Stauber T. ClC-7 is a slowly voltage-gated $2Cl^-/1H^{(+)}$-exchanger and requires Ostm1 for transport activity. *EMBO J* 30: 2140–2152, 2011. doi:10.1038/emboj.2011.137.

454. Li C, Huang D, Tang J, Chen M, Lu Q, Li H, Zhang M, Xu B, Mao J. ClC-3 chloride channel is involved in isoprenaline-induced cardiac hypertrophy. *Gene* 642: 335–342, 2018. doi:10.1016/j.gene.2017.11.045.

455. Li DQ, Jing X, Salehi A, Collins SC, Hoppa MB, Rosengren AH, Zhang E, Lundquist I, Olofsson CS, Mörgelin M, Eliasson L, Rorsman P, Renström E. Suppression of sulfonylurea- and glucose-induced insulin secretion in vitro and in vivo in mice lacking the chloride transport protein ClC-3. *Cell Metab* 10: 309–315, 2009. doi:10.1016/j.cmet.2009.08.011.

456. Li X, Shimada K, Showalter LA, Weinman SA. Biophysical properties of ClC-3 differentiate it from swelling-activated chloride channels in Chinese hamster ovary-K1 cells. *J Biol Chem* 275: 35994–35998, 2000. doi:10.1074/jbc.M002712200.

457. Li X, Wang T, Zhao Z, Weinman SA. The ClC-3 chloride channel promotes acidification of lysosomes in CHO-K1 and Huh-7 cells. *Am J Physiol Cell Physiol* 282: C1483–C1491, 2002. doi:10.1152/ajpcell.00504.2001.

458. Liantonio A, Accardi A, Carbonara G, Fracchiolla G, Loiodice F, Tortorella P, Traverso S, Guida P, Pierno S, De Luca A, Camerino DC, Pusch M. Molecular requisites for drug binding to muscle CLC-1 and renal CLC-K channel revealed by the use of phenoxy-alkyl derivatives of 2-(*p*-chlorophenoxy)propionic acid. *Mol Pharmacol* 62: 265–271, 2002. doi:10.1124/mol.62.2.265.

459. Liantonio A, De Luca A, Pierno S, Didonna MP, Loiodice F, Fracchiolla G, Tortorella P, Antonio L, Bonerba E, Traverso S, Elia L, Picollo A, Pusch M, Camerino DC. Structural requisites of 2-(*p*-chlorophenoxy)propionic acid analogues for activity on native rat skeletal muscle chloride conductance and on heterologously expressed CLC-1. *Br J Pharmacol* 139: 1255–1264, 2003. doi:10.1038/sj.bjp.0705364.

460. Liantonio A, Giannuzzi V, Picollo A, Babini E, Pusch M, Conte Camerino D. Niflumic acid inhibits chloride conductance of rat skeletal muscle by directly inhibiting the CLC-1 channel and by increasing intracellular calcium. *Br J Pharmacol* 150: 235–247, 2007. doi:10.1038/sj.bjp.0706954.

461. Liantonio A, Gramegna G, Camerino GM, Dinardo MM, Scaramuzzi A, Potenza MA, Montagnani M, Procino G, Lasorsa DR, Mastrofrancesco L, Laghezza A, Fracchiolla G, Loiodice F, Perrone MG, Lopedota A, Conte S, Penza R, Valenti G, Svelto M, Camerino DC. In-vivo administration of CLC-K kidney chloride channels inhibitors increases water diuresis in rats: a new drug target for hypertension? *J Hypertens* 30: 153–167, 2012. doi:10.1097/HJH.0b013e32834d9eb9.

462. Liantonio A, Imbrici P, Camerino GM, Fracchiolla G, Carbonara G, Giannico D, Gradogna A, Mangiatordi GF, Nicolotti O, Tricarico D, Pusch M, Camerino DC. Kidney CLC-K chloride channels inhibitors: structure-based studies and efficacy in hypertension and associated CLC-K polymorphisms. *J Hypertens* 34: 981–992, 2016. doi:10.1097/HJH.0000000000000876.

463. Liantonio A, Picollo A, Babini E, Carbonara G, Fracchiolla G, Loiodice F, Tortorella V, Pusch M, Camerino DC. Activation and inhibition of kidney CLC-K chloride channels by fenamates. *Mol Pharmacol* 69: 165–173, 2006. doi:10.1124/mol.105.017384.

464. Liantonio A, Picollo A, Carbonara G, Fracchiolla G, Tortorella P, Loiodice F, Laghezza A, Babini E, Zifarelli G, Pusch M, Camerino DC. Molecular switch for CLC-K Cl^- channel block/activation: optimal pharmacophoric requirements towards high-affinity ligands. *Proc Natl Acad Sci USA* 105: 1369–1373, 2008. doi:10.1073/pnas.0708977105.

465. Liantonio A, Pusch M, Picollo A, Guida P, De Luca A, Pierno S, Fracchiolla G, Loiodice F, Tortorella P, Conte Camerino D. Investigations of pharmacologic properties of the renal CLC-K1 chloride channel co-expressed with barttin by the use of 2-(*p*-chlorophenoxy)propionic acid derivatives and other structurally unrelated chloride channels blockers. *J Am Soc Nephrol* 15: 13–20, 2004. doi:10.1097/01.ASN.0000103226.28798.EA.

466. Licchetta L, Bisulli F, Naldi I, Mainieri G, Tinuper P. Limbic encephalitis with anti-GAD antibodies and Thomsen myotonia: a casual or causal association? *Epileptic Disord* 16: 362–365, 2014. doi:10.1684/epd.2014.0668.

467. Lim HH, Miller C. Intracellular proton-transfer mutants in a CLC Cl^-/H^+ exchanger. *J Gen Physiol* 133: 131–138, 2009. doi:10.1085/jgp.200810112.

468. Lim HH, Shane T, Miller C. Intracellular proton access in a Cl^-/H^+ antiporter. *PLoS Biol* 10: e1001441, 2012. doi:10.1371/journal.pbio.1001441.

469. Lim HH, Stockbridge RB, Miller C. Fluoride-dependent interruption of the transport cycle of a CLC Cl^-/H^+ antiporter. *Nat Chem Biol* 9: 721–725, 2013. doi:10.1038/nchembio.1336.

470. Lin CW, Chen TY. Cysteine modification of a putative pore residue in ClC-0: implication for the pore stoichiometry of ClC chloride channels. *J Gen Physiol* 116: 535–546, 2000. doi:10.1085/jgp.116.4.535.

471. Lin CW, Chen TY. Probing the pore of ClC-0 by substituted cysteine accessibility method using methane thiosulfonate reagents. *J Gen Physiol* 122: 147–159, 2003. doi:10.1085/jgp.200308845.

472. Lin YW, Lin CW, Chen TY. Elimination of the slow gating of ClC-0 chloride channel by a point mutation. *J Gen Physiol* 114: 1–12, 1999. doi:10.1085/jgp.114.1.1.

473. Lin Z, Jin S, Duan X, Wang T, Martini S, Hulamm P, Cha B, Hubbard A, Donowitz M, Guggino SE. Chloride channel (Clc)-5 is necessary for exocytic trafficking of Na^+/H^+ exchanger 3 (NHE3). *J Biol Chem* 286: 22833–22845, 2011. doi:10.1074/jbc.M111.224998.

474. Lindskog S. Structure and mechanism of carbonic anhydrase. *Pharmacol Ther* 74: 1–20, 1997. doi:10.1016/S0163-7258(96)00198-2.

475. Lipecka J, Bali M, Thomas A, Fanen P, Edelman A, Fritsch J. Distribution of ClC-2 chloride channel in rat and human epithelial tissues. *Am J Physiol Cell Physiol* 282: C805–C816, 2002. doi:10.1152/ajpcell.00291.2001.

476. Lipicky RJ, Bryant SH. Sodium, potassium, and chloride fluxes in intercostal muscle from normal goats and goats with hereditary myotonia. *J Gen Physiol* 50: 89–111, 1966. doi:10.1085/jgp.50.1.89.

477. Lipicky RJ, Bryant SH, Salmon JH. Cable parameters, sodium, potassium, chloride, and water content, and potassium efflux in isolated external intercostal muscle of normal volunteers and patients with myotonia congenita. *J Clin Invest* 50: 2091–2103, 1971. doi:10.1172/JCI106703.

478. Lísal J, Maduke M. The ClC-0 chloride channel is a 'broken' Cl^-/H^+ antiporter. *Nat Struct Mol Biol* 15: 805–810, 2008. doi:10.1038/nsmb.1466.

479. Lísal J, Maduke M. Review. Proton-coupled gating in chloride channels. *Philos Trans R Soc Lond B Biol Sci* 364: 181–187, 2009. doi:10.1098/rstb.2008.0123.

480. Liu F, Zhang Z, Csanády L, Gadsby DC, Chen J. Molecular Structure of the Human CFTR Ion Channel. *Cell* 169: 85–95.e8, 2017. doi:10.1016/j.cell.2017.02.024.

481. Lloyd SE, Pearce SH, Fisher SE, Steinmeyer K, Schwappach B, Scheinman SJ, Harding B, Bolino A, Devoto M, Goodyer P, Rigden SP, Wrong O, Jentsch TJ, Craig IW, Thakker RV. A common molecular basis for three inherited kidney stone diseases. *Nature* 379: 445–449, 1996. doi:10.1038/379445a0.

482. Lobet S, Dutzler R. Ion-binding properties of the ClC chloride selectivity filter. *EMBO J* 25: 24–33, 2006. doi:10.1038/sj.emboj.7600909.

483. López-Hernández T, Ridder MC, Montolio M, Capdevila-Nortes X, Polder E, Sirisi S, Duarri A, Schulte U, Fakler B, Nunes V, Scheper GC, Martínez A, Estévez R, van der Knaap MS. Mutant GlialCAM causes megalencephalic leukoencephalopathy with subcortical cysts, benign familial macrocephaly, and macrocephaly with retardation and autism. *Am J Hum Genet* 88: 422–432, 2011. doi:10.1016/j.ajhg.2011.02.009.

484. Lorenz C, Pusch M, Jentsch TJ. Heteromultimeric CLC chloride channels with novel properties. *Proc Natl Acad Sci USA* 93: 13362–13366, 1996. doi:10.1073/pnas.93.23.13362.

485. Lossin C, George AL Jr. Myotonia congenita. *Adv Genet* 63: 25–55, 2008. doi:10.1016/S0065-2660(08)01002-X.

486. Louet M, Bitam S, Bakouh N, Bignon Y, Planelles G, Lagorce D, Miteva MA, Eladari D, Teulon J, Villoutreix BO. In silico model of the human ClC-Kb chloride channel: pore mapping, biostructural pathology and drug screening. *Sci Rep* 7: 7249, 2017. doi:10.1038/s41598-017-07794-5.

487. Lourdel S, Grand T, Burgos J, González W, Sepúlveda FV, Teulon J. ClC-5 mutations associated with Dent's disease: a major role of the dimer interface. *Pflugers Arch* 463: 247–256, 2012. doi:10.1007/s00424-011-1052-0.

488. Lowe CU, Terrey M, MacLACHLAN EA. Organic-aciduria, decreased renal ammonia production, hydrophthalmos, and mental retardation; a clinical entity. *AMA Am J Dis Child* 83: 164–184, 1952.

489. Ludewig U, Jentsch TJ, Pusch M. Analysis of a protein region involved in permeation and gating of the voltage-gated *Torpedo* chloride channel ClC-0. *J Physiol* 498: 691–702, 1997. doi:10.1113/jphysiol.1997.sp021893.

490. Ludewig U, Jentsch TJ, Pusch M. Inward rectification in ClC-0 chloride channels caused by mutations in several protein regions. *J Gen Physiol* 110: 165–171, 1997. doi:10.1085/jgp.110.2.165.

491. Ludewig U, Pusch M, Jentsch TJ. Independent gating of single pores in CLC-0 chloride channels. *Biophys J* 73: 789–797, 1997. doi:10.1016/S0006-3495(97)78111-6.

492. Ludewig U, Pusch M, Jentsch TJ. Two physically distinct pores in the dimeric ClC-0 chloride channel. *Nature* 383: 340–343, 1996. doi:10.1038/383340a0.

493. Ludwig CF, Ullrich F, Leisle L, Stauber T, Jentsch TJ. Common gating of both CLC transporter subunits underlies voltage-dependent activation of the $2Cl^-/1H^+$ exchanger ClC-7/Ostm1. *J Biol Chem* 288: 28611–28619, 2013. doi:10.1074/jbc.M113.509364.

494. Ludwig M, Utsch B. Dent disease-like phenotype and the chloride channel ClC-4 (*CLCN4*) gene. *Am J Med Genet A* 128A: 434–435, 2004. doi:10.1002/ajmg.a.30204.

495. Lueck JD, Lungu C, Mankodi A, Osborne RJ, Welle SL, Dirksen RT, Thornton CA. Chloride channelopathy in myotonic dystrophy resulting from loss of posttranscriptional regulation for CLCN1. *Am J Physiol Cell Physiol* 292: C1291–C1297, 2007. doi:10.1152/ajpcell.00336.2006.

496. Lueck JD, Mankodi A, Swanson MS, Thornton CA, Dirksen RT. Muscle chloride channel dysfunction in two mouse models of myotonic dystrophy. *J Gen Physiol* 129: 79–94, 2007. doi:10.1085/jgp.200609635.

497. Lueck JD, Rossi AE, Thornton CA, Campbell KP, Dirksen RT. Sarcolemmal-restricted localization of functional ClC-1 channels in mouse skeletal muscle. *J Gen Physiol* 136: 597–613, 2010. doi:10.1085/jgp.201010526.

498. Lurin C, Geelen D, Barbier-Brygoo H, Guern J, Maurel C. Cloning and functional expression of a plant voltage-dependent chloride channel. *Plant Cell* 8: 701–711, 1996. doi:10.1105/tpc.8.4.701.

499. Lutter D, Ullrich F, Lueck JC, Kempa S, Jentsch TJ. Selective transport of neurotransmitters and modulators by distinct volume-regulated LRRC8 anion channels. *J Cell Sci* 130: 1122–1133, 2017. doi:10.1242/jcs.196253.

500. Luyckx VA, Goda FO, Mount DB, Nishio T, Hall A, Hebert SC, Hammond TG, Yu AS. Intrarenal and subcellular localization of rat CLC5. *Am J Physiol Renal Fluid Electrolyte Physiol* 275: F761–F769, 1998.

501. Luyckx VA, Leclercq B, Dowland LK, Yu AS. Diet-dependent hypercalciuria in transgenic mice with reduced CLC5 chloride channel expression. *Proc Natl Acad Sci USA* 96: 12174–12179, 1999. doi:10.1073/pnas.96.21.12174.

502. Lv Q, Tang R, Liu H, Gao X, Li Y, Zheng HH, Zhang H. Cloning and molecular analysis of the *Arabidopsis thaliana* chloride channel gene family. *Plant Sci* 176: 650–661, 2009. doi:10.1016/j.plantsci.2009.02.006.

503. Ma L, Rychkov GY, Bretag AH. Functional study of cytoplasmic loops of human skeletal muscle chloride channel, hClC-1. *Int J Biochem Cell Biol* 41: 1402–1409, 2009. doi:10.1016/j.biocel.2008.12.006.

504. Ma L, Rychkov GY, Bykova EA, Zheng J, Bretag AH. Movement of hClC-1 C-termini during common gating and limits on their cytoplasmic location. *Biochem J* 436: 415–428, 2011. doi:10.1042/BJ20102153.

505. Ma L, Rychkov GY, Hughes BP, Bretag AH. Analysis of carboxyl tail function in the skeletal muscle Cl^- channel hClC-1. *Biochem J* 413: 61–69, 2008. doi:10.1042/BJ20071489.

506. Ma MM, Lin CX, Liu CZ, Gao M, Sun L, Tang YB, Zhou JG, Wang GL, Guan YY. Threonine532 phosphorylation in ClC-3 channels is required for angiotensin II-induced Cl^- current and migration in cultured vascular smooth muscle cells. *Br J Pharmacol* 173: 529–544, 2016. doi:10.1111/bph.13385.

507. Macías MJ, Teijido O, Zifarelli G, Martin P, Ramirez-Espain X, Zorzano A, Palacín M, Pusch M, Estévez R. Myotonia-related mutations in the distal C-terminus of ClC-1 and ClC-0 chloride channels affect the structure of a poly-proline helix. *Biochem J* 403: 79–87, 2007. doi:10.1042/BJ20061230.

508. Madison DV, Malenka RC, Nicoll RA. Phorbol esters block a voltage-sensitive chloride current in hippocampal pyramidal cells. *Nature* 321: 695–697, 1986. doi:10.1038/321695a0.

509. Madry C, Attwell D. Receptors, ion channels, and signaling mechanisms underlying microglial dynamics. *J Biol Chem* 290: 12443–12450, 2015. doi:10.1074/jbc.R115.637157.

510. Maduke M, Miller C, Mindell JA. A decade of CLC chloride channels: structure, mechanism, and many unsettled questions. *Annu Rev Biophys Biomol Struct* 29: 411–438, 2000. doi:10.1146/annurev.biophys.29.1.411.

511. Maduke M, Pheasant DJ, Miller C. High-level expression, functional reconstitution, and quaternary structure of a prokaryotic ClC-type chloride channel. *J Gen Physiol* 114: 713–722, 1999. doi:10.1085/jgp.114.5.713.

512. Maduke M, Williams C, Miller C. Formation of CLC-0 chloride channels from separated transmembrane and cytoplasmic domains. *Biochemistry* 37: 1315–1321, 1998. doi:10.1021/bi972418o.

513. Maehara H, Okamura HO, Kobayashi K, Uchida S, Sasaki S, Kitamura K. Expression of CLC-KB gene promoter in the mouse cochlea. *Neuroreport* 14: 1571–1573, 2003. doi:10.1097/00001756-200308260-00006.

514. Majumdar A, Capetillo-Zarate E, Cruz D, Gouras GK, Maxfield FR. Degradation of Alzheimer's amyloid fibrils by microglia requires delivery of ClC-7 to lysosomes. *Mol Biol Cell* 22: 1664–1676, 2011. doi:10.1091/mbc.E10-09-0745.

515. Makara JK, Petheö GL, Tóth A, Spät A. pH-sensitive inwardly rectifying chloride current in cultured rat cortical astrocytes. *Glia* 34: 52–58, 2001. doi:10.1002/glia.1039.

516. Makara JK, Rappert A, Matthias K, Steinhäuser C, Spät A, Kettenmann H. Astrocytes from mouse brain slices express ClC-2-mediated Cl^- currents regulated during development and after injury. *Mol Cell Neurosci* 23: 521–530, 2003. doi:10.1016/S1044-7431(03)00080-0.

517. Malinowska DH, Kupert EY, Bahinski A, Sherry AM, Cuppoletti J. Cloning, functional expression, and characterization of a PKA-activated gastric Cl- channel. *Am J Physiol Cell Physiol* 268: C191–C200, 1995. doi:10.1152/ajpcell.1995.268.1.C191.

518. Mankodi A, Takahashi MP, Jiang H, Beck CL, Bowers WJ, Moxley RT, Cannon SC, Thornton CA. Expanded CUG repeats trigger aberrant splicing of ClC-1 chloride channel pre-mRNA and hyperexcitability of skeletal muscle in myotonic dystrophy. *Mol Cell* 10: 35–44, 2002. doi:10.1016/S1097-2765(02)00563-4.

519. Mansour-Hendili L, Blanchard A, Le Pottier N, Roncelin I, Lourdel S, Treard C, González W, Vergara-Jaque A, Morin G, Colin E, Holder-Espinasse M, Bacchetta J, Baudouin V, Benoit S, Bérard E, Bourdat-Michel G, Bouchireb K, Burtey S, Cailliez M, Cardon G, Cartery C, Champion G, Chauveau D, Cochat P, Dahan K, De la Faille R, Debray FG, Dehoux L, Deschenes G, Desport E, Devuyst O, Dieguez S, Emma F, Fischbach M, Fouque D, Fourcade J, François H, Gilbert-Dussardier B, Hannedouche T, Houillier P, Izzedine H, Janner M, Karras A, Knebelmann B, Lavocat MP, Lemoine S, Leroy V, Loirat C, Macher MA, Martin-Coignard D, Morin D, Niaudet P, Nivet H, Nobili F, Novo R, Faivre L, Rigothier C, Roussey-Kesler G, Salomon R, Schleich A, Sellier-Leclerc AL, Soulami K, Tiple A, Ulinski T, Vanhille P, Van Regemorter N, Jeunemaître X, Vargas-Poussou R. Mutation Update of the *CLCN5* Gene Responsible for Dent Disease 1. *Hum Mutat* 36: 743–752, 2015. doi:10.1002/humu.22804.

520. Mao J, Chen L, Xu B, Wang L, Wang W, Li M, Zheng M, Li H, Guo J, Li W, Jacob TJ, Wang L. Volume-activated chloride channels contribute to cell-cycle-dependent regulation of HeLa cell migration. *Biochem Pharmacol* 77: 159–168, 2009. doi:10.1016/j.bcp.2008.10.009.

521. Maranda B, Chabot G, Décarie JC, Pata M, Azeddine B, Moreau A, Vacher J. Clinical and cellular manifestations of *OSTM1*-related infantile osteopetrosis. *J Bone Miner Res* 23: 296–300, 2008. doi:10.1359/jbmr.071015.

522. Marcoline FV, Ishida Y, Mindell JA, Nayak S, Grabe M. A mathematical model of osteoclast acidification during bone resorption. *Bone* 93: 167–180, 2016. doi:10.1016/j.bone.2016.09.007.

523. Maritzen T, Keating DJ, Neagoe I, Zdebik AA, Jentsch TJ. Role of the vesicular chloride transporter ClC-3 in neuroendocrine tissue. *J Neurosci* 28: 10587–10598, 2008. doi:10.1523/JNEUROSCI.3750-08.2008.

524. Maritzen T, Lisi S, Botta R, Pinchera A, Fanelli G, Viacava P, Marcocci C, Marinò M. ClC-5 does not affect megalin expression and function in the thyroid. *Thyroid* 16: 725–730, 2006. doi:10.1089/thy.2006.16.725.

525. Maritzen T, Rickheit G, Schmitt A, Jentsch TJ. Kidney-specific upregulation of vitamin D_3 target genes in ClC-5 KO mice. *Kidney Int* 70: 79–87, 2006. doi:10.1038/sj.ki.5000445.

526. Markovic S, Dutzler R. The structure of the cytoplasmic domain of the chloride channel ClC-Ka reveals a conserved interaction interface. *Structure* 15: 715–725, 2007. doi:10.1016/j.str.2007.04.013.

527. Marmagne A, Vinauger-Douard M, Monachello D, de Longevialle AF, Charon C, Allot M, Rappaport F, Wollman FA, Barbier-Brygoo H, Ephritikhine G. Two members of the Arabidopsis CLC (chloride channel) family, AtCLCe and AtCLCf, are associated with thylakoid and Golgi membranes, respectively. *J Exp Bot* 58: 3385–3393, 2007. doi:10.1093/jxb/erm187.

528. Martinez GQ, Maduke M. A cytoplasmic domain mutation in ClC-Kb affects long-distance communication across the membrane. *PLoS One* 3: e2746, 2008. doi:10.1371/journal.pone.0002746.

529. Matsuda JJ, Filali MS, Collins MM, Volk KA, Lamb FS. The ClC-3 Cl^-/H^+ antiporter becomes uncoupled at low extracellular pH. *J Biol Chem* 285: 2569–2579, 2010. doi:10.1074/jbc.M109.018002.

530. Matsuda JJ, Filali MS, Moreland JG, Miller FJ, Lamb FS. Activation of swelling-activated chloride current by tumor necrosis factor-alpha requires ClC-3-dependent endosomal reactive oxygen production. *J Biol Chem* 285: 22864–22873, 2010. doi:10.1074/jbc.M109.099838.

531. Matsuda JJ, Filali MS, Volk KA, Collins MM, Moreland JG, Lamb FS. Overexpression of CLC-3 in HEK293T cells yields novel currents that are pH dependent. *Am J Physiol Cell Physiol* 294: C251–C262, 2008. doi:10.1152/ajpcell.00338.2007.

532. Matsumura Y, Uchida S, Kondo Y, Miyazaki H, Ko SB, Hayama A, Morimoto T, Liu W, Arisawa M, Sasaki S, Marumo F. Overt nephrogenic diabetes insipidus in mice lacking the CLC-K1 chloride channel. *Nat Genet* 21: 95–98, 1999. doi:10.1038/5036.

533. Matulef K, Howery AE, Tan L, Kobertz WR, Du Bois J, Maduke M. Discovery of potent CLC chloride channel inhibitors. *ACS Chem Biol* 3: 419–428, 2008. doi:10.1021/cb800083a.

534. Matulef K, Maduke M. Side-dependent inhibition of a prokaryotic ClC by DIDS. *Biophys J* 89: 1721–1730, 2005. doi:10.1529/biophysj.105.066522.

535. Mazón MJ, Barros F, De la Peña P, Quesada JF, Escudero A, Cobo AM, Pascual-Pascual SI, Gutiérrez-Rivas E, Guillén E, Arpa J, Eraso P, Portillo F, Molano J. Screening for mutations in Spanish families with myotonia. Functional analysis of novel mutations in *CLCN1* gene. *Neuromuscul Disord* 22: 231–243, 2012. doi:10.1016/j.nmd.2011.10.013.

536. Meadows NA, Sharma SM, Faulkner GJ, Ostrowski MC, Hume DA, Cassady AI. The expression of *Clcn7* and *Ostm1* in osteoclasts is coregulated by microphthalmia transcription factor. *J Biol Chem* 282: 1891–1904, 2007. doi:10.1074/jbc.M608572200.

537. Mehrke G, Brinkmeier H, Jockusch H. The myotonic mouse mutant ADR: electrophysiology of the muscle fiber. *Muscle Nerve* 11: 440–446, 1988. doi:10.1002/mus.880110505.

538. Menichella DM, Goodenough DA, Sirkowski E, Scherer SS, Paul DL. Connexins are critical for normal myelination in the CNS. *J Neurosci* 23: 5963–5973, 2003. doi:10.1523/JNEUROSCI.23-13-05963.2003.

539. Menichella DM, Majdan M, Awatramani R, Goodenough DA, Sirkowski E, Scherer SS, Paul DL. Genetic and physiological evidence that oligodendrocyte gap junctions contribute to spatial buffering of potassium released during neuronal activity. *J Neurosci* 26: 10984–10991, 2006. doi:10.1523/JNEUROSCI.0304-06.2006.

540. Meyer-Kleine C, Steinmeyer K, Ricker K, Jentsch TJ, Koch MC. Spectrum of mutations in the major human skeletal muscle chloride channel gene (*CLCN1*) leading to myotonia. *Am J Hum Genet* 57: 1325–1334, 1995.

541. Meyer S, Dutzler R. Crystal structure of the cytoplasmic domain of the chloride channel ClC-0. *Structure* 14: 299–307, 2006. doi:10.1016/j.str.2005.10.008.

542. Meyer S, Savaresi S, Forster IC, Dutzler R. Nucleotide recognition by the cytoplasmic domain of the human chloride transporter ClC-5. *Nat Struct Mol Biol* 14: 60–67, 2007. doi:10.1038/nsmb1188.

543. Middleton RE, Pheasant DJ, Miller C. Homodimeric architecture of a ClC-type chloride ion channel. *Nature* 383: 337–340, 1996. doi:10.1038/383337a0.

544. Middleton RE, Pheasant DJ, Miller C. Purification, reconstitution, and subunit composition of a voltage-gated chloride channel from *Torpedo electroplax*. *Biochemistry* 33: 13189–13198, 1994. doi:10.1021/bi00249a005.

545. Miller C. ClC channels: reading eukaryotic function through prokaryotic spectacles. *J Gen Physiol* 122: 129–131, 2003. doi:10.1085/jgp.200308898.

546. Miller C. ClC chloride channels viewed through a transporter lens. *Nature* 440: 484–489, 2006. doi:10.1038/nature04713.

547. Miller C. In the beginning: a personal reminiscence on the origin and legacy of ClC-0, the '*Torpedo* Cl^- channel'. *J Physiol* 593: 4085–4090, 2015. doi:10.1113/jphysiol.2014.286260.

548. Miller C. Open-state substructure of single chloride channels from *Torpedo electroplax*. *Philos Trans R Soc Lond B Biol Sci* 299: 401–411, 1982. doi:10.1098/rstb.1982.0140.

549. Miller C, White MM. Dimeric structure of single chloride channels from *Torpedo* electroplax. *Proc Natl Acad Sci USA* 81: 2772–2775, 1984. doi:10.1073/pnas.81.9.2772.

550. Miller C, White MM. A voltage-dependent chloride conductance channel from *Torpedo* electroplax membrane. *Ann N Y Acad Sci* 341: 534–551, 1980. doi:10.1111/j.1749-6632.1980.tb47197.x.

551. Miller JW, Urbinati CR, Teng-Umnuay P, Stenberg MG, Byrne BJ, Thornton CA, Swanson MS. Recruitment of human muscleblind proteins to $(CUG)_{(n)}$ expansions associated with myotonic dystrophy. *EMBO J* 19: 4439–4448, 2000. doi:10.1093/emboj/19.17.4439.

552. Miloshevsky GV, Jordan PC. Anion pathway and potential energy profiles along curvilinear bacterial ClC Cl^- pores: electrostatic effects of charged residues. *Biophys J* 86: 825–835, 2004. doi:10.1016/S0006-3495(04)74158-2.

553. Mindell JA, Maduke M, Miller C, Grigorieff N. Projection structure of a ClC-type chloride channel at 6.5 A resolution. *Nature* 409: 219–223, 2001. doi:10.1038/35051631.

554. Mitchell J, Wang X, Zhang G, Gentzsch M, Nelson DJ, Shears SB. An expanded biological repertoire for Ins(3,4,5,6)P_4 through its modulation of ClC-3 function. *Curr Biol* 18: 1600–1605, 2008. doi:10.1016/j.cub.2008.08.073.

555. Miyamura N, Matsumoto K, Taguchi T, Tokunaga H, Nishikawa T, Nishida K, Toyonaga T, Sakakida M, Araki E. Atypical Bartter syndrome with sensorineural deafness with G47R mutation of the β-subunit for ClC-Ka and ClC-Kb chloride channels, barttin. *J Clin Endocrinol Metab* 88: 781–786, 2003. doi:10.1210/jc.2002-021398.

556. Miyazaki H, Kaneko T, Uchida S, Sasaki S, Takei Y. Kidney-specific chloride channel, OmClC-K, predominantly expressed in the diluting segment of freshwater-adapted tilapia kidney. *Proc Natl Acad Sci USA* 99: 15782–15787, 2002. doi:10.1073/pnas.242611099.

557. Miyazaki H, Strange K. Differential regulation of a CLC anion channel by SPAK kinase ortholog-mediated multisite phosphorylation. *Am J Physiol Cell Physiol* 302: C1702–C1712, 2012. doi:10.1152/ajpcell.00419.2011.

558. Miyazaki H, Uchida S, Takei Y, Hirano T, Marumo F, Sasaki S. Molecular cloning of CLC chloride channels in *Oreochromis mossambicus* and their functional complementation of yeast CLC gene mutant. *Biochem Biophys Res Commun* 255: 175–181, 1999. doi:10.1006/bbrc.1999.0166.

559. Mo L, Hellmich HL, Fong P, Wood T, Embesi J, Wills NK. Comparison of amphibian and human ClC-5: similarity of functional properties and inhibition by external pH. *J Membr Biol* 168: 253–264, 1999. doi:10.1007/s002329900514.

560. Mo L, Xiong W, Qian T, Sun H, Wills NK. Coexpression of complementary fragments of ClC-5 and restoration of chloride channel function in a Dent's disease mutation. *Am J Physiol Cell Physiol* 286: C79–C89, 2004. doi:10.1152/ajpcell.00009.2003.

561. Moeser AJ, Nighot PK, Engelke KJ, Ueno R, Blikslager AT. Recovery of mucosal barrier function in ischemic porcine ileum and colon is stimulated by a novel agonist of the ClC-2 chloride channel, lubiprostone. *Am J Physiol Gastrointest Liver Physiol* 292: G647–G656, 2007. doi:10.1152/ajpgi.00183.2006.

562. Moh MC, Zhang C, Luo C, Lee LH, Shen S. Structural and functional analyses of a novel ig-like cell adhesion molecule, hepaCAM, in the human breast carcinoma MCF7 cells. *J Biol Chem* 280: 27366–27374, 2005. doi:10.1074/jbc.M500852200.

563. Moh MC, Zhang T, Lee LH, Shen S. Expression of hepaCAM is downregulated in cancers and induces senescence-like growth arrest via a p53/p21-dependent pathway in human breast cancer cells. *Carcinogenesis* 29: 2298–2305, 2008. doi:10.1093/carcin/bgn226.

564. Mohammad-Panah R, Ackerley C, Rommens J, Choudhury M, Wang Y, Bear CE. The chloride channel ClC-4 co-localizes with cystic fibrosis transmembrane conductance regulator and may mediate chloride flux across the apical membrane of intestinal epithelia. *J Biol Chem* 277: 566–574, 2002. doi:10.1074/jbc.M106968200.

565. Mohammad-Panah R, Gyomorey K, Rommens J, Choudhury M, Li C, Wang Y, Bear CE. ClC-2 contributes to native chloride secretion by a human intestinal cell line, Caco-2. *J Biol Chem* 276: 8306–8313, 2001. doi:10.1074/jbc.M006764200.

566. Mohammad-Panah R, Harrison R, Dhani S, Ackerley C, Huan LJ, Wang Y, Bear CE. The chloride channel ClC-4 contributes to endosomal acidification and trafficking. *J Biol Chem* 278: 29267–29277, 2003. doi:10.1074/jbc.M304357200.

567. Mohammad-Panah R, Wellhauser L, Steinberg BE, Wang Y, Huan LJ, Liu XD, Bear CE. An essential role for ClC-4 in transferrin receptor function revealed in studies of fibroblasts derived from Clcn4-null mice. *J Cell Sci* 122: 1229–1237, 2009. doi:10.1242/jcs.037317.

568. Monteagudo LV, Tejedor MT, Ramos JJ, Lacasta D, Ferrer LM. Ovine congenital myotonia associated with a mutation in the muscle chloride channel gene. *Vet J* 204: 128–129, 2015. doi:10.1016/j.tvjl.2015.01.014.

569. Moran O, Traverso S, Elia L, Pusch M. Molecular modeling of *p*-chlorophenoxyacetic acid binding to the CLC-0 channel. *Biochemistry* 42: 5176–5185, 2003. doi:10.1021/bi027368o.

570. Moreland JG, Davis AP, Bailey G, Nauseef WM, Lamb FS. Anion channels, including ClC-3, are required for normal neutrophil oxidative function, phagocytosis, and transendothelial migration. *J Biol Chem* 281: 12277–12288, 2006. doi:10.1074/jbc.M511030200.

571. Moreland JG, Davis AP, Matsuda JJ, Hook JS, Bailey G, Nauseef WM, Lamb FS. Endotoxin priming of neutrophils requires NADPH oxidase-generated oxidants and is regulated by the anion transporter ClC-3. *J Biol Chem* 282: 33958–33967, 2007. doi:10.1074/jbc.M705289200.

572. Moss SJ, Smart TG. Constructing inhibitory synapses. *Nat Rev Neurosci* 2: 240–250, 2001. doi:10.1038/35067500.

573. Murer H, Forster I, Hernando N, Lambert G, Traebert M, Biber J. Posttranscriptional regulation of the proximal tubule NaPi-II transporter in response to PTH and dietary P(i). *Am J Physiol Renal Fluid Electrolyte Physiol* 277: F676–F684, 1999.

574. Murray CB, Morales MM, Flotte TR, McGrath-Morrow SA, Guggino WB, Zeitlin PL. ClC-2: a developmentally dependent chloride channel expressed in the fetal lung and downregulated after birth. *Am J Respir Cell Mol Biol* 12: 597–604, 1995. doi:10.1165/ajrcmb.12.6.7766424.

575. Nagasaki M, Ye L, Duan D, Horowitz B, Hume JR. Intracellular cyclic AMP inhibits native and recombinant volume-regulated chloride channels from mammalian heart. *J Physiol* 523: 705–717, 2000. doi:10.1111/j.1469-7793.2000.00705.x.

576. Neagoe I, Stauber T, Fidzinski P, Bergsdorf EY, Jentsch TJ. The late endosomal ClC-6 mediates proton/chloride countertransport in heterologous plasma membrane expression. *J Biol Chem* 285: 21689–21697, 2010. doi:10.1074/jbc.M110.125971.

577. Nehrke K, Arreola J, Nguyen HV, Pilato J, Richardson L, Okunade G, Baggs R, Shull GE, Melvin JE. Loss of hyperpolarization-activated Cl^- current in salivary acinar cells from *Clcn2* knockout mice. *J Biol Chem* 277: 23604–23611, 2002. doi:10.1074/jbc.M202900200.

578. Nehrke K, Begenisich T, Pilato J, Melvin JE. Into ion channel and transporter function. *Caenorhabditis elegans* ClC-type chloride channels: novel variants and functional expression. *Am J Physiol Cell Physiol* 279: C2052–C2066, 2000. doi:10.1152/ajpcell.2000.279.6.C2052.

579. Neusch C, Rozengurt N, Jacobs RE, Lester HA, Kofuji P. Kir4.1 potassium channel subunit is crucial for oligodendrocyte development and in vivo myelination. *J Neurosci* 21: 5429–5438, 2001. doi:10.1523/JNEUROSCI.21-15-05429.2001.

580. Neutzsky-Wulff AV, Karsdal MA, Henriksen K. Characterization of the bone phenotype in ClC-7-deficient mice. *Calcif Tissue Int* 83: 425–437, 2008. doi:10.1007/s00223-008-9185-7.

581. Neyroud N, Tesson F, Denjoy I, Leibovici M, Donger C, Barhanin J, Fauré S, Gary F, Coumel P, Petit C, Schwartz K, Guicheney P. A novel mutation in the potassium channel gene *KVLQT1* causes the Jervell and Lange-Nielsen cardioauditory syndrome. *Nat Genet* 15: 186–189, 1997. doi:10.1038/ng0297-186.

582. Nguitragool W, Miller C. CLC Cl /H^+ transporters constrained by covalent cross-linking. *Proc Natl Acad Sci USA* 104: 20659–20665, 2007. doi:10.1073/pnas.0708639104.

583. Nguitragool W, Miller C. Uncoupling of a CLC Cl^-/H^+ exchange transporter by polyatomic anions. *J Mol Biol* 362: 682–690, 2006. doi:10.1016/j.jmb.2006.07.006.

584. Nguyen CT, Agorio A, Jossier M, Depré S, Thomine S, Filleur S. Characterization of the Chloride Channel-Like, AtCLCg, Involved in Chloride Tolerance in *Arabidopsis thaliana*. *Plant Cell Physiol* 57: 764–775, 2016. doi:10.1093/pcp/pcv169.

585. Nguyen DK, Yang F, Kaul R, Alkan C, Antonellis A, Friery KF, Zhu B, de Jong PJ, Disteche CM. Clcn4-2 genomic structure differs between the X locus in *Mus spretus* and the autosomal locus in *Mus musculus*: AT motif enrichment on the X. *Genome Res* 21: 402–409, 2011. doi:10.1101/gr.108563.110.

586. Niemeyer MI, Cid LP, Sepúlveda FV, Blanz J, Auberson M, Jentsch TJ. No evidence for a role of *CLCN2* variants in idiopathic generalized epilepsy. *Nat Genet* 42: 3, 2010. doi:10.1038/ng0110-3.

587. Niemeyer MI, Cid LP, Yusef YR, Briones R, Sepúlveda FV. Voltage-dependent and -independent titration of specific residues accounts for complex gating of a ClC chloride channel by extracellular protons. *J Physiol* 587: 1387–1400, 2009. doi:10.1113/jphysiol.2008.167353.

588. Niemeyer MI, Cid LP, Zúñiga L, Catalán M, Sepúlveda FV. A conserved pore-lining glutamate as a voltage- and chloride-dependent gate in the ClC-2 chloride channel. *J Physiol* 553: 873–879, 2003. doi:10.1113/jphysiol.2003.055988.

589. Niemeyer MI, Yusef YR, Cornejo I, Flores CA, Sepúlveda FV, Cid LP. Functional evaluation of human ClC-2 chloride channel mutations associated with idiopathic generalized epilepsies. *Physiol Genomics* 19: 74–83, 2004. doi:10.1152/physiolgenomics.00070.2004.

590. Nighot MP, Nighot PK, Ma TY, Malinowska DH, Shull GE, Cuppoletti J, Blikslager AT. Genetic Ablation of the ClC-2 Cl^- Channel Disrupts Mouse Gastric Parietal Cell Acid Secretion. *PLoS One* 10: e0138174, 2015. doi:10.1371/journal.pone.0138174.

591. Nighot PK, Blikslager AT. ClC-2 regulates mucosal barrier function associated with structural changes to the villus and epithelial tight junction. *Am J Physiol Gastrointest Liver Physiol* 299: G449–G456, 2010. doi:10.1152/ajpgi.00520.2009.

592. Nin F, Hibino H, Doi K, Suzuki T, Hisa Y, Kurachi Y. The endocochlear potential depends on two K^+ diffusion potentials and an electrical barrier in the stria vascularis of the inner ear. *Proc Natl Acad Sci USA* 105: 1751–1756, 2008. doi:10.1073/pnas.0711463105.

593. Nissant A, Lourdel S, Baillet S, Paulais M, Marvao P, Teulon J, Imbert-Teboul M. Heterogeneous distribution of chloride channels along the distal convoluted tubule probed by single-cell RT-PCR and patch clamp. *Am J Physiol Renal Physiol* 287: F1233–F1243, 2004. doi:10.1152/ajprenal.00155.2004.

594. Nissant A, Paulais M, Lachheb S, Lourdel S, Teulon J. Similar chloride channels in the connecting tubule and cortical collecting duct of the mouse kidney. *Am J Physiol Renal Physiol* 290: F1421–F1429, 2006. doi:10.1152/ajprenal.00274.2005.

595. Nobile M, Pusch M, Rapisarda C, Ferroni S. Single-channel analysis of a ClC-2-like chloride conductance in cultured rat cortical astrocytes. *FEBS Lett* 479: 10–14, 2000. doi:10.1016/S0014-5793(00)01876-7.

596. Noda M, Takahashi H, Tanabe T, Toyosato M, Furutani Y, Hirose T, Asai M, Inayama S, Miyata T, Numa S. Primary structure of alpha-subunit precursor of *Torpedo californica* acetylcholine receptor deduced from cDNA sequence. *Nature* 299: 793–797, 1982. doi:10.1038/299793a0.

597. Nomura N, Kamiya K, Ikeda K, Yui N, Chiga M, Sohara E, Rai T, Sakaki S, Uchida S. Treatment with 17-allylamino-17-demethoxygeldanamycin ameliorated symptoms of Bartter syndrome type IV caused by mutated *Bsnd* in mice. *Biochem Biophys Res Commun* 441: 544–549, 2013. doi:10.1016/j.bbrc.2013.10.129.

598. Nomura N, Tajima M, Sugawara N, Morimoto T, Kondo Y, Ohno M, Uchida K, Mutig K, Bachmann S, Soleimani M, Ohta E, Ohta A, Sohara E, Okado T, Rai T, Jentsch TJ, Sasaki S, Uchida S. Generation and analyses of R8L barttin knockin mouse. *Am J Physiol Renal Physiol* 301: F297–F307, 2011. doi:10.1152/ajprenal.00604.2010.

599. Norimatsu Y, Moran AR, MacDonald KD. Lubiprostone activates CFTR, but not ClC-2, via the prostaglandin receptor ($EP(_4)$). *Biochem Biophys Res Commun* 426: 374–379, 2012. doi:10.1016/j.bbrc.2012.08.097.

600. Novarino G, Weinert S, Rickheit G, Jentsch TJ. Endosomal chloride-proton exchange rather than chloride conductance is crucial for renal endocytosis. *Science* 328: 1398–1401, 2010. doi:10.1126/science.1188070.

601. Nozu K, Inagaki T, Fu XJ, Nozu Y, Kaito H, Kanda K, Sekine T, Igarashi T, Nakanishi K, Yoshikawa N, Iijima K, Matsuo M. Molecular analysis of digenic inheritance in Bartter syndrome with sensorineural deafness. *J Med Genet* 45: 182–186, 2008. doi:10.1136/jmg.2007.052944.

602. Oana K, Oma Y, Suo S, Takahashi MP, Nishino I, Takeda S, Ishiura S. Manumycin A corrects aberrant splicing of *Clcn1* in myotonic dystrophy type 1 (DM1) mice. *Sci Rep* 3: 2142, 2013. doi:10.1038/srep02142.

603. Obermüller N, Gretz N, Kriz W, Reilly RF, Witzgall R. The swelling-activated chloride channel ClC-2, the chloride channel ClC-3, and ClC-5, a chloride channel mutated in kidney stone disease, are expressed in distinct subpopulations of renal epithelial cells. *J Clin Invest* 101: 635–642, 1998. doi:10.1172/JCI1496.

604. Ogura T, Furukawa T, Toyozaki T, Yamada K, Zheng YJ, Katayama Y, Nakaya H, Inagaki N. ClC-3B, a novel ClC-3 splicing variant that interacts with EBP50 and facilitates expression of CFTR-regulated ORCC. *FASEB J* 16: 863–865, 2002. doi:10.1096/fj.01-0845fje.

605. Oh U, Jung J. Cellular functions of TMEM16/anoctamin. *Pflugers Arch* 468: 443–453, 2016. doi:10.1007/s00424-016-1790-0.

606. Ohgi K, Okamoto F, Kajiya H, Sakagami R, Okabe K. Antibodies against ClC7 inhibit extracellular acidification-induced Cl^- currents and bone resorption activity in mouse osteoclasts. *Naunyn Schmiedebergs Arch Pharmacol* 383: 79–90, 2011. doi:10.1007/s00210-010-0576-8.

607. Ohkubo K, Matsuzaki T, Yuki M, Yoshida R, Terawaki Y, Maeyama A, Kawashima H, Ono J, Yanase T, Matsunaga A. A novel mutation of *CLCNKB* in a Japanese patient of Gitelman-like phenotype with diuretic insensitivity to thiazide administration. *Meta Gene* 2: 342–348, 2014. doi:10.1016/j.mgene.2014.04.005.

608. Ohtaki H, Ohara K, Song D, Miyamoto K, Tsumuraya T, Yofu S, Dohi K, Tanabe S, Sasaki S, Uchida S, Matsunaga M, Shioda S. Accumulation of autofluorescent storage material in brain is accelerated by ischemia in chloride channel 3 gene-deficient mice. *J Neurosci Res* 90: 2163–2172, 2012. doi:10.1002/jnr.23110.

609. Okada T, Akita T, Sato-Numata K, Islam MR, Okada Y. A newly cloned ClC-3 isoform, ClC-3d, as well as ClC-3a mediates Cd-sensitive outwardly rectifying anion currents. *Cell Physiol Biochem* 33: 539–556, 2014. doi:10.1159/000358633.

610. Okamoto F, Kajiya H, Toh K, Uchida S, Yoshikawa M, Sasaki S, Kido MA, Tanaka T, Okabe K. Intracellular ClC-3 chloride channels promote bone resorption in vitro through organelle acidification in mouse osteoclasts. *Am J Physiol Cell Physiol* 294: C693–C701, 2008. doi:10.1152/ajpcell.00251.2007.

611. Okkenhaug H, Weylandt KH, Carmena D, Wells DJ, Higgins CF, Sardini A. The human ClC-4 protein, a member of the CLC chloride channel/transporter family, is localized to the endoplasmic reticulum by its N-terminus. *FASEB J* 20: 2390–2392, 2006. doi:10.1096/fj.05-5588fje.

612. Orhan G, Fahlke C, Alekov AK. Anion- and proton-dependent gating of ClC-4 anion/proton transporter under uncoupling conditions. *Biophys J* 100: 1233–1241, 2011. doi:10.1016/j.bpj.2011.01.045.

613. Osteen JD, Mindell JA. Insights into the ClC-4 transport mechanism from studies of Zn^{2+} inhibition. *Biophys J* 95: 4668–4675, 2008. doi:10.1529/biophysj.108.137158.

614. Otte L, Wiedemann U, Schlegel B, Pires JR, Beyermann M, Schmieder P, Krause G, Volkmer-Engert R, Schneider-Mergener J, Oschkinat H. WW domain sequence activity relationships identified using ligand recognition propensities of 42 WW domains. *Protein Sci* 12: 491–500, 2003. doi:10.1110/ps.0233203.

615. Overholt KM, Rose MJ, Joshi S, Herman GE, Bajwa R, Abu-Arja R, Rangarajan HG, Horwitz EM. Hematopoietic cell transplantation for a child with OSTM1 osteopetrosis. *Blood Adv* 1: 279–281, 2016. doi:10.1182/bloodadvances.2016002345.

616. Pacheco-Alvarez D, Gamba G. WNK3 is a putative chloride-sensing kinase. *Cell Physiol Biochem* 28: 1123–1134, 2011. doi:10.1159/000335848.

617. Palade PT, Barchi RL. Characteristics of the chloride conductance in muscle fibers of the rat diaphragm. *J Gen Physiol* 69: 325–342, 1977. doi:10.1085/jgp.69.3.325.

618. Palade PT, Barchi RL. On the inhibition of muscle membrane chloride conductance by aromatic carboxylic acids. *J Gen Physiol* 69: 879–896, 1977. doi:10.1085/jgp.69.6.879.

619. Palmada M, Dieter M, Boehmer C, Waldegger S, Lang F. Serum and glucocorticoid inducible kinases functionally regulate ClC-2 channels. *Biochem Biophys Res Commun* 321: 1001–1006, 2004. doi:10.1016/j.bbrc.2004.07.064.

620. Palmer EE, Stuhlmann T, Weinert S, Haan E, Van Esch H, Holvoet M, Boyle J, Leffler M, Raynaud M, Moraine C, van Bokhoven H, Kleefstra T, Kahrizi K, Najmabadi H, Ropers HH, Delgado MR, Sirsi D, Golla S, Sommer A, Pietryga MP, Chung WK, Wynn J, Rohena L, Bernardo E, Hamlin D, Faux BM, Grange DK, Manwaring L, Tolmie J, Joss S, Cobben JM, Duijkers FAM, Goehringer JM, Challman TD, Hennig F, Fischer U, Grimme A, Suckow V, Musante L, Nicholl J, Shaw M, Lodh SP, Niu Z, Rosenfeld JA, Stankiewicz P, Jentsch TJ, Gecz J, Field M, Kalscheuer VM; DDD Study. De novo and inherited mutations in the X-linked gene *CLCN4* are associated with syndromic intellectual disability and behavior and seizure disorders in males and females. *Mol Psychiatry* 23: 222–230, 2018. doi:10.1038/mp.2016.135.

621. Palmer S, Perry J, Ashworth A. A contravention of Ohno's law in mice. *Nat Genet* 10: 472–476, 1995. doi:10.1038/ng0895-472.

622. Pandruvada SN, Beauregard J, Benjannet S, Pata M, Lazure C, Seidah NG, Vacher J. Role of Ostm1 Cytosolic Complex with Kinesin 5B in Intracellular Dispersion and Trafficking. *Mol Cell Biol* 36: 507–521, 2016. doi:10.1128/MCB.00656-15.

623. Pang Q, Chi Y, Zhao Z, Xing X, Li M, Wang O, Jiang Y, Liao R, Sun Y, Dong J, Xia W. Novel mutations of *CLCN7* cause autosomal dominant osteopetrosis type II (ADO-II) and intermediate autosomal recessive osteopetrosis (IARO) in Chinese patients. *Osteoporos Int* 27: 1047–1055, 2016. doi:10.1007/s00198-015-3320-x.

624. Pangrazio A, Poliani PL, Megarbane A, Lefranc G, Lanino E, Di Rocco M, Rucci F, Lucchini F, Ravanini M, Facchetti F, Abinun M, Vezzoni P, Villa A, Frattini A. Mutations in *OSTM1* (grey lethal) define a particularly severe form of autosomal recessive osteopetrosis with neural involvement. *J Bone Miner Res* 21: 1098–1105, 2006. doi:10.1359/jbmr.060403.

625. Papponen H, Kaisto T, Myllylä VV, Myllylä R, Metsikkö K. Regulated sarcolemmal localization of the muscle-specific ClC-1 chloride channel. *Exp Neurol* 191: 163–173, 2005. doi:10.1016/j.expneurol.2004.07.018.

626. Papponen H, Nissinen M, Kaisto T, Myllylä VV, Myllylä R, Metsikkö K. F413C and A531V but not R894X myotonia congenita mutations cause defective endoplasmic reticulum export of the muscle-specific chloride channel CLC-1. *Muscle Nerve* 37: 317–325, 2008. doi:10.1002/mus.20922.

627. Park CW, Lim JH, Youn DY, Chung S, Lim MH, Kim YK, Chang YS, Lee JH. Renal dysfunction and barttin expression in Bartter syndrome Type IV associated with a G47R mutation in *BSND* in a family. *Clin Nephrol* 75, Suppl 1: 69–74, 2011.

628. Park E, Campbell EB, MacKinnon R. Structure of a CLC chloride ion channel by cryo-electron microscopy. *Nature* 541: 500–505, 2017. doi:10.1038/nature20812.

629. Park K, Arreola J, Begenisich T, Melvin JE. Comparison of voltage-activated Cl^- channels in rat parotid acinar cells with ClC-2 in a mammalian expression system. *J Membr Biol* 163: 87–95, 1998. doi:10.1007/s002329900373.

630. Park K, Begenisich T, Melvin JE. Protein kinase A activation phosphorylates the rat ClC-2 Cl^- channel but does not change activity. *J Membr Biol* 182: 31–37, 2001. doi:10.1007/s00232-001-0026-0.

631. Pata M, Héraud C, Vacher J. OSTM1 bone defect reveals an intercellular hematopoietic crosstalk. *J Biol Chem* 283: 30522–30530, 2008. doi:10.1074/jbc.M805242200.

632. Pata M, Vacher J. Ostm1 bifunctional roles in osteoclast maturation: insights from a mouse model mimicking a human OSTM1 mutation. *J Bone Miner Res*, 2018. doi:10.1002/jbmr.3378.

633. Paulais M, Teulon J. cAMP-activated chloride channel in the basolateral membrane of the thick ascending limb of the mouse kidney. *J Membr Biol* 113: 253–260, 1990. doi:10.1007/BF01870076.

634. Pedersen SF, Klausen TK, Nilius B. The identification of a volume-regulated anion channel: an amazing Odyssey. *Acta Physiol (Oxf)* 213: 868–881, 2015. doi:10.1111/apha.12450.

635. Pedersen SF, Okada Y, Nilius B. Biophysics and Physiology of the Volume-Regulated Anion Channel (VRAC)/Volume-Sensitive Outwardly Rectifying Anion Channel (VSOR). *Pflugers Arch* 468: 371–383, 2016. doi:10.1007/s00424-015-1781-6.

636. Pedersen TH, de Paoli F, Nielsen OB. Increased excitability of acidified skeletal muscle: role of chloride conductance. *J Gen Physiol* 125: 237–246, 2005. doi:10.1085/jgp.200409173.

637. Pedersen TH, de Paoli FV, Flatman JA, Nielsen OB. Regulation of ClC-1 and K_{ATP} channels in action potential-firing fast-twitch muscle fibers. *J Gen Physiol* 134: 309–322, 2009. doi:10.1085/jgp.200910290.

638. Pedersen TH, Macdonald WA, de Paoli FV, Gurung IS, Nielsen OB. Comparison of regulated passive membrane conductance in action potential-firing fast- and slow-twitch muscle. *J Gen Physiol* 134: 323–337, 2009. doi:10.1085/jgp.200910291.

639. Pedersen TH, Nielsen OB, Lamb GD, Stephenson DG. Intracellular acidosis enhances the excitability of working muscle. *Science* 305: 1144–1147, 2004. doi:10.1126/science.1101141.

640. Pedersen TH, Riisager A, de Paoli FV, Chen TY, Nielsen OB. Role of physiological ClC-1 Cl^- ion channel regulation for the excitability and function of working skeletal muscle. *J Gen Physiol* 147: 291–308, 2016. doi:10.1085/jgp.201611582.

641. Peña-Münzenmayer G, Catalán M, Cornejo I, Figueroa CD, Melvin JE, Niemeyer MI, Cid LP, Sepúlveda FV. Basolateral localization of native ClC-2 chloride channels in absorptive intestinal epithelial cells and basolateral sorting encoded by a CBS-2 domain di-leucine motif. *J Cell Sci* 118: 4243–4252, 2005. doi:10.1242/jcs.02525.

642. Pérez-Rius C, Gaitán-Peñas H, Estévez R, Barrallo-Gimeno A. Identification and characterization of the zebrafish ClC-2 chloride channel orthologs. *Pflugers Arch* 467: 1769–1781, 2015. doi:10.1007/s00424-014-1614-z.

643. Petheö GL, Molnár Z, Róka A, Makara JK, Spät A. A pH-sensitive chloride current in the chemoreceptor cell of rat carotid body. *J Physiol* 535: 95–106, 2001. doi:10.1111/j.1469-7793.2001.00095.x.

644. Phadke SR, Fischer B, Gupta N, Ranganath P, Kabra M, Kornak U. Novel mutations in Indian patients with autosomal recessive infantile malignant osteopetrosis. *Indian J Med Res* 131: 508–514, 2010.

645. Phillips S, Brammer AE, Rodriguez L, Lim HH, Stary-Weinzinger A, Matulef K. Surprises from an unusual CLC homolog. *Biophys J* 103: L44–L46, 2012. doi:10.1016/j.bpj.2012.08.063.

646. Piala AT, Moon TM, Akella R, He H, Cobb MH, Goldsmith EJ. Chloride sensing by WNK1 involves inhibition of autophosphorylation. *Sci Signal* 7: ra41, 2014. doi:10.1126/scisignal.2005050.

647. Picollo A, Liantonio A, Babini E, Camerino DC, Pusch M. Mechanism of interaction of niflumic acid with heterologously expressed kidney CLC-K chloride channels. *J Membr Biol* 216: 73–82, 2007. doi:10.1007/s00232-007-9034-z.

648. Picollo A, Liantonio A, Didonna MP, Elia L, Camerino DC, Pusch M. Molecular determinants of differential pore blocking of kidney CLC-K chloride channels. *EMBO Rep* 5: 584–589, 2004. doi:10.1038/sj.embor.7400169.

649. Picollo A, Malvezzi M, Accardi A. Proton block of the CLC-5 Cl^-/H^+ exchanger. *J Gen Physiol* 135: 653–659, 2010. doi:10.1085/jgp.201010428.

650. Picollo A, Malvezzi M, Houtman JC, Accardi A. Basis of substrate binding and conservation of selectivity in the CLC family of channels and transporters. *Nat Struct Mol Biol* 16: 1294–1301, 2009. doi:10.1038/nsmb.1704.

651. Picollo A, Pusch M. Chloride/proton antiporter activity of mammalian CLC proteins ClC-4 and ClC-5. *Nature* 436: 420–423, 2005. doi:10.1038/nature03720.

652. Picollo A, Xu Y, Johner N, Bernèche S, Accardi A. Synergistic substrate binding determines the stoichiometry of transport of a prokaryotic H^+/Cl^- exchanger. *Nat Struct Mol Biol* 19: 525–531, 2012. doi:10.1038/nsmb.2277.

653. Pierno S, Camerino GM, Cippone V, Rolland JF, Desaphy JF, De Luca A, Liantonio A, Bianco G, Kunic JD, George AL Jr, Conte Camerino D. Statins and fenofibrate affect skeletal muscle chloride conductance in rats by differently impairing ClC-1 channel regulation and expression. *Br J Pharmacol* 156: 1206–1215, 2009. doi:10.1111/j.1476-5381.2008.00079.x.

654. Pierno S, De Luca A, Beck CL, George AL Jr, Conte Camerino D. Aging-associated down-regulation of ClC-1 expression in skeletal muscle: phenotypic-independent

relation to the decrease of chloride conductance. *FEBS Lett* 449: 12–16, 1999. doi:10.1016/S0014-5793(99)00202-1.

655. Pierno S, Desaphy JF, Liantonio A, De Bellis M, Bianco G, De Luca A, Frigeri A, Nicchia GP, Svelto M, Léoty C, George AL Jr, Camerino DC. Change of chloride ion channel conductance is an early event of slow-to-fast fibre type transition during unloading-induced muscle disuse. *Brain* 125: 1510–1521, 2002. doi:10.1093/brain/awf162.

656. Pierno S, Desaphy JF, Liantonio A, De Luca A, Zarrilli A, Mastrofrancesco L, Procino G, Valenti G, Conte Camerino D. Disuse of rat muscle in vivo reduces protein kinase C activity controlling the sarcolemma chloride conductance. *J Physiol* 584: 983–995, 2007. doi:10.1113/jphysiol.2007.141358.

657. Pifferi S, Dibattista M, Menini A. TMEM16B induces chloride currents activated by calcium in mammalian cells. *Pflugers Arch* 458: 1023–1038, 2009. doi:10.1007/s00424-009-0684-9.

658. Pinelli L, Nissant A, Edwards A, Lourdel S, Teulon J, Paulais M. Dual regulation of the native ClC-K2 chloride channel in the distal nephron by voltage and pH. *J Gen Physiol* 148: 213–226, 2016. doi:10.1085/jgp.201611623.

659. Piret SE, Gorvin CM, Trinh A, Taylor J, Lise S, Taylor JC, Ebeling PR, Thakker RV. Autosomal dominant osteopetrosis associated with renal tubular acidosis is due to a *CLCN7* mutation. *Am J Med Genet A* 170: 2988–2992, 2016. doi:10.1002/ajmg.a.37755.

660. Pirozzi G, McConnell SJ, Uveges AJ, Carter JM, Sparks AB, Kay BK, Fowlkes DM. Identification of novel human WW domain-containing proteins by cloning of ligand targets. *J Biol Chem* 272: 14611–14616, 1997. doi:10.1074/jbc.272.23.14611.

661. Piwon N, Günther W, Schwake M, Bösl MR, Jentsch TJ. ClC-5 Cl^--channel disruption impairs endocytosis in a mouse model for Dent's disease. *Nature* 408: 369–373, 2000. doi:10.1038/35042597.

662. Planells-Cases R, Lutter D, Guyader C, Gerhards NM, Ullrich F, Elger DA, Kucukosmanoglu A, Xu G, Voss FK, Reincke SM, Stauber T, Blomen VA, Vis DJ, Wessels LF, Brummelkamp TR, Borst P, Rottenberg S, Jentsch TJ. Subunit composition of VRAC channels determines substrate specificity and cellular resistance to Pt-based anti-cancer drugs. *EMBO J* 34: 2993–3008, 2015. doi:10.15252/embj.201592409.

663. Poët M, Kornak U, Schweizer M, Zdebik AA, Scheel O, Hoelter S, Wurst W, Schmitt A, Fuhrmann JC, Planells-Cases R, Mole SE, Hübner CA, Jentsch TJ. Lysosomal storage disease upon disruption of the neuronal chloride transport protein ClC-6. *Proc Natl Acad Sci USA* 103: 13854–13859, 2006. doi:10.1073/pnas.0606137103.

664. Pohl M, Shan Q, Petsch T, Styp-Rekowska B, Matthey P, Bleich M, Bachmann S, Theilig F. Short-term functional adaptation of aquaporin-1 surface expression in the proximal tubule, a component of glomerulotubular balance. *J Am Soc Nephrol* 26: 1269–1278, 2015. doi:10.1681/ASN.2014020148.

665. Ponting CP. CBS domains in CIC chloride channels implicated in myotonia and nephrolithiasis (kidney stones). *J Mol Med (Berl)* 75: 160–163, 1997.

666. Pook MA, Wrong O, Wooding C, Norden AG, Feest TG, Thakker RV. Dent's disease, a renal Fanconi syndrome with nephrocalcinosis and kidney stones, is associated with a microdeletion involving DXS255 and maps to Xp11.22. *Hum Mol Genet* 2: 2129–2134, 1993. doi:10.1093/hmg/2.12.2129.

667. Portaro S, Altamura C, Licata N, Camerino GM, Imbrici P, Musumeci O, Rodolico C, Conte Camerino D, Toscano A, Desaphy JF. Clinical, Molecular, and Functional Characterization of *CLCN1* Mutations in Three Families with Recessive Myotonia Congenita. *Neuromolecular Med* 17: 285–296, 2015. doi:10.1007/s12017-015-8356-8.

668. Pressey SN, O'Donnell KJ, Stauber T, Fuhrmann JC, Tyynelä J, Jentsch TJ, Cooper JD. Distinct neuropathologic phenotypes after disrupting the chloride transport proteins ClC-6 or ClC-7/Ostm1. *J Neuropathol Exp Neurol* 69: 1228–1246, 2010. doi:10.1097/NEN.0b013e3181ffe742.

669. Pusch M. Knocking on channel's door. The permeating chloride ion acts as the gating charge in ClC-0. *J Gen Physiol* 108: 233–236, 1996. doi:10.1085/jgp.108.4.233.

670. Pusch M. Myotonia caused by mutations in the muscle chloride channel gene *CLCN1*. *Hum Mutat* 19: 423–434, 2002. doi:10.1002/humu.10063.

671. Pusch M, Accardi A, Liantonio A, Ferrera L, De Luca A, Camerino DC, Conti F. Mechanism of block of single protopores of the *Torpedo* chloride channel ClC-0 by 2-(*p*-chlorophenoxy)butyric acid (CPB). *J Gen Physiol* 118: 45–62, 2001. doi:10.1085/jgp.118.1.45.

672. Pusch M, Accardi A, Liantonio A, Guida P, Traverso S, Camerino DC, Conti F. Mechanisms of block of muscle type CLC chloride channels (Review). *Mol Membr Biol* 19: 285–292, 2002. doi:10.1080/09687680210166938.

673. Pusch M, Jentsch TJ. Molecular physiology of voltage-gated chloride channels. *Physiol Rev* 74: 813–827, 1994. doi:10.1152/physrev.1994.74.4.813.

674. Pusch M, Jordt SE, Stein V, Jentsch TJ. Chloride dependence of hyperpolarization-activated chloride channel gates. *J Physiol* 515: 341–353, 1999. doi:10.1111/j.1469-7793.1999.341ac.x.

675. Pusch M, Liantonio A, Bertorello L, Accardi A, De Luca A, Pierno S, Tortorella V, Camerino DC. Pharmacological characterization of chloride channels belonging to the ClC family by the use of chiral clofibric acid derivatives. *Mol Pharmacol* 58: 498–507, 2000. doi:10.1124/mol.58.3.498.

676. Pusch M, Ludewig U, Jentsch TJ. Temperature dependence of fast and slow gating relaxations of ClC-0 chloride channels. *J Gen Physiol* 109: 105–116, 1997. doi:10.1085/jgp.109.1.105.

677. Pusch M, Ludewig U, Rehfeldt A, Jentsch TJ. Gating of the voltage-dependent chloride channel CIC-0 by the permeant anion. *Nature* 373: 527–531, 1995. doi:10.1038/373527a0.

678. Pusch M, Steinmeyer K, Jentsch TJ. Low single channel conductance of the major skeletal muscle chloride channel, ClC-1. *Biophys J* 66: 149–152, 1994. doi:10.1016/S0006-3495(94)80753-2.

679. Pusch M, Steinmeyer K, Koch MC, Jentsch TJ. Mutations in dominant human myotonia congenita drastically alter the voltage dependence of the ClC-1 chloride channel. *Neuron* 15: 1455–1463, 1995. doi:10.1016/0896-6273(95)90023-3.

680. Pusch M, Zifarelli G. ClC-5: Physiological role and biophysical mechanisms. *Cell Calcium* 58: 57–66, 2015. doi:10.1016/j.ceca.2014.09.007.

681. Qiu Z, Dubin AE, Mathur J, Tu B, Reddy K, Miraglia LJ, Reinhardt J, Orth AP, Patapoutian A. SWELL1, a plasma membrane protein, is an essential component of volume-regulated anion channel. *Cell* 157: 447–458, 2014. doi:10.1016/j.cell.2014.03.024.

682. Qu C, Liang F, Hu W, Shen Z, Spicer SS, Schulte BA. Expression of CLC-K chloride channels in the rat cochlea. *Hear Res* 213: 79–87, 2006. doi:10.1016/j.heares.2005.12.012.

683. Quarello P, Forni M, Barberis L, Defilippi C, Campagnoli MF, Silvestro L, Frattini A, Chalhoub N, Vacher J, Ramenghi U. Severe malignant osteopetrosis caused by a *GL* gene mutation. *J Bone Miner Res* 19: 1194–1199, 2004. doi:10.1359/JBMR.040407.

684. Quraishi IH, Raphael RM. Computational model of vectorial potassium transport by cochlear marginal cells and vestibular dark cells. *Am J Physiol Cell Physiol* 292: C591–C602, 2007. doi:10.1152/ajpcell.00560.2005.

685. Quraishi IH, Raphael RM. Generation of the endocochlear potential: a biophysical model. *Biophys J* 94: L64–L66, 2008. doi:10.1529/biophysj.107.128082.

686. Rai T, Uchida S, Sasaki S, Marumo F. Isolation and characterization of kidney-specific CLC-K2 chloride channel gene promoter. *Biochem Biophys Res Commun* 261: 432–438, 1999. doi:10.1006/bbrc.1999.1038.

687. Raja Rayan DL, Haworth A, Sud R, Matthews E, Fialho D, Burge J, Portaro S, Schorge S, Tuin K, Lunt P, McEntagart M, Toscano A, Davis MB, Hanna MG. A new explanation for recessive myotonia congenita: exon deletions and duplications in *CLCN1*. *Neurology* 78: 1953–1958, 2012. doi:10.1212/WNL.0b013e318259e19c.

688. Rajan I, Read R, Small DL, Perrard J, Vogel P. An alternative splicing variant in *Clcn7*$^{-/-}$ mice prevents osteopetrosis but not neural and retinal degeneration. *Vet Pathol* 48: 663–675, 2011. doi:10.1177/0300985810370164.

689. Rajapurohitam V, Chalhoub N, Benachenhou N, Neff L, Baron R, Vacher J. The mouse osteopetrotic grey-lethal mutation induces a defect in osteoclast maturation/function. *Bone* 28: 513–523, 2001. doi:10.1016/S8756-3282(01)00416-1.

690. Ramírez A, Faupel J, Goebel I, Stiller A, Beyer S, Stöckle C, Hasan C, Bode U, Kornak U, Kubisch C. Identification of a novel mutation in the coding region of the grey-lethal gene *OSTM1* in human malignant infantile osteopetrosis. *Hum Mutat* 23: 471–476, 2004. doi:10.1002/humu.20028.

691. Ramjeesingh M, Li C, She YM, Bear CE. Evaluation of the membrane-spanning domain of ClC-2. *Biochem J* 396: 449–460, 2006. doi:10.1042/BJ20060043.

692. Ratté S, Prescott SA. ClC-2 channels regulate neuronal excitability, not intracellular chloride levels. *J Neurosci* 31: 15838–15843, 2011. doi:10.1523/JNEUROSCI.2748-11.2011.

693. Reed AA, Loh NY, Terryn S, Lippiat JD, Partridge C, Galvanovskis J, Williams SE, Jouret F, Wu FT, Courtoy PJ, Nesbit MA, Rorsman P, Devuyst O, Ashcroft FM, Thakker RV. CLC-5 and KIF3B interact to facilitate CLC-5 plasma membrane expression, endocytosis, and microtubular transport: relevance to pathophysiology of Dent's disease. *Am J Physiol Renal Physiol* 298: F365–F380, 2010. doi:10.1152/ajprenal.00038.2009.

694. Rhodes TH, Vite CH, Giger U, Patterson DF, Fahlke C, George AL Jr. A missense mutation in canine ClC-1 causes recessive myotonia congenita in the dog. *FEBS Lett* 456: 54–58, 1999. doi:10.1016/S0014-5793(99)00926-6.

695. Riazanski V, Deriy LV, Shevchenko PD, Le B, Gomez EA, Nelson DJ. Presynaptic CLC-3 determines quantal size of inhibitory transmission in the hippocampus. *Nat Neurosci* 14: 487–494, 2011. doi:10.1038/nn.2775.

696. Riazuddin S, Anwar S, Fischer M, Ahmed ZM, Khan SY, Janssen AG, Zafar AU, Scholl U, Husnain T, Belyantseva IA, Friedman PL, Riazuddin S, Friedman TB, Fahlke C. Molecular basis of DFNB73: mutations of *BSND* can cause nonsyndromic deafness or Bartter syndrome. *Am J Hum Genet* 85: 273–280, 2009. doi:10.1016/j.ajhg.2009.07.003.

697. Richard EA, Miller C. Steady-state coupling of ion-channel conformations to a transmembrane ion gradient. *Science* 247: 1208–1210, 1990. doi:10.1126/science.2156338.

698. Richardson RC, Tarleton JC, Bird TD, Gospe SM Jr. Truncating *CLCN1* mutations in myotonia congenita: variable patterns of inheritance. *Muscle Nerve* 49: 593–600, 2014. doi:10.1002/mus.23976.

699. Rickheit G, Maier H, Strenzke N, Andreescu CE, De Zeeuw CI, Muenscher A, Zdebik AA, Jentsch TJ. Endocochlear potential depends on Cl^- channels: mechanism underlying deafness in Bartter syndrome IV. *EMBO J* 27: 2907–2917, 2008. doi:10.1038/emboj.2008.203.

700. Rickheit G, Wartosch L, Schaffer S, Stobrawa SM, Novarino G, Weinert S, Jentsch TJ. Role of ClC-5 in renal endocytosis is unique among ClC exchangers and does not require PY-motif-dependent ubiquitylation. *J Biol Chem* 285: 17595–17603, 2010. doi:10.1074/jbc.M110.115600.

701. Riisager A, de Paoli FV, Yu WP, Pedersen TH, Chen TY, Nielsen OB. Protein kinase C-dependent regulation of ClC-1 channels in active human muscle and its effect on fast and slow gating. *J Physiol* 594: 3391–3406, 2016. doi:10.1113/JP271556.

702. Rinke I, Artmann J, Stein V. ClC-2 voltage-gated channels constitute part of the background conductance and assist chloride extrusion. *J Neurosci* 30: 4776–4786, 2010. doi:10.1523/JNEUROSCI.6299-09.2010.

703. Riordan JR, Rommens JM, Kerem B, Alon N, Rozmahel R, Grzelczak Z, Zielenski J, Lok S, Plavsic N, Chou JL, et al. Identification of the cystic fibrosis gene: cloning and characterization of complementary DNA. *Science* 245: 1066–1073, 1989. doi:10.1126/science.2475911.

704. Rivera C, Voipio J, Payne JA, Ruusuvuori E, Lahtinen H, Lamsa K, Pirvola U, Saarma M, Kaila K. The K^+/Cl^- co-transporter KCC2 renders GABA hyperpolarizing during neuronal maturation. *Nature* 397: 251–255, 1999. doi:10.1038/16697.

705. Robertson JL, Kolmakova-Partensky L, Miller C. Design, function and structure of a monomeric ClC transporter. *Nature* 468: 844–847, 2010. doi:10.1038/nature09556.

706. Robinson NC, Huang P, Kaetzel MA, Lamb FS, Nelson DJ. Identification of an N-terminal amino acid of the CLC-3 chloride channel critical in phosphorylation-dependent activation of a CaMKII-activated chloride current. *J Physiol* 556: 353–368, 2004. doi:10.1113/jphysiol.2003.058032.

707. Robitaille P, Merouani A, He N, Pei Y. Bartter syndrome in two sisters with a novel mutation of the *CLCNKB* gene, one with deafness. *Eur J Pediatr* 170: 1209–1211, 2011. doi:10.1007/s00431-011-1464-z.

708. Rodríguez-Soriano J, Vallo A, Pérez de Nanclares G, Bilbao JR, Castaño L. A founder mutation in the *CLCNKB* gene causes Bartter syndrome type III in Spain. *Pediatr Nephrol* 20: 891–896, 2005. doi:10.1007/s00467-005-1867-z.

709. Romanenko VG, Nakamoto T, Catalán MA, Gonzalez-Begne M, Schwartz GJ, Jaramillo Y, Sepúlveda FV, Figueroa CD, Melvin JE. *Clcn2* encodes the hyperpolarization-activated chloride channel in the ducts of mouse salivary glands. *Am J Physiol Gastrointest Liver Physiol* 295: G1058–G1067, 2008. doi:10.1152/ajpgi.90384.2008.

710. Ronstedt K, Sternberg D, Detro-Dassen S, Gramkow T, Begemann B, Becher T, Kilian P, Grieschat M, Machtens JP, Schmalzing G, Fischer M, Fahlke C. Impaired surface membrane insertion of homo- and heterodimeric human muscle chloride channels carrying amino-terminal myotonia-causing mutations. *Sci Rep* 5: 15382, 2015. doi:10.1038/srep15382.

711. Rosenbohm A, Rüdel R, Fahlke C. Regulation of the human skeletal muscle chloride channel hClC-1 by protein kinase C. *J Physiol* 514: 677–685, 1999. doi:10.1111/j.1469-7793.1999.677ad.x.

712. Rüdel R, Lehmann-Horn F. Membrane changes in cells from myotonia patients. *Physiol Rev* 65: 310–356, 1985. doi:10.1152/physrev.1985.65.2.310.

713. Rugarli EI, Adler DA, Borsani G, Tsuchiya K, Franco B, Hauge X, Disteche C, Chapman V, Ballabio A. Different chromosomal localization of the *Clcn4* gene in *Mus spretus* and C57BL/6J mice. *Nat Genet* 10: 466–471, 1995. doi:10.1038/ng0895-466.

714. Ruivo R, Bellenchi GC, Chen X, Zifarelli G, Sagné C, Debacker C, Pusch M, Supplisson S, Gasnier B. Mechanism of proton/substrate coupling in the heptahelical lysosomal transporter cystinosin. *Proc Natl Acad Sci USA* 109: E210–E217, 2012. doi:10.1073/pnas.1115581109.

715. Ruiz-Lafuente N, Alcaraz-García MJ, Sebastián-Ruiz S, García-Serna AM, Gómez-Espuch J, Moraleda JM, Minguela A, García-Alonso AM, Parrado A. IL-4 Up-Regulates MiR-21 and the MiRNAs Hosted in the *CLCN5* Gene in Chronic Lymphocytic Leukemia. *PLoS One* 10: e0124936, 2015. doi:10.1371/journal.pone.0124936.

716. Rutledge E, Bianchi L, Christensen M, Boehmer C, Morrison R, Broslat A, Beld AM, George AL Jr, Greenstein D, Strange K. CLH-3, a ClC-2 anion channel ortholog activated during meiotic maturation in *C. elegans* oocytes. *Curr Biol* 11: 161–170, 2001. doi:10.1016/S0960-9822(01)00051-3.

717. Rutledge E, Denton J, Strange K. Cell cycle- and swelling-induced activation of a *Caenorhabditis elegans* ClC channel is mediated by CeGLC-7α/β phosphatases. *J Cell Biol* 158: 435–444, 2002. doi:10.1083/jcb.200204142.

718. Ryan A, Rüdel R, Kuchenbecker M, Fahlke C. A novel alteration of muscle chloride channel gating in myotonia levior. *J Physiol* 545: 345–354, 2002. doi:10.1113/jphysiol.2002.027037.

719. Rychkov GY, Astill DS, Bennetts B, Hughes BP, Bretag AH, Roberts ML. pH-dependent interactions of Cd^{2+} and a carboxylate blocker with the rat ClC-1 chloride channel and its R304E mutant in the Sf-9 insect cell line. *J Physiol* 501: 355–362, 1997. doi:10.1111/j.1469-7793.1997.355bn.x.

720. Rychkov GY, Pusch M, Astill DS, Roberts ML, Jentsch TJ, Bretag AH. Concentration and pH dependence of skeletal muscle chloride channel ClC-1. *J Physiol* 497: 423–435, 1996. doi:10.1113/jphysiol.1996.sp021778.

721. Rychkov GY, Pusch M, Roberts ML, Bretag AH. Interaction of hydrophobic anions with the rat skeletal muscle chloride channel ClC-1: effects on permeation and gating. *J Physiol* 530: 379–393, 2001. doi:10.1111/j.1469-7793.2001.0379k.x.

722. Rychkov GY, Pusch M, Roberts ML, Jentsch TJ, Bretag AH. Permeation and block of the skeletal muscle chloride channel, ClC-1, by foreign anions. *J Gen Physiol* 111: 653–665, 1998. doi:10.1085/jgp.111.5.653.

723. Sabirov RZ, Merzlyak PG, Islam MR, Okada T, Okada Y. The properties, functions, and pathophysiology of maxi-anion channels. *Pflugers Arch* 468: 405–420, 2016. doi:10.1007/s00424-015-1774-5.

724. Sabirov RZ, Merzlyak PG, Okada T, Islam MR, Uramoto H, Mori T, Makino Y, Matsuura H, Xie Y, Okada Y. The organic anion transporter SLCO2A1 constitutes the core component of the Maxi-Cl channel. *EMBO J* 36: 3309–3324, 2017. doi:10.15252/embj.201796685.

725. Sage CL, Marcus DC. Immunolocalization of ClC-K chloride channel in strial marginal cells and vestibular dark cells. *Hear Res* 160: 1–9, 2001. doi:10.1016/S0378-5955(01)00308-2.

726. Saint-Martin C, Gauvain G, Teodorescu G, Gourfinkel-An I, Fedirko E, Weber YG, Maljevic S, Ernst JP, Garcia-Olivares J, Fahlke C, Nabbout R, LeGuern E, Lerche H, Poncer JC, Depienne C. Two novel *CLCN2* mutations accelerating chloride channel deactivation are associated with idiopathic generalized epilepsy. *Hum Mutat* 30: 397–405, 2009. doi:10.1002/humu.20876.

727. Saito M, Hanson PI, Schlesinger P. Luminal chloride-dependent activation of endosome calcium channels: patch clamp study of enlarged endosomes. *J Biol Chem* 282: 27327–27333, 2007. doi:10.1074/jbc.M702557200.

728. Sakamoto H, Sado Y, Naito I, Kwon TH, Inoue S, Endo K, Kawasaki M, Uchida S, Nielsen S, Sasaki S, Marumo F. Cellular and subcellular immunolocalization of ClC-5 channel in mouse kidney: colocalization with H^+-ATPase. *Am J Physiol Renal Physiol* 277: F957–F965, 1999.

729. Salazar G, Love R, Styers ML, Werner E, Peden A, Rodriguez S, Gearing M, Wainer BH, Faundez V. AP-3-dependent mechanisms control the targeting of a chloride channel (ClC-3) in neuronal and non-neuronal cells. *J Biol Chem* 279: 25430–25439, 2004. doi:10.1074/jbc.M402331200.

730. Sánchez-Rodríguez JE, De Santiago-Castillo JA, Arreola J. Permeant anions contribute to voltage dependence of ClC-2 chloride channel by interacting with the protopore gate. *J Physiol* 588: 2545–2556, 2010. doi:10.1113/jphysiol.2010.189175.

731. Sánchez-Rodríguez JE, De Santiago-Castillo JA, Contreras-Vite JA, Nieto-Delgado PG, Castro-Chong A, Arreola J. Sequential interaction of chloride and proton ions with the fast gate steer the voltage-dependent gating in ClC-2 chloride channels. *J Physiol* 590: 4239–4253, 2012. doi:10.1113/jphysiol.2012.232660.

732. Sander T, Schulz H, Saar K, Gennaro E, Riggio MC, Bianchi A, Zara F, Luna D, Bulteau C, Kaminska A, Ville D, Cieuta C, Picard F, Prud'homme JF, Bate L, Sundquist A, Gardiner RM, Janssen GA, de Haan GJ, Kasteleijn-Nolst-Trenité DG, Bader A, Lindhout D, Riess O, Wienker TF, Janz D, Reis A. Genome search for susceptibility loci of common idiopathic generalised epilepsies. *Hum Mol Genet* 9: 1465–1472, 2000. doi:10.1093/hmg/9.10.1465.

733. Sardiello M, Palmieri M, di Ronza A, Medina DL, Valenza M, Gennarino VA, Di Malta C, Donaudy F, Embrione V, Polishchuk RS, Banfi S, Parenti G, Cattaneo E, Ballabio A. A gene network regulating lysosomal biogenesis and function. *Science* 325: 473–477, 2009. doi:10.1126/science.1174447.

734. Sartelet A, Stauber T, Coppieters W, Ludwig CF, Fasquelle C, Druet T, Zhang Z, Ahariz N, Cambisano N, Jentsch TJ, Charlier C. A missense mutation accelerating the gating of the lysosomal Cl^-/H^+-exchanger ClC-7/Ostm1 causes osteopetrosis with gingival hamartomas in cattle. *Dis Model Mech* 7: 119–128, 2014. doi:10.1242/dmm.012500.

735. Sasaki Y, Nagai J, Kitahara Y, Takai N, Murakami T, Takano M. Expression of chloride channel, ClC-5, and its role in receptor-mediated endocytosis of albumin in OK cells. *Biochem Biophys Res Commun* 282: 212–218, 2001. doi:10.1006/bbrc.2001.4557.

736. Sato-Numata K, Numata T, Inoue R, Okada Y. Distinct pharmacological and molecular properties of the acid-sensitive outwardly rectifying (ASOR) anion channel from those of the volume-sensitive outwardly rectifying (VSOR) anion channel. *Pflugers Arch* 468: 795–803, 2016. doi:10.1007/s00424-015-1786-1.

737. Sato-Numata K, Numata T, Okada T, Okada Y. Acid-sensitive outwardly rectifying (ASOR) anion channels in human epithelial cells are highly sensitive to temperature and independent of ClC-3. *Pflugers Arch* 465: 1535–1543, 2013. doi:10.1007/s00424-013-1296-y.

738. Satoh N, Yamada H, Yamazaki O, Suzuki M, Nakamura M, Suzuki A, Ashida A, Yamamoto D, Kaku Y, Sekine T, Seki G, Horita S. A pure chloride channel mutant of CLC-5 causes Dent's disease via insufficient V-ATPase activation. *Pflugers Arch* 468: 1183–1196, 2016. doi:10.1007/s00424-016-1808-7.

739. Saviane C, Conti F, Pusch M. The muscle chloride channel ClC-1 has a double-barreled appearance that is differentially affected in dominant and recessive myotonia. *J Gen Physiol* 113: 457–468, 1999. doi:10.1085/jgp.113.3.457.

740. Sayer JA, Stewart GS, Boese SH, Gray MA, Pearce SH, Goodship TH, Simmons NL. The voltage-dependent Cl^- channel ClC-5 and plasma membrane Cl^- conductances of mouse renal collecting duct cells (mIMCD-3). *J Physiol* 536: 769–783, 2001. doi:10.1111/j.1469-7793.2001.00769.x.

741. Schaller S, Henriksen K, Sveigaard C, Heegaard AM, Hélix N, Stahlhut M, Ovejero MC, Johansen JV, Solberg H, Andersen TL, Hougaard D, Berryman M, Shiødt CB, Sørensen BH, Lichtenberg J, Christophersen P, Foged NT, Delaissé JM, Engsig MT, Karsdal MA. The chloride channel inhibitor NS3736 prevents bone resorption in ovariectomized rats without changing bone formation. *J Bone Miner Res* 19: 1144–1153, 2004. doi:10.1359/JBMR.040302.

742. Scheel O, Zdebik AA, Lourdel S, Jentsch TJ. Voltage-dependent electrogenic chloride/proton exchange by endosomal CLC proteins. *Nature* 436: 424–427, 2005. doi:10.1038/nature03860.

743. Scheinman SJ. X-linked hypercalciuric nephrolithiasis: clinical syndromes and chloride channel mutations. *Kidney Int* 53: 3–17, 1998. doi:10.1046/j.1523-1755.1998.00718.x.

744. Scheinman SJ, Pook MA, Wooding C, Pang JT, Frymoyer PA, Thakker RV. Mapping the gene causing X-linked recessive nephrolithiasis to Xp11.22 by linkage studies. *J Clin Invest* 91: 2351–2357, 1993. doi:10.1172/JCI116467.

745. Schenck S, Wojcik SM, Brose N, Takamori S. A chloride conductance in VGLUT1 underlies maximal glutamate loading into synaptic vesicles. *Nat Neurosci* 12: 156–162, 2009. doi:10.1038/nn.2248.

746. Scheper GC, van Berkel CG, Leisle L, de Groot KE, Errami A, Jentsch TJ, Van der Knaap MS. Analysis of *CLCN2* as candidate gene for megalencephalic leukoencephalopathy with subcortical cysts. *Genet Test Mol Biomarkers* 14: 255–257, 2010. doi:10.1089/gtmb.2009.0148.

747. Scholl UI, Stölting G, Schewe J, Thiel A, Tan H, Nelson-Williams C, Vichot AA, Jin SC, Loring E, Untiet V, Yoo T, Choi J, Xu S, Wu A, Kirchner M, Mertins P, Rump LC, Onder AM, Gamble C, McKenney D, Lash RW, Jones DP, Chune G, Gagliardi P, Choi M, Gordon R, Stowasser M, Fahlke C, Lifton RP. *CLCN2* chloride channel mutations in familial hyperaldosteronism type II. *Nat Genet* 50: 349–354, 2018. doi:10.1038/s41588-018-0048-5.

748. Schlingmann KP, Konrad M, Jeck N, Waldegger P, Reinalter SC, Holder M, Seyberth HW, Waldegger S. Salt wasting and deafness resulting from mutations in two chloride channels. *N Engl J Med* 350: 1314–1319, 2004. doi:10.1056/NEJMoa032843.

749. Schmidt-Rose T, Jentsch TJ. Reconstitution of functional voltage-gated chloride channels from complementary fragments of CLC-1. *J Biol Chem* 272: 20515–20521, 1997. doi:10.1074/jbc.272.33.20515.

750. Schmidt-Rose T, Jentsch TJ. Transmembrane topology of a CLC chloride channel. *Proc Natl Acad Sci USA* 94: 7633–7638, 1997. doi:10.1073/pnas.94.14.7633.

751. Schmieder S, Lindenthal S, Ehrenfeld J. Tissue-specific *N*-glycosylation of the ClC-3 chloride channel. *Biochem Biophys Res Commun* 286: 635–640, 2001. doi:10.1006/bbrc.2001.5407.

752. Schofield PR, Darlison MG, Fujita N, Burt DR, Stephenson FA, Rodriguez H, Rhee LM, Ramachandran J, Reale V, Glencorse TA, Seeburg PH, Barnard EA. Sequence and functional expression of the GABA A receptor shows a ligand-gated receptor superfamily. *Nature* 328: 221–227, 1987. doi:10.1038/328221a0.

753. Scholey JM. Kinesin-2: a family of heterotrimeric and homodimeric motors with diverse intracellular transport functions. *Annu Rev Cell Dev Biol* 29: 443–469, 2013. doi:10.1146/annurev-cellbio-101512-122335.

754. Scholl U, Hebeisen S, Janssen AG, Müller-Newen G, Alekov A, Fahlke C. Barttin modulates trafficking and function of ClC-K channels. *Proc Natl Acad Sci USA* 103: 11411–11416, 2006. doi:10.1073/pnas.0601631103.

755. Schriever AM, Friedrich T, Pusch M, Jentsch TJ. CLC chloride channels in *Caenorhabditis elegans*. *J Biol Chem* 274: 34238–34244, 1999. doi:10.1074/jbc.274.48.34238.

756. Schroeder BC, Cheng T, Jan YN, Jan LY. Expression cloning of TMEM16A as a calcium-activated chloride channel subunit. *Cell* 134: 1019–1029, 2008. doi:10.1016/j.cell.2008.09.003.

757. Schulz P, Werner J, Stauber T, Henriksen K, Fendler K. The G215R mutation in the Cl^-/H^+-antiporter ClC-7 found in ADO II osteopetrosis does not abolish function but causes a severe trafficking defect. *PLoS One* 5: e12585, 2010. doi:10.1371/journal.pone.0012585.

758. Schulze-Bahr E, Wang Q, Wedekind H, Haverkamp W, Chen Q, Sun Y, Rubie C, Hördt M, Towbin JA, Borggrefe M, Assmann G, Qu X, Somberg JC, Breithardt G, Oberti C, Funke H. *KCNE1* mutations cause jervell and Lange-Nielsen syndrome. *Nat Genet* 17: 267–268, 1997. doi:10.1038/ng1197-267.

759. Schwake M, Friedrich T, Jentsch TJ. An internalization signal in ClC-5, an endosomal Cl^- channel mutated in Dent's disease. *J Biol Chem* 276: 12049–12054, 2001. doi:10.1074/jbc.M010642200.

760. Schwappach B, Stobrawa S, Hechenberger M, Steinmeyer K, Jentsch TJ. Golgi localization and functionally important domains in the NH_2 and COOH terminus of the yeast CLC putative chloride channel Gef1p. *J Biol Chem* 273: 15110–15118, 1998. doi:10.1074/jbc.273.24.15110.

761. Schwartzberg PL, Xing L, Hoffmann O, Lowell CA, Garrett L, Boyce BF, Varmus HE. Rescue of osteoclast function by transgenic expression of kinase-deficient Src in *src*$^{-/-}$ mutant mice. *Genes Dev* 11: 2835–2844, 1997. doi:10.1101/gad.11.21.2835.

762. Schwiebert EM, Cid-Soto LP, Stafford D, Carter M, Blaisdell CJ, Zeitlin PL, Guggino WB, Cutting GR. Analysis of ClC-2 channels as an alternative pathway for chloride conduction in cystic fibrosis airway cells. *Proc Natl Acad Sci USA* 95: 3879–3884, 1998. doi:10.1073/pnas.95.7.3879.

763. Scott JW, Hawley SA, Green KA, Anis M, Stewart G, Scullion GA, Norman DG, Hardie DG. CBS domains form energy-sensing modules whose binding of adenosine ligands is disrupted by disease mutations. *J Clin Invest* 113: 274–284, 2004. doi:10.1172/JCI19874.

764. Sekine T, Komoda F, Miura K, Takita J, Shimadzu M, Matsuyama T, Ashida A, Igarashi T. Japanese Dent disease has a wider clinical spectrum than Dent disease in Europe/USA: genetic and clinical studies of 86 unrelated patients with low-molecular-weight proteinuria. *Nephrol Dial Transplant* 29: 376–384, 2014. doi:10.1093/ndt/gft394.

765. Sethi SK, Ludwig M, Kabra M, Hari P, Bagga A. Vitamin A responsive night blindness in Dent's disease. *Pediatr Nephrol* 24: 1765–1770, 2009. doi:10.1007/s00467-009-1198-6.

766. Seyberth HW. An improved terminology and classification of Bartter-like syndromes. *Nat Clin Pract Nephrol* 4: 560–567, 2008. doi:10.1038/ncpneph0912.

767. Seyberth HW, Schlingmann KP. Bartter- and Gitelman-like syndromes: salt-losing tubulopathies with loop or DCT defects. *Pediatr Nephrol* 26: 1789–1802, 2011. doi:10.1007/s00467-011-1871-4.

768. Seys E, Andrini O, Keck M, Mansour-Hendili L, Courand PY, Simian C, Deschenes G, Kwon T, Bertholet-Thomas A, Bobrie G, Borde JS, Bourdat-Michel G, Decramer S, Cailliez M, Krug P, Cozette P, Delbet JD, Dubourg L, Chaveau D, Fila M, Jourde-Chiche N, Knebelmann B, Lavocat MP, Lemoine S, Djeddi D, Llanas B, Louillet F, Merieau E, Mileva M, Mota-Vieira L, Mousson C, Nobili F, Novo R, Roussey-Kesler G, Vrillon I, Walsh SB, Teulon J, Blanchard A, Vargas-Poussou R. Clinical and Genetic Spectrum of Bartter Syndrome Type 3. *J Am Soc Nephrol* 28: 2540–2552, 2017. doi:10.1681/ASN.2016101057.

769. Shafique S, Siddiqi S, Schraders M, Oostrik J, Ayub H, Bilal A, Ajmal M, Seco CZ, Strom TM, Mansoor A, Mazhar K, Shah ST, Hussain A, Azam M, Kremer H, Qamar R. Genetic spectrum of autosomal recessive non-syndromic hearing loss in Pakistani families. *PLoS One* 9: e100146, 2014. doi:10.1371/journal.pone.0100146.

770. Shalata A, Furman H, Adir V, Adir N, Hujeirat Y, Shalev SA, Borochowitz ZU. Myotonia congenita in a large consanguineous Arab family: insight into the clinical spectrum of carriers and double heterozygotes of a novel mutation in the chloride channel *CLCN1* gene. *Muscle Nerve* 41: 464–469, 2010. doi:10.1002/mus.21525.

771. Sherry AM, Malinowska DH, Morris RE, Ciraolo GM, Cuppoletti J. Localization of ClC-2 Cl^- channels in rabbit gastric mucosa. *Am J Physiol Cell Physiol* 280: C1599–C1606, 2001. doi:10.1152/ajpcell.2001.280.6.C1599.

772. Shimada K, Li X, Xu G, Nowak DE, Showalter LA, Weinman SA. Expression and canalicular localization of two isoforms of the ClC-3 chloride channel from rat hepatocytes. *Am J Physiol Gastrointest Liver Physiol* 279: G268–G276, 2000. doi:10.1152/ajpgi.2000.279.2.G268.

773. Shinmura K, Igarashi H, Kato H, Koda K, Ogawa H, Takahashi S, Otsuki Y, Yoneda T, Kawanishi Y, Funai K, Takayama T, Ozono S, Sugimura H. BSND and ATP6V1G3: Novel Immunohistochemical Markers for Chromophobe Renal Cell Carcinoma. *Medicine (Baltimore)* 94: e989, 2015. doi:10.1097/MD.0000000000000989.

774. Shinmura K, Kato H, Kawanishi Y, Kamo T, Inoue Y, Yoshimura K, Sugiyama K, Misawa K, Hosokawa S, Mineta H, Sugimura H. BSND is a Novel Immunohistochemical Marker for Oncocytic Salivary Gland Tumors. *Pathol Oncol Res* 24: 439–444, 2018. doi:10.1007/s12253-017-0248-9.

775. Shrimpton AE, Hoopes RR Jr, Knohl SJ, Hueber P, Reed AA, Christie PT, Igarashi T, Lee P, Lehman A, White C, Milford DV, Sanchez MR, Unwin R, Wrong OM, Thakker RV, Scheinman SJ. *OCRL1* mutations in Dent 2 patients suggest a mechanism for phenotypic variability. *Nephron, Physiol* 112: 27–36, 2009. doi:10.1159/000213506.

776. Sigworth FJ. The patch clamp is more useful than anyone had expected. *Fed Proc* 45: 2673–2677, 1986.

777. Sík A, Smith RL, Freund TF. Distribution of chloride channel-2-immunoreactive neuronal and astrocytic processes in the hippocampus. *Neuroscience* 101: 51–65, 2000. doi:10.1016/S0306-4522(00)00360-2.

778. Sile S, Velez DR, Gillani NB, Narsia T, Moore JH, George AL Jr, Vanoye CG, Williams SM. CLCNKB-T481S and essential hypertension in a Ghanaian population. *J Hypertens* 27: 298–304, 2009. doi:10.1097/HJH.0b013e3283140c9e.

779. Silva IV, Cebotaru V, Wang H, Wang XT, Wang SS, Guo G, Devuyst O, Thakker RV, Guggino WB, Guggino SE. The ClC-5 knockout mouse model of Dent's disease has renal hypercalciuria and increased bone turnover. *J Bone Miner Res* 18: 615–623, 2003. doi:10.1359/jbmr.2003.18.4.615.

780. Simon DB, Bindra RS, Mansfield TA, Nelson-Williams C, Mendonca E, Stone R, Schurman S, Nayir A, Alpay H, Bakkaloglu A, Rodriguez-Soriano J, Morales JM, Sanjad SA, Taylor CM, Pilz D, Brem A, Trachtman H, Griswold W, Richard GA, John E, Lifton RP. Mutations in the chloride channel gene, *CLCNKB*, cause Bartter's syndrome type III. *Nat Genet* 17: 171–178, 1997. doi:10.1038/ng1097-171.

781. Simon DB, Karet FE, Hamdan JM, DiPietro A, Sanjad SA, Lifton RP. Bartter's syndrome, hypokalaemic alkalosis with hypercalciuria, is caused by mutations in the Na-K-2Cl cotransporter NKCC2. *Nat Genet* 13: 183–188, 1996. doi:10.1038/ng0696-183.

782. Simon DB, Karet FE, Rodriguez-Soriano J, Hamdan JH, DiPietro A, Trachtman H, Sanjad SA, Lifton RP. Genetic heterogeneity of Bartter's syndrome revealed by mutations in the K^+ channel, ROMK. *Nat Genet* 14: 152–156, 1996. doi:10.1038/ng1096-152.

783. Simon DB, Nelson-Williams C, Bia MJ, Ellison D, Karet FE, Molina AM, Vaara I, Iwata F, Cushner HM, Koolen M, Gainza FJ, Gitleman HJ, Lifton RP. Gitelman's variant of Bartter's syndrome, inherited hypokalaemic alkalosis, is caused by mutations in the thiazide-sensitive Na-Cl cotransporter. *Nat Genet* 12: 24–30, 1996. doi:10.1038/ng0196-24.

784. Simpson BJ, Height TA, Rychkov GY, Nowak KJ, Laing NG, Hughes BP, Bretag AH. Characterization of three myotonia-associated mutations of the *CLCN1* chloride channel gene via heterologous expression. *Hum Mutat* 24: 185, 2004. doi:10.1002/humu.9260.

785. Sirisi S, Elorza-Vidal X, Arnedo T, Armand-Ugón M, Callejo G, Capdevila-Nortes X, López-Hernández T, Schulte U, Barrallo-Gimeno A, Nunes V, Gasull X, Estévez R. Depolarization causes the formation of a ternary complex between GlialCAM, MLC1 and ClC-2 in astrocytes: implications in megalencephalic leukoencephalopathy. *Hum Mol Genet* 26: 2436–2450, 2017. doi:10.1093/hmg/ddx134.

786. Sly WS, Hewett-Emmett D, Whyte MP, Yu YS, Tashian RE. Carbonic anhydrase II deficiency identified as the primary defect in the autosomal recessive syndrome of osteopetrosis with renal tubular acidosis and cerebral calcification. *Proc Natl Acad Sci USA* 80: 2752–2756, 1983. doi:10.1073/pnas.80.9.2752.

787. Smith AJ, Lippiat JD. Direct endosomal acidification by the outwardly rectifying CLC-5 Cl^-/H^+ exchanger. *J Physiol* 588: 2033–2045, 2010. doi:10.1113/jphysiol.2010.188540.

788. Smith AJ, Lippiat JD. Voltage-dependent charge movement associated with activation of the CLC-5 $2Cl^-/1H^+$ exchanger. *FASEB J* 24: 3696–3705, 2010. doi:10.1096/fj.09-150649.

789. Smith AJ, Reed AA, Loh NY, Thakker RV, Lippiat JD. Characterization of Dent's disease mutations of CLC-5 reveals a correlation between functional and cell biological consequences and protein structure. *Am J Physiol Renal Physiol* 296: F390–F397, 2009. doi:10.1152/ajprenal.90526.2008.

790. Smith RL, Clayton GH, Wilcox CL, Escudero KW, Staley KJ. Differential expression of an inwardly rectifying chloride conductance in rat brain neurons: a potential mechanism for cell-specific modulation of postsynaptic inhibition. *J Neurosci* 15: 4057–4067, 1995. doi:10.1523/JNEUROSCI.15-05-04057.1995.

791. Sobacchi C, Villa A, Schulz A, Kornak U. *CLCN7*-Related Osteopetrosis. In: *GeneReviews*, edited by Pagon RA, Adam MP, Ardinger HH, Wallace SE, Amemiya A, Bean LJH, Bird TD, Ledbetter N, Mefford HC, Smith RJH, Stephens K. Seattle, WA: Univ. of Washington, Seattle, 2007.

792. Sonawane ND, Thiagarajah JR, Verkman AS. Chloride concentration in endosomes measured using a ratioable fluorescent Cl^- indicator: evidence for chloride accumulation during acidification. *J Biol Chem* 277: 5506–5513, 2002. doi:10.1074/jbc.M110818200.

793. Souraty N, Noun P, Djambas-Khayat C, Chouery E, Pangrazio A, Villa A, Lefranc G, Frattini A, Mégarbané A. Molecular study of six families originating from the Middle-East and presenting with autosomal recessive osteopetrosis. *Eur J Med Genet* 50: 188–199, 2007. doi:10.1016/j.ejmg.2007.01.005.

794. Spät A, Hunyady L. Control of aldosterone secretion: a model for convergence in cellular signaling pathways. *Physiol Rev* 84: 489–539, 2004. doi:10.1152/physrev.00030.2003.

795. Speake T, Kajita H, Smith CP, Brown PD. Inward-rectifying anion channels are expressed in the epithelial cells of choroid plexus isolated from ClC-2 'knock-out' mice. *J Physiol* 539: 385–390, 2002. doi:10.1113/jphysiol.2001.014548.

796. Speirs HJ, Wang WY, Benjafield AV, Morris BJ. No association with hypertension of *CLCNKB* and *TNFRSF1B* polymorphisms at a hypertension locus on chromosome 1p36. *J Hypertens* 23: 1491–1496, 2005. doi:10.1097/01.hjh.0000174300.73992.cc.

797. Staley K. The role of an inwardly rectifying chloride conductance in postsynaptic inhibition. *J Neurophysiol* 72: 273–284, 1994. doi:10.1152/jn.1994.72.1.273.

798. Staley K, Smith R, Schaack J, Wilcox C, Jentsch TJ. Alteration of $GABA_A$ receptor function following gene transfer of the CLC-2 chloride channel. *Neuron* 17: 543–551, 1996. doi:10.1016/S0896-6273(00)80186-5.

799. Staub O, Gautschi I, Ishikawa T, Breitschopf K, Ciechanover A, Schild L, Rotin D. Regulation of stability and function of the epithelial Na^+ channel (ENaC) by ubiquitination. *EMBO J* 16: 6325–6336, 1997. doi:10.1093/emboj/16.21.6325.

800. Stauber T, Jentsch TJ. Chloride in vesicular trafficking and function. *Annu Rev Physiol* 75: 453–477, 2013. doi:10.1146/annurev-physiol-030212-183702.

801. Stauber T, Jentsch TJ. Sorting motifs of the endosomal/lysosomal CLC chloride transporters. *J Biol Chem* 285: 34537–34548, 2010. doi:10.1074/jbc.M110.162545.

802. Stauber T, Weinert S, Jentsch TJ. Cell biology and physiology of CLC chloride channels and transporters. *Compr Physiol* 2: 1701–1744, 2012. doi:10.1002/cphy.c110038.

803. Steinberg BE, Huynh KK, Brodovitch A, Jabs S, Stauber T, Jentsch TJ, Grinstein S. A cation counterflux supports lysosomal acidification. *J Cell Biol* 189: 1171–1186, 2010. doi:10.1083/jcb.200911083.

804. Steinke KV, Gorinski N, Wojciechowski D, Todorov V, Guseva D, Ponimaskin E, Fahlke C, Fischer M. Human CLC-K Channels Require Palmitoylation of Their Accessory Subunit Barttin to Be Functional. *J Biol Chem* 290: 17390–17400, 2015. doi:10.1074/jbc.M114.631705.

805. Steinmeyer K, Klocke R, Ortland C, Gronemeier M, Jockusch H, Gründer S, Jentsch TJ. Inactivation of muscle chloride channel by transposon insertion in myotonic mice. *Nature* 354: 304–308, 1991. doi:10.1038/354304a0.

806. Steinmeyer K, Lorenz C, Pusch M, Koch MC, Jentsch TJ. Multimeric structure of ClC-1 chloride channel revealed by mutations in dominant myotonia congenita (Thomsen). *EMBO J* 13: 737–743, 1994.

807. Steinmeyer K, Ortland C, Jentsch TJ. Primary structure and functional expression of a developmentally regulated skeletal muscle chloride channel. *Nature* 354: 301–304, 1991. doi:10.1038/354301a0.

808. Steinmeyer K, Schwappach B, Bens M, Vandewalle A, Jentsch TJ. Cloning and functional expression of rat CLC-5, a chloride channel related to kidney disease. *J Biol Chem* 270: 31172–31177, 1995. doi:10.1074/jbc.270.52.31172.

809. Steward CG. Neurological aspects of osteopetrosis. *Neuropathol Appl Neurobiol* 29: 87–97, 2003. doi:10.1046/j.1365-2990.2003.00474.x.

810. Stobrawa SM, Breiderhoff T, Takamori S, Engel D, Schweizer M, Zdebik AA, Bösl MR, Ruether K, Jahn H, Draguhn A, Jahn R, Jentsch TJ. Disruption of ClC-3, a chloride channel expressed on synaptic vesicles, leads to a loss of the hippocampus. *Neuron* 29: 185–196, 2001. doi:10.1016/S0896-6273(01)00189-1.

811. Stockbridge RB, Lim HH, Otten R, Williams C, Shane T, Weinberg Z, Miller C. Fluoride resistance and transport by riboswitch-controlled CLC antiporters. *Proc Natl Acad Sci USA* 109: 15289–15294, 2012. doi:10.1073/pnas.1210896109.

812. Stogmann E, Lichtner P, Baumgartner C, Schmied M, Hotzy C, Asmus F, Leutmezer F, Bonelli S, Assem-Hilger E, Vass K, Hatala K, Strom TM, Meitinger T, Zimprich F, Zimprich A. Mutations in the *CLCN2* gene are a rare cause of idiopathic generalized epilepsy syndromes. *Neurogenetics* 7: 265–268, 2006. doi:10.1007/s10048-006-0057-x.

813. Stölting G, Bungert-Plümke S, Franzen A, Fahlke C. Carboxyl-terminal Truncations of ClC-Kb Abolish Channel Activation by Barttin Via Modified Common Gating and Trafficking. *J Biol Chem* 290: 30406–30416, 2015. doi:10.1074/jbc.M115.675827.

814. Stölting G, Fischer M, Fahlke C. ClC-1 and ClC-2 form hetero-dimeric channels with novel protopore functions. *Pflugers Arch* 466: 2191–2204, 2014. doi:10.1007/s00424-014-1490-6.

815. Stölting G, Teodorescu G, Begemann B, Schubert J, Nabbout R, Toliat MR, Sander T, Nürnberg P, Lerche H, Fahlke C. Regulation of ClC-2 gating by intracellular ATP. *Pflugers Arch* 465: 1423–1437, 2013. doi:10.1007/s00424-013-1286-0.

816. Strange K. Putting the pieces together: a crystal clear window into CLC anion channel regulation. *Channels (Austin)* 5: 101–105, 2011. doi:10.4161/chan.5.2.14694.

817. Suetterlin K, Männikkö R, Hanna MG. Muscle channelopathies: recent advances in genetics, pathophysiology and therapy. *Curr Opin Neurol* 27: 583–590, 2014. doi:10.1097/WCO.0000000000000127.

818. Sun H, Tsunenari T, Yau KW, Nathans J. The vitelliform macular dystrophy protein defines a new family of chloride channels. *Proc Natl Acad Sci USA* 99: 4008–4013, 2002. doi:10.1073/pnas.052692999.

819. Supanchart C, Wartosch L, Schlack C, Kühnisch J, Felsenberg D, Fuhrmann JC, de Vernejoul MC, Jentsch TJ, Kornak U. ClC-7 expression levels critically regulate bone turnover, but not gastric acid secretion. *Bone* 58: 92–102, 2014. doi:10.1016/j.bone.2013.09.022.

820. Suzuki T, Rai T, Hayama A, Sohara E, Suda S, Itoh T, Sasaki S, Uchida S. Intracellular localization of ClC chloride channels and their ability to form hetero-oligomers. *J Cell Physiol* 206: 792–798, 2006. doi:10.1002/jcp.20516.

821. Syeda R, Qiu Z, Dubin AE, Murthy SE, Florendo MN, Mason DE, Mathur J, Cahalan SM, Peters EC, Montal M, Patapoutian A. LRRC8 Proteins Form Volume-Regulated Anion Channels that Sense Ionic Strength. *Cell* 164: 499–511, 2016. doi:10.1016/j.cell.2015.12.031.

822. Tajima M, Hayama A, Rai T, Sasaki S, Uchida S. Barttin binds to the outer lateral surface of the ClC-K2 chloride channel. *Biochem Biophys Res Commun* 362: 858–864, 2007. doi:10.1016/j.bbrc.2007.08.097.

823. Tajima T, Nawate M, Takahashi Y, Mizoguchi Y, Sugihara S, Yoshimoto M, Murakami M, Adachi M, Tachibana K, Mochizuki H, Fujieda K. Molecular analysis of the *CLCNKB* gene in Japanese patients with classic Bartter syndrome. *Endocr J* 53: 647–652, 2006. doi:10.1507/endocrj.K06-034.

824. Takamori S, Holt M, Stenius K, Lemke EA, Grønborg M, Riedel D, Urlaub H, Schenck S, Brügger B, Ringler P, Müller SA, Rammner B, Gräter F, Hub JS, De Groot BL, Mieskes G, Moriyama Y, Klingauf J, Grubmüller H, Heuser J, Wieland F, Jahn R. Molecular anatomy of a trafficking organelle. *Cell* 127: 831–846, 2006. doi:10.1016/j.cell.2006.10.030.

825. Tan H, Bungert-Plümke S, Fahlke C, Stölting G. Reduced Membrane Insertion of CLC-K by V33L Barttin Results in Loss of Hearing, but Leaves Kidney Function Intact. *Front Physiol* 8: 269, 2017. doi:10.3389/fphys.2017.00269.

826. Tanaka K, Terryn S, Geffers L, Garbay S, Pontoglio M, Devuyst O. The transcription factor HNF1α regulates expression of chloride-proton exchanger ClC-5 in the renal proximal tubule. *Am J Physiol Renal Physiol* 299: F1339–F1347, 2010. doi:10.1152/ajprenal.00077.2010.

827. Tang CY, Chen TY. Physiology and pathophysiology of CLC-1: mechanisms of a chloride channel disease, myotonia. *J Biomed Biotechnol* 2011: 685328, 2011. doi:10.1155/2011/685328.

828. Tank DW, Miller C, Webb WW. Isolated-patch recording from liposomes containing functionally reconstituted chloride channels from *Torpedo* electroplax. *Proc Natl Acad Sci USA* 79: 7749–7753, 1982. doi:10.1073/pnas.79.24.7749.

829. Tavira B, Gómez J, Ortega F, Tranche S, Díaz-Corte C, Alvarez F, Ortiz A, Santos F, Sánchez-Niño MD, Coto E. A *CLCNKA* polymorphism (rs10927887; p.Arg83Gly) previously linked to heart failure is associated with the estimated glomerular filtration rate in the RENASTUR cohort. *Gene* 527: 670–672, 2013. doi:10.1016/j.gene.2013.06.055.

830. Terker AS, Zhang C, Erspamer KJ, Gamba G, Yang CL, Ellison DH. Unique chloride-sensing properties of WNK4 permit the distal nephron to modulate potassium homeostasis. *Kidney Int* 89: 127–134, 2016. doi:10.1038/ki.2015.289.

831. Terryn S, Tanaka K, Lengelé JP, Olinger E, Dubois-Laforgue D, Garbay S, Kozyraki R, Van Der Smissen P, Christensen EI, Courtoy PJ, Bellanné-Chantelot C, Timsit J, Pontoglio M, Devuyst O. Tubular proteinuria in patients with HNF1α mutations:

HNF1α drives endocytosis in the proximal tubule. *Kidney Int* 89: 1075–1089, 2016. doi:10.1016/j.kint.2016.01.027.

832. Thiemann A, Gründer S, Pusch M, Jentsch TJ. A chloride channel widely expressed in epithelial and non-epithelial cells. *Nature* 356: 57–60, 1992. doi:10.1038/356057a0.

833. Thompson CH, Fields DM, Olivetti PR, Fuller MD, Zhang ZR, Kubanek J, McCarty NA. Inhibition of ClC-2 chloride channels by a peptide component or components of scorpion venom. *J Membr Biol* 208: 65–76, 2005. doi:10.1007/s00232-005-0818-8.

834. Thompson CH, Olivetti PR, Fuller MD, Freeman CS, McMaster D, French RJ, Pohl J, Kubanek J, McCarty NA. Isolation and characterization of a high affinity peptide inhibitor of ClC-2 chloride channels. *J Biol Chem* 284: 26051–26062, 2009. doi:10.1074/jbc.M109.031724.

835. Thomsen J. Tonische Krämpfe in willkürlich beweglichen Muskeln in Folge von ererbter psychischer Disposition. *Arch Psychiatr Nervenkr* 6: 702–718, 1876. doi:10.1007/BF02164912.

836. Tosetto E, Addis M, Caridi G, Meloni C, Emma F, Vergine G, Stringini G, Papalia T, Barbano G, Ghiggeri GM, Ruggeri L, Miglietti N, D Angelo A, Melis MA, Anglani F. Locus heterogeneity of Dent's disease: OCRL1 and TMEM27 genes in patients with no CLCN5 mutations. *Pediatr Nephrol* 24: 1967–1973, 2009. doi:10.1007/s00467-009-1228-4.

837. Tosetto E, Casarin A, Salviati L, Familiari A, Lieske JC, Anglani F. Complexity of the 5'UTR region of the *CLCN5* gene: eleven 5'UTR ends are differentially expressed in the human kidney. *BMC Med Genomics* 7: 41, 2014. doi:10.1186/1755-8794-7-41.

838. Traverso S, Elia L, Pusch M. Gating competence of constitutively open CLC-0 mutants revealed by the interaction with a small organic Inhibitor. *J Gen Physiol* 122: 295–306, 2003. doi:10.1085/jgp.200308784.

839. Traverso S, Zifarelli G, Aiello R, Pusch M. Proton sensing of CLC-0 mutant E166D. *J Gen Physiol* 127: 51–65, 2006. doi:10.1085/jgp.200509340.

840. Tricarico D, Conte Camerino D, Govoni S, Bryant SH. Modulation of rat skeletal muscle chloride channels by activators and inhibitors of protein kinase C. *Pflugers Arch* 418: 500–503, 1991. doi:10.1007/BF00497778.

841. Tseng PY, Bennetts B, Chen TY. Cytoplasmic ATP inhibition of CLC-1 is enhanced by low pH. *J Gen Physiol* 130: 217–221, 2007. doi:10.1085/jgp.200709817.

842. Tseng PY, Yu WP, Liu HY, Zhang XD, Zou X, Chen TY. Binding of ATP to the CBS domains in the C-terminal region of CLC-1. *J Gen Physiol* 137: 357–368, 2011. doi:10.1085/jgp.201010495.

843. Tsujino A, Kaibara M, Hayashi H, Eguchi H, Nakayama S, Sato K, Fukuda T, Tateishi Y, Shirabe S, Taniyama K, Kawakami A. A *CLCN1* mutation in dominant myotonia congenita impairs the increment of chloride conductance during repetitive depolarization. *Neurosci Lett* 494: 155–160, 2011. doi:10.1016/j.neulet.2011.03.002.

844. Uchida S, Rai T, Yatsushige H, Matsumura Y, Kawasaki M, Sasaki S, Marumo F. Isolation and characterization of kidney-specific ClC-K1 chloride channel gene promoter. *Am J Physiol Renal Fluid Electrolyte Physiol* 274: F602–F610, 1998.

845. Uchida S, Sasaki S, Furukawa T, Hiraoka M, Imai T, Hirata Y, Marumo F. Molecular cloning of a chloride channel that is regulated by dehydration and expressed predominantly in kidney medulla [published erratum appears in J Biol Chem 1994 Jul 22; 269(29):19192]. *J Biol Chem* 268: 3821–3824, 1993.

846. Uchida S, Sasaki S, Marumo F. Isolation of a novel zinc finger repressor that regulates the kidney-specific CLC-K1 promoter. *Kidney Int* 60: 416–421, 2001. doi:10.1046/j.1523-1755.2001.060002416.x.

847. Uchida S, Sasaki S, Nitta K, Uchida K, Horita S, Nihei H, Marumo F. Localization and functional characterization of rat kidney-specific chloride channel, ClC-K1. *J Clin Invest* 95: 104–113, 1995. doi:10.1172/JCI117626.

848. Uchida S, Tanaka Y, Ito H, Saitoh-Ohara F, Inazawa J, Yokoyama KK, Sasaki S, Marumo F. Transcriptional regulation of the CLC-K1 promoter by myc-associated zinc finger protein and kidney-enriched Krüppel-like factor, a novel zinc finger repressor. *Mol Cell Biol* 20: 7319–7331, 2000. doi:10.1128/MCB.20.19.7319-7331.2000.

849. Ugarte G, Delgado R, O'Day PM, Farjah F, Cid LP, Vergara C, Bacigalupo J. Putative ClC-2 chloride channel mediates inward rectification in *Drosophila* retinal photoreceptors. *J Membr Biol* 207: 151–160, 2005. doi:10.1007/s00232-005-0810-3.

850. Van den Hove MF, Croizet-Berger K, Jouret F, Guggino SE, Guggino WB, Devuyst O, Courtoy PJ. The loss of the chloride channel, ClC-5, delays apical iodide efflux and induces a euthyroid goiter in the mouse thyroid gland. *Endocrinology* 147: 1287–1296, 2006. doi:10.1210/en.2005-1149.

851. Van Mil HG, Geukes Foppen RJ, Siegenbeek van Heukelom J. The influence of bumetanide on the membrane potential of mouse skeletal muscle cells in isotonic and hypertonic media. *Br J Pharmacol* 120: 39–44, 1997. doi:10.1038/sj.bjp.0700887.

852. Van Slegtenhorst MA, Bassi MT, Borsani G, Wapenaar MC, Ferrero GB, de Conciliis L, Rugarli EI, Grillo A, Franco B, Zoghbi HY, Ballabio A. A gene from the Xp22.3 region shares homology with voltage-gated chloride channels. *Hum Mol Genet* 3: 547–552, 1994. doi:10.1093/hmg/3.4.547.

853. Vandewalle A, Cluzeaud F, Bens M, Kieferle S, Steinmeyer K, Jentsch TJ. Localization and induction by dehydration of ClC-K chloride channels in the rat kidney. *Am J Physiol Renal Fluid Electrolyte Physiol* 272: F678–F688, 1997.

854. Vandewalle A, Cluzeaud F, Peng KC, Bens M, Lüchow A, Günther W, Jentsch TJ. Tissue distribution and subcellular localization of the ClC-5 chloride channel in rat intestinal cells. *Am J Physiol Cell Physiol* 280: C373–C381, 2001. doi:10.1152/ajpcell.2001.280.2.C373.

855. Vanoye CG, George AL Jr. Functional characterization of recombinant human ClC-4 chloride channels in cultured mammalian cells. *J Physiol* 539: 373–383, 2002. doi:10.1113/jphysiol.2001.013115.

856. Varela D, Niemeyer MI, Cid LP, Sepúlveda FV. Effect of an N-terminus deletion on voltage-dependent gating of the ClC-2 chloride channel. *J Physiol* 544: 363–372, 2002. doi:10.1113/jphysiol.2002.026096.

857. Veeramah KR, Johnstone L, Karafet TM, Wolf D, Sprissler R, Salogiannis J, Barth-Maron A, Greenberg ME, Stuhlmann T, Weinert S, Jentsch TJ, Pazzi M, Restifo LL, Talwar D, Erickson RP, Hammer MF. Exome sequencing reveals new causal mutations in children with epileptic encephalopathies. *Epilepsia* 54: 1270–1281, 2013. doi:10.1111/epi.12201.

858. Vetter DE, Mann JR, Wangemann P, Liu J, McLaughlin KJ, Lesage F, Marcus DC, Lazdunski M, Heinemann SF, Barhanin J. Inner ear defects induced by null mutation of the isk gene. *Neuron* 17: 1251–1264, 1996. doi:10.1016/S0896-6273(00)80255-X.

859. Vicinanza M, Di Campli A, Polishchuk E, Santoro M, Di Tullio G, Godi A, Levtchenko E, De Leo MG, Polishchuk R, Sandoval L, Marzolo MP, De Matteis MA. OCRL controls trafficking through early endosomes via PtdIns4,5P_2-dependent regulation of endosomal actin. *EMBO J* 30: 4970–4985, 2011. doi:10.1038/emboj.2011.354.

860. Vien M, Basilio D, Leisle L, Accardi A. Probing the conformation of a conserved glutamic acid within the Cl^- pathway of a CLC H^+/Cl^- exchanger. *J Gen Physiol* 149: 523–529, 2017. doi:10.1085/jgp.201611682.

861. Vindas-Smith R, Fiore M, Vásquez M, Cuenca P, Del Valle G, Lagostena L, Gaitán-Peñas H, Estévez R, Pusch M, Morales F. Identification and Functional Characterization of *CLCN1* Mutations Found in Nondystrophic Myotonia Patients. *Hum Mutat* 37: 74–83, 2016. doi:10.1002/humu.22916.

862. Vitzthum H, Castrop H, Meier-Meitinger M, Riegger GA, Kurtz A, Krämer BK, Wolf K. Nephron specific regulation of chloride channel CLC-K2 mRNA in the rat. *Kidney Int* 61: 547–554, 2002. doi:10.1046/j.1523-1755.2002.00165.x.

863. Von der Fecht-Bartenbach J, Bogner M, Dynowski M, Ludewig U. CLC-b-mediated NO^-_3/H^+ exchange across the tonoplast of *Arabidopsis* vacuoles. *Plant Cell Physiol* 51: 960–968, 2010. doi:10.1093/pcp/pcq062.

864. Von der Fecht-Bartenbach J, Bogner M, Krebs M, Stierhof YD, Schumacher K, Ludewig U. Function of the anion transporter AtCLC-d in the *trans*-Golgi network. *Plant J* 50: 466–474, 2007. doi:10.1111/j.1365-313X.2007.03061.x.

865. Voss FK, Ullrich F, Münch J, Lazarow K, Lutter D, Mah N, Andrade-Navarro MA, von Kries JP, Stauber T, Jentsch TJ. Identification of LRRC8 heteromers as an essential component of the volume-regulated anion channel VRAC. *Science* 344: 634–638, 2014. doi:10.1126/science.1252826.

866. Wächter A, Schwappach B. The yeast CLC chloride channel is proteolytically processed by the furin-like protease Kex2p in the first extracellular loop. *FEBS Lett* 579: 1149–1153, 2005. doi:10.1016/j.febslet.2005.01.011.

867. Waguespack SG, Koller DL, White KE, Fishburn T, Carn G, Buckwalter KA, Johnson M, Kocisko M, Evans WE, Foroud T, Econs MJ. Chloride channel 7 (*ClCN7*) gene

mutations and autosomal dominant osteopetrosis, type II. *J Bone Miner Res* 18: 1513–1518, 2003. doi:10.1359/jbmr.2003.18.8.1513.

868. Waldegger S, Jeck N, Barth P, Peters M, Vitzthum H, Wolf K, Kurtz A, Konrad M, Seyberth HW. Barttin increases surface expression and changes current properties of ClC-K channels. *Pflugers Arch* 444: 411–418, 2002. doi:10.1007/s00424-002-0819-8.

869. Waldegger S, Jentsch TJ. Functional and structural analysis of ClC-K chloride channels involved in renal disease. *J Biol Chem* 275: 24527–24533, 2000. doi:10.1074/jbc.M001987200.

870. Walden M, Accardi A, Wu F, Xu C, Williams C, Miller C. Uncoupling and turnover in a Cl^-/H^+ exchange transporter. *J Gen Physiol* 129: 317–329, 2007. doi:10.1085/jgp.200709756.

871. Wang B, Xie J, He HY, Huang EW, Cao QH, Luo L, Liao YS, Guo Y. Suppression of CLC-3 chloride channel reduces the aggressiveness of glioma through inhibiting nuclear factor-κB pathway. *Oncotarget* 8: 63788–63798, 2017. doi:10.18632/oncotarget.19093.

872. Wang D, Voth GA. Proton transport pathway in the ClC Cl^-/H^+ antiporter. *Biophys J* 97: 121–131, 2009. doi:10.1016/j.bpj.2009.04.038.

873. Wang H, Huo N, Li F, Fu S, Xue Y, Yang T, Wen X, Ding Y, Duan X. Osteogenic role of endosomal chloride channels in MC3T3-E1 cells. *Mol Cell Biochem* 342: 191–199, 2010. doi:10.1007/s11010-010-0483-9.

874. Wang H, Pan M, Ni J, Zhang Y, Zhang Y, Gao S, Liu J, Wang Z, Zhang R, He H, Wu B, Duan X. ClC-7 Deficiency Impairs Tooth Development and Eruption. *Sci Rep* 6: 19971, 2016. doi:10.1038/srep19971.

875. Wang H, Xu M, Kong Q, Sun P, Yan F, Tian W, Wang X. Research and progress on ClC-2 (Review). *Mol Med Rep* 16: 11–22, 2017. doi:10.3892/mmr.2017.6600.

876. Wang J, Xu H, Morishima S, Tanabe S, Jishage K, Uchida S, Sasaki S, Okada Y, Shimizu T. Single-channel properties of volume-sensitive Cl^- channel in ClC-3-deficient cardiomyocytes. *Jpn J Physiol* 55: 379–383, 2005. doi:10.2170/jjphysiol.S655.

877. Wang L, Ma W, Zhu L, Ye D, Li Y, Liu S, Li H, Zuo W, Li B, Ye W, Chen L. ClC-3 is a candidate of the channel proteins mediating acid-activated chloride currents in nasopharyngeal carcinoma cells. *Am J Physiol Cell Physiol* 303: C14–C23, 2012. doi:10.1152/ajpcell.00145.2011.

878. Wang SS, Devuyst O, Courtoy PJ, Wang XT, Wang H, Wang Y, Thakker RV, Guggino S, Guggino WB. Mice lacking renal chloride channel, CLC-5, are a model for Dent's disease, a nephrolithiasis disorder associated with defective receptor-mediated endocytosis. *Hum Mol Genet* 9: 2937–2945, 2000. doi:10.1093/hmg/9.20.2937.

879. Wang T, Weinman SA. Involvement of chloride channels in hepatic copper metabolism: ClC-4 promotes copper incorporation into ceruloplasmin. *Gastroenterology* 126: 1157–1166, 2004. doi:10.1053/j.gastro.2004.01.015.

880. Wang X, Anglani F, Beara-Lasic L, Mehta AJ, Vaughan LE, Herrera Hernandez L, Cogal A, Scheinman SJ, Ariceta G, Isom R, Copelovitch L, Enders FT, Del Prete D, Vezzoli G, Paglialonga F, Harris PC, Lieske JC; Investigators of the Rare Kidney Stone Consortium. Glomerular Pathology in Dent Disease and Its Association with Kidney Function. *Clin J Am Soc Nephrol* 11: 2168–2176, 2016. doi:10.2215/CJN.03710416.

881. Wang XQ, Deriy LV, Foss S, Huang P, Lamb FS, Kaetzel MA, Bindokas V, Marks JD, Nelson DJ. CLC-3 channels modulate excitatory synaptic transmission in hippocampal neurons. *Neuron* 52: 321–333, 2006. doi:10.1016/j.neuron.2006.08.035.

882. Wang Y, Cai H, Cebotaru L, Hryciw DH, Weinman EJ, Donowitz M, Guggino SE, Guggino WB. ClC-5: role in endocytosis in the proximal tubule. *Am J Physiol Renal Physiol* 289: F850–F862, 2005. doi:10.1152/ajprenal.00011.2005.

883. Wang Y, Du X, Bin R, Yu S, Xia Z, Zheng G, Zhong J, Zhang Y, Jiang YH, Wang Y. Genetic Variants Identified from Epilepsy of Unknown Etiology in Chinese Children by Targeted Exome Sequencing. *Sci Rep* 7: 40319, 2017. doi:10.1038/srep40319.

884. Wangemann P. Supporting sensory transduction: cochlear fluid homeostasis and the endocochlear potential. *J Physiol* 576: 11–21, 2006. doi:10.1113/jphysiol.2006.112888.

885. Wangemann P, Wittner M, Di Stefano A, Englert HC, Lang HJ, Schlatter E, Greger R. Cl^--channel blockers in the thick ascending limb of the loop of Henle. Structure activity relationship. *Pflugers Arch* 407, Suppl 2: S128–S141, 1986. doi:10.1007/BF00584942.

886. Warnstedt M, Sun C, Poser B, Escriva MJ, Tranebjaerg L, Torbergsen T, van Ghelue M, Fahlke C. The myotonia congenita mutation A331T confers a novel hyperpolarization-activated gate to the muscle chloride channel ClC-1. *J Neurosci* 22: 7462–7470, 2002. doi:10.1523/JNEUROSCI.22-17-07462.2002.

887. Warsi J, Hosseinzadeh Z, Elvira B, Bissinger R, Shumilina E, Lang F. Regulation of ClC-2 activity by SPAK and OSR1. *Kidney Blood Press Res* 39: 378–387, 2014. doi:10.1159/000355816.

888. Wartosch L, Fuhrmann JC, Schweizer M, Stauber T, Jentsch TJ. Lysosomal degradation of endocytosed proteins depends on the chloride transport protein ClC-7. *FASEB J* 23: 4056–4068, 2009. doi:10.1096/fj.09-130880.

889. Watanabe M, Fukuda A. Development and regulation of chloride homeostasis in the central nervous system. *Front Cell Neurosci* 9: 371, 2015. doi:10.3389/fncel.2015.00371.

890. Waters CW, Varuzhanyan G, Talmadge RJ, Voss AA. Huntington disease skeletal muscle is hyperexcitable owing to chloride and potassium channel dysfunction. *Proc Natl Acad Sci USA* 110: 9160–9165, 2013. doi:10.1073/pnas.1220068110.

891. Watkins WJ, Watts DC. Biological features of the new A2G–adr mouse mutant with abnormal muscle function. *Lab Anim* 18: 1–6, 1984. doi:10.1258/002367784780865036.

892. Wege S, De Angeli A, Droillard MJ, Kroniewicz L, Merlot S, Cornu D, Gambale F, Martinoia E, Barbier-Brygoo H, Thomine S, Leonhardt N, Filleur S. Phosphorylation of the vacuolar anion exchanger AtCLCa is required for the stomatal response to abscisic acid. *Sci Signal* 7: ra65, 2014. doi:10.1126/scisignal.2005140.

893. Wege S, Jossier M, Filleur S, Thomine S, Barbier-Brygoo H, Gambale F, De Angeli A. The proline 160 in the selectivity filter of the Arabidopsis NO_3^-/H^+ exchanger AtCLCa is essential for nitrate accumulation in planta. *Plant J* 63: 861–869, 2010. doi:10.1111/j.1365-313X.2010.04288.x.

894. Weinberger S, Wojciechowski D, Sternberg D, Lehmann-Horn F, Jurkat-Rott K, Becher T, Begemann B, Fahlke C, Fischer M. Disease-causing mutations C277R and C277Y modify gating of human ClC-1 chloride channels in myotonia congenita. *J Physiol* 590: 3449–3464, 2012. doi:10.1113/jphysiol.2012.232785.

895. Weinert S, Jabs S, Hohensee S, Chan WL, Kornak U, Jentsch TJ. Transport activity and presence of ClC-7/Ostm1 complex account for different cellular functions. *EMBO Rep* 15: 784–791, 2014. doi:10.15252/embr.201438553.

896. Weinert S, Jabs S, Supanchart C, Schweizer M, Gimber N, Richter M, Rademann J, Stauber T, Kornak U, Jentsch TJ. Lysosomal pathology and osteopetrosis upon loss of H^+-driven lysosomal Cl^- accumulation. *Science* 328: 1401–1403, 2010. doi:10.1126/science.1188072.

897. Weinreich F, Jentsch TJ. Pores formed by single subunits in mixed dimers of different CLC chloride channels. *J Biol Chem* 276: 2347–2353, 2001. doi:10.1074/jbc.M005733200.

898. Wellhauser L, Kuo HH, Stratford FL, Ramjeesingh M, Huan LJ, Luong W, Li C, Deber CM, Bear CE. Nucleotides bind to the C-terminus of ClC-5. *Biochem J* 398: 289–294, 2006. doi:10.1042/BJ20060142.

899. Wellhauser L, Luna-Chavez C, D'Antonio C, Tainer J, Bear CE. ATP induces conformational changes in the carboxyl-terminal region of ClC-5. *J Biol Chem* 286: 6733–6741, 2011. doi:10.1074/jbc.M110.175877.

900. Wen X, Lacruz RS, Paine ML. Dental and Cranial Pathologies in Mice Lacking the Cl^-/H^+-Exchanger ClC-7. *Anat Rec (Hoboken)* 298: 1502–1508, 2015. doi:10.1002/ar.23118.

901. Weylandt KH, Nebrig M, Jansen-Rosseck N, Amey JS, Carmena D, Wiedenmann B, Higgins CF, Sardini A. ClC-3 expression enhances etoposide resistance by increasing acidification of the late endocytic compartment. *Mol Cancer Ther* 6: 979–986, 2007. doi:10.1158/1535-7163.MCT-06-0475.

902. Weylandt KH, Valverde MA, Nobles M, Raguz S, Amey JS, Diaz M, Nastrucci C, Higgins CF, Sardini A. Human ClC-3 is not the swelling-activated chloride channel involved in cell volume regulation. *J Biol Chem* 276: 17461–17467, 2001. doi:10.1074/jbc.M011667200.

903. Wheeler TM, Lueck JD, Swanson MS, Dirksen RT, Thornton CA. Correction of ClC-1 splicing eliminates chloride channelopathy and myotonia in mouse models of myotonic dystrophy. *J Clin Invest* 117: 3952–3957, 2007. doi:10.1172/JCI33355.

904. White MM, Miller C. Probes of the conduction process of a voltage-gated Cl^- channel from *Torpedo* electroplax. *J Gen Physiol* 78: 1–18, 1981. doi:10.1085/jgp.78.1.1.

905. White MM, Miller C. A voltage-gated anion channel from the electric organ of *Torpedo californica*. *J Biol Chem* 254: 10161–10166, 1979.

906. Wijnberg ID, Owczarek-Lipska M, Sacchetto R, Mascarello F, Pascoli F, Grünberg W, van der Kolk JH, Drögemüller C. A missense mutation in the skeletal muscle chloride channel 1 (*CLCN1*) as candidate causal mutation for congenital myotonia in a New Forest pony. *Neuromuscul Disord* 22: 361–367, 2012. doi:10.1016/j.nmd.2011.10.001.

907. Wingo CS, Stockand JD. Alkaline activation of ClC-K2 chloride channels switches renal cells from reabsorbing to secreting. *J Gen Physiol* 148: 195–199, 2016. doi:10.1085/jgp.201611669.

908. Winters CJ, Zimniak L, Reeves WB, Andreoli TE. Cl^- channels in basolateral renal medullary membranes. XII. Anti-rbClC-Ka antibody blocks MTAL Cl^- channels. *Am J Physiol Renal Fluid Electrolyte Physiol* 273: F1030–F1038, 1997.

909. Wischmeyer E, Nolte E, Klocke R, Jockusch H, Brinkmeier H. Development of electrical myotonia in the ADR mouse: role of chloride conductance in myotubes and neonatal animals. *Neuromuscul Disord* 3: 267–274, 1993. doi:10.1016/0960-8966(93)90019-G.

910. Wojciechowski D, Fischer M, Fahlke C. Tryptophan Scanning Mutagenesis Identifies the Molecular Determinants of Distinct Barttin Functions. *J Biol Chem* 290: 18732–18743, 2015. doi:10.1074/jbc.M114.625376.

911. Wolf K, Meier-Meitinger M, Bergler T, Castrop H, Vitzthum H, Riegger GA, Kurtz A, Krämer BK. Parallel down-regulation of chloride channel CLC-K1 and barttin mRNA in the thin ascending limb of the rat nephron by furosemide. *Pflugers Arch* 446: 665–671, 2003. doi:10.1007/s00424-003-1098-8.

912. Wollnik B, Kubisch C, Steinmeyer K, Pusch M. Identification of functionally important regions of the muscular chloride channel ClC-1 by analysis of recessive and dominant myotonic mutations. *Hum Mol Genet* 6: 805–811, 1997. doi:10.1093/hmg/6.5.805.

913. Wong JA, Fu L, Schneider EG, Thomason DB. Molecular and functional evidence for Na^+-K^+-$2Cl^-$ cotransporter expression in rat skeletal muscle. *Am J Physiol Regul Integr Comp Physiol* 277: R154–R161, 1999.

914. Wright J, Morales MM, Sousa-Menzes J, Ornellas D, Sipes J, Cui Y, Cui I, Hulamm P, Cebotaru V, Cebotaru L, Guggino WB, Guggino SE. Transcriptional adaptation to *Clcn5* knockout in proximal tubules of mouse kidney. *Physiol Genomics* 33: 341–354, 2008. doi:10.1152/physiolgenomics.00024.2008.

915. Wrong OM, Norden AG, Feest TG. Dent's disease; a familial proximal renal tubular syndrome with low-molecular-weight proteinuria, hypercalciuria, nephrocalcinosis, metabolic bone disease, progressive renal failure and a marked male predominance. *QJM* 87: 473–493, 1994.

916. Wu F, Reed AA, Williams SE, Loh NY, Lippiat JD, Christie PT, Large O, Bettinelli A, Dillon MJ, Goldraich NP, Hoppe B, Lhotta K, Loirat C, Malik R, Morel D, Kotanko P, Roussel B, Rubinger D, Schrander-Stumpel C, Serdaroglu E, Nesbit MA, Ashcroft F, Thakker RV. Mutational analysis of CLC-5, cofilin and CLC-4 in patients with Dent's disease. *Nephron, Physiol* 112: 53–62, 2009. doi:10.1159/000225944.

917. Wu F, Roche P, Christie PT, Loh NY, Reed AA, Esnouf RM, Thakker RV. Modeling study of human renal chloride channel (hCLC-5) mutations suggests a structural-functional relationship. *Kidney Int* 63: 1426–1432, 2003. doi:10.1046/j.1523-1755.2003.00859.x.

918. Wu FF, Ryan A, Devaney J, Warnstedt M, Korade-Mirnics Z, Poser B, Escriva MJ, Pegoraro E, Yee AS, Felice KJ, Giuliani MJ, Mayer RF, Mongini T, Palmucci L, Marino M, Rüdel R, Hoffman EP, Fahlke C. Novel *CLCN1* mutations with unique clinical and electrophysiological consequences. *Brain* 125: 2392–2407, 2002. doi:10.1093/brain/awf246.

919. Wu M, Moh MC, Schwarz H. HepaCAM associates with connexin 43 and enhances its localization in cellular junctions. *Sci Rep* 6: 36218, 2016. doi:10.1038/srep36218.

920. Wu W, Rychkov GY, Hughes BP, Bretag AH. Functional complementation of truncated human skeletal-muscle chloride channel (hClC-1) using carboxyl tail fragments. *Biochem J* 395: 89–97, 2006. doi:10.1042/BJ20050966.

921. Xiong D, Heyman NS, Airey J, Zhang M, Singer CA, Rawat S, Ye L, Evans R, Burkin DJ, Tian H, McCloskey DT, Valencik M, Britton FC, Duan D, Hume JR. Cardiac-specific, inducible ClC-3 gene deletion eliminates native volume-sensitive chloride channels and produces myocardial hypertrophy in adult mice. *J Mol Cell Cardiol* 48: 211–219, 2010. doi:10.1016/j.yjmcc.2009.07.003.

922. Xiong D, Wang GX, Burkin DJ, Yamboliev IA, Singer CA, Rawat S, Scowen P, Evans R, Ye L, Hatton WJ, Tian H, Keller PS, McCloskey DT, Duan D, Hume JR. Cardiac-specific overexpression of the human short CLC-3 chloride channel isoform in mice. *Clin Exp Pharmacol Physiol* 36: 386–393, 2009. doi:10.1111/j.1440-1681.2008.05069.x.

923. Xiong H, Li C, Garami E, Wang Y, Ramjeesingh M, Galley K, Bear CE. ClC-2 activation modulates regulatory volume decrease. *J Membr Biol* 167: 215–221, 1999. doi:10.1007/s002329900485.

924. Xue Y, Wang W, Mao T, Duan X. Report of two Chinese patients suffering from *CLCN7*-related osteopetrosis and root dysplasia. *J Craniomaxillofac Surg* 40: 416–420, 2012. doi:10.1016/j.jcms.2011.07.014.

925. Yamada T, Bhate MP, Strange K. Regulatory phosphorylation induces extracellular conformational changes in a CLC anion channel. *Biophys J* 104: 1893–1904, 2013. doi:10.1016/j.bpj.2013.03.026.

926. Yamamoto-Mizuma S, Wang GX, Liu LL, Schegg K, Hatton WJ, Duan D, Horowitz TL, Lamb FS, Hume JR. Altered properties of volume-sensitive osmolyte and anion channels (VSOACs) and membrane protein expression in cardiac and smooth muscle myocytes from *Clcn3*$^{-/-}$ mice. *J Physiol* 557: 439–456, 2004. doi:10.1113/jphysiol.2003.059261.

927. Yamamoto T, Shimojima K, Sangu N, Komoike Y, Ishii A, Abe S, Yamashita S, Imai K, Kubota T, Fukasawa T, Okanishi T, Enoki H, Tanabe T, Saito A, Furukawa T, Shimizu T, Milligan CJ, Petrou S, Heron SE, Dibbens LM, Hirose S, Okumura A. Single nucleotide variations in *CLCN6* identified in patients with benign partial epilepsies in infancy and/or febrile seizures. *PLoS One* 10: e0118946, 2015. doi:10.1371/journal.pone.0118946.

928. Yang YD, Cho H, Koo JY, Tak MH, Cho Y, Shim WS, Park SP, Lee J, Lee B, Kim BM, Raouf R, Shin YK, Oh U. TMEM16A confers receptor-activated calcium-dependent chloride conductance. *Nature* 455: 1210–1215, 2008. doi:10.1038/nature07313.

929. Yin J, Kuang Z, Mahankali U, Beck TL. Ion transit pathways and gating in ClC chloride channels. *Proteins* 57: 414–421, 2004. doi:10.1002/prot.20208.

930. Yoshikawa M, Uchida S, Ezaki J, Rai T, Hayama A, Kobayashi K, Kida Y, Noda M, Koike M, Uchiyama Y, Marumo F, Kominami E, Sasaki S. CLC-3 deficiency leads to phenotypes similar to human neuronal ceroid lipofuscinosis. *Genes Cells* 7: 597–605, 2002. doi:10.1046/j.1365-2443.2002.00539.x.

931. Yoshikawa M, Uchida S, Yamauchi A, Miyai A, Tanaka Y, Sasaki S, Marumo F. Localization of rat CLC-K2 chloride channel mRNA in the kidney. *Am J Physiol Renal Physiol* 276: F552–F558, 1999.

932. Yu B, Pulit SL, Hwang SJ, Brody JA, Amin N, Auer PL, Bis JC, Boerwinkle E, Burke GL, Chakravarti A, Correa A, Dreisbach AW, Franco OH, Ehret GB, Franceschini N, Hofman A, Lin DY, Metcalf GA, Musani SK, Muzny D, Palmas W, Raffel L, Reiner A, Rice K, Rotter JI, Veeraraghavan N, Fox E, Guo X, North KE, Gibbs RA, van Duijn CM, Psaty BM, Levy D, Newton-Cheh C, Morrison AC; CHARGE Consortium and the National Heart, Lung, and Blood Institute GO ESP*. Rare Exome Sequence Variants in *CLCN6* Reduce Blood Pressure Levels and Hypertension Risk. *Circ Cardiovasc Genet* 9: 64–70, 2016. doi:10.1161/CIRCGENETICS.115.001215.

933. Yu Y, Tsai MF, Yu WP, Chen TY. Modulation of the slow/common gating of CLC channels by intracellular cadmium. *J Gen Physiol* 146: 495–508, 2015. doi:10.1085/jgp.201511413.

934. Yu Y, Xu C, Pan X, Ren H, Wang W, Meng X, Huang F, Chen N. Identification and functional analysis of novel mutations of the *CLCNKB* gene in Chinese patients with classic Bartter syndrome. *Clin Genet* 77: 155–162, 2010. doi:10.1111/j.1399-0004.2009.01288.x.

935. Yusef YR, Zúñiga L, Catalán M, Niemeyer MI, Cid LP, Sepúlveda FV. Removal of gating in voltage-dependent ClC-2 chloride channel by point mutations affecting the pore and C-terminus CBS-2 domain. *J Physiol* 572: 173–181, 2006. doi:10.1113/jphysiol.2005.102392.

936. Zaika O, Mamenko M, Boukelmoune N, Pochynyuk O. IGF-1 and insulin exert opposite actions on ClC-K2 activity in the cortical collecting ducts. *Am J Physiol Renal Physiol* 308: F39–F48, 2015. doi:10.1152/ajprenal.00545.2014.

937. Zaika O, Tomilin V, Mamenko M, Bhalla V, Pochynyuk O. New perspective of ClC-Kb/2 Cl^- channel physiology in the distal renal tubule. *Am J Physiol Renal Physiol* 310: F923–F930, 2016. doi:10.1152/ajprenal.00577.2015.

938. Zanardi I, Zifarelli G, Pusch M. An optical assay of the transport activity of ClC-7. *Sci Rep* 3: 1231, 2013. doi:10.1038/srep01231.

939. Zdebik AA, Cuffe JE, Bertog M, Korbmacher C, Jentsch TJ. Additional disruption of the ClC-2 Cl^- channel does not exacerbate the cystic fibrosis phenotype of CFTR mouse models. *J Biol Chem* 279: 22276–2226783, 2004. doi:10.1074/jbc.M309899200.

940. Zdebik AA, Wangemann P, Jentsch TJ. Potassium ion movement in the inner ear: insights from genetic disease and mouse models. *Physiology (Bethesda)* 24: 307–316, 2009. doi:10.1152/physiol.00018.2009.

941. Zdebik AA, Zifarelli G, Bergsdorf E-Y, Soliani P, Scheel O, Jentsch TJ, Pusch M. Determinants of anion-proton coupling in mammalian endosomal CLC proteins. *J Biol Chem* 283: 4219–4227, 2008. doi:10.1074/jbc.M708368200.

942. Zelikovic I, Szargel R, Hawash A, Labay V, Hatib I, Cohen N, Nakhoul F. A novel mutation in the chloride channel gene, *CLCNKB*, as a cause of Gitelman and Bartter syndromes. *Kidney Int* 63: 24–32, 2003. doi:10.1046/j.1523-1755.2003.00730.x.

943. Zeng B, Li R, Hu Y, Hu B, Zhao Q, Liu H, Yuan P, Wang Y. A novel mutation and a known mutation in the *CLCN7* gene associated with relatively stable infantile malignant osteopetrosis in a Chinese patient. *Gene* 576: 176–181, 2016. doi:10.1016/j.gene.2015.10.021.

944. Zeydan B, Uygunoglu U, Altintas A, Saip S, Siva A, Abbink TEM, van der Knaap MS, Yalcinkaya C. Identification of 3 Novel Patients with *CLCN2*-Related Leukoencephalopathy due to *CLCN2* Mutations. *Eur Neurol* 78: 125–127, 2017. doi:10.1159/000478089.

945. Zhang HN, Zhou JG, Qiu QY, Ren JL, Guan YY. ClC-3 chloride channel prevents apoptosis induced by thapsigargin in PC12 cells. *Apoptosis* 11: 327–336, 2006. doi:10.1007/s10495-006-3980-2.

946. Zhang J, Bendahhou S, Sanguinetti MC, Ptácek LJ. Functional consequences of chloride channel gene (CLCN1) mutations causing myotonia congenita. *Neurology* 54: 937–942, 2000. doi:10.1212/WNL.54.4.937.

947. Zhang J, Sanguinetti MC, Kwiecinski H, Ptácek LJ. Mechanism of inverted activation of ClC-1 channels caused by a novel myotonia congenita mutation. *J Biol Chem* 275: 2999–3005, 2000. doi:10.1074/jbc.275.4.2999.

949. Zhang L, Zhang T, Xiang Z, Lu S. The rs3737964 single-nucleotide polymorphism of the chloride channel-6 gene as a risk factor for coronary heart disease. *Mol Genet Genomic Med* 3: 537–542, 2015. doi:10.1002/mgg3.163.

950. Zhang X, Hartz PA, Philip E, Racusen LC, Majerus PW. Cell lines from kidney proximal tubules of a patient with Lowe syndrome lack OCRL inositol polyphosphate 5-phosphatase and accumulate phosphatidylinositol 4,5-bisphosphate. *J Biol Chem* 273: 1574–1582, 1998. doi:10.1074/jbc.273.3.1574.

951. Zhang XD, Chen TY. Amphiphilic blockers punch through a mutant CLC-0 pore. *J Gen Physiol* 133: 59–68, 2009. doi:10.1085/jgp.200810005.

952. Zhang XD, Li Y, Yu WP, Chen TY. Roles of K149, G352, and H401 in the channel functions of ClC-0: testing the predictions from theoretical calculations. *J Gen Physiol* 127: 435–447, 2006. doi:10.1085/jgp.200509460.

953. Zhang XD, Tseng PY, Chen TY. ATP inhibition of CLC-1 is controlled by oxidation and reduction. *J Gen Physiol* 132: 421–428, 2008. doi:10.1085/jgp.200810023.

954. Zhang XD, Tseng PY, Yu WP, Chen TY. Blocking pore-open mutants of CLC-0 by amphiphilic blockers. *J Gen Physiol* 133: 43–58, 2009. doi:10.1085/jgp.200810004.

955. Zhang XD, Yu WP, Chen TY. Accessibility of the CLC-0 pore to charged methanethiosulfonate reagents. *Biophys J* 98: 377–385, 2010. doi:10.1016/j.bpj.2009.09.066.

956. Zhang X, Jefferson AB, Auethavekiat V, Majerus PW. The protein deficient in Lowe syndrome is a phosphatidylinositol-4,5-bisphosphate 5-phosphatase. *Proc Natl Acad Sci USA* 92: 4853–4856, 1995. doi:10.1073/pnas.92.11.4853.

957. Zhang Y, Voth GA. The coupled proton transport in the ClC-ec1 Cl^-/H^+ antiporter. *Biophys J* 101: L47–L49, 2011. doi:10.1016/j.bpj.2011.10.021.

958. Zhao Z, Li X, Hao J, Winston JH, Weinman SA. The ClC-3 chloride transport protein traffics through the plasma membrane via interaction of an N-terminal dileucine cluster with clathrin. *J Biol Chem* 282: 29022–29031, 2007. doi:10.1074/jbc.M703506200.

959. Zheng H, Shao C, Zheng Y, He JW, Fu WZ, Wang C, Zhang ZL. Two novel mutations of *CLCN7* gene in Chinese families with autosomal dominant osteopetrosis (type II). *J Bone Miner Metab* 34: 440–446, 2016. doi:10.1007/s00774-015-0682-2.

959a. Zheng J, Trudeau M (Editors). *Handbook of Ion Channels*. Boca Raton, FL: CRC, 2015. doi:10.1201/b18027

960. Zhou JG, Ren JL, Qiu QY, He H, Guan YY. Regulation of intracellular Cl^- concentration through volume-regulated ClC-3 chloride channels in A10 vascular smooth muscle cells. *J Biol Chem* 280: 7301–7308, 2005. doi:10.1074/jbc.M412813200.

961. Zifarelli G, De Stefano S, Zanardi I, Pusch M. On the mechanism of gating charge movement of ClC-5, a human Cl^-/H^+ antiporter. *Biophys J* 102: 2060–2069, 2012. doi:10.1016/j.bpj.2012.03.067.

962. Zifarelli G, Liantonio A, Gradogna A, Picollo A, Gramegna G, De Bellis M, Murgia AR, Babini E, Camerino DC, Pusch M. Identification of sites responsible for the potentiating effect of niflumic acid on ClC-Ka kidney chloride channels. *Br J Pharmacol* 160: 1652–1661, 2010. doi:10.1111/j.1476-5381.2010.00822.x.

963. Zifarelli G, Murgia AR, Soliani P, Pusch M. Intracellular proton regulation of ClC-0. *J Gen Physiol* 132: 185–198, 2008. doi:10.1085/jgp.200809999.

964. Zifarelli G, Pusch M. CLC chloride channels and transporters: a biophysical and physiological perspective. *Rev Physiol Biochem Pharmacol* 158: 23–76, 2007.

965. Zifarelli G, Pusch M. CLC transport proteins in plants. *FEBS Lett* 584: 2122–2127, 2010. doi:10.1016/j.febslet.2009.12.042.

966. Zifarelli G, Pusch M. Conversion of the 2 Cl^-/1 H^+ antiporter ClC-5 in a NO_3^-/H^+ antiporter by a single point mutation. *EMBO J* 28: 175–182, 2009. doi:10.1038/emboj.2008.284.

967. Zifarelli G, Pusch M. Intracellular regulation of human ClC-5 by adenine nucleotides. *EMBO Rep* 10: 1111–1116, 2009. doi:10.1038/embor.2009.159.

968. Zifarelli G, Pusch M. The muscle chloride channel ClC-1 is not directly regulated by intracellular ATP. *J Gen Physiol* 131: 109–116, 2008. doi:10.1085/jgp.200709899.

969. Zifarelli G, Pusch M. Relaxing messages from the sarcolemma. *J Gen Physiol* 136: 593–596, 2010. doi:10.1085/jgp.201010567.

970. Zifarelli G, Pusch M. The role of protons in fast and slow gating of the *Torpedo* chloride channel ClC-0. *Eur Biophys J* 39: 869–875, 2010. doi:10.1007/s00249-008-0393-x.

971. Zúñiga L, Niemeyer MI, Varela D, Catalán M, Cid LP, Sepúlveda FV. The voltage-dependent ClC-2 chloride channel has a dual gating mechanism. *J Physiol* 555: 671–682, 2004. doi:10.1113/jphysiol.2003.060046.